UNIVERSITÀ DEGLI STUDI DI PALERMO
Dottorato in Energia e Tecnologie dell'Informazione
Dipartimento di Ingegneria
Settore Scientifico Disciplinare ING-IND/33

MULTI-OBJECTIVE OPTIMISATION OF BUILDINGS AND BUILDING CLUSTERS PERFORMANCE: A LIFE CYCLE THINKING APPROACH

IL DOTTORE
ING. FRANCESCO MONTANA

IL COORDINATORE
PROF. MAURIZIO CELLURA

IL TUTOR
PROF.SSA ELEONORA RIVA SANSEVERINO

CO TUTOR
DOTT. ING. SONIA LONGO

CICLO XXXII
ANNO 2020

Prefazione

Il lavoro descritto in questa tesi è stato condotto principalmente presso il Dipartimento di Ingegneria dell'Università degli Studi di Palermo, in parte presso Engineering Ingegneria Informatica S.p.A., un'azienda internazionale di ingegneria informatica il cui reparto di Ricerca e Sviluppo è situato a Palermo, e in parte presso il Danish Building Research Institute (Statens Byggeforskningsinstitut, SBi), un dipartimento della Aalborg University Copenhagen.

Il progetto è stato finanziato interamente dal Ministero dell'Istruzione, dell'Università e della Ricerca tramite il Programma Operativo Nazionale "FSE-FESR Ricerca e Innovazione 2014-2020, Azione I.1", dedicato a supportare le università insistenti nelle regioni italiane con uno sviluppo economico ridotto. La mia tutor principale è stata la Professoressa Eleonora Riva Sanseverino, Professore Ordinario di Sistemi Elettrici per l'Energia con specializzazione in smart grids, microgrids e ottimizzazione euristica multi-obiettivo, mentre la mia co-tutor è stata la Dr. Sonia Longo, Ricercatore in Fisica Tecnica Ambientale specializzata in Life Cycle Assessment di sistemi energetici e in termofisica degli edifici.

Durante il mio progetto di dottorato di ricerca ho sviluppato un approccio metodologico su cui basare il progetto e la ristrutturazione di edifici e di cluster di edifici che permette di identificare le migliori soluzioni progettuali di compromesso tra vari criteri secondo un approccio multi-obiettivo. In particolare, ho integrato la metodologia del LCA in un problema di ottimizzazione impiegando gli impatti di ciclo di vita come funzioni obiettivo; la risoluzione di questo problema individua le soluzioni progettuali ed i materiali che minimizzano gli impatti di ciclo di vita dell'edificio dal punto di vista energetico ed ambientale e i principali aspetti economici per l'acquisto e l'esercizio dei componenti.

Scopo di questo progetto di dottorato di ricerca è stato quindi fornire alle comunità scientifica e tecnica internazionali una metodologia olistica che possa essere impiegata per il progetto di edifici ad alte prestazioni energetiche, in modo che essi riducano i consumi e gli impatti in tutto il loro ciclo di vita, anziché soltanto nella loro fase d'uso.

Il documento è diviso in tre sezioni principali: background, revisione della letteratura esistente e presentazione della metodologia; casi studio sull'ottimizzazione di un singolo edificio; casi studio sull'ottimizzazione di cluster di edifici e micro-reti.

Palermo, 10 gennaio 2021

Francesco Montana

Preface

The work described in this thesis has been conducted mainly at the Department of Engineering at University of Palermo, partly at Engineering Ingegneria Informatica S.p.A., a multinational software engineering company with a Research and Development laboratory located in Palermo, and partly at the Danish Building Research Institute (Statens Byggeforskningsinstitut, SBi), one of the departments of the Aalborg University Copenhagen.

The project has been entirely financed by the Italian Ministry of Education, University and Research through the National Operating Program "FSE-FESR Ricerca e Innovazione 2014-2020, Azione I.1", dedicated to the universities located in Italian regions whose development is lagging. My thesis has been supervised by Professor Eleonora Riva Sanseverino, Full Professor in power systems with expertise in smart grids, microgrids and multi-objective heuristic optimisation, and co-supervised by Sonia Longo, Assistant Professor in Life Cycle Assessment of energy systems and building physics.

During my PhD project, I have developed an innovative framework for the design and refurbishment of buildings and clusters of buildings aimed at identifying the best compromise solution according to different criteria through a multi-objective optimisation approach. More in detail, I integrated the LCA methodology into the optimisation using life cycle impacts as objective functions, to identify interventions and materials that allow minimising energy and environmental impacts over the life cycle of the building and the economic cost for purchase and operation of the building components.

This PhD research project aims at providing the scientific and technical international communities with a comprehensive method that can be used for the rational design of high performing buildings, allowing the attainment of energy saving along the complete life cycle of the building instead of just focusing on its use phase.

The work consists of three main parts:

- background, review of the existing literature and presentation of the methodology;
- case studies on single-building optimisation;
- case studies on the cluster of buildings and microgrids optimisation.

Palermo, January, 10th 2021

Francesco Montana

Acknowledgements

There are many persons that I wish to acknowledge because of their help and support in this three-year path.

First of all, I would like to thank my main supervisor, Professor Eleonora Riva Sanseverino, and my co-supervisor, Dr Sonia Longo, who always provided me with suggestions derived from their huge experience in their respective research fields. Although we did not know each other before the beginning of my PhD, we started working immediately with mutual respect and they have always encouraged my new ideas and my professional and personal growth.

I warmly wish to thank PhD students at the University of Palermo, Domenico, Pietro, Giuseppe, Francesca, Daniele, Milagros, and Quynh, who were my companions in this wonderful adventure between study, lectures, collaborations, suggestions, but also recreation and laughs.

Thanks to Prof. Maurizio Cellura, Dr. Enrico Telaretti and Dr. Gaetano Zizzo from the University of Palermo, who were always ready to give me opportunities for comparing our ideas and to give me their suggestions.

I thank my former boss at Business Integration Partners S.p.A., Claudio Lui, who encouraged me when I decided to start this PhD, allowing me to suspend my job in the company to find the career that suits me best.

I wish to thank my supervisors at the Research and Development laboratory of Engineering Ingegneria Informatica S.p.A., Diego Arnone and Alessandro Rossi, together with their team, made up by Ferdinando, Enrico, Marzia, Giuseppe, Alessio, and Angelo, who helped me with their expertise in the development of the software tools that I have used to accomplish this research project.

I warmly thank my supervisors at Aalborg University Copenhagen, Dr. Harpa Birgisdottir, Dr. Kai Kanafani, and Kim Wittchen, who were enthusiastic to collaborate from the very first moment and supervised my research on the optimisation of a real case study in Copenhagen, also providing useful data on typical Danish constructions and challenging my building modelling skills. I also wish to thank the researchers of SBi department, Athanasia, Alessandro, Roberta, Joanna, Freja, Gianluca, and Regitze, for making me feel at home in a different country with their friendship.

I really thank the evaluators of this PhD thesis, Prof. Amjad Anvari-Moghaddam from the Aalborg University and Prof. Shady Attia from the Liege University, for their fundamental, useful suggestions and for their appreciation to my research project.

And last but not least, my family: my parents, for supporting my every choice, even when they do not agree with me, and my fiancée, who shared with me the experience of the PhD, listening to my doubts and trying to provide me with useful tips.

Thank you very much to all of you for making me a better person.

Sommario

Il tema della riduzione dei consumi energetici negli edifici sta ricevendo un interesse sempre crescente negli ultimi anni poiché il settore edilizio è uno dei più energivori nei paesi sviluppati. Il lavoro descritto in questa tesi propone un framework metodologico per valutare e minimizzare gli impatti energetici e ambientali di ciclo di vita ed i costi degli edifici con alte prestazioni energetiche. La metodologia è stata concepita per essere quanto più generica e inclusiva possibile, in modo da poter essere impiegata per il progetto di nuovi edifici o per la ristrutturazione di costruzioni esistenti. Inoltre, il metodo consente di analizzare e ottimizzare anche i cluster di edifici, schematizzati come micro-reti, per dimensionare e gestire in maniera coordinata i sistemi di climatizzazione e produzione di acqua calda sanitaria, gli impianti a fonti rinnovabili e i relativi sistemi di accumulo elettrico e termico, migliorando in tal modo l'efficienza energetica e riducendo gli impatti ed i costi al livello del cluster. Quest'approccio potrebbe essere d'interesse anche per i decisori pubblici, permettendo loro di identificare la strategia energetica o incentivante da preferire e perseguire.

Sebbene la maggior parte delle politiche energetiche si focalizzi sulla riduzione dei consumi durante la fase d'uso di un edificio, esiste un altro contributo di energia da considerare, cioè l'energia necessaria per l'estrazione delle materie prime, la costruzione e la demolizione dei materiali, che è nota in letteratura con il nome di *embodied energy*. Nonostante questo termine sia stato spesso trascurato in passato nello studio degli edifici, dato il suo valore ridotto, lo sviluppo di edifici ad alte prestazioni energetiche ha dimostrato che questo contributo può diventare predominante, o comunque non più trascurabile rispetto all'energia di fase d'uso. Questa evidenza suggerisce che è necessario adottare un approccio olistico per ridurre efficacemente i consumi e gli impatti del comparto edilizio.

Pertanto, questo progetto di dottorato è stato orientato all'ottimizzazione del progetto e della ristrutturazione di edifici, adottando come funzioni obiettivo la minimizzazione degli indicatori d'impatto energetico e ambientale di ciclo di vita e degli aspetti economici. L'approccio di ottimizzazione è stato incluso nello studio poiché esso garantisce l'identificazione della soluzione o delle soluzioni ottimali, qualora si adotti un approccio multi-obiettivo. Inoltre, l'impiego di strategie di ottimizzazione euristiche consente un'investigazione approfondita dello spazio di ricerca che sarebbe altrimenti proibita in una semplice analisi parametrica, che è l'approccio solitamente più adottato a oggi in ambito edilizio. Ciò accade poiché l'algoritmo di ottimizzazione esplora lo spazio delle variabili in maniera intelligente, valutando progressivamente solo le alternative che appaiono più promettenti anziché verificarle tutte.

In particolare, l'ottimizzazione multi-obiettivo descritta in questa tesi, partendo da un modello preliminare di edificio o di cluster di edifici, permette di identificare un insieme di soluzioni che riducono contemporaneamente la Domanda Energetica Cumulativa (Cumulative Energy Demand) il Potenziale di Riscaldamento Globale (Global Warming Potential) e i costi di investimento e operativi relativi al ciclo di vita dell'edificio. Per dimostrare la fattibilità della metodologia esposta e per fornire qualche

indicazione e linee guida sui benefici potenzialmente conseguibili, sono stati sviluppati alcuni casi studio dimostrativi in diverse condizioni climatiche. L'impiego di dati di input e di software disponibili gratuitamente è stato considerato come criterio principale nella gran parte di questi casi studio. Sebbene il minimo assoluto delle funzioni obiettivo si raggiunga solo raramente negli studi di ottimizzazione multi-obiettivo, poiché gli obiettivi sono in contrasto tra loro, ognuno di essi risulta ampiamente ridotto.

Riguardo all'ottimizzazione di un singolo edificio, è stato adottato un approccio di ottimizzazione *simulation-based*, cioè un accoppiamento tra un software che analizza un fenomeno tramite una simulazione dedicata ed un metodo di ottimizzazione. In questo modo, le prestazioni termiche dell'edificio sono state valutate accuratamente attraverso un software di certificazione energetica o di simulazione termofisica; questi risultati sono stati sfruttati per identificare le tecniche progettuali o gli interventi di ristrutturazione ottimali per l'involucro e per gli impianti tecnici dell'edificio. Sono stati sviluppati tre casi studio su questa applicazione:

- uno studio dimostrativo effettuato su un edificio fittizio nel contesto climatico mediterraneo di Palermo (Italia);
- uno studio su un edificio residenziale esistente situato in una citta con clima oceanico (Hvalsø, Danimarca);
- uno studio su una abitazione mono-familiare esistente situata in una citta con clima caldo-umido (Palermo, Italia).

Nonostante i casi studio sul singolo edificio presentati in questa tesi riguardino unicamente la ristrutturazione di edifici residenziali, la metodologia illustrata può essere adattata anche a contesti non residenziali o al progetto di nuovi edifici. Questi studi sono stati condotti accoppiando un software di simulazione delle prestazioni dell'edificio con un software di ottimizzazione. In particolare, nello studio dimostrativo e per il caso studio sull'edificio situato a Palermo, EnergyPlus e MOBO sono stati impiegati per l'ottimizzazione dell'involucro edilizio e uno script sviluppato su MATLAB è stato impiegato per ottimizzare gli impianti energetici. Invece, per il caso studio relativo a Hvalsø, Be18 e MOBO sono stati accoppiati per l'ottimizzazione sia dell'involucro che degli impianti. Così facendo, la metodologia è stata testata sia con un software di simulazione dettagliata come EnergyPlus sia con uno strumento di certificazione energetica come Be18, ampliando la platea di soggetti potenzialmente interessati all'impiego del metodo.

L'ottimizzazione di cluster di edifici, condotta tramite un modello matematico di *energy hub*, permette di identificare la combinazione ottimale di impianti, le loro taglie e il loro programma di gestione oraria in un'unica ottimizzazione, ottenendo quindi di andare incontro alle domande energetiche di un insieme di utilizzatori in maniera centralizzata. I due casi studio sviluppati riguardano:

- uno studio dimostrativo effettuato su un quartiere urbano fittizio in due diversi contesti energetico-economici: Palermo (Italia) e Hanoi (Vietnam);
- un caso studio applicativo sull'isola mediterranea di Pantelleria (Italia).

Questi due studi sono stati basati su diversi approcci per la stima della domanda energetica, principalmente a causa della differenza di dati a disposizione, ed entrambi gli studi sono stati condotti tramite uno script in MATLAB sviluppato durante il progetto di dottorato.

La metodologia e gran parte dei casi studio sviluppati in questo progetto di dottorato di ricerca sono stati pubblicati su riviste o atti di conferenze. Inoltre, la parte dello studio riguardante i singoli edifici è stata inserita tra le attività dell'International Energy Agency (IEA) – Energy in Buildings and Communities Programme (EBC) Annex 72 "Assessing Life Cycle Related Environmental Impacts Caused by Buildings", il cui scopo principale è la valutazione degli impatti ambientali di ciclo di vita provocati dal settore edilizio. In particolare, questo lavoro fa parte dell'Activity 3.3 dell'Annex, dove sono stati classificati e confrontati diversi casi studio sull'ottimizzazione delle prestazioni energetiche e dell'effetto serra degli edifici.

Abstract

The topic of reducing energy consumption in buildings is gaining an increasing interest in the last years since the building sector is one of the most energy-intensive in industrialised countries. The work depicted in this thesis proposes a methodological framework to assess and minimise life cycle energy and environmental impacts and costs related to buildings with very high-energy performance. The methodology was conceived to be as generic as possible, in order to be applicable to the preliminary design of new buildings or refurbishment of existing ones. Furthermore, the method allows to analyse and optimise even clusters of buildings operated as a microgrid, to design and manage HVAC plants, renewable systems and their storages in a coordinated way, thus improving energy efficiency and reducing the related environmental impacts at a cluster level. This approach may be of interest also for policymakers to identify which energy strategy should be followed.

Although most of existing policies often focus on the reduction of buildings' operating energy, there is another energy and impact contribution to take into account, *i.e.* the energy required for the resources extraction, materials construction and demolition, known in the scientific literature as embodied energy. Concerning buildings, although this term has been often disregarded in the past for its low value in traditional buildings, the development of low energy buildings has proven that embodied energy becomes a predominant contribution, or at least non-negligible to the operating term. This feature suggests that a holistic approach has to be adopted to effectively reduce consumptions and impacts in the building sector.

For what above, this PhD research project was focused on the optimisation of buildings' design and refurbishment adopting Life Cycle Assessment energy and environmental impact indicators and economic aspects as objective functions. The optimisation approach was included in the study since it allows identifying effectively the optimal solution or solutions (in the case of multi-objective optimisation). Moreover, the employment of heuristic optimisation strategies enables a comprehensive investigation of the variable space that would be forbidden for a simple parametric analysis, namely the most popular approach currently adopted for the studies on buildings. For this reason, this is most commonly used in the building sector. This aspect occurs since the algorithm investigates the variables space smartly without analysing every single alternative, but only the most promising ones.

In detail, starting from a preliminary building or cluster of buildings model, the multi-objective optimisation method developed in this thesis allows obtaining a set of solutions that simultaneously reduce the Cumulative Energy Demand, the Global Warming Potential, and the investment and operating costs related to the life cycle of the building. To demonstrate the feasibility of the methodology and to provide an indication of achievable benefits and guidelines, some applicative case studies in different climatic conditions were developed. The use of free-of-charge input data and software has been preferred in most of the case studies. Although the absolute minimum of objective functions is hardly achieved in multi-objective optimisation, since the

objectives are usually conflicting, the implementation of compromise solutions allows a huge reduction of every single objective.

Regarding the optimisation of a single building, a simulation-based optimisation approach was adopted to accurately assess the building thermal performance through a software for energy rating or building physics simulation, whose results are exploited by the optimisation to identify the optimal design strategies or retrofit interventions for the envelope and the equipment. On this application, three case studies were analysed:

- A demonstrative study performed on a fictitious building in the Mediterranean climate of Palermo (Italy);
- A real case study on a residential building located in an oceanic climate city (Hvalsø, Denmark);
- A real case study on a single-family house located in a warm climate city (Palermo, Italy).

Although the single building case studies shown in this work are related to the retrofitting of residential buildings only, the methodology can be employed also for non-residential applications and designs of new buildings. These studies were developed coupling a building energy performance simulation software tool with an optimisation software tool. For the demonstrative study and the real case study in Palermo, EnergyPlus and MOBO were coupled for the building envelope optimisation while a MATLAB script was employed for optimising the equipment. For the real case study in Halsø, Be18 and MOBO were coupled for both the building envelope and the equipment optimisation. This also allowed proving that the methodology can be developed using both a detailed dynamic simulation software as EnergyPlus or a simplified tool for energy rating as Be18, allowing a wider audience to be interested in adopting this kind of approach.

The buildings cluster optimisation, performed through an energy hub mathematical model, allows identifying the optimal combination of equipment, their sizes and their operating schedule in a unique optimisation, thus allowing to fulfil the demand of a district in a centralised way. The two case studies on buildings cluster optimisation describe:

- A demonstrative study performed on a fictitious urban district cluster in two different energy and economic contexts: Palermo (Italy) and Hanoi (Vietnam);
- A real case study on the Mediterranean island of Pantelleria (Italy).

These studies were based on different approaches for the energy demand evaluation because of different data availability, while the optimisation was performed through a MATLAB script developed during this project.

The methodology and most of the case studies developed during this PhD research project have been published on international journals and conference proceedings, and have been also included within the activities of International Energy Agency (IEA) – Energy in Buildings and Communities Programme (EBC) Annex 72 “Assessing Life

Cycle Related Environmental Impacts Caused by Buildings”, whose main aim is the assessment of the life cycle related environmental impacts caused by buildings. More in detail, this work was part of the Activity 3.3 of this Annex, where case studies on the life cycle energy and carbon performance of buildings are classified and compared.

Contents

List of Figures

List of Tables

Abbreviations

ADP	*Abiotic Depletion Potential*
ANSI	*American National Standards Institute*
AP	*Acidification Potential*
ASHRAE	*American Society of Heating, Refrigerating and Air-conditioning Engineers*
BPO	*Building Performance Optimisation*
BPS	*Building Performance Simulation*
CED	*Cumulative Energy Demand*
CEN	*European Committee for Standardization*
CHP	*Combined Heat and Power*
CIS	*Commonwealth of Independent States*
DES	*Desalination system*
DG	*Diesel Generators*
DHW	*Domestic Hot Water*
DM	*Decision Makers*
DU	*Declared Unit*
EB	*Electric Boiler*
EBC	*Energy in Buildings and Communities programme*
EE	*Embodied Energy*
EGWP	*Embodied Global Warming Potential*
ELCD	*European reference Life Cycle Database*
EP	*Eutrophication Potential*
EPBD	*Energy Performance of Buildings Directive*
EPD	*Environmental Product Declarations*
EPS	*Expanded Polystyrene*
EU	*European Union*
FU	*Functional Unit*
GER	*Gross Energy Requirement*
GHG	*Greenhouse Gas*
GWP	*Global Warming Potential*

HB	*Heat Balance method*
HP	*Heat Pump*
HVAC	*Heating, Ventilation and Air Conditioning*
IEA	*International Energy Agency*
ILCD	*International reference Life Cycle Data system*
IPCC	*Intergovernmental Panel on Climate Change*
ISO	*International Organization for Standardization*
LC-ZEB	*Life Cycle Zero-Energy Building*
LCA	*Life Cycle Assessment*
LCC	*Life Cycle Costing*
LULUCF	*Land Use, Land-Use Change, and Forestry*
MILP	*Mixed Integer Linear Programming*
MOBO	*Multi Objective Building Optimization tool*
MOO	*Multi-Objective Optimisation*
MS	*Member States*
NGB	*Natural Gas Boiler*
NPV	*Net Present Value*
NSGA	*Non-dominated Sorting Genetic Algorithm*
NZEB	*Net Zero-Energy Building*
nZEB	*Nearly Zero-Energy Building*
ODP	*Ozone Depletion Potential*
PE	*Primary Energy use*
PMV	*Predicted Mean Vote*
POCP	*Photochemical Ozone Creation Potential*
PPD	*Predicted Percentage of Dissatisfied*
PV	*Photovoltaic*
RES	*Renewable Energy Source*
RTS	*Radiant Time Series method*
SDG	*Sustainable Development Goal*
SHGC	*Solar Heat Gain Coefficient*
SOO	*Single-Objective Optimisation*
STC	*Solar Thermal Collector*
STO_e	*Electrical Storage*

STO_h	*Thermal Storage*
STO_w	*Freshwater Storage*
UCRF	*Uniform Capital Recovery Factor*
UEC	*Unit Embodied Carbon factor*
UEE	*Unit Embodied Energy factor*
UK	*United Kingdom*
UL	*Useful Life*
UP	*Unit Price*
USPWF	*Uniform Series Present-Worth Factor*
WWR	*Window to Wall Ratio*
ZEB	*Zero Emission Building*

Chapter One – Introduction

1.1. Motivation and research gaps

The humankind has always tried to adapt the surrounding environment to its primary requirements, first finding repair from the weathering in caves and then creating houses. Nevertheless, since the human population growth rate underwent an exponential growth rate in last seventy years, passing from 2.5 billion to almost 8 billion (as shown in Fig. 1.1), and considering also the recent climate emergency, new ways to fulfil our needs must be found to ensure the sustainable development, thus letting also to future generations to provide for their needs.

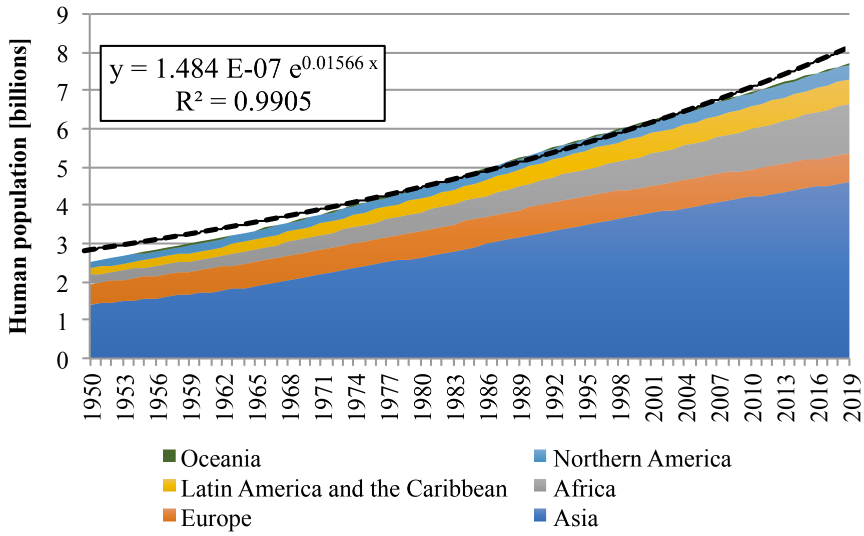

Fig 1.1. Human population trend from 1950 according to the continent (data from [1])

One of the most important needs of humankind is energy, namely the capacity of a physical system to do work. It is used in many forms in the everyday life, as for air conditioning, lighting or transports. The world primary energy consumption trend in the last 55 years is shown in Fig. 1.2.

It is possible to state that, apart from some small decreasing periods, the trend has a monotonic rising behaviour, and although many developed countries invested in energy-saving policies in the last few years, developing countries in Asia overbalanced their efforts (Fig. 1.2a). Another important evidence is that, notwithstanding the increasing penetration and promotion of renewable energies related to the last 20 years, fossil fuels still compose the highest share of the mix (Fig. 1.2b).

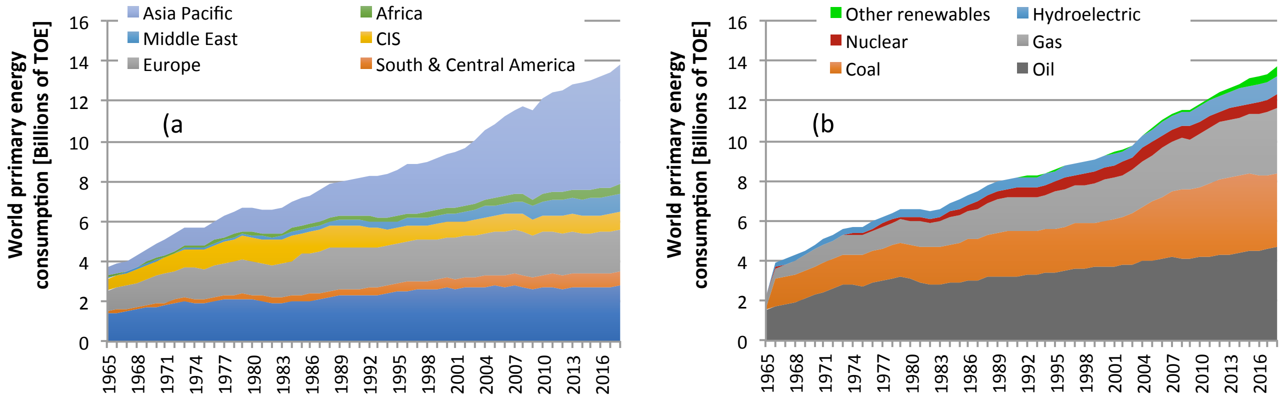

Fig 1.2. World energy consumption from 1965 according to the continent (a) and the source (b) [2]

As well known, the fossil fuels combustion is the primary cause of greenhouse gases (GHG) emission, whose concentration in the atmospheric air is considered the primary cause of the rising of average air temperature. To confirm this statement, in Fig. 1.3 it is possible to see that, neglecting the oscillations, carbon dioxide concentration in the atmospheric air and average temperature anomalies had similar general rising trends since 1958, when the first CO_2 measurements started.

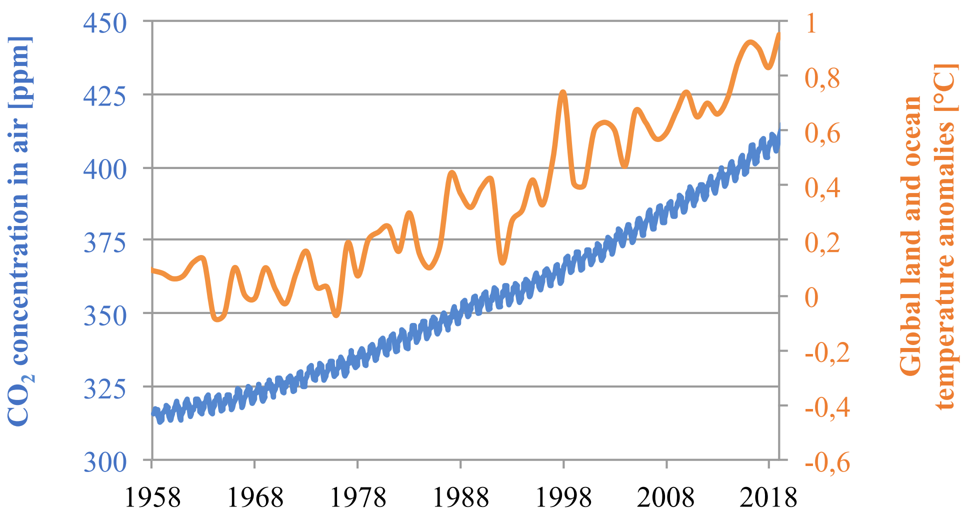

Fig 1.3. Blue trend: Carbon dioxide concentration in air measured on Mauna Loa laboratory [3]; Orange trend: average global land and ocean temperature anomalies [4]

To face this problem and allow our ecosystem to find a new balance that can be compatible with humankind life and wellbeing, many international agreements have been made, the first and most known of whom being the Kyoto Protocol in 1992 [5]. More recently, energy was considered as one of the key elements included in the 17

Sustainable Development Goals (SDGs) of the United Nations' 2030 Agenda for Sustainable Development [6], since energy and environmental issues directly influence SDGs 1, 3, 6, 7, 11, 13, and 15 [7]. The topics of 2030 Agenda SDGs are shown in Fig. 1.4.

One of the main actors in the attainment of these goals is the European Union (EU), who in 2007 undertook a roadmap to achieve challenging targets with the so-called "2020 climate & energy package" [8]. This package consists of three energy-related targets to be attained within 2020, *i.e.* a reduction of at least 20% in GHG emissions with respect to the 1990 levels, a 20% penetration in the share of renewable energies in EU energy consumption and a saving of 20% of primary energy consumptions compared to forecasted levels. The current status (2018) is reported in Table 1.1.

Fig 1.4. List of Sustainable Development Goals of the United Nations' 2030 Agenda for Sustainable Development [6]

Table 1.1. 2020 package targets status [9]

EUROPEAN UNION (27 COUNTRIES) + UNITED KINGDOM	**2007 levels**	**2018 levels**	**Target**	**Status**
GHG emissions, base year 1990	92.7%	76.8%	80.0%	Overcome
Share of renewable energy in gross final energy consumption	10.6%	18.0%	20.0%	To be reached
Primary energy consumption	1,701.6 MTOE	1,551.9 MTOE	1,483.0 MTOE	To be reached

With the currently reached levels, Europeans managed to successfully decouple GHG emissions from economic growth, since in the period between 1990 and 2016, energy use was reduced by almost 2%, GHG emissions by 22% while Gross Domestic Product grew by 54% [10]. With the approaching of the deadline for 2020 targets, EU Commission decided to update these targets for the subsequent decade, in detail a 40% reduction of GHG emissions with respect to the 1990 levels, a 32% share of renewable energies in EU energy consumption and a saving of 32.5% of primary energy consumptions [11]. Furthermore, in 2011 a long-term strategy was set, in order to achieve an 80% CO_2 emissions reduction within 2050 [12], that was ultimately updated to a climate-neutral economy in 2018, as shown in Fig. 1.5. In the figure legend, LULUCF indicates emissions reduction for Land use, land-use change, and forestry. With this challenging policy, EU aims at complying with the Paris Agreement, limiting the global temperature increase to 1.5 °C above pre-industrial levels and attaining a development model based on the balance between carbon production and consumption [10]. The latest and the most challenging policy is the European Green Deal that, in addition to a carbon neutral economy by 2050, also aims at attaining an economic growth decoupled from the resource use, boosting the circular economy and the sustainability in buildings, agriculture, mobility and industry [13].

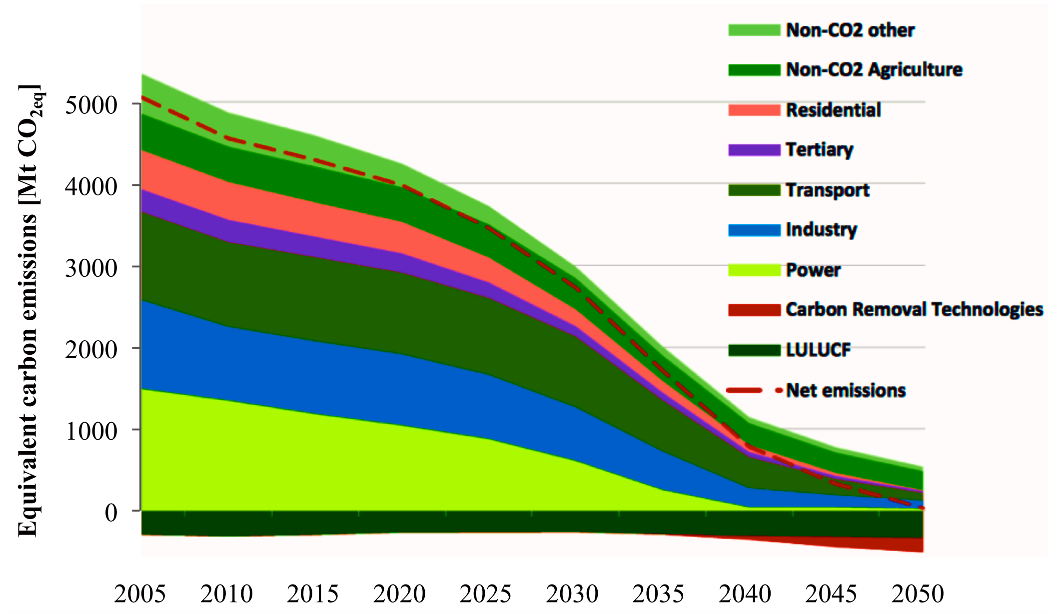

Fig 1.5. European Union 2050 long-term strategy to a climate-neutral economy [10]

In the depicted framework, the topic of reducing energy consumption in buildings gained an increasing interest in the last years, since the building sector is one of the most energy-intensive in developed countries. According to a report issued by the International Energy Agency (IEA), buildings construction and operations accounted for 36% of global final energy use, and for nearly 40% of global energy-related carbon dioxide emissions in 2017, including both direct emissions from the use of fossil fuels for heating purposes and indirect emissions through the electricity and/or district heating use [14]. Furthermore, buildings' energy load is estimated to keep increasing in the next decades and is predicted to augment by about 50% in 2050 [15].

Focusing on the 27 countries of the EU and the United Kingdom (UK), buildings are the cause of about 40% of the energy consumption and 36% of CO_2 emissions [16]. As shown in Fig. 1.6 [17], where the sector is divided in households and commercial & services, the primary energy consumption in final uses was responsible for 41% of the EU demand in 2017, meaning between 408 and 479 MTOE in the period from 2010 and 2017. Further detail on final energy uses in buildings is provided in Fig. 1.7, where space heating and Domestic Hot Water (DHW) production are proved to be the most significant terms. Nevertheless, space cooling is currently the fastest-growing energy use in buildings, according to an IEA report, both in advanced countries where people has high thermal comfort expectations and in hot and humid emerging economies [18].

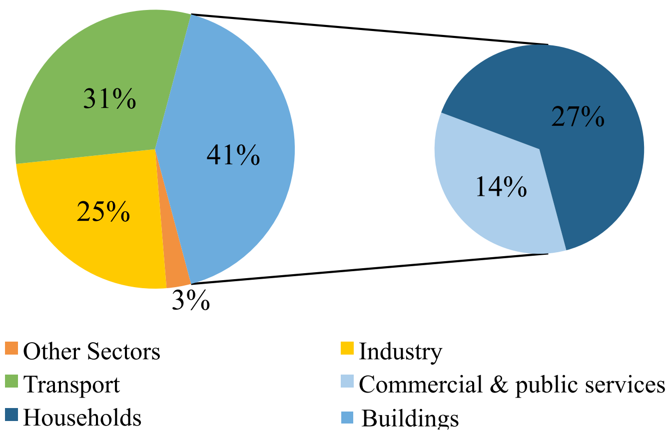

Fig 1.6. European Union and UK primary energy consumption in main final uses in 2017 (percentage) [17]

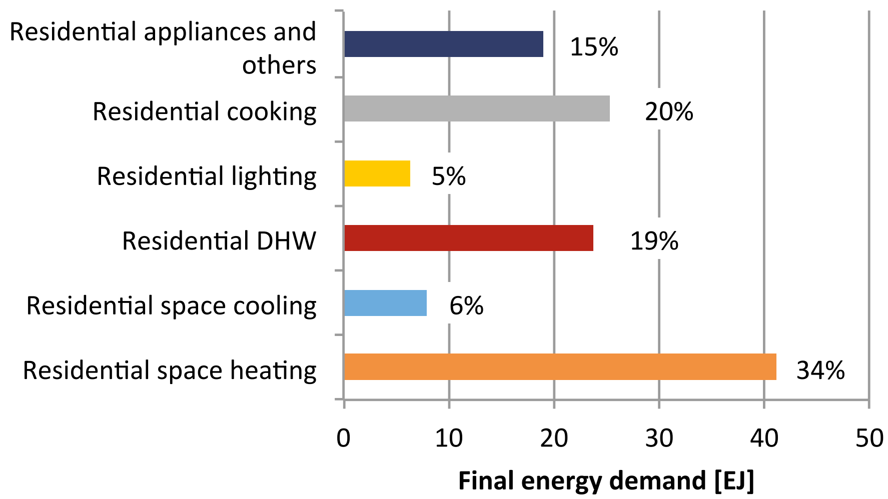

Fig 1.7. World final energy demand in buildings in 2017 (author's elaborations on [14])

In order to reduce the final energy uses, and coherently with directives and targets previously described, EU Commission issued some directives on energy efficiency in last 15 years, both in general terms [19,20] and specific for energy performance of buildings [21–23], known as Energy Performance of Buildings Directive (EPBD).

One of the tools identified by the EU commission to reduce energy uses in buildings is the nearly Zero-Energy Building (or nZEB) paradigm, defined in the EPBD Recast in 2010 as “a building that has a very high energy performance. The nearly zero or very low amount of energy required should be covered to a very significant extent by energy from renewable sources, including energy from renewable sources produced on-site or nearby” [22]. This definition is very generic and provides only with principles to follow for the design of an nZEB, since each Member States (MS) is responsible to set the quantitative limits for the renewable energy integration and the maximum energy consumption in national laws. According to this definition, the design of nZEBs should be mainly based on the reduction of energy consumption for air conditioning, through the rise of thermal resistance of the envelope and the adoption of passive strategies. In the EU Commission’s vision, the diffusion of low-energy buildings should improve the energy and carbon footprint of the building sector, mainly regarding the residential districts.

The EPBD Recast imposes to all new buildings from 31 December 2020 to be designed as nZEBs. Nevertheless, acting only on new buildings would not be very profitable, since about 35% of buildings in EU are over 50 years old, with many of them being inefficient and very few of them being renovated [16]. To remedy to this aspect, the newest version of EPBD explicitly promotes the renovation of buildings using more efficient systems and smart technologies [23,24]. In this way, the massive introduction of nZEBs in the European context should be a valid help for the reduction of primary energy demand and the fulfilment of the international targets and agreements, since nZEBs affect the energy system reducing energy consumption due to energy efficiency measures and increasing distributed renewable energy production.

Although EPBD, as well as most of the current policies, often focus on the reduction of operating energy in buildings, the research on low energy buildings has proven that the *embodied energy*, often disregarded in the past for its low value in traditional buildings, becomes a predominant term, or at least non-negligible, in this kind of building. In detail, the embodied energy is the energy required for the resources extraction, materials construction and demolition. The main reason of this feature is related to the adoption of additional materials with low thermal transmittance and technological components as renewables, which simultaneously decrease the net operating energy demand and increase the embodied energy of the whole construction.

Moreover, many literature case studies describe a phenomenon, referred to as *phase shifting*, where the interventions for the reduction of the use phase energy demand cause an embodied energy rising that nullify each effort [25]. This feature suggests that a holistic approach has to be adopted to effectively reduce energy consumption in the building sector. The adoption of this point of view is also briefly suggested in the newest EPBD, where it is recommended that “in their long-term renovation strategies, … Member States could … [consider] opportune moments in *the life cycle of a building* …for carrying out energy efficiency renovations.”

The designers of low-energy buildings and nZEBs often have to assess different solutions and perform many dynamic simulations of building performance to find the configuration with the lowest energy demand and to correctly design the components aimed at covering this demand (*e.g.* boilers, heat pumps, renewable energies). This is due to three main reasons:

- The availability of multiple energy efficiency solutions: designers have to take into account the huge series of commercial energy efficiency solutions on the market, related to both passive and active measures (*i.e.* envelope insulation, renewables, building automation technologies);

- The presence of conflicting measures: solutions that might produce benefits and disadvantages to the building at the same time. An example is the installation of large windows, whose installation may lower the electrical energy requirement for lighting but also increase the thermal transmittance of the building and the solar heat gains (positive in winter but negative in summer);

- The attainment of several objectives: each of the involved actors, as designers, Decision Makers (DM) and dwellers, want to obtain the optimum according to different points of view, *e.g.* minimum cost, maximum energy saving or maximum internal comfort, which can be conflicting objectives. When two or more goals have to be attained in the same building, the search of an optimal technical solution for a low-energy building becomes a Multi-Criteria or a Multi-Objective Optimisation (MOO) problem, characterized by constraints such as structural problems, legal obligations or cost-efficiency.

For the above reasons, researchers and designers often combine Building Performance Simulation (BPS) and mathematical optimisation techniques to identify the optimal combination of technical solutions for the building. When a dedicated software tool for the assessment of energy performance and an optimisation tool are combined, the approach is referred to as simulation-based optimisation. This approach links together different areas of knowledge that are distant from each other and can hardly be part of the cultural baggage of a single professional figure. This happens because the building design process is usually carried out by multi-disciplinary design teams being composed by figures as architects or civil engineers, responsible for aspects as the shape, spacing, and functions of a building, and mechanical engineers, who assess the energy efficiency through sensitivity analyses or optimisation techniques performed through appropriate tools.

Moreover, the European Commission also suggested the application of an optimisation approach, since EPBD guidelines require the nZEBs to be cost-optimal [26,27], where the cost-optimality should be assessed through the comparison of at least ten building variants, although ideally up to forty different configurations should be assessed and compared [28].

For what above, integrating the optimisation approach seems to fit perfectly in the described framework for the design nZEBs, and low energy buildings in general, since its employment allows comparing many alternatives without time-consuming operations. Furthermore, the problem of assessing the effects of conflicting measures can be overcome through a simulation-based approach. The optimisation should be used also to handle many decision criteria through a multi-objective approach. Furthermore, since the design of a building can be assessed according to many decision criteria, as the minimum cost or maximum comfort, a MOO should be carried out. Multi-objective optimisation is considered an effective technique to evaluate, design and identify the optimal compromise solutions since the objectives are usually conflicting. In detail, the results of a MOO study are sets of solutions being part of the Pareto front [29]. The evaluation criteria usually employed for nZEBs' performance assessment are diverse, usually regarding energy or economic savings or maximum thermal comfort.

1.2. Methods

This thesis illustrates the proposal of a methodological framework to assess and minimise life cycle impacts and costs related to buildings with a very high-energy performance. The method was conceived to be as generic as possible, in order to be applicable to the preliminary design of new buildings or refurbishments of existing ones. Furthermore, the method allows to analyse and optimise even clusters of buildings operated as a microgrid, to design and manage Heating, Ventilation and Air Conditioning (HVAC) plants and renewable energy systems (RES) in a coordinated way, thus improving energy efficiency and reducing the related environmental impacts.

More in detail, the research project is focused on the multi-objective optimisation of buildings' design and refurbishment adopting Life Cycle Assessment (LCA) energy and environmental indicators and economic aspects as objective functions. The LCA is a powerful methodology allowing for the holistic evaluation of the performance of a product or a service throughout its life cycle, according to the "cradle to grave" approach. In this way, starting from a preliminary building model, a multi-objective optimisation algorithm allows obtaining many retrofitting solutions that simultaneously minimise the Cumulative Energy Demand (CED), the Global Warming Potential (GWP), and the investment and operating costs related to the life cycle of the building, thus avoiding the phase shifting phenomenon.

A simulation-based optimisation was carried out for the single building optimisation, connecting a BPS or an energy rating tool to the optimisation software, adopting a different approach for each of these cases. In detail, a dual step approach was adopted in the first case, with the BPS employed for the optimisation of building's loads through interventions on the envelope, while an accurate simulation model developed in MATLAB environment was exploited to simulate and optimise the performance of HVAC, RES and storages. This approach was adopted to have a better control on the simulation models describing each component, also resembling the conventional approach to the design of a building, where architects and civil engineers are usually involved in the structural design while mechanical or industrial engineers are dedicated on equipment sizing. For the second case, since the energy rating is usually based on a monthly calculation, the output of this kind of method was not indicated for the optimal sizing of equipment, thus a unique optimisation was carried out in lieu of a dual step approach.

The buildings cluster optimisation, performed through a modified version of the MATLAB model developed for the single building equipment sizing, allows identifying the optimal combination of components, their sizes and their operating schedule in a unique optimisation, thus allowing to fulfil the energy demand of a district in a centralised way. This script is based on an energy hub model [30,31], an efficient mathematical formulation allowing to perform an optimisation of energy systems and microgrids through some simplifying assumptions that reduce the computational burden.

The envelope optimisation was performed through the multi-objective genetic algorithms NSGA II [32] or Omni-Optimizer [33], the former being one of the most popular and effective algorithms employed in the building sector [34] while the latter proved to have better performance in some applications. The energy hub model optimisation was based on the scalarization technique, involving the weighted and normalised sum of the objectives, and was solved through the Branch and Bound algorithm available in MATLAB for Mixed Integer Linear Programming (MILP) problems.

The study was developed using different software tools, summarized below:

- SketchUp Make 2017, a 3D modeller developed by Trimble that was used for the geometrical design of the building for some single building optimisations (the model may represent the existing building in the case of refurbishment or a preliminary shape in the case of design of a new building) and to develop an EnergyPlus input file;

- EnergyPlus v8.7.0, a dynamic building performance simulation software developed by the USA Department of Energy, that was used for the definition of thermal features on SketchUp preliminary models and the calculation of building's use phase energy requirement for some single building optimisations;

- Be18, an energy rating tool developed by the Danish Building Research Institute, that was used alternatively to SketchUp and EnergyPlus to model the building for the Danish single building optimisations case study;

- MOBO© (Multi Objective Building Optimization) Beta 0.3b developed at Aalto University, a building optimisation tool that was used to define the optimisation problem for the single building optimisations and was linked to EnergyPlus or Be18 to manage the optimisation process, evaluate the fitness of each solution and identify the best compromise solution between the objective functions;

- MATLAB, a programming platform where some scripts were developed containing cost and environmental impact data on RES and HVAC systems, allows identifying the size and the operation schedule of a set of components in order to satisfy the energy requirement of the building or the cluster of buildings.

The case studies included in this thesis are mainly aimed at proving the effectiveness of the methodology developed for the present project. The data collection phase was performed in different ways and with a different level of accuracy for each study, thus affecting the reliability of results. For this reason, the outcomes of the case studies should not be considered as a reference or guidelines for the actual design or renovation of buildings, although they comply with the common design practice. The main data sources employed for the case studies are summarized below:

- Environmental Product Declarations and literature papers for the specific impact factors of building envelope materials in Italian context;
- European reference Life Cycle Database (ELCD) for the specific impact factors of electricity and natural gas from public networks in Italian context;
- Companies pricelists and market reports for the cost data of building envelope materials, equipment and energy carriers in Italian context;
- Ökobau database, for the specific impact factors of building envelope materials, equipment and energy carriers in Danish context;
- Molio database, for the cost data of building envelope materials, equipment and energy carriers in the Danish context;
- Public reports from the main national grid operator and literature papers for the Vietnamese context.

The development of the methodology deriving from this PhD research project and some of the case studies are part of the research activities of IEA – Energy in Buildings and Communities Programme (EBC) Annex 72 "Assessing Life Cycle Related Environmental Impacts Caused by Buildings", that is focused on the assessment of the life cycle related environmental impacts caused by buildings. More in detail, this work was part of the Activity 3.3 of this Annex, where case studies on the life cycle energy and carbon performance of buildings are classified and compared to develop guidelines on optimal retrofit actions. Moreover, the method and some of the case studies were described in papers published on international journals and peer-reviewed conference proceedings.

1.3. Contributions

The present PhD project aims at include most of the building performance optimisation studies already present in literature in a larger methodological framework, where the most common approaches are considered as a part of a holistic and more comprehensive picture. The goal of this framework is the evaluation and minimisation of life cycle performance of the buildings or the building clusters. This kind of approach ambitiously aims at supporting the current international strategies in energy-saving and conservation in the building sector, also providing indications on the best materials and interventions to be adopted in refurbishments and thus whose employment should be promoted. The adoption of this method by the scientific community, the practitioners or the policymakers will allow the building sector to be energy-efficient, cost-effective and also less carbon-intensive.

The main research question here addressed involve the critical analysis and the illustration of the basic steps on how to properly carry out the optimisation of the performance of a building or a cluster of buildings, related to only one or more objective functions, and including the use phase or the whole life cycle performance, since the assessment of the use phase may be considered as a reduced LCA analysis.

From a methodological point of view, one important result of the study is that a preliminary comparison of the life cycle impact indicators should be performed, to avoid the selection of non-conflicting objectives in the optimisation studies. Although the results of the case study may be strongly influenced from site-specific aspects, the main results from the single building optimisations are that low carbon insulation materials as cellulose should be preferred to more impacting synthetic materials as expanded polystyrene (EPS), proving also to be cost-effective, that better thermal performance of windows should be preferred for North-oriented walls rather than in South ones, both in Mediterranean and Oceanic climates, and that the district heating technology should be preferred to more energy-efficient technologies like heat pumps or solar collectors in cold climates. The building clusters optimisation case studies proved that it is relatively easy to identify the compromise solution between the objective functions since the possible alternatives composing the Pareto front are limited, and that when large surfaces are available for solar technologies installation, the photovoltaic should be preferred to solar collectors in terms of embodied impacts, using the electricity combined with electric heaters to produce domestic hot water and to feed the heat pumps, although the economic criterion instead leads to the installation of solar collectors.

1.4. Thesis structure

This thesis is organised as follows. Chapter 2 presents the context and the background for the research developed in this thesis, providing an overview on the various areas of knowledge that were combined in this study, namely the life cycle assessment, the building physics and the optimisation techniques. Chapter 3 illustrates a review on literature studies about the performance optimisation of low energy buildings and a literature review on the optimisation of life cycle assessment of buildings. This section was necessary to identify a general framework for the existing studies, to detect existing research gaps and to develop the methodology for the present research project. Chapter 4 presents and discusses the main approach of the methodology, showing the mathematical model for single building and cluster of buildings optimisation, describing and discussing on the approaches, strengths and weaknesses and employed software tools. In order to demonstrate the feasibility of the methodology and to provide an indication of achievable benefits, some case studies developed in different climatic conditions are illustrated in Chapters 5 and 6, related to single building and cluster of buildings optimisation, respectively. Although the single building optimisation case studies shown in this work are related to the retrofitting of residential buildings only, the methodology can be also employed for non-residential applications and designs of new buildings. The main conclusions of the thesis are outlined in Chapter 7, together with recommendations for future research.

1.5. References

[1] United Nations. World Population Prospects 2019. Total population (both sexes combined) by region, subregion and country, annually for 1950-2100 (thousands) 2019. https://population.un.org/wpp/Download/Standard/Population (accessed September 3, 2019).

[2] British Petroleum (BP). Statistical Review of World Energy 2019. http://www.bp.com/statisticalreview (accessed September 26, 2019).

[3] National Oceanic and Atmospheric Administration. Carbon dioxide concentration in air measured on Mauna Loa laboratory 2019. https://www.esrl.noaa.gov/gmd/ccgg/trends (accessed September 4, 2019).

[4] National Oceanic and Atmospheric Administration. Average Global Land and Ocean Temperature Anomalies 2019. https://www.ncdc.noaa.gov/cag/global/time-series/globe/land_ocean/ytd/12/1880-2016 (accessed September 4, 2019).

[5] The Guardian. What is the Kyoto protocol and has it made any difference? n.d.

[6] United Nations. Sustainable Development Goals n.d. https://www.un.org/sustainabledevelopment/sustainable-development-goals/ (accessed September 26, 2019).

[7] Basosi R, Cellura M, Longo S, Parisi ML. Life Cycle Assessment of Energy Systems and Sustainable Energy Technologies: The Italian Experience. Springer Nature; 2018.

[8] European Commission. Communication 2008/30 - 20 20 by 2020 - Europe's climate change opportunity 2008.

[9] Eurostat. Tables on EU policy - Europe 2020 indicators 2019.

[10] European Commission. Communication 2018/773 - A Clean Planer for all. A European strategic long-term vision for a prosperous, modern, competitive and climate neutral economy 2018.

[11] European Commission. Clean energy for all Europeans. 2019.

[12] European Commission. Communication 2011/112 - A roadmap for moving to a competitive low carbon economy in 2050 2011.

[13] European Commission. A European Green Deal 2019. https://ec.europa.eu/info/strategy/priorities-2019-2024/european-green-deal_en.

[14] International Energy Agency (IEA), Global Alliance for Buildings and Construction (GlobalABC). 2018 Global Status Report. 2018.

[15] International Energy Agency (IEA). Transition to sustainable buildings: strategies and opportunities to 2050. 2013.

[16] European Union. Energy performance of buildings n.d. https://ec.europa.eu/energy/en/topics/energy-efficiency/buildings (accessed September 30, 2019).

[17] Eurostat. Complete energy balance 2019 edition 2019. https://ec.europa.eu/eurostat/web/energy/data/energy-balances (accessed September 30, 2019).

[18] International Energy Agency (IEA). The Future of Cooling. Opportunities for energy efficient air conditioning. 2018.

[19] European Parliament And Council. Directive 2012/27/EU of 25 October 2012 on energy efficiency, amending Directives 2009/125/EC and 2010/30/EU and repealing Directives 2004/8/EC and 2006/32/EC. 2012.

[20] European Parliament And Council. Directive (EU) 2018/2002 of 11 December 2018 amending Directive 2012/27/EU on energy efficiency. 2018.

[21] European Parliament And Council. Directive 2002/91/EC of 16 December 2002 on the energy performance of buildings. 2003.

[22] European Parliament And Council. Directive 2010/31/EU of 19 May 2010 on the energy performance of buildings (recast). 2010.

[23] European Parliament and Council. Directive (EU) 2018/844 of 30 May 2018 amending Directive 2010/31/EU on the energy performance of buildings and Directive 2012/27/EU on energy efficiency. 2018.

[24] European Commission. Commission Recommendation (EU) 2019/786 of 8 May 2019 on building renovation 2019.

[25] Beccali M, Cellura M, Fontana M, Longo S, Mistretta M. Energy retrofit of a single-family house: Life cycle net energy saving and environmental benefits. Renew Sustain Energy Rev 2013;27:283–93. doi:10.1016/j.rser.2013.05.040.

[26] European Commission. Commission Delegated Regulation (EU) No 244/2012 of 16 January 2012 supplementing Directive 2010/31/EU of European Parliament and of the Council. 2012.

[27] European Commission. Guidelines accompanying Commission Delegated Regulation (EU) No 244/2012 of 16 January 2012 supplementing Directive 2010/31/EU of the European Parliament and of the Council. 2012.

[28] Thomsen KE, Wittchen KB. Energy performance requirements using cost-

optimal levels. Overview and outcomes. In: Maldonado E, editor. Implement. Energy Perform. Build. Dir. Featur. Ctry. reports, 2015, p. 41–56.

[29] Harkouss F. Optimal design of net zero energy buildings under different climates. PhD Thesis - Université Côte d'Azur, 2018.

[30] Geidl M. Integrated Modeling and Optimization of Multi-Carrier Energy Systems. PhD Thesis - Swiss Federal Institute of Technology (ETH), Zurich, 2007. doi:10.3929/ethz-a-005377890.

[31] Geidl M, Andersson G. Optimal Power Flow of Multiple Energy Carriers. IEEE Trans Power Syst 2007;22.

[32] Deb K, Pratab S, Agarwal S, Meyarivan T. A Fast and Elitist Multiobjective Genetic Algorithm: NGSA-II. IEEE Trans Evol Comput 2002;6:182–97. doi:10.1109/4235.996017.

[33] Deb K, Tiwari S. Omni-optimizer: A Procedure for Single and Multi-objective Optimization. In: Coello Coello CA, Hernández Aguirre A, Zitzler E, editors. Int. Conf. Evol. Multi-Criterion Optim. EMO 2005, Berlin, Heidelberg: Springer; 2005, p. 47–61.

[34] Longo S, Montana F, Riva Sanseverino E. A review on optimization and cost-optimal methodologies in low-energy buildings design and environmental considerations. Sustain Cities Soc 2019;45:87–104.

Chapter Two – Background

2.1. Background on Life Cycle Assessment

In the last decades, policymakers and industries paid higher attention to environment-related issues with respect to the beginning of the Third Industrial Revolution. In detail, an increased interest was dedicated to methods to assess and reduce the potential impacts related to processes and products. One of the main issues to be deepened was the waste disposal and recycle. In this view, a focus on the whole life cycle of the products was quickly developed. The Life Cycle Assessment (LCA) is a widely used methodology that allows assessing the potential environmental impacts of products and processes throughout their life cycle. The life cycle can be schematised as the sequence of the following phases: raw material extraction/acquisition, production, use, end-of-life. The popularity of this methodology lies on its rigorousness, being based on mass and energy balances, and on the flexibility, allowing the analysis of a process with higher or lower detail depending on the availability of data. The application of this method allows identifying the main sub-processes to be analysed and improved to reduce the impacts.

The first example of an LCA study dates back to 1969, when the Midwest Research Institute (MRI) performed a comparison among different beverage containers for the Coca Cola Company. The conceptualisation of the basics of the method occurred in the subsequent few decades, with diverging approaches, terminologies, and results, and only in the 1990s a standardisation process started [1]. Nowadays, the procedure to properly perform an LCA study is standardised by ISO inside the ISO 14000 family, focused on the environmental management. In detail, the main standards are ISO 14040:2006 [2], dedicated to the principles and the framework of the methodology, and ISO 14044:2006 [3], describing the requirements and providing guidelines. According to the standards, an LCA study is composed of four stages, each one interacting with others:

1. Goal and scope definition;
2. Inventory analysis;
3. Impact assessment;
4. Results interpretation.

The scope, the boundary and the level of detail of an LCA depend on the aim and the intended use of the study. Nevertheless, although the deepness and the amplitude of the included details may vary from one analysis to another, the generic framework to be used is the same. During the first stage, the analyst should define the *functional unit*, which defines precisely the product or process that is studied in that analysis. All the input and output process flows are referred to the functional unit, and its definition is necessary to compare many studies on the same basis [4].

The philosophy behind the application of the LCA is known as Life Cycle Thinking. In the last years, three main "dimensions" of the Life Cycle Thinking have been developed, according to the three dimensions of the sustainable development:

- Environmental dimension: Life Cycle Assessment;
- Economic dimension: Life Cycle Costing (LCC);
- Social dimension: Social Life Cycle Assessment.

The level of accuracy of an LCA study depends on which method is chosen. In detail, three families of impact assessment methods can be listed: process-based analysis, input-output analysis or hybrid analysis. The process-based analysis method is a bottom-up technique based on the analysis of energy and mass flows of the specific case study. It is considered to be the easiest one, but it is also seen to have major limitations, mainly related to system boundary incompleteness because, when a specific boundary is set up, many input flows are neglected during the quantification of inputs to a product or process [5]. The level of incompleteness varies with the type of product or process and depth of study and can reach up to 50% or more [6]. A higher level of detail is provided by the input-output analysis methods, a top-down statistical technique based on financial transactions, which is systemically complete [5]. This method involves the use of aggregate data on how much each sector of the economy contributes to an environmental impact and how much each sector purchases from other sectors. This analysis method allows evaluating the interactions between economic sectors in long product chains, that are common in a linked economic system [7]. For example, building an automobile requires steel components that are made through machinery in other factories made up of steel, and so on. Nevertheless, it is hard to find representative data on each economic sector of each country, and the aggregation of all the products in a specific sector in a unique impact intensity may be an inaccurate hypothesis [5]. The hybrid analysis methods try to combine the best aspects of both the previous methods, using process data when available and filling the gaps with data from input-output methods in order to assess the whole supply chain of a product [5].

The strategic importance of the adoption of the LCA method in research and industrial fields as a scientific basis to account for the environmental impacts has gained a large popularity at international level. For example, LCA is proposed as a tool to support decisions in many EU calls for research funding, and it is mandatory to adopt the LCA method for some products labelling systems as EU Ecolabel. An interesting application in the industrial field are the Environmental Product Declarations (EPD), public reports based on ISO 14025 [8] and EN 15804 [9] standards that are developed by companies to improve their efforts in sustainability, to understand how to attain some goals, and to demonstrate their attention to the environment-related issues to their customers [10].

In the development of an LCA, a compromise between rigorousness and clarity should be inevitably found, in order to give useful information to the audience. For this reason, the results of an LCA are expressed through impact indicators describing a specific phenomenon, which may be further synthesised in indexes to avoid that an unskilled reader might misunderstand the results, although a synthetic index gives less information than the indicators making it up. A balance between clarity and readability should thus be found. In LCA literature studies, many indicators are employed to assess the energy and environmental performance. The most important indicators used in the building sector are:

- The Global Warming Potential (GWP) indicates how much heat a greenhouse gas traps in the lower atmosphere. It is calculated over a specific time interval, commonly 20, 100 or 500 years. The most common substances related to this effect are the carbon dioxide, the methane and the nitrogen protoxide. It is referred to the equivalent mass of carbon dioxide producing the same effect [11];
- The Ozone Depletion Potential (ODP) indicates how much the ozone layer in the stratosphere is reduced by the emission of a substance, increasing the ultraviolet radiations in the atmosphere. The chlorofluorocarbons are the main responsible for this effect. It is referred to the equivalent mass of trichlorofluoromethane producing the same effect;
- The Acidification Potential (AP) expresses the possibility to produce acid emissions or to acidify lands and water. One of the effects is to provoke acid rains, thus reducing the pH of the atmospheric water introducing H^+ ions. The most common substances related to this effect are the sulphur and nitrogen oxides and the ammonia. It is referred to the equivalent mass of sulphur dioxide producing the same effect;
- The Photochemical Ozone Creation Potential (POCP) expresses the airborne substances' potential for forming atmospheric oxidants at ground level as ozone. This effect is mainly due to the presence of volatile organic compounds. It is referred to the equivalent mass of ethene producing the same effect;
- The Eutrophication Potential (EP) indicates the reduction in oxygen contained in the waters as a consequence of increased nutrients in the water. This effect derives from the excessive growth of algae and plants, disturbing the balance between species It is referred to the equivalent mass of phosphorus tetroxide producing the same effect;
- The Abiotic Depletion Potential (ADP) expresses the consumption of limited mineral resources being non-renewable. It is referred to the equivalent mass of antimony producing the same effect;
- The primary energy demand may be assessed through the Cumulative Energy Demand (CED) or the Gross Energy Requirement (GER), which are usually synonyms.

As every technique, LCA necessarily has some limitation to be taken into account in its use. The main issues, that are nevertheless common to other assessment techniques (*e.g.* environmental impact assessment), is provided here:

- Being based on a physical model, a LCA study is a simplified representation of the reality, preventing a complete description of the effects on the environment;
- The accuracy of the analysis is limited by the availability of high-quality information and data;

- The models used for the inventory or to assess the environmental impacts are limited by their founding assumptions;
- Results deriving from a specific study should not be extended to a wider framework as they are. For example, the results of one region cannot be related to the whole country;
- The analysis may be affected by the subjectivity of the analyst, introducing some effect related to his beliefs or bias.

Focusing on buildings and building materials, a specific LCA methodology framework exists for the evaluation of energy and environmental performance. This methodology is illustrated in the EN 15978:2011 European standard [12]. This standard specifies the method to assess the environmental performance of a building according to the LCA approach and provides the correct means for the reporting and the communication of the outcomes. EN 15978 standard suggests rationalising the results to the *functional equivalent*, namely a representation of the required technical characteristics and functionalities of the building. Furthermore, the standard specifies the life cycle stages and boundaries of the study, dividing the life cycle of the building in product fabrication and construction (A modules), use (B modules), end of life (C modules) and benefits (D modules). The detail on the modules is specified in Table 2.1.

Table 2.1. Building life cycle stages according to EN 15978:2011 [12]

Product fabrication stage			**Building construction process stage**		**Use stage**							**End of life stage**			
Raw material supply	Transport	Manufacturing	Transport	Construction-installation process	Use	Maintenance	Repair	Replacement	Refurbishment	Operational energy use	Operational water use	Deconstruction, demolition	Transport	Waste processing	Disposal
A1	A2	A3	A4	A5	B1	B2	B3	B4	B5	B6	B7	C1	C2	C3	C4

Regarding the modules describing the life cycle of buildings, the impacts may be split between embodied and operating terms. Although there is not a fixed definition in literature, the embodied terms may be related to the fabrication of the materials, the building construction and the end of life, thus including A and C modules, while the operating term should incorporate the B module. For example, the embodied energy is the sum of primary energy used for raw materials' extraction, transportation, final component production, building construction and end-of-life [13,14]. Although the embodied energy term is often neglected in ordinary buildings, the development of low-energy buildings or net zero-energy buildings gave rise to the investigation of this term, because it becomes predominant compared to the operational term since the latter is very low or null in these structures.

Regarding the LCC, this is a cost accounting method taking into account the cost or cash flows of all the main phases in the life of a product or service, *i.e.* relevant costs (and income and externalities if included in the agreed scope) arising from acquisition through operation to disposal. An LCC analysis typically includes a comparison between some alternatives or an estimate of the future costs agreed throughout the analysis. Concerning the limits of the generic LCA method, an additional element of uncertainty exists in LCC studies, related to the prediction of average interest and inflation rates throughout the period of analysis.

The LCC of studies involving buildings or their parts was standardised at international level by the ISO 15686-5:2017 [15]. Another international standard, the EN 15459 [16], was emitted at European level in the set of standards supporting the EPBD and regulating the energy renovation of buildings. EN 15459 standard introduced the concept of the global cost of a building as shown in Eq. (2.1). It is defined as the sum of the initial investment cost (C_I), the annual cost at the year i due to the j-th component ($C_{a,i}(j)$) (sum of energy supply, running and replacement costs), and the final value of the component ($V_{f,\tau}(j)$), whether the expected lifetime of the building is longer than the reference period considered in the analysis. The annual terms are actualised with the discount rate $R_d(i)$.

$$C_G(\tau) = C_I + \sum_j \left\{ \sum_{i=1}^{\tau} \left[C_{a,i}(j) \cdot R_d(i) \right] - V_{f,\tau}(j) \right\} \tag{2.1}$$

This set of terms is quite similar to the cost categorisation systems usually adopted for the LCC. This methodology was explicitly mentioned in the EU's legislative framework since the EPBD Recast introduced the concept of nZEB. In detail, in order to make the nZEBs diffusion more appealing for the building sector, the accompanying notes to EPBD Recast [17] stated that nZEBs should be designed according to the cost-optimal methodology, calculating the global cost of several building alternatives and then selecting the one with best Net Present Value (NPV).

2.2. Background on building physics and low-energy buildings

The building physics is the branch of science applying the principles of thermodynamics and heat transfer to the built environment. Taking into account the heat generation and heat and mass transfer mechanisms between the indoor and the outdoor environment through the building envelope, building physics allows assessing the energy performance of a building. The results of the building physics are employed to design HVAC systems, to identify and contrast the main thermal losses, increasing the energy efficiency in the building sector and reducing its fossil fuel dependence, or to rate the building performance in standard conditions.

The driving force behind the application of building physics is to guarantee the thermal comfort to the occupants, keeping the indoor conditions inside a determined range defined as the *comfort zone*. The main quantities influencing the thermal comfort are related to environmental conditions (air temperature, air relative humidity, air velocity, and air mean radiant temperature) and to personal factors (thermal resistance of clothes and metabolic rate) [18,19].

2.2.1. Basic building physics considerations

The study of the thermal performance of buildings may be investigated adopting different mathematical models available in the literature, each of them having different accuracy levels and applications. For example, the design of heating systems is usually performed fixing constant indoor and outdoor temperatures and calculating the thermal power flowing from the building to the environment in steady-state conditions [20]. This calculation is simplified neglecting the influence of solar radiation and internal gains, thus slightly oversizing the equipment [21]. For the design of cooling equipment, on the opposite, all the heating sources are to be modelled in transient conditions, usually identifying a design day with maximum load and simulating the hourly distribution of the heat gains. The transient conditions introduce a further complexity in the calculations given by the heat capacity of the envelope, causing a delay between the instantaneous heat gains from the outdoor, *e.g.* the solar radiation, and the effective cooling load to be removed. A visual example of the difference between the instantaneous heat gain and the actual cooling load is provided in Fig. 2.1. Higher values of the heat capacity of the structure cause a reduction in the heat wave peak and an increase of the time delay (Fig. 2.2), and a correct design of massive structures should necessarily take into account for these aspects to implement energy-saving and passive techniques, avoiding the oversizing of the equipment. For example, a time delay of six or eight hours between the solar peak occurring at noon and the actual cooling load might be a very effective energy saving strategy because in this way the heat removal can be performed by opening the windows, since at late evening the outdoor air temperature is usually lower than the indoor conditions.

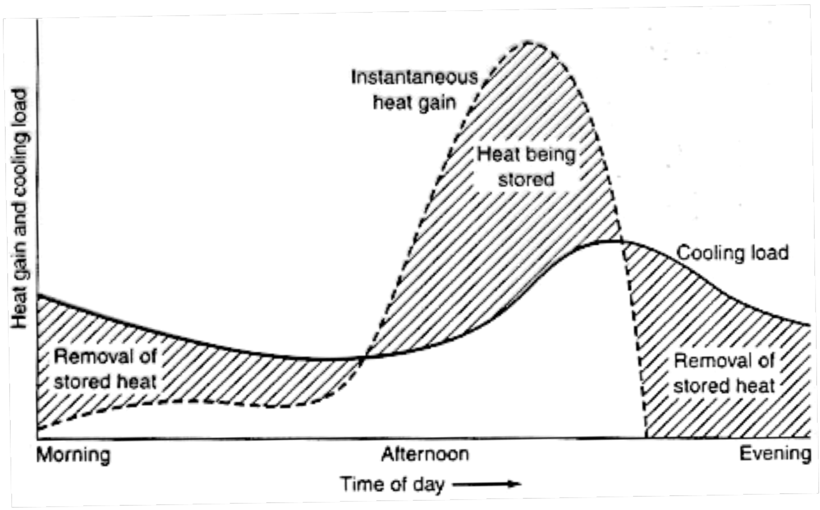

Fig. 2.1. Difference between instantaneous heat gain and actual cooling load in a massive building (adapted from [22]*)*

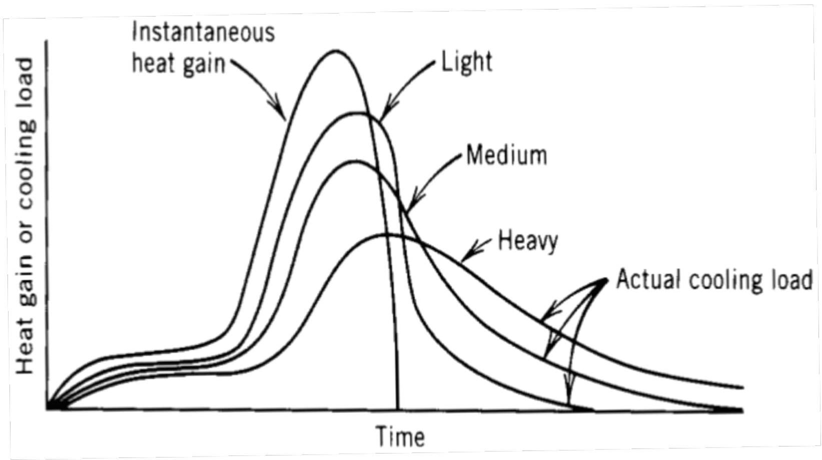

Fig. 2.2. Different actual cooling load in three buildings with different heat capacity corresponding to the same instantaneous heat gain (adapted from [22]*)*

These basic building physics considerations make evident that designers should spend more efforts to properly design a building in cooling dominated climates according to energy saving criteria.

In order to identify the set of parameters that mainly influence the thermal behaviour of a building, it is possible to refer to a generic solid body with any shape and material. If this body has a different temperature with respect to its surroundings, the temperature will change according to the laws describing the three main heat transfer mechanisms, in general terms. Furthermore, the body may also experience an internal heat generation. Applying the law of conservation of energy to this body, the mathematical description of the evolution of the temperature with the time can be easily obtained.

Although an accurate description of the terms of this equation is out of the scope of this chapter, since it might be found in any heat transfer textbook, it is important to describe the two physical quantities resulting from this analysis and that are recurrent in building physics: the thermal diffusivity α, shown in Eq. (2.2), and the surface-to-volume ratio.

$$\alpha = \frac{\lambda}{\rho \cdot c} \tag{2.2}$$

In this equation, λ is the thermal conductivity, ρ is the density and c is the specific heat capacity. The thermal diffusivity is always taken into account in thermal transient applications since this parameter physically represents the ratio between the heat flowing through the body and the heat stored into the body. Massive materials, *i.e.* substances with low diffusivity, are to be preferred for the envelope of buildings in cooling dominated climates since they are able to temporally shift the heat gain and to reduce the entity of the cooling load. In detail, the heat wave penetration depth, that is the depth of material (wall, roof) where the intensity of the heat wave is reduced to $1/e \cong 37\%$, where e is the Napier constant, is directly influenced by the thermal diffusivity.

The surface-to-volume ratio, or shape factor, is another useful quantity in this subject. In detail, for a given volume, the higher is the external surface of the building and the higher the heat exchange will be. Thus, this ratio has to be kept as low as possible, in order to reduce the rated size of HVAC and to improve the indoor thermal comfort. In order to suggest the importance of this term, Danielski identified a linear relationship between the annual energy use and the shape factor [23]. Moreover, the energy-saving policies and the national regulations in some countries explicitly categorise buildings according to this ratio [24,25].

The phenomena occurring in building heat transfer with transient conditions are among the main causes of non-linearity in this kind of studies. For this reason, simplified calculation methods bring to approximations that neglect these aspects, making dynamic methods more accurate and reliable, although some corrective factor may be introduced in steady-state calculations.

2.2.2. Building performance simulation

Focusing the attention on the assessment of the energy performance of buildings, different methods are available in the literature. An overview of the most commonly used methods, both currently and in the past, might be found in [26,27]. Since the energy demand and the environmental impacts related to the operation of the building sector became a pressing issue in developed countries, many software tools were developed for various applications as the energy efficiency rating or research applications. Nowadays, thermal simulation of buildings became a routine procedure in both research and design fields, even because of the growing computational capacity of personal computers.

The building energy simulation started being investigated in the '60s, and in about 20 years were developed the foundation theory behind the heat transfer and the main criteria and algorithms for the prediction of heating and cooling loads. For example, in this period, the Total Equivalent Temperature Differential Method and the Z Transfer Function Method were invented and developed. Although these methods were widely used by designers for decades, modern methods based on fewer simplifications and reducing the required calculations at the same time are available now. For example, the Radiant Time Series (RTS) method was developed to offer a rigorous approach without requiring iterative calculations. This method is suitable for peak design cooling load calculations, but its simplifications prevent its employment for annual energy simulations [27].

A more detailed version of the RTS method is the Heat Balance (HB) method, one of the most recent and employed methods available, combining both rigorousness and avoidance of physical and numerical assumptions. As the name suggests, this algorithm is based on the energy balance of the thermal contributions to each envelope component and on each thermal zone, namely rooms or sets of rooms whose temperature may be considered uniform, having the same heating system and the same set-point temperature. Starting from the outdoor face, an energy balance is evaluated considering the absorbed solar radiation, the convection with the air and the long-wave radiations. The convection heat transfer between the outdoor and indoor faces of the surface is calculated, and then another balance is evaluated on the indoor face, considering the convection and radiation with the indoor air and the internal equipment. The indoor air is considered as being well mixed, thus having a uniform temperature, and is modelled as an additional surface [27]. This process is repeated for each surface and each thermal zone. A visual illustration of the contributions considered for the heat balance in this method is provided in Fig. 2.3, where front wall and window and the air thermal mass are not shown. The output of the method is the hourly average temperature of the air and of each surface of each thermal zone.

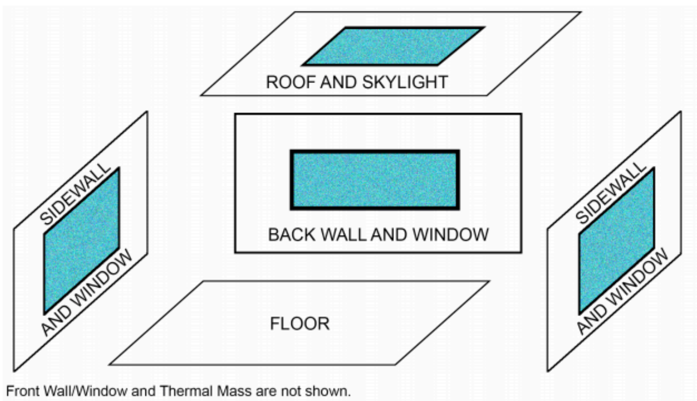

Fig. 2.3. Schematic of the heating and cooling contributions considered in the Heat Balance Method [27]

Software tools implementing these algorithms to simulate the thermal performance of buildings are collectively known as Building Performance Simulation (BPS) tools. The growing number of available solutions pushed the US Department of Energy to create a web resource, the Building Energy Software Tools Directory, collecting main features of commercial BPS. The resource is now managed by IBPSA-USA and describes more than 200 entries. EnergyPlus and TRNSYS are probably the most commonly used BPS tools, both in research and advanced design applications, and are based on the Conduction Transfer Function method [28][29]. Since BPS tools are based on standard meteorological input data and simplified assumptions of the heat exchange model, in many cases it is not possible to obtain the exact energy use of the building operation from the simulation. Therefore, the model should be fine-tuned to the energy being used by the buildings using information from energy bills, monitoring devices or surveys among the residents [30].

2.2.3. International regulatory framework

The calculation methods for the evaluation of buildings energy performance are standardized at the international level to make the energy-saving in buildings uniform. Until 2017, the international standard ISO 13790:2008 was the reference for energy calculation in buildings, providing guidelines for the design or the energy rating. The standard describes a quasi-steady-state method, based on monthly energy balances, and a simple hourly method, providing tips also on a detailed dynamic simulation procedure. The quasi-steady-state method owes its name to the steady-state balances that are evaluated in each month, but the variability between one month and the others makes it sufficiently representative of the standard year. In this way, the method allows evaluating the different space heating and cooling needs due to season variations but neglects the transient effects typical of cooling dominated climates, that are taken into account through correction factors [31]. Although these factors may cause excessive underestimations of the cooling loads, this approach has shown an optimal balance between accuracy and computational burden for heating-dominated climates [32].

The ISO 13790:2008 standard was explicitly mentioned in the European guidelines for the application of EPBD as the method to be followed for the energy rating of buildings in the member states so that many software tools based on this standard were developed to calculate the buildings energy performance according to each country's rules. This standard was replaced by ISO 52016-1:2017 [33], being part of a set of about 90 standards related to the building energy performance. The important innovation contained in this standard is the introduction of a detailed hourly-based dynamic assessment of building energy performance, provided with a monthly-based calculation method similar to the model already available in ISO 13790:2008.

2.2.4. Low-energy and zero-energy buildings

As shown in Chapter 1, the building sector is responsible for a large share of the energy demand and emissions of the developed countries. The increasing attention on energy saving and conservation pushed designers and researchers to develop techniques to improve the efficiency of buildings and reducing their operating energy demand. Depending on the specific target of each study, different definitions were invented to describe the building categories. Some examples are *low-energy buildings*, whose may be considered as the most similar to nZEBs, and *plus-energy buildings*, namely buildings generating more energy than their requirement through local renewable generation, mainly relying on photovoltaic (PV) systems or small wind turbines.

Another common definition of high performing building is the *Net Zero Energy Building* (NZEB). According to the most common definition, a NZEB is a building exchanging energy with the surrounding grids, realizing an annual zero balance between exported and delivered energy [34]. In some applications, the zero balance was also set monthly [35]. The energy balance may be evaluated considering the building as a black box, thus assessing only the energy import and export, or analysing the local balance between local loads and generation [34], as in Eqn. (2.3):

Import-Export balance for NZEBs *Load-Generation balance for NZEBs*

$$\sum_{t=t_1}^{t_2}\left[\sum_{k=k_1}^{k_2}\left(I_k \cdot w_{i,k}\right)-\sum_{j=j_1}^{j_2}\left(E_j \cdot w_{e,j}\right)\right] \leq 0 \qquad \sum_{t=t_1}^{t_2}\left[\sum_{k=k_1}^{k_2}\left(L_k \cdot w_{l,k}\right)-\sum_{j=j_1}^{j_2}\left(G_j \cdot w_{g,j}\right)\right] \leq 0 \qquad (2.3)$$

where G_j are the building generation flows, L_k the building loads, E_j the building exports, I_k the building imports and w indicate weighing factors, adopted to make homogeneous the energy quantities. The use of weights allows expressing the balance in primary or final energy terms, using conventional conversion factors, or in different quantities as costs or emissions. A further categorisation exists according to the boundary adopted for the evaluation of the building's energy balance, as the local generation may be installed on the building or nearby, or even be just related to the national grid mix share (this is the case of Danish regulation [36]). A description of the different boundaries was schematised by Marszal et al. [37] as in Fig. 2.4.

Although a widespread number of definitions currently coexist, the approach to the design of a high performing building should always be based on the following rules [38]:

- Minimising the building's thermal loads, through the reduction of the envelope transmittance;
- Employing passive energy techniques, through the removal of a part of the thermal loads' exploiting natural phenomena;
- Implementing efficient technical systems, as radiant floors or, in general, low-temperature heating and high-temperature cooling systems;
- Adopting RES technologies to cover a (generally) high share of the remaining thermal and electrical loads.

This set of actions was effectively synthesised by Sartori et al. with specific reference to NZEBs [37], as in Fig. 2.5.

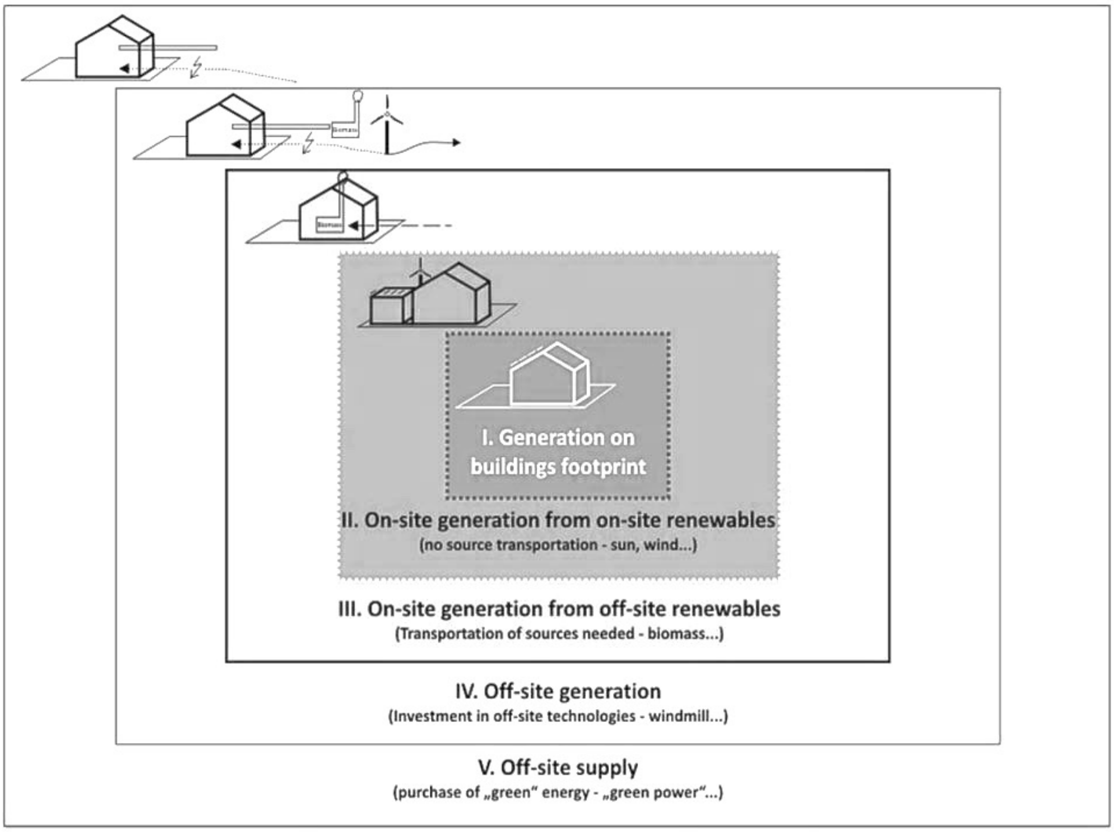

Fig. 2.4. Different definitions of boundaries for NZEBs [37]

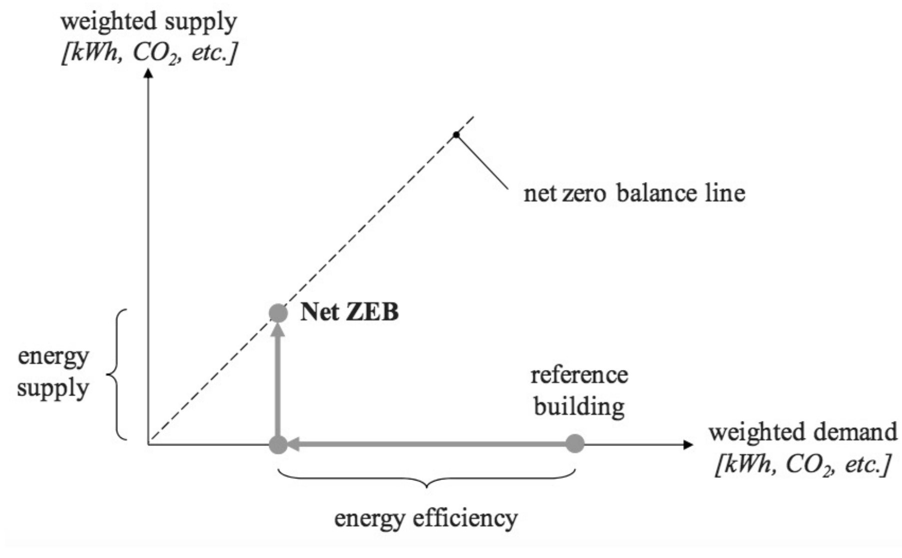

Fig. 2.5. Main actions to reach the NZEB level [37]

Since the embodied energy becomes an important contribution to the life cycle primary energy demand of nZEBs or NZEBs, some tentative to extend the above-mentioned criteria including a life cycle thinking approach were done. A first approach available in the literature was proposed by Cellura *et al.* with specific reference to NZEBs and plus-energy buildings [39], proposing a relation that can be considered as a more detailed and exploitable form of Eq. (2.3), including three additional terms in the Import-Export balance. In detail, the annualized initial embodied energy $EE_{i,a}$, the annualized recurring embodied energy $EE_{r,a}$ and the annualized demolition energy DE_a were included, as in Eq. (2.4):

$$\sum_{t=t_1}^{t_2}\left[\sum_{j=j_1}^{j_2}\left(E_j \cdot w_{e,j}\right)-\sum_{k=k_1}^{k_2}\left(I_k \cdot w_{i,k}\right)\right]-\left(EE_{i,a}+EE_{r,a}+DE_a\right)\geq 0 \qquad (2.4)$$

Another interesting approach was proposed by Hernandez and Kenny in a series of papers [40–42], defining and exploring the concept of *Life Cycle Zero-Energy Building (LC-ZEB)*. This is a refurbished building producing (exporting) enough energy during its life cycle to compensate the embodied energy increase undergone during the renovation. A clear understanding of the effort to be spent to build a LC-ZEB was depicted by the authors as in Fig. 2.6. In detail, in the authors' view, the energy balance in a LC-ZEB is composed setting to zero the *Annualized Life Cycle Energy*, namely the sum of annualized primary embodied energy and annual primary energy use.

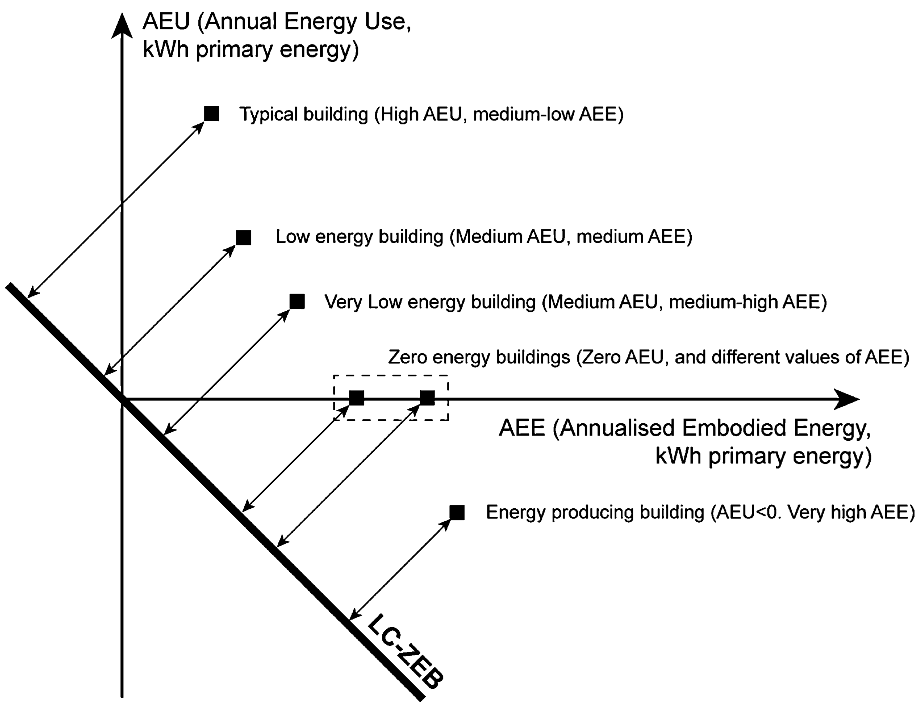

Fig. 2.6. Distance between common categories of buildings and the LC-ZEB target [42]

A further proposal was made by the Norwegian Research Centre on Zero Emission Buildings in [37,43]. The authors measure the energy balance using the greenhouse gas equivalent emissions factors as weights, defining the Zero Emission Building (ZEB). With specific reference to the modules defined in the EN 15978:2011 European standard, various ZEB levels were defined, as shown in Fig. 2.7, starting from the operation of the technical equipment (O EQ), and going to the whole operating emissions (O), the operating and embodied emissions (OM), also including the construction and installation stages (COM) and, finally, including the end of life (COME). Although these ideas are very interesting and they might make the reader suppose that a great interest in the topic is growing, further work is still necessary to make these concepts and criteria be adopted by the construction companies.

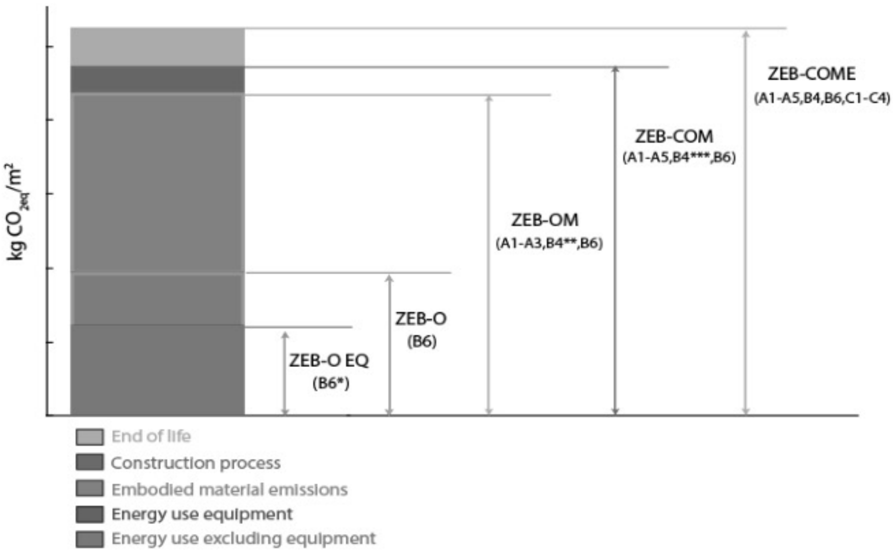

Fig. 2.7. Various levels of Zero Emission Building [44]

2.3. Background on optimisation techniques

2.3.1. Mathematical theory

In general terms, mathematical programming or optimisation is the branch of applied mathematics aimed at developing methods to find maximum and minimum points of an Objective Function (OF) by changing the values assumed by the independent variables. Although in generic mathematical programming this may not be a strict rule, the variables are usually subject to physical bounds and constraints in most of the engineering optimisation problems. For example, with specific reference to buildings, the annual energy demand may be subject to an upper bound due to legal requirements, while the available rooftop surface may limit the installation of PV systems. The difference between bounds and constraints is that each variable has a lower and an upper bound on its own, but the values of some variables of the problem may be confined by equality and inequality constraints, identifying the feasibility space. For example, the available surface to install PV system may be bound between zero and the rooftop surface, but, in the case of installation of other systems in the same area (solar thermal collectors, rooftop air handling units), a constraint should be included in the problem linking the necessary surface for each kind of system to the maximum available.

Multiple categories of optimisation problems and algorithms can be listed. Depending on the variables and on the OF's analytical representation, optimisation problems can be classified as linear or non-linear, integer or real, convex or non-convex, and different algorithms are available for each kind of problem. Linear problems with real variables are the easiest to analyse, and analytical (or deterministic) algorithms are available, as the simplex algorithm. For non-linear problems, the interior-point or the Lagrange multipliers methods are available. The higher complexity behind the latter category of algorithms is due to the multiple maxima or minima characterising non-linear functions, that might mislead the algorithm in the identification of the true optimum. For this reason, non-linear functions have many local optima but only one global or absolute optimum value [45].

Further complexity may be introduced when the mathematical functions describing the problem have discontinuities, as may be the case of variables with integer values. Although integer problems may be solved with dedicated techniques, problems composed by both real and integer variables, named Mixed Integer Linear Programming (MILP), are more complex to face, since the discontinuities usually prevent the calculation of the function derivatives. The classical algorithm employed for the solution of MILP problems is the *Branch and Bound* algorithm, based on the generation of every possible combination of variables. For this reason, it is a slow algorithm. Broadly speaking, this algorithm is based on the following steps:

1. The algorithm solves the linear relaxation of the original MILP problem, for example using the simplex algorithm, that is considered as the lower bound of the true problem;
2. Based on the solution of the linear relaxation, the algorithm generates a set of additional optimisation problems where constraints are added to the linear relaxation;
3. This sequence of additional optimisation problems is used by the algorithm to establish some lower and upper bounds to the optimal value of the objective function of the original MILP problem;
4. The lower bound continuously increases and the upper bound decreases, until the optimal solution is found.

Because of this long series of steps, the adoption of a deterministic method is often omitted in these cases, preferring heuristic approaches. Although the true behaviour of the real-world phenomena is always non-linear, the adoption of simplifications in optimisation studies is very common, with the aim to identify quickly the absolute optimal value of the simplified problem and to verify its optimality in a more complex simulation model [45].

The number of OFs included in an optimisation problem is used to distinguish between Single-Objective Optimisation (SOO) and Multi-Objective Optimisation (MOO) problems. In detail, in SOO problems, the OF typically has only one optimum value and only one best solution exists (or none, eventually). On the opposite, the solution of a MOO problem is a vector of decision variables simultaneously satisfying the constraints and optimising a vector function whose elements represent the OFs. These functions create a mathematical description of the performance criteria, which usually conflict with each other so that minimising each OF separately would give a different solution. In detail, optimising a single OF would give the absolute optimal value of the problem according to the selected criterion without taking into account for the remaining OFs, while the solutions obtained from the multi-objective optimisation algorithm attaining the best value of a single objective function at a time are known as *extreme solutions*. They are thus compromise solutions from the MOO algorithm that should not be confused with the absolute minima of a single function in the search space. For this reason, the solution of a MOO problem is a set of trade-off solutions that are considered equally optimal if no preference is expressed, *i.e.* it may happen that solution A outperforms solution B according to one OF but B is better than A according to another one. Thus, since these two solutions are equally optimal if no preference is included among the optimisation criteria, the output of a MOO problem is a set of equally optimal compromise solutions, called Pareto front [46]. In detail, the Pareto front is made up by a set of solutions that outperform or are equal to all the other solutions for all the criteria, while strictly outperform all the other solutions for at least one criterion. The solutions in the Pareto front are thus a set of compromise solutions, characterized by very low values of each objective function, although not as low as the true minimum. This condition is known as the dominance of the solutions and a solution dominates the others when this condition occurs. To easily understand the concept of dominance, Fig. 2.8 shows the typical trend of a two-dimensional Pareto front. Depending on the features of a problem, this trend may not occur in MOO problems with three or more objectives.

The analysis of a MOO study involves introducing decision-making techniques in order to identify the best compromise solution from the Pareto front to be actually realised. MOO algorithms may thus be further categorised according to the moment when the selection is performed, distinguishing between *a priori* or *a posteriori* methods [47]. *A priori* methods require specifying a priority between the OFs has to be specified before the optimisation run, thus a deep knowledge of the problem before performing the optimisation is necessary. *A posteriori* methods, instead, are oriented to identify the whole Pareto front, to obtain diversified solutions that may facilitate the decision-making process.

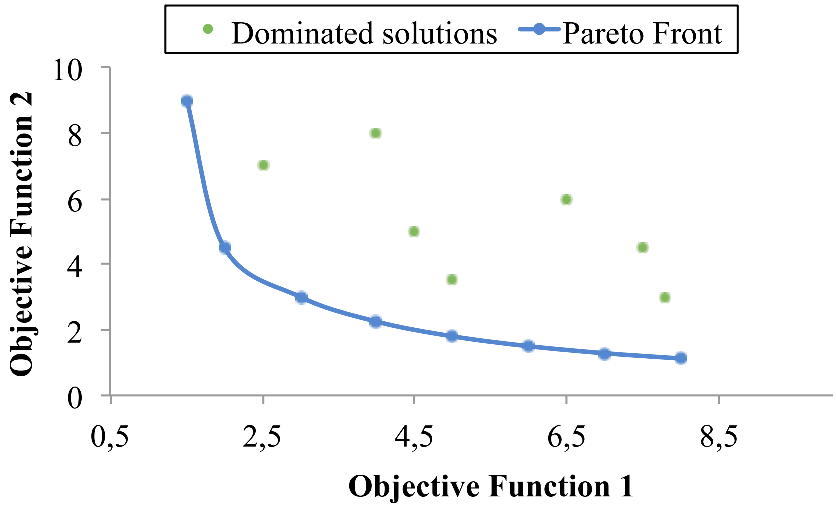

Fig. 2.8. Example of a two-dimensional Pareto front

One of the first techniques developed to solve multi-objective optimisation problems is known as the *scalarization technique*, based on the optimisation of the weighted sum of the objective functions to convert the MOO problem to an SOO. The employment of weights classifies this method in the *a priory* category. Since the employment of this technique would give only one solution, many optimisations with different weights should be performed to identify the solutions of the Pareto Front. Although this method is quite easy to implement, it can be proved that some drawbacks related to non-convex problems exist, since this technique is not able to explore non-convex parts of the Pareto Front. Moreover, objective functions have to be properly normalised in order to have similar orders of magnitude [48].

Another classification of optimisation algorithms consists in the method of exploration of the feasibility space. According to this criterion, algorithms may be classified as deterministic or exact methods and heuristic methods. The deterministic methods are based on mathematical operations that involve derivatives so that they require the OF to be expressed in a continuous and differentiable analytical form. When an analytical and continuous expression is not allowed, heuristic methods are preferred. This category of algorithms is based on criteria derived from the experience of the analyst, and they generally do not require continuity and differentiability of the OF. The easiest example of a heuristic algorithm is a random investigation of the variables and a comparison of the solutions space. The investigation may be stopped setting a maximum number of iterations or through the evaluation of a fitness function (deriving from the OF). The last difference depends on the number of alternatives considered for each iteration, classifying the algorithms as single-point (or local search) or population-based. In detail, single-point algorithms allow the perturbation of the variables one-by-one, while population-based algorithms can manage multiple sets of values of decision variables in each iteration.

In the last years, a category of heuristic, population-based, *a posteriori* method has gained popularity, namely the evolutionary algorithms. These algorithms are based on the biological evolution criteria discovered by Charles Darwin in the mid-19th century. In detail, these algorithms usually combine the values assumed by the decision variables in the high performing solutions to create better solutions. This combination is performed miming biological evolution mechanisms such as reproduction, mutation, recombination, and selection. A sub-category of the evolutionary algorithms is known as genetic algorithms. Since these algorithms are intrinsically population-based, it is possible to exploit this feature to easily extend the investigation to MOO problems. Being based on heuristics, non-linear or integer problems can be efficiently handled with genetic algorithms. The mutation rate is one of the typical parameters of these algorithms and it is employed to shake the values of variables, avoiding to fall into local minima.

2.3.2. Optimisation of building performance

The optimisation of building performance may be considered as the process aimed at identifying the set of features (design) or interventions (renovation) on the building envelope and on the technical systems, whose combination optimises the objective function. The main advantage of the adoption of optimisation techniques in place of classic parametric analyses is to automatically investigate a number of variables that is usually at least one order of magnitude higher. In detail, although an optimisation study requires a basic knowledge of techniques and a longer preliminary setting of the problem, the rapid simulation phase allows a global time saving up to 2.5 times, as described by Naboni *et al.* [49].

Differently from the sequential approach illustrated in Section 2.2.4 for the design of low-energy buildings, during an optimisation study the categories of interventions are assessed all at the same time. As previously stated, the design of a building with very high-energy performance can be considered as a SOO or a MOO problem. A review paper in 2013 stated that 70% of the interviewed designers usually perform multi-objective optimisation [50,51]. This aspect should clarify the complexity of the energy optimisation of a building.

In most of the cases, especially in the last few years, one of the objective functions is related to the energy consumption during the use phase or to the economic aspects. Without loss of generality, the mathematical problem of the optimisation of building performance during the use phase may be expressed referencing to a prosumer building, *i.e.* a building being both an energy consumer and producer, modifying Eq. (2.3) as in Eq. (2.5):

Import-Export minimisation *Load-Generation minimisation*

$$\min \sum_{t=t_1}^{t_2} \left[\sum_{k=k_1}^{k_2} \left(I_k \cdot w_{i,k} \right) - \sum_{j=j_1}^{j_2} \left(E_j \cdot w_{e,j} \right) \right] \qquad \min \sum_{t=t_1}^{t_2} \left[\sum_{k=k_1}^{k_2} \left(L_k \cdot w_{l,k} \right) - \sum_{j=j_1}^{j_2} \left(G_j \cdot w_{g,j} \right) \right] \quad (2.5)$$

For a building without local generation, using these equations will only minimise the local import or loads, since $E_j = G_j = 0$ in this case. Although these equations have a simple and linear expression, the accurate evaluation of the hourly energy flows is highly complicated and requires the employment of BPS. Unless the optimisation tool is already embedded in the BPS, this feature hides the mathematical form of the energy flows, preventing from the calculation of derivatives to identify the best combination of alternatives for the building. This is the main reason why heuristic algorithms are particularly attractive and are often employed in the optimisation of buildings performance [52].

Although many differences exist in the aims and the approaches of the literature studies on the optimisation of building performance, it is possible to recognise a general scheme that was generally followed by researchers [14,53,54], based on the following steps, also depicted in Fig. 2.9:

- Modelling of the initial building configuration (*e.g.* existing building, preliminary design);
- Assessment of the variables and the objective functions to be optimised (generally minimised);
- Execution of the algorithm to start a loop of iterations, adopting a convergence criterion based on a fitness function;
- Data post-processing and analysis.

Another commonly used objective is the cost minimisation since this is one of the most important aspects for the customers. The cost function may be assessed with multiple approaches; with increasing level of detail, a study may incorporate:

- The investment or both investment and labour cost, thus the initial expense due to the project;
- The investment and operating costs (*e.g.* electric energy purchase), namely the most common approach;
- The investment, operating and maintenance and/or refurbishment costs;
- The LCC or the global cost, considering all the costs quantities occurring during the life of the buildings.

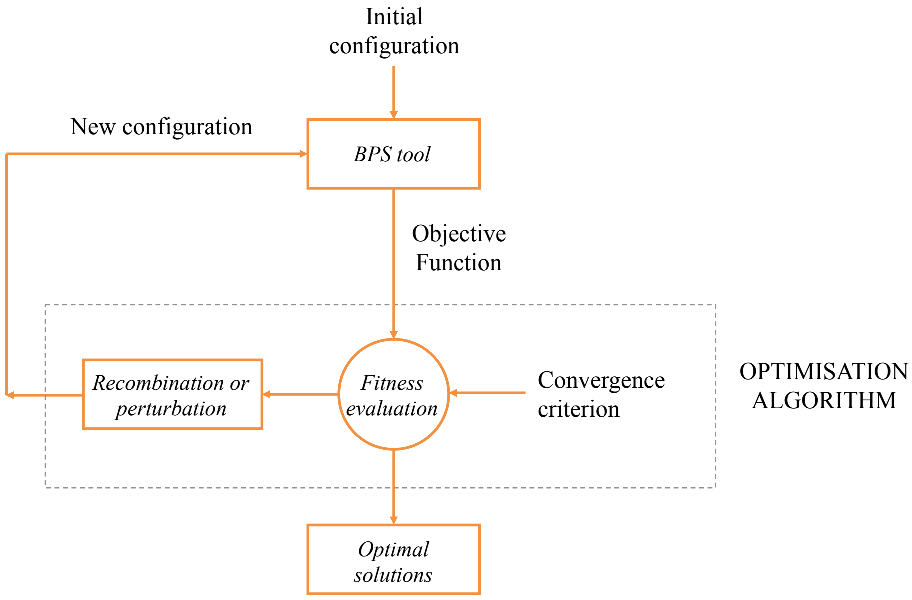

Fig. 2.9. The basic principle of heuristic optimisation algorithms in a simulation-based optimisation

Other OFs usually employed in literature assess:

- The CO_2 emissions, in terms of direct emissions, direct equivalent emissions or also embodied emissions through the GWP [55–62];
- The internal comfort, in terms of thermal [61,63–71] or visual internal comfort [68,72]. Thermal comfort is usually assessed through the Predicted Mean Vote (PMV) and the Predicted Percentage of Dissatisfied (PPD) static indicators [19,73], that correlate the metabolic rate of the occupants and some psychrometric quantities to estimate the people satisfaction, or the dynamic indicator Weighted Discomfort Time [69]. Visual comfort may be evaluated through the Discomfort Glare Index (DGI) or the Useful Daylight Illuminance (UDI) [68];
- The interactions between a prosumer building and the electrical grid [58–60,64,74] (*e.g.* Grid Interaction Index (GII) [75].

Although it was not employed in the optimisation studies investigated during this project, another physical quantity employed in the literature studies on low-energy buildings is the exergy consumption [76], where the exergy is the maximum available work in a process. The exergy analysis is related to the Second Law of Thermodynamics and its adoption can be useful to identify, and thus reduce, the main avoidable primary energy losses in building processes.

The application of optimisation techniques in building design and performance simulation, also called Building Performance Optimisation (BPO), is slowly moving out from the academic environment to design companies, although it still cannot be defined as a popular technique either in research applications. Contrarily to classic optimisation, where the problem is usually simplified to speed up the investigation of the search space, a recent common approach is to combine BPS and BPO tools in the so-defined simulation-based optimisation studies. For this sake, although specific optimisation tools for building applications already exist, researchers often employ optimisation software suitable for each kind of application [68,71,77–79]. A description of selected tools highlighting main features and interoperability is provided in Table 2.2, while a brief list with the most common tools used for the simulation-based building optimisation is reported in Table 2.3.

Table 2.2. Main features of selected software for simulation-based building optimisation

Software	Category	Interactions with Geometrical Tools	Interactions with BPS Tools	Interactions with Generic Optimisation Tools	Interactions with Specific Optimisation Tools
EnergyPlus	BPS	DesignBuilder [70,81] OpenStudio [49] Rhinoceros [72], [81] SketchUp [82]	-	GenOpt [50,83] MATLAB [66] MOBO [84] modeFRONTIER [50] Rhinoceros [72]	jEPlus [81] jEPlus+EA [83] Opt-E-Plus [50,83]
TRNSYS	BPS	SketchUp (through TRNSYS3D) [81]	-	GenOpt [50,83] MATLAB [81] MOBO [83]	BEopt [50,83] Multiopt2 [83] TRNOPT [83]
IDA-ICE	BPS	ArchiCAD [81] MagiCAD [81] Revit [81] SketchUp [81]	-	GenOpt [50,83] MATLAB [85] MOBO [83]	IDA-ESBO
MATLAB	Programming environment Optimisation tool	-	EnergyPlus [66] TRNSYS [81] IDA-ICE [85]	-	-

Table 2.3. Most common tools for the simulation-based building optimisation

Building Performance Simulation	Building Performance Optimisation
DOE-2 [86]	BEopt [87]
EnergyPlus [88]	GenOpt [89]
ESP-r [90]	MATLAB Optimisation Toolbox [80]
IDA-ICE [91]	modeFRONTIER [92]
TRNSYS [93]	Opt-E-Plus [94]

2.4. Scientific literature contributions

Part of the work shown in this chapter was published in the following scientific papers:

JOURNAL ARTICLES

- Sonia Longo, Francesco Montana, Eleonora Riva Sanseverino, "A review on optimization and cost-optimal methodologies in low-energy buildings design and environmental considerations", Sustainable Cities and Society vol. 45, pp. 87–104, 2019.

INTERNATIONAL CONFERENCE PROCEEDINGS

- Maurizio Cellura, Sonia Longo, Francesco Montana, Eleonora Riva Sanseverino, "Multi-Objective Building Envelope Optimization through a Life Cycle Assessment Approach", 2019 IEEE International Conference on Environment and Electrical Engineering and 2019 IEEE Industrial and Commercial Power Systems Europe (EEEIC / I&CPS Europe), Genoa, Italy, 2019, pp. 1-6.

NATIONAL CONFERENCE PROCEEDINGS

- Maurizio Cellura, Sonia Longo, Francesco Montana, Eleonora Riva Sanseverino, "Ottimizzazione Multi-Obiettivo delle Prestazioni Energetiche e Ambientali di un Edificio Residenziale", Atti del XIII Convegno della Rete Italiana LCA – VIII Convegno dell'Associazione Rete Italiana LCA (Proceedings of the XIII Conference of Italian LCA Network), Rome, Italy, 2019, pp. 1-10.

2.5. References

[1] Guinée JB, Heijungs R, Huppes G, Zamagni A, Masoni P, Buonamici R, et al. Life Cycle Assessment: Past, Present, and Future. Environ Sci Technol 2011;45:90–6. doi:10.1021/es101316v.

[2] International Organization for Standardization (ISO). ISO 14040:2006 - Environmental management. Life cycle assessment. Principles and framework 2006.

[3] International Organization for Standardization (ISO). ISO 14044:2006 + Amd 1:2017 - Environmental management. Life cycle assessment. Requirements and guidelines 2017.

[4] Rebitzer G, Ekvall T, Frischknecht R, Hunkeler D, Norris G, Rydberg T, et al. Life cycle assessment: Part 1: Framework, goal and scope definition, inventory

analysis, and applications. Environ Int 2004;30:701–20. doi:https://doi.org/10.1016/j.envint.2003.11.005.

[5] Stephan A, Crawford RH, Myttenaere K De. Towards a comprehensive life cycle energy analysis framework for residential buildings. Energy Build 2012;55:592–600. doi:10.1016/j.enbuild.2012.09.008.

[6] Crawford RH, Treloar GJ, Fuller RJ, Bazilian M. Life-cycle energy analysis of building integrated photovoltaic systems (BiPVs) with heat recovery unit 2006;10:559–75. doi:10.1016/j.rser.2004.11.005.

[7] Hendrickson C, Lave L, Matthews H, Horvath A, Joshi S, Maclean H, et al. Environmental Life Cycle Assessment of Goods and Services: An Input-Output Approach. vol. 2. 2006.

[8] International Organization for Standardization (ISO). ISO 14025:2006 - Environmental labels and declarations. Type III environmental declarations. Principles and procedures 2006.

[9] European Committee for Standardization (CEN). EN 15804:2012 - Sustainability of construction works. Environmental product declarations. Core rules for the product category of construction products 2012.

[10] The International EPD® System. Environmental Product Declarations (EPD) n.d. https://www.environdec.com/ (accessed March 27, 2020).

[11] Intergovernmental Panel on Climate Change (IPCC). Climate Change 2001: The Scientific Basis. Contribution of Working Group I to the Third Assessment Report of the Intergovernmental Panel on Climate Change. 2001. doi:10.1256/004316502320517344.

[12] European Committee for Standardization (CEN). EN 15978:2011 - Sustainability of construction works. Assessment of environmental performance of buildings. Calculation method 2011.

[13] Tumminia G, Guarino F, Longo S, Ferraro M, Cellura M, Antonucci V. Life cycle energy performances and environmental impacts of a prefabricated building module. Renew Sustain Energy Rev 2018;92:272–83. doi:https://doi.org/10.1016/j.rser.2018.04.059.

[14] Schwartz Y, Raslan R, Mumovic D. Implementing multi objective genetic algorithm for life cycle carbon footprint and life cycle cost minimisation: A building refurbishment case study. Energy 2016;97:58–68. doi:10.1016/j.energy.2015.11.056.

[15] International Organization for Standardization (ISO). ISO 15686-5:2017 – Buildings and constructed assets – Service life planning – Part 5: Life-cycle costing 2017.

[16] European Committee for Standardization (CEN). EN 15459:2007 - Energy

performance of buildings. Economic evaluation procedure for energy systems in buildings 2007.

[17] European Commission. Guidelines accompanying Commission Delegated Regulation (EU) No 244/2012 of 16 January 2012 supplementing Directive 2010/31/EU of the European Parliament and of the Council. 2012.

[18] ANSI, ASHRAE. ANSI/ASHRAE Standard 55-2017 - Thermal Environmental Conditions for Human Occupancy 2017.

[19] International Organization for Standardization (ISO). ISO 7730 - Ergonomics of the thermal environment. Analytical determination and interpretation of thermal comfort using calculation of the PMV and PPD indices and local thermal comfort criteria 2005.

[20] Cengel Y, Ghajar A. Heat and Mass Transfer: Fundamentals and Applications. 5th ed. McGraw Hill; 2015.

[21] European Committee for Standardization (CEN). EN 12831:2003 - Heating systems in buildings. Method for calculation of the design heat load 2003.

[22] Carrier Air Conditioning Company. Handbook of Air Conditioning System Design. McGraw Hill; 1965.

[23] Danielski I. Energy variations in apartment buildings due to different shape factors and relative size of common areas. Proc. World Renew. Energy Congr., Linköping, Sweden: 2011.

[24] Italian Ministry for the Economic Development. Decreto Ministeriale 11/3/2008 – Attuazione dell'articolo 1, comma 24, lettera a), della legge 24 dicembre 2007, n. 244, per la definizione dei valori limite di fabbisogno di energia primaria annuo e di trasmittanza termica ai fini dell'applicazione dei c. 2008.

[25] Italian Government. Decreto Legislativo 19 agosto 2005, n. 192 – Attuazione della direttiva 2002/91/CE relativa al rendimento energetico nell'edilizia. 2005.

[26] Davies MG. Building Heat Transfer. John Wiley & Sons, Ltd; 2006. doi:10.1002/0470020555.

[27] American Society of Heating Refrigerating and Air-Conditioning Engineers. ASHRAE Handbook - Fundamentals. 2017.

[28] Crawley DB, Lawrie LK, Pedersen CO, Winkelmann FC. EnergyPlus: Energy Simulation Program. ASHRAE J 2000;42:49–56. doi:10.1.1.122.6852.

[29] Delcroix B, Kummert M, Daoud A, Hiller M. Conduction Transfer Functions in TRNSYS Multizone Building Model: Current Implementation, Limitations and Possible Improvements. Fifth Natl. Conf. IBPSA-USA, 2012, p. 219–26.

[30] Sánchez Ramos J, Guerrero Delgado Mc, Álvarez Domínguez S, Molina Félix

JL, de la Flor FJ, Tenorio Ríos JA. Systematic Simplified Simulation Methodology for Deep Energy Retrofitting Towards Nze Targets Using Life Cycle Energy Assessment. Energies 2019;12. doi:10.3390/en12163038.

[31] International Organization for Standardization (ISO). ISO 13790:2008 - Energy performance of buildings. Calculation of energy use for space heating and cooling 2008.

[32] Kiss B, Szalay Z. The applicability of different energy performance calculation methods for building life cycle environmental optimization. Int Rev Appl Sci Eng 2019;9:115–21.

[33] International Organization for Standardization (ISO). ISO 52016-1:2017 - Energy Performance of Buildings - Energy Needs for Heating and Cooling, Internal Temperatures and Sensible and Latent Heat Loads - Part 1: Calculation Procedures 2017.

[34] Marszal AJ, Heiselberg P, Bourrelle JS, Musall E, Voss K, Sartori I, et al. Zero Energy Building - A review of definitions and calculation methodologies. Energy Build 2011;43:971–9. doi:10.1016/j.enbuild.2010.12.022.

[35] AlAjmi A, Abou-Ziyan H, Ghoneim A. Achieving annual and monthly net-zero energy of existing building in hot climate. Appl Energy 2016;165:511–21. doi:https://doi.org/10.1016/j.apenergy.2015.11.073.

[36] Aggerholm S. SBi 2018:13 - Cost-optimal levels of minimum energy performance requirements in the Danish Building Regulations. 2018.

[37] Dokka TH, Sartori I, Thyholt M, Lien K, Lindberg KB. A Norwegian Zero Emission Building Definition. Proc. Passiv. Nord. 2013 Conf., Göteborg, Sweden: 2013.

[38] Longo S, Montana F, Riva Sanseverino E. A review on optimization and cost-optimal methodologies in low-energy buildings design and environmental considerations. Sustain Cities Soc 2019;45:87–104.

[39] Cellura M, Guarino F, Longo S, Mistretta M. Energy life-cycle approach in Net zero energy buildings balance: Operation and embodied energy of an Italian case study. Energy Build 2014;72:371–81. doi:10.1016/j.enbuild.2013.12.046.

[40] Hernandez P. Life Cycle Energy Performance Evaluation. In: Pacheco Torgal F., Mistretta M., Kaklauskas A., Granqvist C. CL, editor. Nearly Zero Energy Build. Refurb., Springer; 2013. doi:https://doi.org/10.1007/978-1-4471-5523-2_8.

[41] Hernandez P, Kenny P. Defining Zero Energy Buildings - A life cycle perspective. PLEA 2008 – 25th Conf. Passiv. Low Energy Archit., Dublin: n.d.

[42] Hernandez P, Kenny P. From net energy to zero energy buildings: Defining life cycle zero energy buildings (LC-ZEB). Energy Build 2010;42:815–21. doi:10.1016/j.enbuild.2009.12.001.

[43] Kristjansdottir T, Fjeldheim H, Selvig E, Risholt B, Time B, Georges L, et al. A Norwegian ZEB-definition embodied emission. ZEB Proj Rep 17 2014.

[44] Fufa SM, Schlanbusch RD, Sørnes K, Inman M, Andresen I. A Norwegian ZEB Definition Guideline. ZEB Proj Rep 29 2016.

[45] Sioshansi R, Conejo A. Optimization in Engineering. Models and Algorithms. Springer Nature; 2017. doi:10.1007/978-3-319-56769-3.

[46] Deb K. Multi-Objective Optimization Using Evolutionary Algorithms. John Wiley Sons, LTD 2001:497.

[47] Alarcon-Rodriguez A, Ault G, Galloway S. Multi-objective planning of distributed energy resources: A review of the state-of-the-art. Renew Sustain Energy Rev 2010;14:1353–66. doi:10.1016/j.rser.2010.01.006.

[48] Liu GP, Yang JB, Whidborne JF. Multiobjective optimisation and control. 2003.

[49] Naboni E, Maccarini A, Korolija I, Zhang Y. Comparison of Conventional, Parametric and Evolutionary Optimization Approaches for the Architectural Design of Nearly Zero Energy Buildings. Proc BS2013 2013.

[50] Attia S, Hamdy M, O'Brien W, Carlucci S. Assessing gaps and needs for integrating building performance optimization tools in net zero energy buildings design. Energy Build 2013;60:110–24. doi:10.1016/j.enbuild.2013.01.016.

[51] Attia S, Hamdy M, O'Brien W, Carlucci S. Computational optimisation for zero energy building design: Interviews results with twenty eight international experts. 13th Conf Int Build Perform Simul Assoc 2013:3698–705.

[52] Recht T, Schalbart P, Peuportier B. Ecodesign of a 'plus-energy' house using stochastic occupancy model, life-cycle assessment and multi-objective optimisation. In: Hamza N, Underwood C, editors. Build. Simul. Optim. Conf., Newcastle upon Tyne, United Kingdom: 2016.

[53] Niemelä T, Kosonen R, Jokisalo J. Cost-optimal energy performance renovation measures of educational buildings in cold climate. Appl Energy 2016;183:1005–20. doi:10.1016/j.apenergy.2016.09.044.

[54] Hamdy M, Nguyen A-T, Hensen JLM. A performance comparison of multi-objective optimization algorithms for solving nearly-zero-energy-building design problems. Energy Build 2016;121:57–71. doi:10.1016/j.enbuild.2016.03.035.

[55] Diakaki C, Grigoroudis E, Kabelis N, Kolokotsa D, Kalaitzakis K, Stavrakakis G. A multi-objective decision model for the improvement of energy efficiency in buildings. Energy 2010;35:5483–96. doi:10.1016/j.energy.2010.05.012.

[56] Antipova E, Boer D, Guillén-Gosálbez G, Cabeza LF, Jiménez L. Multi-objective optimization coupled with life cycle assessment for retrofitting buildings. Energy Build 2014;82:92–9. doi:10.1016/j.enbuild.2014.07.001.

[57] Stadler M, Groissböck M, Cardoso G, Marnay C. Optimizing Distributed Energy Resources and building retrofits with the strategic DER-CAModel. Appl Energy 2014;132:557–67. doi:10.1016/j.apenergy.2014.07.041.

[58] Lu Y, Wang S, Zhao Y, Yan C. Renewable energy system optimization of low/zero energy buildings using single-objective and multi-objective optimization methods. Energy Build 2015;89:61–75. doi:10.1016/j.enbuild.2014.12.032.

[59] Lu Y, Wang S, Yan C, Shan K. Impacts of renewable energy system design inputs on the performance robustness of net zero energy buildings. Energy 2015;93:1595–606. doi:10.1016/j.energy.2015.10.034.

[60] Lu Y, Wang S, Yan C, Huang Z. Robust optimal design of renewable energy system in nearly/net zero energy buildings under uncertainties. Appl Energy 2017;187:62–71. doi:10.1016/j.apenergy.2016.11.042.

[61] Gilles F, Bernard S, Ioannis A, Simon R. Decision-making based on network visualization applied to building life cycle optimization. Sustain Cities Soc 2017;35:565–73. doi:10.1016/j.scs.2017.09.006.

[62] Kang HJ. Development of an nearly Zero Emission Building (nZEB) life cycle cost assessment tool for fast decision making in the early design phase. Energies 2017;10. doi:10.3390/en10010059.

[63] Asadi E, da Silva MG, Antunes CH, Dias L. A multi-objective optimization model for building retrofit strategies using TRNSYS simulations, GenOpt and MATLAB. Build Environ 2012;56:370–8. doi:10.1016/j.buildenv.2012.04.005.

[64] Sun Y, Huang P, Huang G. A multi-criteria system design optimization for net zero energy buildings under uncertainties. Energy Build 2015;97:196–204. doi:10.1016/j.enbuild.2015.04.008.

[65] Negendahl K, Nielsen TR. Building energy optimization in the early design stages: A simplified method. Energy Build 2015;105:88–99.

[66] Ascione F, Bianco N, De Masi RF, Mauro GM, Vanoli GP. Design of the Building Envelope: A Novel Multi-Objective Approach for the Optimization of Energy Performance and Thermal Comfort. Sustainability 2015;7:10809–36. doi:10.3390/su70810809.

[67] Yu Z (Jerry), Chen J, Sun Y, Zhang G. A GA-based system sizing method for net-zero energy buildings considering multi-criteria performance requirements under parameter uncertainties. Energy Build 2016;129:524–34. doi:10.1016/j.enbuild.2016.08.032.

[68] Carlucci S, Cattarin G, Causone F, Pagliano L. Multi-objective optimization of a nearly zero-energy building based on thermal and visual discomfort minimization using a non-dominated sorting genetic algorithm (NSGA-II). Energy Build 2015;104:378–94. doi:10.1016/j.enbuild.2015.06.064.

[69] Penna P, Prada A, Cappelletti F, Gasparella A. Multi-objectives optimization of Energy Efficiency Measures in existing buildings. Energy Build 2015;95:57–69. doi:10.1016/j.enbuild.2014.11.003.

[70] Ascione F, De Masi RF, de Rossi F, Ruggiero S, Vanoli GP. Optimization of building envelope design for nZEBs in Mediterranean climate: Performance analysis of residential case study. Appl Energy 2016;183:938–57. doi:10.1016/j.apenergy.2016.09.027.

[71] Ascione F, Bianco N, De Masi RF, Mauro GM, Vanoli GP. Energy retrofit of educational buildings: Transient energy simulations, model calibration and multi-objective optimization towards nearly zero-energy performance. Energy Build 2017;144:303–19. doi:10.1016/j.enbuild.2017.03.056.

[72] Konis K, Gamas A, Kensek K. Passive performance and building form: An optimization framework for early-stage design support. Sol Energy 2016;125:161–79. doi:10.1016/j.solener.2015.12.020.

[73] European Committee for Standardization (CEN). EN 15251:2007 - Indoor environmental input parameters for design and assessment of energy performance of buildings addressing indoor air quality, thermal environment, lighting and acoustics 2007.

[74] Zhang S, Huang P, Sun Y. A multi-criterion renewable energy system design optimization for net zero energy buildings under uncertainties. Energy 2016;94:654–65. doi:10.1016/j.energy.2015.11.044.

[75] Salom J, Widén J, Candanedo J a, Sartori I, Voss K, Marszal AJ. Understanding Net Zero Energy Buildings: Evaluation of load matching and grid interaction indicators. Proc Build Simul 2011 2011;6:14–6. doi:ISBN: 9870646565101.

[76] Picallo-Perez A. New Exergetic Methodology to Promote Improvements in nZEB. In: Hidalgo-Betanzos J-M, editor., Rijeka: IntechOpen; 2018, p. Ch. 5. doi:10.5772/intechopen.73153.

[77] Ferrara M, Fabrizio E, Virgone J, Filippi M. Appraising the effect of the primary systems on the cost optimal design of nZEB: A case study in two different climates. Energy Procedia 2015;78:2028–33. doi:10.1016/j.egypro.2015.11.200.

[78] Baglivo C, Congedo PM. Design method of high performance precast external walls for warm climate by multi-objective optimization analysis. Energy 2015;90:1645–61. doi:10.1016/j.energy.2015.06.132.

[79] Diakaki C, Grigoroudis E, Kolokotsa D. Towards a multi-objective optimization approach for improving energy efficiency in buildings. Energy Build 2008;40:1747–54. doi:10.1016/j.enbuild.2008.03.002.

[80] Mathworks. MATLAB web page n.d. https://www.mathworks.com/products/matlab.html (accessed March 22, 2020).

[81] IBPSA-USA. Building Energy Software Tools (BEST) Directory n.d. https://www.buildingenergysoftwaretools.com/.

[82] Becchio C, Dabbene P, Fabrizio E, Monetti V, Filippi M. Cost optimality assessment of a single family house: Building and technical systems solutions for the nZEB target. Energy Build 2015;90:173–87. doi:10.1016/j.enbuild.2014.12.050.

[83] Palonen M, Hamdy M, Hasan A. MOBO A New Software for Multi-Objective Building Performance Optimization. 13th Conf Int Build Perform Simul Assoc 2013:2567–74.

[84] Cellura M, Longo S, Montana F, Riva Sanseverino E. Multi-Objective Building Envelope Optimization through a Life Cycle Assessment Approach. 2019 IEEE Int. Conf. Environ. Electr. Eng. 2019 IEEE Ind. Commer. Power Syst. Eur. (EEEIC / I&CPS Eur., Genoa, Italy: Institute of Electrical and Electronics Engineers (IEEE); 2019, p. 1–6.

[85] Hamdy M, Hasan A, Sirén K. A multi-stage optimization method for cost-optimal and nearly-zero-energy building solutions in line with the EPBD-recast 2010. Energy Build 2013;56:189–203. doi:10.1016/j.enbuild.2012.08.023.

[86] DOE-2 web page n.d. http://doe2.com/doe2/.

[87] BEopt web page n.d. https://beopt.nrel.gov/ (accessed March 27, 2020).

[88] U.S. Department of Energy. EnergyPlus web page n.d. https://energyplus.net/ (accessed April 28, 2020).

[89] GenOpt web page n.d. https://simulationresearch.lbl.gov/GO/ (accessed March 27, 2020).

[90] ESP-r web page n.d. http://www.esru.strath.ac.uk/Programs/ESP-r.htm.

[91] EQUA Simulation AB. IDA-ICE web page n.d. https://www.equa.se/en/ida-ice (accessed March 27, 2020).

[92] modeFRONTIER web page n.d. http://www.esteco.com/modefrontier (accessed March 27, 2020).

[93] TRNSYS web page n.d. http://www.trnsys.com/ (accessed March 27, 2020).

[94] Opt-E-Plus web page n.d. https://www.nrel.gov/tech_deployment/pdfs/45620.pdf (accessed March 27, 2020).

Chapter Three – Literature review

3.1. Brief review on the optimisation of the life cycle performance of buildings

During the activities of the IEA EBC Annex 72, a brief review of case studies on the optimisation of life cycle impacts of buildings available in literature was performed. These studies were developed by the components of the Annex, and a set of thirteen case studies was collected, including the three cases described in the Chapter 5 of this thesis. Besides the works performed by these authors, very few works on the topic were found in the literature. A possible explanation of this aspect might be the difficulty of finding researchers specialised in all of these techniques. Even Gilles et al. discussed this aspect in 2017, highlighting the difficulties in the interactions between building performance simulators and life cycle assessment studies because there is a lack of software tools [1]. An extract of the review is here reported.

3.1.1. Optimisation workflow

Analysing the studies on the optimisation of buildings performance, and specifically, the works focused on minimising LCA impacts, a generic workflow may be identified [2]:

- First, the base geometrical model is created and used as an input. In this model, the building details as materials and layer thickness for each envelope component or the type of building services are indicated;
- Next, auxiliary data as the climate file and the reference period are defined;
- The variables of the problem are specified, the optimisation run starts, usually assessing the embodied and operating (or use phase) terms of each impact function separately and then aggregating these terms;
- The fitness function of each building alternative is evaluated until the optimisation ends;
- The results are investigated to identify the values of the variables in the best solution, thus the optimal interventions for the building. Normalisation, weighting and aggregation of several impact indicators into a single score may also be performed in this step.

The embodied impacts are obtained directly from the variables selected by the optimisation algorithm for each configuration, multiplying the variable quantity (*e.g.* thickness, mass, kind of material) by its unit impact factor. The use phase contribution may be instead obtained dividing the final energy demand, *i.e.* the output of the energy calculation of each building configuration, by the efficiency of the HVAC system and then multiplying the result by the unit impact factor.

3.1.2. Optimisation approaches and algorithms

The studies analysed in this review may be categorised according to different aspects. Considering the main target of the study, three of the case studies focused on the early design stage of residential buildings [3,4], nine studies analysed the refurbishment of existing buildings [2,5–9], and the last one analysed only the optimal concrete quantity and quality for a construction without including the operating phase [10]. All the studies focused both on the envelope features and the HVAC systems, with the only exception of [10], where analysing the operating phase was unnecessary. Only four works included the RES in the study [3,8,9], with one of these buildings being optimised to reach the plus-energy level [3].

The preferred approach to evaluate the use phase energy demand and impacts of the building was the employment of a dynamic building performance simulation (BPS) software [5–8], while four studies [2,4,9] adopted energy calculations based on the quasi-stationary seasonal method described on the European standard EN ISO 13790:2008 [11] or from the German standard DIN V 18599-2:2011 [12].

Analysing the approaches, about half of the studies adopted an SOO approach [2,4–7,10], while the remaining half employed MOO algorithms [3,4,7–10]. Nevertheless, some SOO studies assessed the minimisation of many LCA indicators one at the time, comparing the optimal renovation actions [2,4], and other studies optimised one impact but also evaluated the other impacts related to the optimal solution [5,6,10]. Almost all the studies adopted heuristic algorithms, mainly genetics, with the only exception being the two case studies described in this thesis developed in the Mediterranean climate, where the Branch and Bound MILP algorithm was employed in the second step.

3.1.3. LCA indicators and variables

The LCA impact assessment indicators employed in the reviewed studies are among the most commonly used in LCA studies on buildings [13,14]. All the studies optimised the use phase of the building employing the GWP as an objective function, indicating a greater attention to the environmental issues rather than to the primary energy. Apart from the GWP, the use phase energy demand of the building was assessed through the CED [2,4–10]. Other indicators identified in these works are the ODP, the AP, the EP, the POCP [2,4,5,10] and less commonly the ADP [2,10].

The variables assessed in the reviewed studies are various, although they are mainly related to the envelope. Nevertheless, the following groups may be identified:

- Early design parameters, as the number of floors or the building orientation;
- Opaque envelope components, namely the materials and thicknesses of each layer;

- Transparent envelope components, as windows glazing or surface;
- HVAC equipment features, as the inclusion or the rated size of a specific technology;
- RES features, as the inclusion or the rated size of a specific technology.

The opaque envelope components are the most common category, and all these studies assessed the optimal thickness or material at least for one envelope component. More in detail, the insulation-related variables (thickness or material) are the most popular variables, but massive materials as concrete and bricks were optimised as well [7,8,10]. The assessment of the best HVAC was also quite common, although it was changed out of the optimisation process parametrically in some cases [5,6]. The heating system is the predominant topic since most of the studies were developed in cold climates, while space cooling or ventilation technologies were hardly included [3,4,8]. Furthermore, the embodied impacts of the equipment were sometimes neglected [6]. Early design parameters were included in only three studies, where two assessed the optimal number of floors [4] and the third the optimal position of the supporting columns of a garage [10]. This is because the renovation of existing buildings is more common than the design of new ones.

3.1.4. LCA unit impact factors and data quality

Using reliable and representative data is a very important issue in LCA studies, since the results may be influenced by site-specific conditions. Nevertheless, all the studies analysed in this review employed secondary data, namely average values from the literature, in order to get generic and simplified results, according to the philosophy that optimisation studies are usually employed to obtain generic indications on the problem to be further investigated with more detailed simulations. LCA impact factors were drawn from international databases as Ecoinvent [3,4], KBOB [6,7], Ökobau [2,5,9], or from the Environmental Product Declarations. In the same way, costs data were collected from databases [3,9] or market reports [8].

3.1.5. Main outcomes

The first outcome of this review is that, although this research branch is still in a developing stage and only a few studies were conducted, many approaches were already attempted, with a tendency to a deep investigation of many alternatives in each case study. In detail, some SOO studies identified the optimal thicknesses of various insulation materials according to different objective functions, while the works involving MOO compared many indicators in a single optimisation. Moreover, use phase energy consumption was investigated with a simulation-based approach every time, rather than employing a simplified estimation of thermal loads.

Regarding the optimal solutions, insulation materials of natural origin (*e.g.* cellulose) are preferred to synthetic ones (*e.g.* EPS) from the point of view of the associated impact, although these substances are usually more expensive. Furthermore, the optimal thickness resulted being very sensitive to the HVAC system, and in the case of air-to-air heat pump powered by electricity from renewable sources, no additional insulation was identified as optimal retrofit solution. Regarding the heating system technology, district heating was preferred to traditional systems and solar collectors in cold climate, even due to the low average solar radiation. Since only two studies were conducted in cooling dominated climate, assessing only air conditioning as technology, it is not possible to gather any consideration. More studies on warm climates are recommended to be investigated, including other technologies as absorption chillers.

3.2. State of the art on the optimisation approaches adopted for low-energy buildings

In this review, literature studies on the energy performance optimisation of a building have been examined, comparing algorithms and methodologies. A bibliometric analysis has been conducted in mid-2018, considering all the papers published until 2017 and using *optimisation* and *NZEB* as keywords in *ScienceDirect, Scopus, IEEE Xplore* and *MDPI* scientific databases. The number of available studies was then expanded including the bibliography of the selected papers, in order to include works not strictly related to zero-energy buildings. Most of the papers found with this approach were found to improperly use the keywords. For example, *NZEB* was often mentioned only in the introduction, or *optimisation* was often used as a synonymous of improvement [5,15–36]. Furthermore, the review considered only the studies optimising the design or refurbishment of buildings, thus neglecting studies involving only optimal control or optimal schedule of the equipment. The final set is composed of 64 works on buildings energy performance optimisation. Nevertheless, since some papers showed more than one study, in most of the categories shown below, the total number of studies will be often different than 64.

3.2.1. General considerations

The EU EPBD recast highly pushed the research on the topic of reducing the energy demand in the building sector. This aspect can be clearly understood from Fig. 2.10, where the year-by-year number of studies available on the *ScienceDirect* database with “low”, “energy” and “buildings” as keywords is illustrated. In detail, the number of papers jumped from about 5400 to more than 36,000 from 2000 to 2018. A similar trend was followed by the studies specifically involving the optimisation of buildings design or renovation aimed at reducing their energy demand, as in Fig. 2.11. Although a peak can be identified in 2015, followed by a decreasing trend, the energy optimisation of buildings still remains a hot topic in the scientific literature.

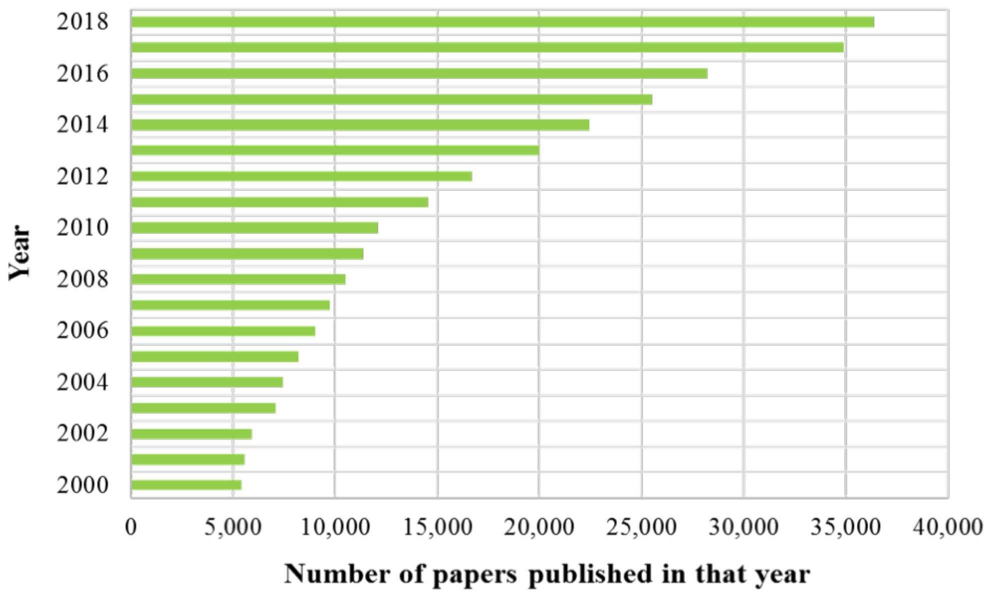

Fig. 3.1. Number of literature papers on low-energy buildings available on the ScienceDirect database after 2000

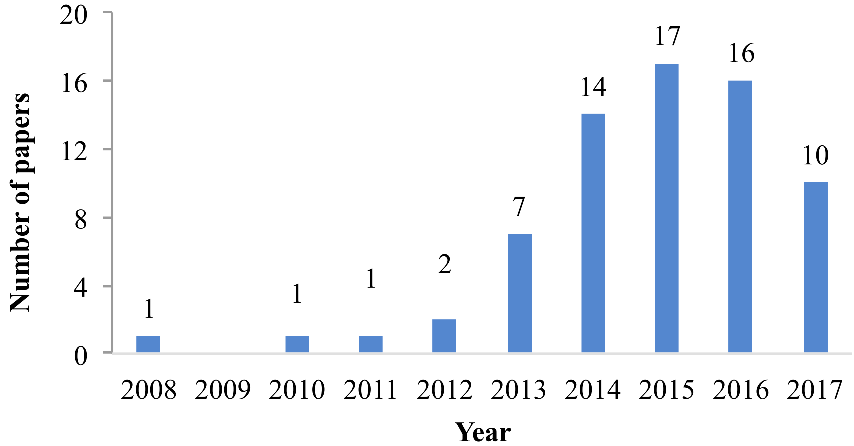

Fig. 3.2. Year-by-year publication trend of the analysed studies

Since the EPBD was emitted in the EU, this continent was the most prolific in investigating the topic focused on this review. Italian researchers were the most interested on the matter, developing 23 studies [37–59], followed by Finnish [60–65], Portuguese [39,66–70] and Spanish [39,71–75] researchers (all of them with 6 studies). Even Asiatic researchers were quite interested, mainly in Hong Kong, while only 3 American and 2 African researchers authored the remaining papers.

3.2.2. Categorisation of the studies

The works may be categorised according to different criteria. Although the greatest part of the literature is concentrated in the residential sector, some studies on industrial or office buildings were developed [52,56,76–78].

Three main topics can be identified: optimisation applied to low-energy buildings without attaining the zero-energy target (13 papers); buildings optimisation to achieve the NZEB or nZEB target (37 papers); works on economic optimisation of nZEBs, performed according to the cost-optimal methodology [79] (23 papers). These three categories can be applied to studies focusing on both new and existing buildings.

Regarding the approach to the building energy demand, most of the available literature assessed the refurbishment of existing structures (31 studies) [37–39,41,47,52,54–57,60–63,65–70,73,77,78,80–87], followed by the design of new buildings (22 studies) [1,40,42–44,48,51,59,64,71,72,74,76,88–96]. Nine works described single building components [45,46,49,50,53,58,97–99], as the optimal materials for an insulation block, and two papers assessed uniquely the use phase energy demand [75,100].

The energy demand was also assessed considering different contributions. Air conditioning is by far the most frequently considered energy contribution in the analysed literature (63 works). Although most of the works considered both space heating and cooling, only one of these two contributions was minimised in selected locations with peculiar climates. The second kind of energy demand mostly investigated in the literature is the lighting demand (39 studies), with natural lighting being also included since larger windows reduce the building envelope thermal resistance. The other energy uses that were considered in the literature are DHW (30 papers), ventilation (22 studies) and embodied energy, that was considered only three times [1,64,95].

In order to attain the target of reducing the consumption of resources to fulfil the energy requirements, different kinds of variables were considered. Referring to the categorisation shown in Section 3.1.3, optimal opaque and transparent envelope components were investigated in more than 40 studies, while the technical systems' features, distinguished in RES and HVAC plants, were optimised in 35 and 30 studies, respectively. The early design stage variables were rarely included in the studies since most of them regarded refurbishment studies. Thus, it is possible to state that building researchers and designers do not have any preference between envelope and equipment to reduce the energy demand of the building sector through optimisation studies.

3.2.3. Optimisation approaches

Investigating the available literature allowed identifying that the optimisation of buildings energy performance is most often considered as a MOO problem, with 38 studies against 19 SOO works. The majority of the studies involves heuristic algorithms, mainly genetic, for the reasons illustrated in Section 2.3.1, while few studies were based on the development of a building heat transfer mathematical model to be employed in a deterministic optimisation. Although many algorithms were employed in literature, the most popular one was NSGA II [101]. This algorithm has shown high performance in the search space investigation in [102], where it was compared with other six multi-objective algorithms, although the Two-Phase genetic algorithm PR_GA [103] overtook all the others.

Another important outcome of this analysis is that the economic aspects are more commonly optimised while the energy demand of the building is considered secondly. This aspect proves a general market-oriented trend of the research. In detail, Global cost, Life Cycle Cost, or investment cost were selected as objective functions in the reviewed studies. More surprising is that the environmental impacts due to the building construction and operation have been often ignored. Thus, although the low-energy buildings have the main goal to reduce the primary energy demand of the building sector, the attention should be oriented to the decarbonisation of the economy holistically, as the application of LCA may allow.

No integrated software tools for the simulation-based optimisation of buildings was adopted, while some optimisation modules may be added to research tools as TRNSYS, EnergyPlus and IDA-ICE, as already shown in the last column of Table 2.2. MATLAB environment has shown great flexibility since it was employed both to evaluate and to optimise energy performance of buildings, although the building physic performance was estimated through simplified models.

Many more details on the reviewed studies were extracted during this literature review. Nevertheless, in order to make this section more coherent with the rest of the thesis, the main data are recapped in Table 3.1. More details on these figures can be found in [33]. With reference to the three main topics investigated in the studies, the following main information was extracted:

Table 3.1. Recap of the main findings from [104]

	Low-energy buildings	**NZEB or nZEB**	**Cost-optimal nZEBs**
Number of studies	13	37	23
OPTIMISATION APPROACH			
SOO problem	3	10	6
MOO problem	10	28	0
OPTIMISATION ALGORITHM			
Deterministic	5	1	0
Heuristic	8	31	6
Not available	0	5	0
OBJECTIVE FUNCTION			
Cost	13	27	24
Energy demand	11	20	6
Carbon emissions	3	9	0
Indoor comfort	2	8	2
Power grid interactions	0	6	0
Envelope features	0	3	0

As a conclusive analysis, in order to demonstrate the advantages deriving from the employment of LCA to the design of a low-energy building, a further deepening was performed on the studies considering the additional insulation among the improvement actions. Since each insulation material employed for buildings has a different embodied impact, depending on its production process, a classification of their performance may be done according to their embodied impact referred to a specific functional unit (FU). For example, Asdrubali performed this kind of classification for the embodied energy of the most common insulation materials in [105], selecting an insulation panel with unit surface and unit thermal resistance was as functional unit.

Choosing arbitrarily two threshold values, namely 100 and 200 MJ/FU, this list of materials provided in [105] can be divided into three regions, namely Low embodied impact (embodied energy < 100 MJ/FU), Mid embodied impact (100 MJ/FU < embodied energy < 200 MJ/FU), and High embodied impact (embodied energy > 200 MJ/FU). Applying this classification to the literature studies analysed in this review, it is possible to see in Fig. 3.3 that 35% used Mid impact materials and 19% of the papers considered High impact materials, while 23% of the analysed studies did not mention the adopted material but only the insulating performance. This simple example proves how the sustainability of the materials, *i.e.* the embodied impacts of the construction components, is often neglected in the scientific literature on optimisation of building performance. Conversely, since NZEBs may aim is the energy demand reduction, it is strongly recommended to adopt a Life Cycle Thinking approach in order to identify the retrofit actions that *really* allow saving energy, thus introducing a building design methodology oriented at the sustainable development.

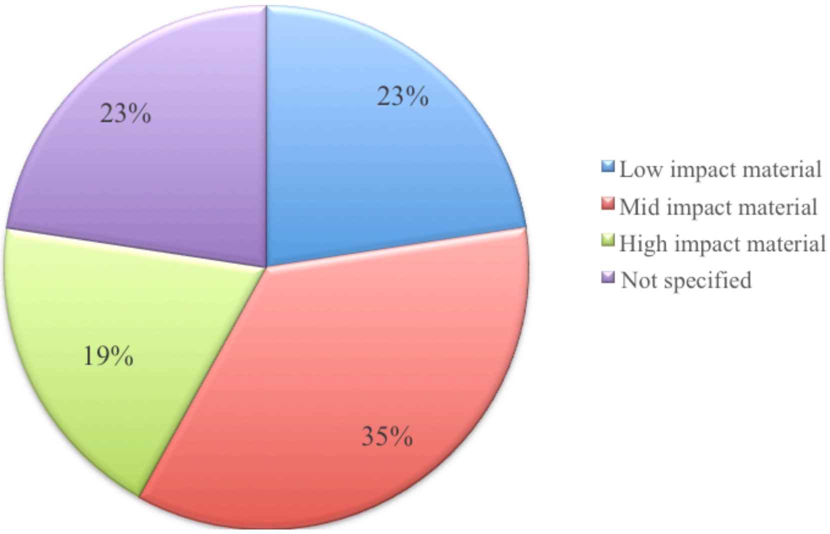

Fig. 3.3. Insulation materials' embodied energy in the analysed papers

3.3. Scientific literature contributions

Part of the work shown in this chapter was published in the following scientific papers:

JOURNAL ARTICLES

- Sonia Longo, Francesco Montana, Eleonora Riva Sanseverino, “A review on optimization and cost-optimal methodologies in low-energy buildings design and environmental considerations”, Sustainable Cities and Society vol. 45, pp. 87–104, 2019.

BOOK CHAPTERS

- Francesco Montana, Sonia Longo, Harpa Birgisdottir, Maurizio Cellura, Rolf Frischknecht, Francesco Guarino, Benedek Kiss, Bruno Peuportier, Thomas Recht, Eleonora Riva Sanseverino, Zsuzsa Szalay, “Multi-criteria oriented optimization of building energy performances: the Annex 72 IEA-EBC experience”, in “Energy Systems Evaluation”, Ed. Springer, 2020, *in press*.

3.4. References

[1] Gilles F, Bernard S, Ioannis A, Simon R. Decision-making based on network visualization applied to building life cycle optimization. Sustain Cities Soc 2017;35:565–73. doi:10.1016/j.scs.2017.09.006.

[2] Hollberg A, Ruth J. LCA in architectural design—a parametric approach. Int J Life Cycle Assess 2016;21:943–60. doi:10.1007/s11367-016-1065-1.

[3] Recht T, Schalbart P, Peuportier B. Ecodesign of a ’plus-energy’ house using stochastic occupancy model, life-cycle assessment and multi-objective optimisation. In: Hamza N, Underwood C, editors. Build. Simul. Optim. Conf., Newcastle upon Tyne, United Kingdom: 2016.

[4] Kiss B, Szalay Z. Modular approach to multi-objective environmental optimization of buildings. Autom Constr 2020;111. doi:10.1016/j.autcon.2019.103044.

[5] Hollberg A, Ruth J. A Parametric Life Cycle Assessment Model for Façade Optimization. Build. Simul. Optim., 2014.

[6] Hollberg A, Ruth J. Parametric performance evaluation and optimization based on life cycle demands. 8th Energy Forum Adv. Build. Ski., Bressanone, Italy: 2013.

[7] Klüber N, Hollberg A, Ruth J. Life cycle optimized application of renewable raw materials for retrofitting measures. World Sustain. Build. 2014, Barcelona, Spain: 2014, p. 1–7.

[8] Cellura M, Longo S, Montana F, Riva Sanseverino E. Multi-Objective Building Envelope Optimization through a Life Cycle Assessment Approach. 2019 IEEE Int. Conf. Environ. Electr. Eng. 2019 IEEE Ind. Commer. Power Syst. Eur. (EEEIC / I&CPS Eur., Genoa, Italy: Institute of Electrical and Electronics Engineers (IEEE); 2019, p. 1–6.

[9] Montana F, Kanafani K, Wittchen K, Birgisdottir H, Longo S, Cellura M, et al. Multi-Objective Optimization of Building Life Cycle Performance. A Housing Renovation Case Study in Northern Europe. Sustainability 2020;12:7807. doi:10.3390/su12187807.

[10] Hollberg A, Heidenreich C, Ruth J, Hartung R, Herzog S. Using evolutionary optimization for low-impact solid constructions. World Sustain. Build. 2014, Barcelona, Spain: 2014.

[11] International Organization for Standardization (ISO). ISO 13790:2008 - Energy performance of buildings. Calculation of energy use for space heating and cooling 2008.

[12] DIN. DIN V 18599-2:2011 - Energetische Bewertung von Gebäuden. Berechnung des Nutz-, End- und Primärenergiebedarfs für Heizung, Kühlung, Lüftung, Trinkwasser und Beleuchtung. Teil 2: Nutzenergiebedarf für Heizen und Kühlen von Gebäudezonen (in German) 2011.

[13] Bahramian M, Yetilmezsoy K. Life cycle assessment of the building industry: an overview of two decades of research (1995–2018). Energy Build 2020;109917.

[14] Lasvaux S, Favre D, Périsset B, Bony J, Hildbrand C, Citherlet S. Life Cycle Assessment of Energy Related Building Renovation: Methodology and Case Study. Energy Procedia 2015;78:3496–501. doi:10.1016/j.egypro.2016.10.132.

[15] Wright JA, Loosemore HA, Farmani R. Optimization of building thermal design and control by multi-criterion genetic algorithm. Energy Build 2002;34.

[16] Antonini E, Longo D, Gianfrate V. Towards nZEB: Modular pre-assembled steel systems for residential buildings 2014.

[17] Micono C, Zanzottera G. Energy modeling for NZEBs: A case-study. Energy Procedia 2015;78:2034–9. doi:10.1016/j.egypro.2015.11.202.

[18] Carpino C, Bevilacqua P, Bruno R, Arcuri N. Energy performances of a passive house for Mediterranean climate: A case study. Build Simul Appl 2015.

[19] Jakica N, Zanelli A. Knowledge based expert system tool for optimization of the complex glass BIPV system panel layout on the cable net structural skin. Energy Procedia 2015;78:2226–31. doi:10.1016/j.egypro.2015.11.339.

[20] Edited by Andreas Athienitis and William O'Brien. Modeling, design, and optimization of net-zero energy buildings. 2015.

[21] Uribe OH, Martin JPS, Garcia-Alegre MC, Santos M, Guinea D. Smart building: Decision making architecture for thermal energy management 2015.

[22] Odonkor P, Lewis K, Wen J, Wu T. Adaptive Energy Optimization Toward Net-Zero Energy Building Clusters 2016.

[23] Mørck OC. Concept Development and Technology Choices for the More-connect Pilot Energy Renovation of Three Apartment Blocks in Denmark 2016.

[24] Raimondi A, Santucci D, Bevilacqua S, Corso A. Daylight Autonomy as a Driver for Office Building Retrofitting 2016.

[25] Ascione F, D'Agostino D, Marino C, Minichiello F. Earth-to-air heat exchanger for NZEB in Mediterranean climate. Renew Energy 2016;99:553–63. doi:10.1016/j.renene.2016.07.025.

[26] Kolokotsa D, Rovas D, Kosmatopoulos E, Kalaitzakis K. A roadmap towards intelligent net zero- and positive-energy buildings. Sol Energy 2011;85:3067–84. doi:10.1016/j.solener.2010.09.001.

[27] Kazmi H, D'Oca S, Delmastro C, Lodeweyckx S, Corgnati SP. Generalizable occupant-driven optimization model for domestic hot water production in NZEB. Appl Energy 2016;175:1–15. doi:10.1016/j.apenergy.2016.04.108.

[28] Suárez R, Fragoso J. Passive strategies for energy optimisation of social housing in the Mediterranean climate [Estrategias pasivas de optimización energética de la vivienda social en clima mediterráneo] 2016.

[29] Aste N, Manfren M, Marenzi G. Building Automation and Control Systems and performance optimization: A framework for analysis 2017.

[30] Todorovic B. Towards Zero Energy Buildings: New and Retrofitted Existing Buildings 2011.

[31] Adhikari RS, Aste N, Manfren M. Optimization concepts in district energy design and management – A case study. Energy Procedia 2012;14:1386–91. doi:10.1016/j.egypro.2011.12.1106.

[32] Doust N, Masera G, Imperadori M. A study on design optimization of a near net-zero energy house. Int J Hous Sci 2013.

[33] Rayegan R, Tao YX. Optimal collector type and temperature in a solar organic rankine cycle system for building-scale power generation in hot and humid climate 2013.

[34] Hong T, Lee M, Kim J. Development of the process for deploying optimal photovoltaic system. Energy Procedia 2014;61:1544–8.

doi:10.1016/j.egypro.2014.12.166.

[35] Rey J, Zubiaurre J, Beristain B, Irusta D. Energy and comfort. Analysis of integrated “low-ex” solutions. Int J Energy a Clean Environ 2014;15.

[36] Buonomano A, Palombo A. NZEBs design and simulation: A new tool for dynamic energy performance analyses 2014.

[37] Ferrara M, Fabrizio E, Virgone J, Filippi M. A simulation-based optimization method for cost-optimal analysis of nearly Zero Energy Buildings. Energy Build 2014;84:442–57. doi:10.1016/j.enbuild.2014.08.031.

[38] Ferrara M, Virgone J, Fabrizio E, Kuznik F, Filippi M. Modelling Zero Energy Buildings: Parametric study for the technical optimization. Energy Procedia 2014;62:200–9. doi:10.1016/j.egypro.2014.12.381.

[39] Aelenei L, Paduos S, Petran H, Tarrés J, Ferreira A, Corrado V, et al. Implementing cost-optimal methodology in existing public buildings. Energy Procedia 2015;78:2022–7. doi:10.1016/j.egypro.2015.11.197.

[40] Carlucci S, Cattarin G, Causone F, Pagliano L. Multi-objective optimization of a nearly zero-energy building based on thermal and visual discomfort minimization using a non-dominated sorting genetic algorithm (NSGA-II). Energy Build 2015;104:378–94. doi:10.1016/j.enbuild.2015.06.064.

[41] Penna P, Prada A, Cappelletti F, Gasparella A. Multi-objectives optimization of Energy Efficiency Measures in existing buildings. Energy Build 2015;95:57–69. doi:10.1016/j.enbuild.2014.11.003.

[42] Becchio C, Bottero MC, Corgnati SP, Ghiglione C. nZEB design: Challenging between energy and economic targets. Energy Procedia 2015;78:2070–5. doi:10.1016/j.egypro.2015.11.226.

[43] Buonomano A, Montanaro U, Palombo A, Vicidomini M. NZEBs in Mediterranean climates: Energy design and optimization for a non-residential building. Energy Procedia 2015;82:458–64. doi:10.1016/j.egypro.2015.11.844.

[44] Méndez Echenagucia T, Capozzoli A, Cascone Y, Sassone M. The early design stage of a building envelope: Multi-objective search through heating, cooling and lighting energy performance analysis. Appl Energy 2015;154:577–91. doi:10.1016/j.apenergy.2015.04.090.

[45] Testi D, Schito E, Conti P. Cost-optimal Sizing of Solar Thermal and Photovoltaic Systems for the Heating and Cooling Needs of a Nearly Zero-Energy Building: Design Methodology and Model Description. Energy Procedia 2016;91:517–27. doi:10.1016/j.egypro.2016.06.286.

[46] Testi D, Schito E, Conti P. Cost-optimal Sizing of Solar Thermal and Photovoltaic Systems for the Heating and Cooling Needs of a Nearly Zero-Energy Building: The Case Study of a Farm Hostel in Italy. Energy Procedia

2016;91:528–36. doi:10.1016/j.egypro.2016.06.286.

[47] Ferrara M, Fabrizio E, Virgone J, Filippi M. Energy systems in cost-optimized design of nearly zero-energy buildings. Autom Constr 2016;70:109–27. doi:10.1016/j.autcon.2016.06.007.

[48] Buonomano A, De Luca G, Montanaro U, Palombo A. Innovative technologies for NZEBs: An energy and economic analysis tool and a case study of a non-residential building for the Mediterranean climate 2016.

[49] Baglivo C, Congedo PM, Fazio A, Laforgia D. Multi-objective optimization analysis for high efficiency external walls of zero energy buildings (ZEB) in the Mediterranean climate. Energy Build 2014;84:483–92. doi:10.1016/j.enbuild.2014.08.043.

[50] Ascione F, Bianco N, De Masi RF, De Stasio C, Mauro GM, Vanoli GP. Multi-objective optimization of the renewable energy mix for a building. Appl Therm Eng 2016;101:612–21. doi:10.1016/j.applthermaleng.2015.12.073.

[51] Ascione F, De Masi RF, de Rossi F, Ruggiero S, Vanoli GP. Optimization of building envelope design for nZEBs in Mediterranean climate: Performance analysis of residential case study. Appl Energy 2016;183:938–57. doi:10.1016/j.apenergy.2016.09.027.

[52] Ascione F, Bianco N, De Masi RF, Mauro GM, Vanoli GP. Energy retrofit of educational buildings: Transient energy simulations, model calibration and multi-objective optimization towards nearly zero-energy performance. Energy Build 2017;144:303–19. doi:10.1016/j.enbuild.2017.03.056.

[53] Baglivo C, Congedo PM, Fazio A. Multi-criteria optimization analysis of external walls according to ITACA protocol for zero energy buildings in the mediterranean climate. Build Environ 2014;82:467–80. doi:10.1016/j.buildenv.2014.09.019.

[54] Ferrara M, Fabrizio E, Virgone J, Filippi M. Appraising the effect of the primary systems on the cost optimal design of nZEB: A case study in two different climates. Energy Procedia 2015;78:2028–33. doi:10.1016/j.egypro.2015.11.200.

[55] Baglivo C, Congedo PM, D'Agostino D, Zacà I. Cost-optimal analysis and technical comparison between standard and high efficient mono-residential buildings in a warm climate. Energy 2015;83:560–75. doi:10.1016/j.energy.2015.02.062.

[56] Congedo PM, Baglivo C, D'Agostino D, Zacà I. Cost-optimal design for nearly zero energy office buildings located in warm climates. Energy 2015;91:967–82. doi:10.1016/j.energy.2015.08.078.

[57] Becchio C, Dabbene P, Fabrizio E, Monetti V, Filippi M. Cost optimality assessment of a single family house: Building and technical systems solutions for the nZEB target. Energy Build 2015;90:173–87.

doi:10.1016/j.enbuild.2014.12.050.

[58] Baglivo C, Congedo PM. Design method of high performance precast external walls for warm climate by multi-objective optimization analysis. Energy 2015;90:1645–61. doi:10.1016/j.energy.2015.06.132.

[59] Ascione F, Bianco N, De Masi RF, Mauro GM, Vanoli GP. Design of the Building Envelope: A Novel Multi-Objective Approach for the Optimization of Energy Performance and Thermal Comfort. Sustainability 2015;7:10809–36. doi:10.3390/su70810809.

[60] Kurnitski J, Saari A, Kalamees T, Vuolle M, Niemelä J, Tark T. Cost optimal and nearly zero (nZEB) energy performance calculations for residential buildings with REHVA definition for nZEB national implementation. Energy Build 2011;43:3279–88. doi:10.1016/j.enbuild.2011.08.033.

[61] Kurnitski J, Saari A, Kalamees T, Vuolle M, Niemelä J, Tark T. Cost optimal and nearly zero energy performance requirements for buildings in Estonia. Est J Eng 2013;19:183–202. doi:10.3176/eng.2013.3.02.

[62] Hamdy M, Hasan A, Sirén K. A multi-stage optimization method for cost-optimal and nearly-zero-energy building solutions in line with the EPBD-recast 2010. Energy Build 2013;56:189–203. doi:10.1016/j.enbuild.2012.08.023.

[63] Niemelä T, Kosonen R, Jokisalo J. Cost-optimal energy performance renovation measures of educational buildings in cold climate. Appl Energy 2016;183:1005–20. doi:10.1016/j.apenergy.2016.09.044.

[64] Pal SK, Takano A, Alanne K, Palonen M, Sirén K. A multi-objective life cycle approach for optimal building design: A case study in Finnish context. J Clean Prod 2017;143:1021–35. doi:10.1016/j.jclepro.2016.12.018.

[65] Hamdy M, Sirén K, Attia S. Impact of financial assumptions on the cost optimality towards nearly zero energy buildings – A case study. Energy Build 2017;153:421–38. doi:10.1016/j.enbuild.2017.08.018.

[66] Asadi E, da Silva MG, Antunes CH, Dias L. A multi-objective optimization model for building retrofit strategies using TRNSYS simulations, GenOpt and MATLAB. Build Environ 2012;56:370–8. doi:10.1016/j.buildenv.2012.04.005.

[67] Asadi E, Da Silva MG, Antunes CH, Dias L. Multi-objective optimization for building retrofit strategies: A model and an application. Energy Build 2012;44:81–7. doi:10.1016/j.enbuild.2011.10.016.

[68] Oliveira Panão MJN, Rebelo MP, Camelo SML. How low should be the energy required by a nearly Zero-Energy Building? the load/generation energy balance of Mediterranean housing. Energy Build 2013;61:161–71. doi:10.1016/j.enbuild.2013.02.031.

[69] Stadler M, Groissböck M, Cardoso G, Marnay C. Optimizing Distributed Energy

Resources and building retrofits with the strategic DER-CAModel. Appl Energy 2014;132:557–67. doi:10.1016/j.apenergy.2014.07.041.

[70] Ferreira M, Almeida M, Rodrigues A. Cost-optimal energy efficiency levels are the first step in achieving cost effective renovation in residential buildings with a nearly-zero energy target. Energy Build 2016;133:724–37. doi:10.1016/j.enbuild.2016.10.017.

[71] Ruiz PA, de la Flor FJS, Felix JLM, Lissén JMS, Martín JG. Applying the HVAC systems in an integrated optimization method for residential building's design. A case study in Spain. Energy Build 2016;119:74–84.

[72] Aparicio Ruiz P, Guadix Martín J, Salmerón Lissén JM, Sánchez De La Flor FJ. An integrated optimisation method for residential building design: A case study in Spain. Energy Build 2014;80:158–68. doi:10.1016/j.enbuild.2014.05.020.

[73] Antipova E, Boer D, Guillén-Gosálbez G, Cabeza LF, Jiménez L. Multi-objective optimization coupled with life cycle assessment for retrofitting buildings. Energy Build 2014;82:92–9. doi:10.1016/j.enbuild.2014.07.001.

[74] Fonseca I Casas P, Fonseca I Casas A, Garrido-Soriano N, Casanovas J. Formal simulation model to optimize building sustainability. Adv Eng Softw 2014;69:62–74. doi:10.1016/j.advengsoft.2013.12.009.

[75] Iturriaga E, Aldasoro U, Campos-Celador A, Sala JM. A general model for the optimization of energy supply systems of buildings. Energy 2017;138:954–66. doi:10.1016/j.energy.2017.07.094.

[76] Konis K, Gamas A, Kensek K. Passive performance and building form: An optimization framework for early-stage design support. Sol Energy 2016;125:161–79. doi:10.1016/j.solener.2015.12.020.

[77] Brinks P, Kornadt O, Oly R. Development of concepts for cost-optimal nearly zero-energy buildings for the industrial steel building sector. Appl Energy 2016;173:343–54. doi:10.1016/j.apenergy.2016.04.007.

[78] Dillon K, Colton J. A design methodology for the economic design of vaccine warehouses in the developing world. Build Environ 2014;82:160–70. doi:10.1016/j.buildenv.2014.07.024.

[79] European Commission. Guidelines accompanying Commission Delegated Regulation (EU) No 244/2012 of 16 January 2012 supplementing Directive 2010/31/EU of the European Parliament and of the Council. 2012.

[80] Diakaki C, Grigoroudis E, Kolokotsa D. Towards a multi-objective optimization approach for improving energy efficiency in buildings. Energy Build 2008;40:1747–54. doi:10.1016/j.enbuild.2008.03.002.

[81] Malatji EM, Zhang J, Xia X. A multiple objective optimisation model for building energy efficiency investment decision. Energy Build 2013;61:81–7.

doi:10.1016/j.enbuild.2013.01.042.

[82] Lee B, Hensen JLM. Towards zero energy industrial halls - Simulation and optimization with integrated design approach 2013.

[83] Wang B, Xia X, Zhang J. A multi-objective optimization model for the life-cycle cost analysis and retrofitting planning of buildings. Energy Build 2014;77:227–35. doi:10.1016/j.enbuild.2014.03.025.

[84] Sun Y, Huang P, Huang G. A multi-criteria system design optimization for net zero energy buildings under uncertainties. Energy Build 2015;97:196–204. doi:10.1016/j.enbuild.2015.04.008.

[85] Kim HY, Kang HJ. A Study on Development of a Cost Optimal and Energy Saving Building Model: Focused on Industrial Building. Energies 2016;9.

[86] Schwartz Y, Raslan R, Mumovic D. Implementing multi objective genetic algorithm for life cycle carbon footprint and life cycle cost minimisation: A building refurbishment case study. Energy 2016;97:58–68. doi:10.1016/j.energy.2015.11.056.

[87] Touloupaki E, Theodosiou T. Optimization of external envelope insulation thickness: A parametric study 2017.

[88] Diakaki C, Grigoroudis E, Kabelis N, Kolokotsa D, Kalaitzakis K, Stavrakakis G. A multi-objective decision model for the improvement of energy efficiency in buildings. Energy 2010;35:5483–96. doi:10.1016/j.energy.2010.05.012.

[89] Naboni E, Maccarini A, Korolija I, Zhang Y. Comparison of Conventional, Parametric and Evolutionary Optimization Approaches for the Architectural Design of Nearly Zero Energy Buildings. Proc BS2013 2013.

[90] Pikas E, Thalfeldt M, Kurnitski J. Cost optimal and nearly zero energy building solutions for office buildings. Energy Build 2014;74:30–42. doi:10.1016/j.enbuild.2014.01.039.

[91] Negendahl K, Nielsen TR. Building energy optimization in the early design stages: A simplified method. Energy Build 2015;105:88–99.

[92] Yu Z (Jerry), Chen J, Sun Y, Zhang G. A GA-based system sizing method for net-zero energy buildings considering multi-criteria performance requirements under parameter uncertainties. Energy Build 2016;129:524–34. doi:10.1016/j.enbuild.2016.08.032.

[93] Zhang S, Huang P, Sun Y. A multi-criterion renewable energy system design optimization for net zero energy buildings under uncertainties. Energy 2016;94:654–65. doi:10.1016/j.energy.2015.11.044.

[94] Kang HJ. Development of an nearly Zero Emission Building (nZEB) life cycle cost assessment tool for fast decision making in the early design phase. Energies

2017;10. doi:10.3390/en10010059.

[95] Touloupaki E, Theodosiou T. Energy Performance Optimization as a Generative Design Tool for Nearly Zero Energy Buildings. Procedia Eng 2017;180:1178–85. doi:10.1016/j.proeng.2017.04.278.

[96] Ferdyn-Grygierek J, Grygierek K. Multi-Variable Optimization of Building Thermal Design Using Genetic Algorithms. Energies 2017;10.

[97] Lu Y, Wang S, Zhao Y, Yan C. Renewable energy system optimization of low/zero energy buildings using single-objective and multi-objective optimization methods. Energy Build 2015;89:61–75. doi:10.1016/j.enbuild.2014.12.032.

[98] Lu Y, Wang S, Yan C, Shan K. Impacts of renewable energy system design inputs on the performance robustness of net zero energy buildings. Energy 2015;93:1595–606. doi:10.1016/j.energy.2015.10.034.

[99] Lu Y, Wang S, Yan C, Huang Z. Robust optimal design of renewable energy system in nearly/net zero energy buildings under uncertainties. Appl Energy 2017;187:62–71. doi:10.1016/j.apenergy.2016.11.042.

[100] Balijepalli VSKM, Khaparde SA. Effect of cost related parameters on optimization of Zero Net Energy Buildings. IEEE Power Energy Soc Gen Meet 2014;2014-Octob:1–5. doi:10.1109/PESGM.2014.6938811.

[101] Deb K, Pratab S, Agarwal S, Meyarivan T. A Fast and Elitist Multiobjective Genetic Algorithm: NGSA-II. IEEE Trans Evol Comput 2002;6:182–97. doi:10.1109/4235.996017.

[102] Hamdy M, Nguyen A-T, Hensen JLM. A performance comparison of multi-objective optimization algorithms for solving nearly-zero-energy-building design problems. Energy Build 2016;121:57–71. doi:10.1016/j.enbuild.2016.03.035.

[103] Mohamed H, Hasan A, Sirén K. Combination of Optimisation Algorithms for a Multi-Objective Building Design Problem. Elev Int IBPSA Conf 2009:173–9.

[104] Longo S, Montana F, Riva Sanseverino E. A review on optimization and cost-optimal methodologies in low-energy buildings design and environmental considerations. Sustain Cities Soc 2019;45:87–104.

[105] Asdrubali F. The role of Life Cycle Assessment (LCA) in the design of sustainable buildings: thermal and sound insulating materials. EURONOISE 2009 - Oct. 26-28, Edinburgh, Scotl., 2009.

Chapter Four – Development of the model for the holistic optimisation of buildings and building clusters

4.1. Introduction and methodology

As stated in the previous chapters, the idea for the development of a comprehensive model for the performance optimisation of buildings and building clusters was suggested by many aspects: regulations on building energy performance, a very high number of alternatives available on the market, the very low rate of refurbishment in developed countries, the scarce inclusion of the life cycle thinking in the optimisation of buildings and the requirement of interventions to be cost-effective.

The development of this framework for the optimisation of the performance of buildings and building clusters was conceived to make it as flexible as possible, to be applicable by each kind of stakeholder as policymakers or building designers, without lacking in accuracy and scientific rigorousness, and to allow the compliance with the regulations.

The method is mainly based on the combination of the following techniques:

- Building physics simulation, allowing an accurate assessment of the use phase final energy demand of the constructions;
- LCA method, that was exploited to evaluate the most common performance indicators, thus ensuring a holistic point of view and avoiding the phase-shifting phenomenon;
- Economic analysis, adopted to calculate the expenditure related to the interventions, providing the investors with a preliminary estimation of their investment;
- Optimisation algorithms, in order to compare a representative number of scenarios automatically with a smart investigation algorithm, not just based on a random search, identifying the best compromise solution between the criteria through a multi-objective logic.

The main foundation of these techniques was outlined in Chapter 2. However, it is strongly recommended to gain a good background on the various topics recapped above before addressing a study on the optimisation of building performance. Beginners should find useful tips in the considerations contained in this chapter.

In LCA literature, many indicators are usually employed to assess resource use (energy and raw materials depletion etc.), environmental impacts (global warming, ozone depletion, acidification etc.), or additional environmental information (hazardous waste, etc.) [1,2]. To select the indicators for the present PhD project, the existing literature was deeply investigated. The main attention was dedicated to reports of IEA projects on energy saving and LCA of buildings. In detail, Annex 31 "Energy Related Environmental Impact of Buildings" [3], Annex 56 "Cost-Effective Energy & CO_2 Emissions Optimization in Building Renovation" [4] and Annex 57 "Evaluation of Embodied Energy and CO_2 Equivalent Emissions for Building Construction" [5] were analysed. Furthermore, since the current international agreements and policies mainly focus on the energy saving, as the EU EPBD [6], and on the greenhouse effect reduction, as the Paris Agreement adopted at the Paris climate conference (COP21) [7], the indicators employed as objective functions in the present project also considered the indications of these regulations.

The energy-saving was ensured through the assessment of the CED, that is given by the sum of an embodied term [8] and an operational term. Although the CED is often split into renewable and non-renewable contributions, this approach was disregarded in this project, in order to ensure the effective attainment of energy saving, regardless from the origin, further reducing the number of objective functions to be assessed. The environmental impact was minimised through the assessment of the GWP that was composed of an embodied and an operational contribution as well. Moreover, these two indicators were also employed during the activities of the IEA EBC Annex 56, focused on the LCA of buildings renovation [9].

The economic analysis was based on the assessment of main costs terms, *i.e.* investments and operating costs, through the evaluation of the Net Present Value (NPV). Replacement costs related to building components were assessed only when reliable data on the useful life of components were available. Although this cost function does not include terms as recurring costs, demolition costs or residual values, it can be considered as a rough estimation of the LCC. In detail, several journal papers involving the LCC of buildings only evaluate the investment (or construction), the operating and, sometimes, the recurring and maintenance costs [10,11,20,21,12–19], mainly because of lack of reliable data on the end-of-life costs. Nevertheless, this OF was defined as "cost" rather than "LCC" in the rest of this thesis to indicate that some important contributions are missing.

Another key point of the present study was the employment of free available input data and software, when possible. For example, most of the life cycle-specific impacts were derived from public databases as Ökobau [22] or ELCD [23], representative of the German and Danish contexts, or were drawn from some EPDs. At the same way, only data from public market reports or scientific papers were employed for the economic analysis, while Molio economic database was consulted for the Danish context [24]. With specific regard to the Vietnamese context, the data collection was mainly based on public reports from EVN, the main national grid operator, and on literature papers. Since no LCA study was found on Vietnamese products or processes, average literature data were considered for both Italy and Vietnam in that study, assuming that materials and equipment are imported from foreign countries in both cases. The unique differentiation was applied to the embodied impact due to electricity generation, since the Vietnamese power mix is still mainly based on coal-fired thermal power plants. This parameter was estimated through a methodology that, although is specific for the Italian context, was considered as a good proxy of the actual impact.

For what above, the results of the case studies that are illustrated in the following Chapters 5 and 6 should be considered as the demonstration that the methodology here depicted can be profitably employed to attain reasonable design or retrofit solutions for a case study, rather than obtaining nonsenses or resulting in diverging simulation. In order to roughly validate the methodology and the input data, the results were compared with the common design practice in each context. The outcome of the comparison was that simulations results usually correspond to the actual retrofit or design solutions, somehow confirming that the data collection was performed with a sufficient level of accuracy. Nevertheless, these solutions should not be considered as guidelines or specific indication to be followed for the design or renovation of buildings.

The same philosophy chosen for data collection was adopted for the software tools used for the simulations and optimisations. In detail, the energy performance tool EnergyPlus was preferred to more user-friendly analogues as TRNSYS or IDA-ICE, and the building optimisation software MOBO was selected among many other commercial tools. The employment of Be18 for the real case study in Denmark was guided by the legal requirement of using this tool for the energy performance simulation, thus making the results comparable with other studies in the same country. MATLAB environment was adopted for the development of the model for equipment optimisation as it is very easy to use and it is broadly used in both research and industrial applications.

The methodology for the optimisation of the life cycle performance of buildings and building clusters conceived in this project is fully described in the following sections. In detail, the single building optimisation was approached in a two-step framework, with the first oriented at reducing the energy demand and the second being employed for the preliminary design of the equipment. The approach adopted for the second step was employed for the building clusters optimisation as well.

4.2. Single building performance optimisation

In the developed methodology, the optimisation of a single building was carried out in a dual step approach, with the first one aimed at optimising envelope features and the latter used to identify optimal design and schedule for HVAC and RES equipment. This division allows to decouple the two main phases of the design of a building and was made in order to provide separate results for the passive or demand part of the retrofit, making the result applicable to a broader range of locations with varying restrictions regarding energy supply. Furthermore, this approach reflects somehow the common design practice, since the envelope design is related to the expertise of architects or civil engineers while the equipment design belongs to the skill set of mechanical engineers.

Step 1 involves the combination of a building physics simulation tool and an optimisation software, and exploits a multi-objective heuristic algorithm, while Step 2, where the outputs of the load optimisation are used as an input, was carried out through a MATLAB script developed using scalarization technique to combine the objective functions and the Branch and Bound MILP algorithm. The main features of these two steps are further detailed in the following sections.

4.2.1. Step 1 – Building loads optimisation

4.2.1.1. Variables and objective functions

In the method of Step 1, different techniques and areas of knowledge are combined with the aim of obtaining the optimal set of retrofit options for the envelope of an existing building or the envelope features of a preliminary design of a new building. In order to correctly evaluate the final energy demand of each building configuration, a simulation-based optimisation through BPS was preferred to a simplified building loads estimation method. This approach ensures the detailed evaluation of energy performance during the use phase of the building, and the adoption of a multi-objective optimisation allows comparing multiple scenarios through a search algorithm (instead of a random comparison) and obtaining an optimal combination of available retrofit options according to multiple aspects (economic, energy and environmental).

In this section, the energy loads of a building are to be intended as space heating and cooling loads, since the other energy demands as electricity or domestic hot water demands are independent on the variables. Thus, the optimisation of the building loads was performed using the envelope features as variables. For this reason, Step 1 may be also referred to as *envelope optimisation*. More in detail, examples of variables may be the insulation materials and their thicknesses, the thermal mass materials and their thicknesses, the external cladding, the windows frames and glazing, the orientation of the building.

In this step, the optimised functions are the use phase final energy demand evaluated in ideal conditions (with HVAC having unit efficiency), the embodied energy (EE), the embodied GWP (EGWP), and the investment cost. In Step 2, these functions are aggregated in the three main objective functions discussed in Section 4.1. The use phase energy demand is evaluated in final energy terms in Step 1 since the equipment is still not specified. This term is transformed in use phase primary energy, use phase GWP and use phase costs in Step 2 through the conversion coefficients related to each equipment's technology. Since aspects as daylight or occupants behaviour were not assessed in this study, the variables influencing the final energy use are only related to the thermal loads for space heating and cooling, and the ideal use phase final energy demand is given by the sum of yearly heating and cooling requirements of the building, multiplied by the assumed useful life of the building, as in Eq. (4.1):

$$OF_1 = Use\ Phase\ Energy\ Demand = UL \cdot \sum_{t=1}^{8760} \sum_{y=1}^{Y} \left(H_{t,y} + C_{t,y} \right) \tag{4.1}$$

where *H* and *C* are the hourly heating and cooling loads of each *y-th* thermal zone required to keep the indoor temperature fixed at the set-point at the *t-th* hour of the year, *Y* is the number of thermal zones in the buildings, 8760 is the number of hours in one standard year and *UL* is the building useful life expressed in years. The remaining objective functions were evaluated as differential terms, considering that the impacts related to the existing building structure are independent on the renovation and assessing only the impacts related to the retrofit actions. Thus, EGWP, EE and the Investment Cost were evaluated according to Eqn. (4.2) - (4.4), respectively:

$$OF_2 = EGWP = \sum_{r=1}^{R} m_r \cdot UEC_r \tag{4.2}$$

$$OF_3 = EE = \sum_{r=1}^{R} m_r \cdot UEE_r \tag{4.3}$$

$$OF_4 = Investment\ Cost = \sum_{r=1}^{R} m_r \cdot UP_r \tag{4.4}$$

where *m* is the significant parameter of the *r-th* retrofit action, *R* is the total number of retrofit actions, and *UEC, UEE* and *UP* are the unit embodied carbon factor, the unit embodied energy factor and the unit price of the *r-th* action, respectively. Examples of the significant parameters are the thicknesses for insulation and thermal mass materials and the related Boolean variable for cladding materials or glazed components. The unit impacts and prices were calculated in order to take into account the ratio between the useful life of the component and the residual life of the building, thus including the replacement during the life cycle. To take into account also for the variable value of the money along the life cycle of the building, the costs related to the maintenance of the building in the *UP* term were actualized through the Uniform Series Present-Worth Factor (*USPWF*), as in Eq. (4.5) [25]:

$$USPWF = \frac{\left(1 + i_{real}\right)^n - 1}{i_{real} \cdot \left(1 + i_{real}\right)^n} \tag{4.5}$$

where *n* is the number of years from the installation of the retrofit action and i_{real} is the real interest rate, calculated using the nominal interest rate i_{nom} and an average inflation rate *f* for the building sector according to in Eq. (4.6):

$$i_{real} = \frac{1 + i_{nom}}{1 + f} - 1 \tag{4.6}$$

4.2.1.2. Software tools

Although the method described in this thesis aims to be generic, some criteria were established to select the software to be used for the case studies. For this step, the following criteria were adopted:

- Research-oriented;
- Interoperability;
- Freeware.

The following review of software tools and the description of their interoperability was developed during the internship at the Research and Development laboratory of Engineering Ingegneria Informatica S.p.A..

According to [26], the most popular BPS tool in the literature on building simulation-based optimisation are TRNSYS [27], IDA ICE [28] and EnergyPlus [29]. Although each of these software has its own peculiarities, their results can be considered to be equivalent [30–32]. The interoperability with optimisation software is also guaranteed by each of these tools, being often employed in previous studies, but EnergyPlus is the only one of them to be freeware since it was developed by the United States Department of Energy rather than a company. EnergyPlus is a BPS program developed in 2000 combining the best features from two existing famous BPS tools, BLAST and DOE-2 [33], including even additional functionalities. It is mainly composed by a simulation engine, there is a limited user interface, and the code is written in Fortran 90 [34]. An example of the input mask of EnergyPlus version 9.0.1 for Microsoft Windows is provided in Fig. 4.1, while the main view of EnergyPlus version 8.7.0 for Macintosh is shown in Fig. 4.2. The simulations for this project were mainly run on a quad-code MacBook Pro. Nevertheless, since the Macintosh version of EnergyPlus has a reduced interface, most of the simulations were conducted on a Virtual Machine implementing a Microsoft Windows operating system.

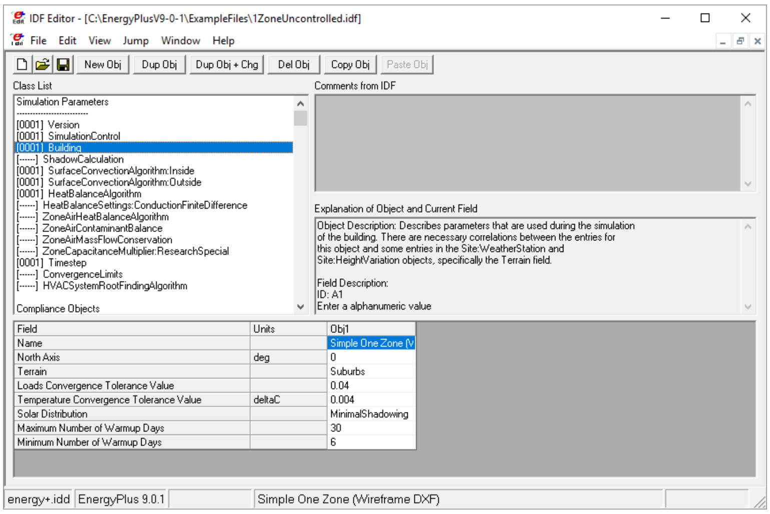

Fig. 4.1. Example of input mask of EnergyPlus version 9.1.0 for Windows

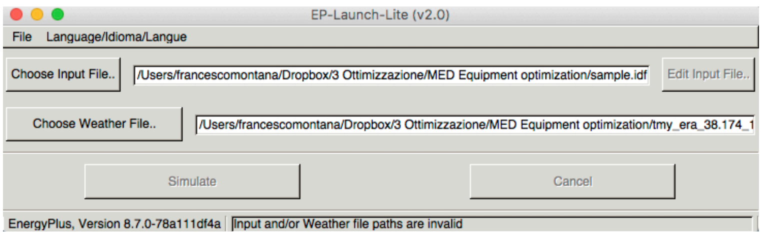

Fig. 4.2. Main mask of EnergyPlus version 8.7.0 for Macintosh

EnergyPlus allows calculating the heating and cooling loads necessary to maintain a fixed temperature set point, the operation of the HVAC systems and the energy consumption of equipment. The required input data are the stratigraphy and thermal description of each building structure component, the users' behaviour schedule, and the outdoor boundary conditions, *e.g.* temperature, relative humidity, solar radiation. Further details may be included for the energy systems like HVAC, cogeneration or photovoltaic, with both simplified and detailed models available, depending on the preferred level of detail of the model. The main algorithm for the heating and cooling load calculation is the Heat Balance Method [35]. Being a dynamic method, a timestep has to be defined; in EnergyPlus, the user can set this value before the simulation, with available values ranging between 10 minutes and 1 hour. Another advantage of EnergyPlus is the availability of the source code on the GitHub online repository, allowing researchers to customise the tool to each specific needs [36].

Although EnergyPlus was selected as the main tool for this project, one of the case studies was developed using Be18 [37], the Danish national energy rating tool. One of the reasons was to show an extension of the methodology to less detailed simulation tools since Be18 is based on a quasi-steady state monthly averaged balance rather than on a dynamic hourly calculation, according to the method shown in the ISO 13790:2008 international standard [38]. This method was uniformly applied in the European Union countries as the reference for the energy rating calculations. A view of the main mask of Be18 is provided in Fig. 4.3, while an example of an input mask is shown in Fig. 4.4.

Regarding the selection of the optimisation software, there are many tools employed in literature on building simulation-based optimisation. The main categorisation can be done between generic optimisation tools, like MATLAB [39], GenOpt [40], modeFRONTIER [41], or MOBO [42], that can be linked to much other software, and customised tools, like TRNOPT [43], jEplus+EA [44], Opt-E-Plus [45], IDA ESBO [46] or BEopt [47], allowing a link only with a specific BPS. Other minor tools specific for EnergyPlus as BCVTB [48] and MLE+ [43] were also investigated. The features of most of the available tools were compared in 2013 by Palonen et al. [49], obtaining the considerations recapped in Table 4.1.

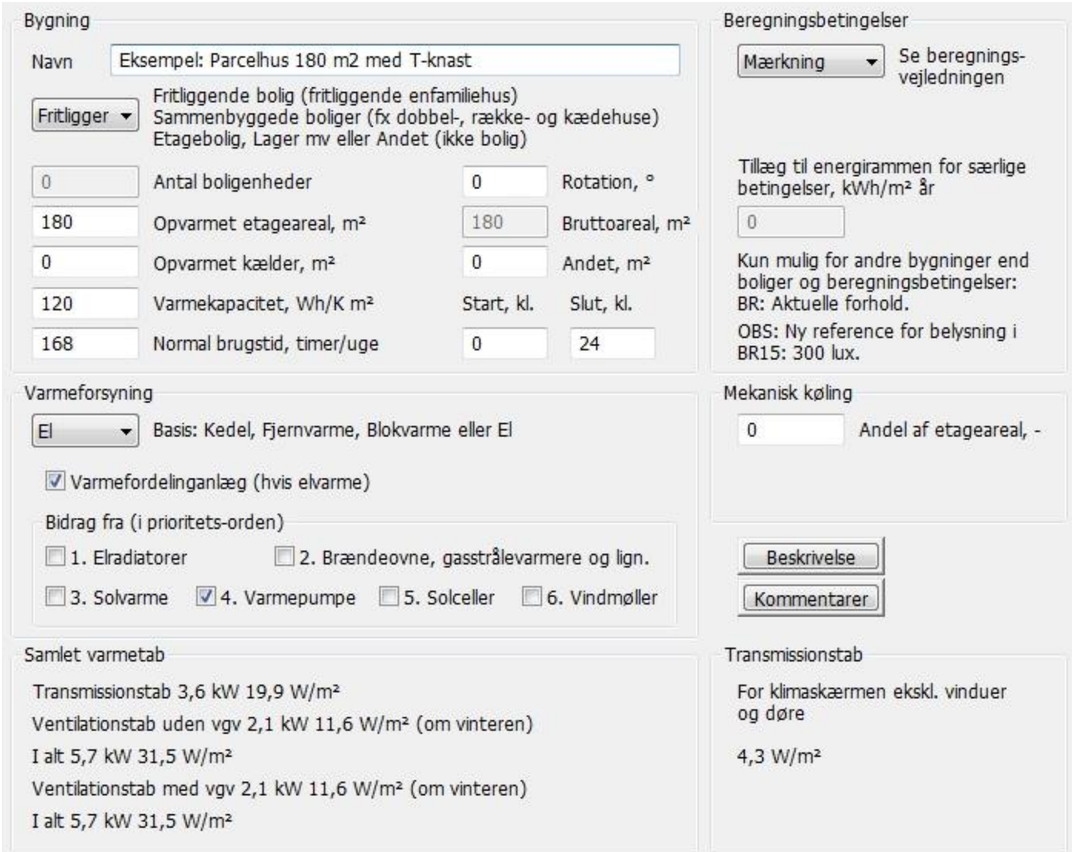

Fig. 4.3. Be18 main input mask (in Danish)

	Ydervægge, tage og gulve	Areal (m²)	U (W/m²K)	b	Ht (W/K)	Dim.Inde	Dim.Ude	Tab (W)
		1376		CtrlClick	243,894			6717,98
+1	Ydervægge (brutto 802,8 m2)	567,8	0,21	1,00	119,238			3815,62
2	Kælderydervægge (brutto 11,4 m2)	3,4	0,21	1,00	0,714			22,848
3	Tag	360,4	0,1	1,00	36,04			1153,28
4	Kælderdæk	313,4	0,24	0,75	56,2118		5	1128,24
5	Skillevægge mod kælder	84	0,4	0,75	25,1106		5	504
6	Kældergulv i trapperum	47	0,2	0,70	6,58		10	94
7								
8								
9								
10								
11								
12								
13								
14								
15								
16								
17								
18								
19								
20								

Fig. 4.4. Example of Be18 input mask, related to the opaque surfaces details (in Danish)

Table 4.1. Comparison between commercial optimisation software

Optimisation Tools		*Freeware*	*Discrete and continuous variables handling*	*Allows MOO*
Generic	MATLAB	No	Yes[1]	Yes
	GenOpt	Yes	Yes	No
	modeFRONTIER	No	Yes	Yes
	MOBO	Yes	Yes	Yes
Customised	TRNOPT	No	Yes	No
	jEPlus+EA	No	No	No
	Opt-E-Plus	Yes	No	No
	BEopt	Yes	No	No

Since all of these tools are research-oriented and allow the interoperability, the first selection criterion was the free availability, but also the possibility to handle continuous and discrete variables at the same time and perform multi-objective optimisations. For these reasons, the unique tool eligible to be employed for this research project was MOBO. Using this tool also involved the advantage of learning how to use a generic tool being linkable with many other BPSs. The main disadvantage was that, being developed only from a few years, its use requires also dealing with bug fixing.

In detail, MOBO was developed in 2013 by researchers of Aalto University and its features were illustrated in [49]. MOBO (Multi Objective Building Optimization tool) was created to provide a freeware able to overcome the limitations of the existing building performance optimisation software, integrating seven different optimisation algorithms (single or multi-objective optimisation, constrained or unconstrained problem, continuous or integer variables) and providing a graphical user interface. MOBO can be combined with EnergyPlus, TRNSYS, IDA-ICE and other BPS tools since it uses only text files as input and outputs. The last version currently available is MOBO Beta 03b, dating back to about mid-2014, suggesting that the project is not being more maintained. Moreover, the technical support is mainly based on the software developers research group, founding their support on the research experience. Nevertheless, the high simplicity and flexibility of this tool largely overbalance its drawbacks. An example of MOBO's input mask is reported in Fig. 4.5, while the online output of MOBO showing the ongoing simulation is shown in Fig. 4.6.

[1] Although the authors of the original reference state that MATLAB optimisation toolbox cannot handle continuous and discrete variables simultaneously, the *intlinprog* function actually can, as shown in Chapters 5 and 6

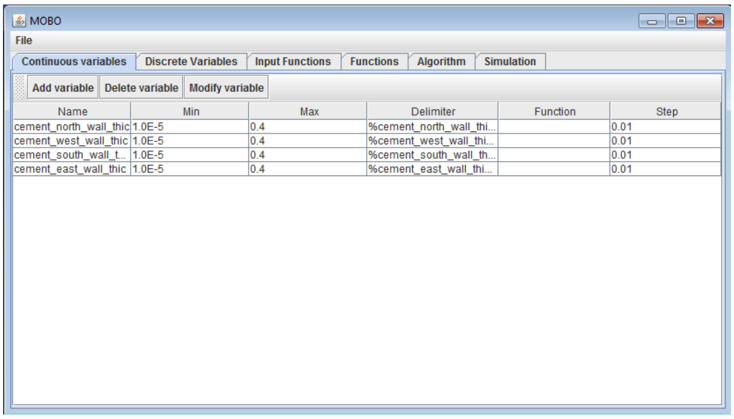

Fig. 4.5. Example of MOBO main input mask

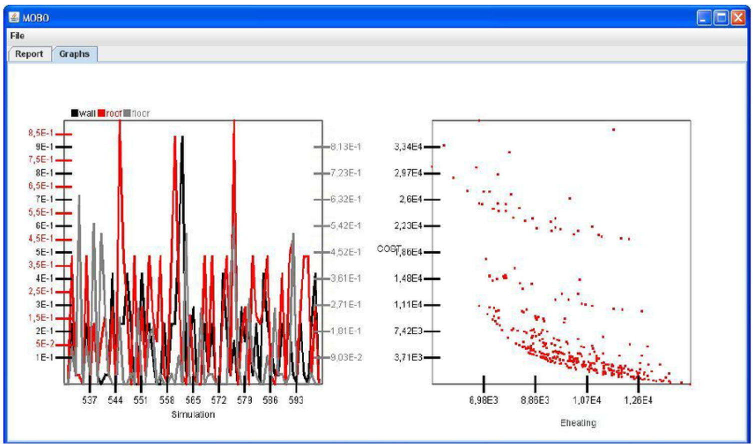

Fig. 4.6. Example of MOBO online output mask

In order to understand the possibilities of MOBO, a literature review on its employment was performed, analysing the papers authored by the software developers, all the studies referencing the paper [49] collected in the *Google Scholar* database, and all the studies with ”MOBO" as a keyword in the *ScienceDirect* database. This research allowed to collect 75 documents, with only 37 of them effectively describing case studies involving the use of MOBO, while the remaining 38 just quoted the above-referenced paper. In detail, 16 journal articles [50,51,60–65,52–59], 12 conference proceedings [66,67,76,77,68–75], and 9 theses [78–86] were investigated. This review was useful to understand how to generically set an optimisation problem in MOBO, although all these studies employed TRNSYS and IDA ICE, thus realizing that the present research was the first, or at least one of the firsts, studies illustrating the combination between MOBO and EnergyPlus.

The interface of MOBO was exploited to set and manage the optimisation problem, specifying the independent variables, their lower and upper bounds, their nature (real or discrete), and equations to calculate the dependent variables, to impose constraints between variables, to collect data from the BPS at each iteration and to specify the objective functions. For example, the thermal mass material thickness was modelled as a real variable while the insulation thickness was modelled as a discrete variable since the insulation is usually manufactured in panels with standardised thickness. The category of discrete variables was exploited to set some auxiliary Boolean variables that were employed even to set the constraints. The data exchange process between MOBO and the BPS is managed using some keywords, known as *delimiters*, which are to be set both in MOBO and in the building model file. Since MOBO was designed to automatically read a text-based output file at each iteration, that is a common feature of the BPS tools, the development of an auxiliary script has been necessary for automating the generation of Be18 output files for the Danish case study. Examples of the input setting masks in MOBO are provided in Fig. 4.7 – Fig. 4.9. In detail:

- In Fig. 4.7, the mask used to set the input discrete variables is shown, where the variable name is specified in the first column, the values of the variables in the second column, and the delimiter in the third column;

- In Fig. 4.8, the mask used to set the dependent variables is shown, where the variable name is specified in the first column, the delimiter in the second column, and the equation to calculate the variable in the third column;

- In Fig. 4.9, the mask used to set the constraints and the objective functions is shown, where the name is specified in the first column, the kind of the equation (equality constraint, inequality constraint, objective function) in the second column, the delimiter in the third column and the related equation in the fourth column.

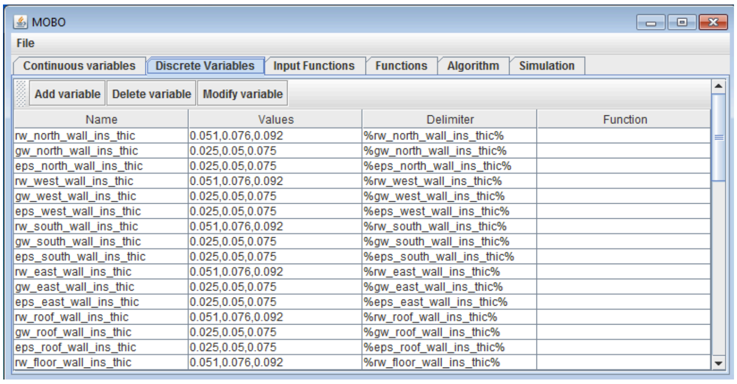

Fig. 4.7. Example of MOBO mask for discrete variables setting

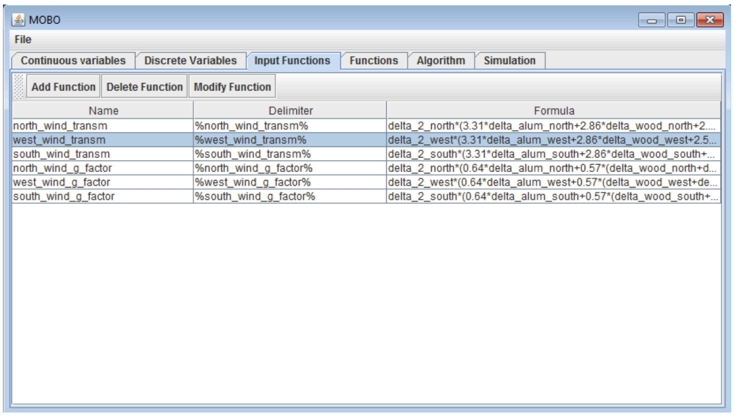

Fig. 4.8. Example of MOBO mask for dependent variables calculation (called "input functions")

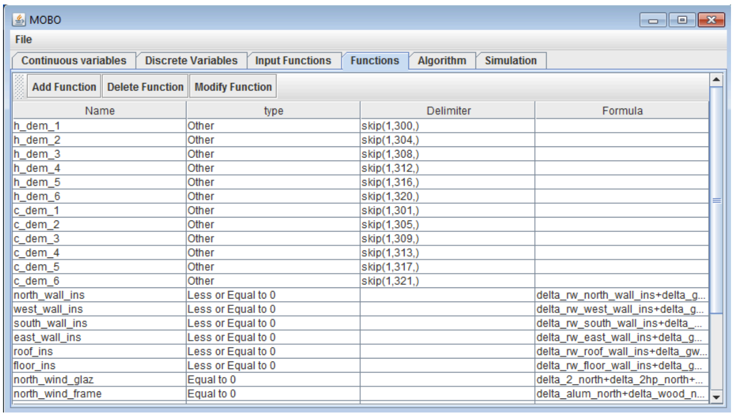

Fig. 4.9. Example of MOBO mask for constraints and objective functions setting (called "functions")

4.2.1.3. Optimisation process

The general process executed in Step 1 is schematised in Fig. 4.10. In detail, a preliminary building model should be developed on the BPS software, representing a preliminary shape of the building in the case of a new design or the existing structure in the case of refurbishment. The physical features of the building components are also specified in this phase. Depending on the case study, different kinds of variables may be decided and specified in the model. Then, the optimisation problem should be specified on the optimisation tool, describing variables and objective functions, and the most suitable algorithm should be selected, setting its parameters. Since the optimisation software does not evaluate the operating final energy demand but it comes from the BPS tool, this objective function lacks a mathematical formulation to be minimised through mathematical derivation, thus requiring the employment of a heuristic optimisation algorithm. When the optimisation loop starts, the algorithm sets the variables values in the preliminary building model at any iteration and then the BPS evaluates the annual operating final energy demand of this building configuration. The optimisation software then assesses and collects the four objective functions and repeats the cycle until the convergence is reached. At the end of the loop, all the details on the buildings evaluated during the optimisation are given as an output of the study, together with the Pareto front.

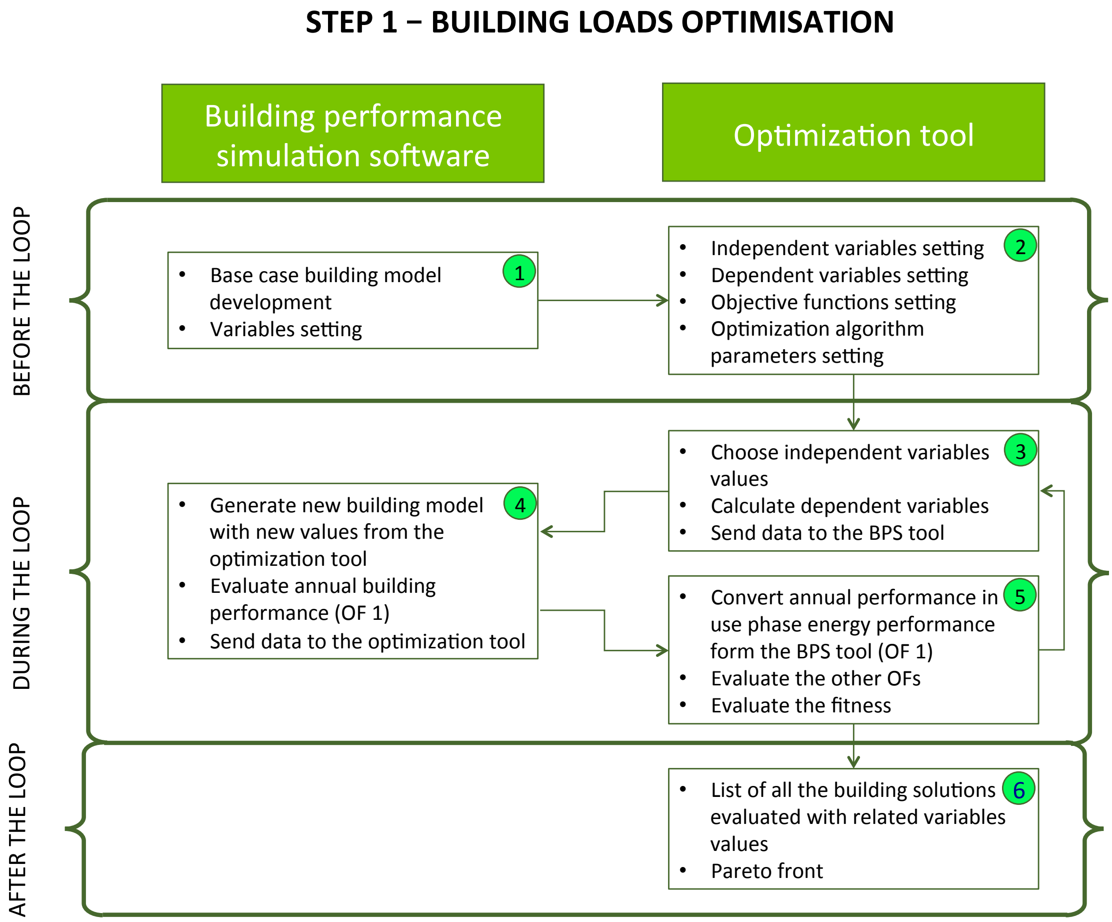

Fig. 4.10. Schematic of the loads' optimisation performed in Step 1

It is important to remark that, since the number of buildings depends on the setting parameters of the optimisation algorithm, they are not the complete set of possible alternatives, *i.e.* the solutions space, but just a subset that was investigated by the algorithm. In the case of genetic algorithms, these solutions features are the result of a progressive improvement from each iteration (generation) to the subsequent one. Instead, in a random search, the fitness of each solution is independent on the number of iterations.

In this kind of problems, the variables may be divided into independent and dependent, since some of the inputs of the BPS may be different from what is calculated by the optimisation tool. For example, with reference to EnergyPlus, if the optimisation sets the windows to have a triple glazing and a wooden frame for a solution, an intermediate calculation of the thermal transmittance and the Solar Heat Gain Coefficient (SHGC) may be required before the transmission of data to the BPS, that in this case requires the numerical values of these quantities.

The output of Step 1 is a set of compromise buildings configurations with very low values of each of the four objective functions, although none of them is the absolute optimum of one of the functions. Since the low values of the objective functions derive from the values assumed by the variables in these solutions, the values of the variables should be analysed to identify the optimal interventions to implement into the analysed building, identifying in this way the optimal envelope configuration.

4.2.1.4. Mathematical model

The mathematical model developed for the present research allows managing the following variables for the renovation of a building:

- Additional insulation material for external walls;
- Additional insulation thickness for external walls;
- Additional thermal mass material for external walls;
- Additional thermal mass thickness for external walls;
- Additional insulation material for roof;
- Additional insulation thickness for roof;
- Additional insulation thickness for basement walls;
- New cladding for external walls;
- New cladding for roof;
- Windows or staircase glazing replacement;
- Windows frame replacement.

The main difference between the mathematical models employed for EnergyPlus and Be18 lays on the calculation of the components' thermal features that are the dependent variables of the mathematical problem. In detail, EnergyPlus calculates the transmittance based on the features of each layer while Be18 requires as an input only the actual transmittance value, disregarding materials and thicknesses. The equations for the dependent variables' calculations are shown in Eq. (4.7)-(4.9), (4.12), (4.15)-(4.20), (4.22)-(4.23), (4.25)-(4.28), while the constraints are reported in Eq. (4.10)-(4.11), (4.13)-(4.14), (4.21), (4.24), (4.29). The dependent variables were calculated according to the laws of the thermodynamics and heat transfer and to the international standards EN 12831:2003 [87], ISO 6946:2007 [88], ISO 10077-1:2006 [89], and ISO

13370:2007 [90]. The variable terms in the following equations were highlighted using a bold font.

HORIZONTAL WALLS (WA)

$$U_{WA} = \frac{1}{\frac{1}{U_{WA.0}} + \sum_{i=1}^{N_{ins}} \left(\frac{\boldsymbol{s_{ins,i}}}{\lambda_{ins.i}} \cdot \boldsymbol{\delta_{ins,i}}\right) + (r_i - r_o) \cdot \sum_{i=1}^{N_{clad,v}} \left(\boldsymbol{\delta_{clad,v,i}}\right) + \sum_{i=1}^{N_{clad,nv}} \left(\frac{\boldsymbol{s_{clad,nv,i}}}{\lambda_{clad.nv.i}} \cdot \boldsymbol{\delta_{clad,nv,i}}\right)} \tag{4.7}$$

$$U_{WABB} = \frac{1}{\frac{1}{U_{EW}} + \left(\sum_{g=0}^{N_{glazing}} \boldsymbol{\delta_{g,balc}}\right) \cdot (r_i - r_o) \cdot \sum_{i=1}^{N_{clad,nv}} \left(\frac{\boldsymbol{s_{clad,nv,i}}}{\lambda_{clad.nv.i}} \cdot \boldsymbol{\delta_{clad,nv,i}}\right)} \tag{4.8}$$

$$b_{WABB} = \sum_{g,balc=0}^{N_{glazing}} \boldsymbol{\delta_{g,balc}} \cdot b_{g,balc} \tag{4.9}$$

$$\sum_{i=1}^{N_{ins}} \boldsymbol{\delta_{ins,i}} \leq 1 \tag{4.10}$$

$$\sum_{i=1}^{N_{clad,v}} \boldsymbol{\delta_{clad,v,i}} + \sum_{i=1}^{N_{clad,nv}} \boldsymbol{\delta_{clad,nv,i}} = 1 \tag{4.11}$$

ROOF (R)

$$U_{R} = \frac{1}{\frac{1}{U_{R,0}} + \sum_{i=1}^{N_{ins}} \left(\frac{\boldsymbol{s_{ins,i}}}{\lambda_{ins,i}} \cdot \boldsymbol{\delta_{ins,i}}\right) + (r_i - r_o) \cdot \sum_{i=1}^{N_{clad,v}} \left(\boldsymbol{\delta_{clad,v,i}}\right) + \sum_{i=1}^{N_{clad,nv}} \left(\frac{\boldsymbol{s_{clad,nv,i}}}{\lambda_{clad,nv,i}} \cdot \boldsymbol{\delta_{clad,nv,i}}\right)} \tag{4.12}$$

$$\sum_{i=1}^{N_{ins}} \boldsymbol{\delta_{ins,i}} \leq 1 \tag{4.13}$$

$$\sum_{i=1}^{N_{clad,v}} \boldsymbol{\delta_{clad,v,i}} + \sum_{i=1}^{N_{clad,nv}} \boldsymbol{\delta_{clad,nv,i}} = 1 \tag{4.14}$$

WINDOWS (W)

$$U_{W} = \frac{1}{\sum_{g,W=0}^{N_{glazing}} \left(\frac{\boldsymbol{\delta_{g,W}}}{U_{g,W}}\right) + r_i + r_o} \tag{4.15}$$

$$U_{WBB} = \frac{1}{\sum_{g,W=0}^{N_{glazing}} \left(\frac{\boldsymbol{\delta_{g,W}}}{U_{g,W}}\right) + r_i + r_i \cdot \sum_{g,balc=1}^{N_{glazing}} \boldsymbol{\delta_{g,balc}} + r_o \cdot \boldsymbol{\delta_{g0,balc}}} \tag{4.16}$$

$$g_{W} = \sum_{g,W=0}^{N_{glazing}} \boldsymbol{\delta_{g,W}} \cdot g_{g} \tag{4.17}$$

$$g_{WBB} = \sum_{g,W=1}^{N_{glazing,W}} \left[\sum_{g,balc=0}^{N_{glazing,balc}} \left(\boldsymbol{\delta_{g,balc}} \cdot g_{g,balc}\right)\right] \cdot \boldsymbol{\delta_{g,W}} \tag{4.18}$$

$$b_{WBB} = \sum_{g,balc=0}^{N_{glazing}} \boldsymbol{\delta_{g,balc}} \cdot b_{g,balc} \tag{4.19}$$

$$F_{f\_WBV} = F_{f,0} \cdot \boldsymbol{\delta_{0\,balc}} + F_{f,1} \cdot \sum_{g,balc=1}^{N_{glazing}} \boldsymbol{\delta_{g,balc}} \tag{4.20}$$

$$\sum_{f=1}^{N_{frames}} \boldsymbol{\delta_f} = 1 \tag{4.21}$$

GLAZED BALCONIES (B)

$$U_B = \frac{\sum_{i=1}^{N_{clad,nv}} \left(\frac{\boldsymbol{s_{clad,nv,i}}}{\lambda_{clad,nv,i}} \cdot \boldsymbol{\delta_{clad,nv,i}}\right)}{\sum_{g,balc=0}^{N_{glazing}} \boldsymbol{\delta_{g,balc}} \cdot \left(\frac{1}{U_{g,balc}} + r_i + r_o\right)} \tag{4.22}$$

$$g_B = \sum_{g,balc=0}^{N_{glazing}} \boldsymbol{\delta_{g,balc}} \cdot g_{g,balc} \tag{4.23}$$

$$\sum_{g,balc=1}^{N_{glazing}} \boldsymbol{\delta_{g,balc}} = 1 \tag{4.24}$$

GLAZED STAIRCASES

$$U_{ST} = \frac{1}{r_i + r_o + \sum_{g,ST=0}^{N_{glazing}} \frac{\boldsymbol{\delta_{g,ST}}}{U_{g,ST}}} \tag{4.25}$$

$$g_{ST} = \sum_{g,ST=0}^{N_{glazing}} \boldsymbol{\delta_{g,ST}} \cdot g_{g,ST} \tag{4.26}$$

$$b_{SAW} = \sum_{g,ST=0}^{N_{glazing}} \boldsymbol{\delta_{g,ST}} \cdot b_{g,ST} \tag{4.27}$$

$$b_{SBF} = \sum_{g,ST=0}^{N_{glazing}} \boldsymbol{\delta_{g,ST}} \cdot b_{g,ST} \tag{4.28}$$

$$\sum_{g,ST=1}^{N_{glazing}} \boldsymbol{\delta_{g,ST}} = 1 \tag{4.29}$$

where U indicates the thermal transmittances, r the thermal resistances, s the layers' thicknesses, λ the thermal conductivities, b the temperature reduction factors defined in the standard EN 12831:2003 [87], g the SHGCs, F_f the ratio between the transparent and total surface of glazed components, δ the Boolean variables associated to multiple alternatives

In Eqn. (4.7) and (4.12), the cladding structures were distinguished in non-ventilated cavities, whose thermal transmittance was assessed, and ventilated air cavities larger than 1500 mm^2 per meter of length, whose transmittance was neglected according to the standard ISO 6946:2007 [88]. This aspect also influences Eq. (4.8) and (4.22).

The mathematical optimisation problem described so far can be characterized by the following features:

- Mixed-integer, because some of the variables are Boolean;
- Non-linear, because of some equations as (4.7) and (4.8) and for the adoption of a simulation-based optimisation;
- Constrained, because equality and inequality constraints were imposed;
- Multi-objective, because four objectives were minimised at the same time.

MOBO library includes four algorithms for multi-objective problems solving, all of them belonging to the family of heuristic algorithms, namely NSGA II [91], Pareto Archive NSGA II [92], Omni-Optimizer [93] and Random Search. This category of algorithms is known to be not indicated to handle constrained problems [94], although MOBO implements an improved constraints handling technique. Nevertheless, the case studies confirmed this feature, since the Pareto Front was often composed of many unfeasible solutions, *i.e.* building solutions not respecting the constraints. However, the heuristic approach was required for the present study since the use phase energy demand was not expressed in an explicit mathematical form. Furthermore, the heuristic algorithms allow minimising several objective functions without requiring further mathematical elaborations. These four algorithms were all employed in the case studies, comparing the resulting Pareto fronts to identify every time the best performing, also using different combinations of parameters for each algorithm. In detail, the unique parameter of the Random Search algorithm is the total number of buildings to evaluate, while the remaining three algorithms require the number of individuals, the number of generations, the crossover rate, and the mutation rate since they are genetic algorithms. The first two parameters influence the total number of buildings investigated during the optimisation, and different combinations were employed to find the best one. The crossover rate was set equal to 0.9. The mutation rate was evaluated according to the formula derived by Mühlenbein, which states that this parameter should be set equal to the reciprocal of the bit-string length [95]. For the present study, this criterion was applied through Eq. (4.30) [96]:

$$mr = \frac{1}{10 \cdot NC + \log_2 \prod_{i=1}^{NI} VI_i} \tag{4.30}$$

where mr is the mutation rate, NC is the number of continuous variables (that are codified through 10 bits per variable), NI is the number of integer variables and VI is the number of values that each integer variable can assume. This formula provides values allowing to change a *gene* per each offspring and per each generation, on average, according to the common practice [97].

4.2.1.5. Optimal solutions selection

Since the single building optimisation was based on a dual step optimisation approach, it was necessary to select an optimised envelope from Step 1 to perform the equipment optimisation in Step 2. The number of non-dominated optimal solutions making up the Pareto front in a multi-objective optimisation can be quite large. The selection process might be long and difficult, mainly because many solutions may be similar to each other. In these situations, two main strategies were developed in literature: the ranking of the solutions using a synthetic index or the analysis of the Pareto front. The first approach consists of creating a performance indicator, for example the weighted sum of the normalised objectives of each solution. This approach has the advantage of being fast and the disadvantage of introducing a subjective weight to each objective function, thus affecting the optimality with the analyst's opinions. The other approach consists in selecting some representative solutions that cover well the optimal design space, for example through a cluster analysis of the solutions. In this way, the number of solutions on the Pareto front can be reduced considerably by selecting a solution closed to the centroid of the cluster [98].

In this study, the first approach was preferred, employing the utopia point criterion. This criterion is based on the evidence that, in the multi-dimensional space of the objective functions, one point can be identified as the ideal alternative having each function with the minimum feasible value. A visual 2D example is provided in Fig. 4.11. Given two solutions, identified by points P_0 and P_1, their Euclidean distance from the origin of axes is the length of vectors s_0 and s_1. In the present study, where each objective function has real values and is always non-negative, this ideal point is located on the origin of axes, where each objective function is null. The origin of axes in the space of solutions of our study is a building with null objective functions, thus the ideal solution. Thus, the closer is a solution to this ideal building, the better this solution is [99]. The distance between each solution of the Pareto front and the utopia point was measured through the Euclidean distance, with each objective function being normalised to avoid that different orders of magnitude affect the result and to sum quantities all expressed as pure numbers. Although the normalisation may include some degree of freedom in the study, this approach was preferred to the weighted sum. In this study, the objective functions were normalised to the maximum theoretical value, *i.e.* the operating final energy demand of the original building and the sum of the investment costs or embodied impacts related to the highest alternative of each variable, respectively.

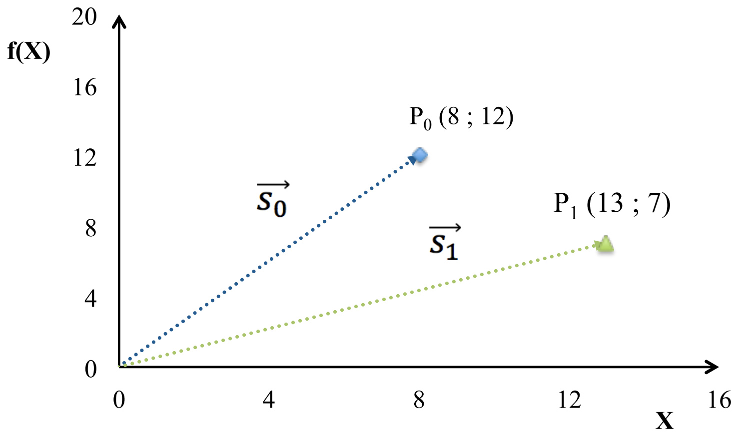

Fig. 4.11. Example of the utopia point criterion in a 2D space

4.2.2. Step 2 – Equipment optimisation

4.2.2.1. Variables and objective functions

The second and final step of the single building optimisation framework is dedicated to the components converting energy and fulfilling the demand of the building assessed in Step 1. In detail, this step is employed for a preliminary sizing, thus the variables of this problem are synthesis, design and operation variables for the equipment and the energy flows from the grids. Synthesis variables indicate whether the component is selected or not and there is one variable for each component. Design variables indicate the size of each component. Operation variables indicate, for each timestep, the amount of energy imported from the electricity and gas networks, energy flowing in and out of each component, and indicating the status of each storage system. For example, the optimisation indicates if it is better to provide the space heating through air-to-air heat pumps fed by a photovoltaic (PV) system, through a natural gas boiler or a combination of both technologies with lower values of rated power. The optimal combination of the variables of this step aims at minimising the objective functions. In this step, the objective functions deriving from Step 1 were combined with the parameters related to the equipment to generate the GWP, the CED and the Cost functions. In detail, the use phase final energy demand was converted in use phase primary energy, use phase GWP and operating costs decoupling the heating and cooling demands and multiplying each term by the conversion factor *k* (unit impact factor or unit cost) related to each *e-th* technology, according to Eq. (4.31):

$$Use\,Phase\,Term = UL \cdot \left[\sum_{e=1}^{E} \sum_{t=1}^{8760} \sum_{y=1}^{Y} \left(H_{t,y} \cdot k_e \right) + \sum_{e=1}^{E} \sum_{t=1}^{8760} \sum_{y=1}^{Y} \left(C_{t,y} \cdot k_e \right) \right] \tag{4.31}$$

This use phase term was added to the embodied impacts and investment costs of the building envelope components selected during the Step 1 and to the embodied impacts and investment costs of the equipment, whose rated sizes and operating schedule are optimised during this step, according to Eq. (4.32) – (4.34):

$$OF_1 = GWP = EGWP + Use\ Phase\ GWP + \sum_{e=1}^{E} m_e \cdot UEC_e \tag{4.32}$$

$$OF_2 = CED = EE + Use\ Phase\ Primary\ Energy + \sum_{e=1}^{E} m_e \cdot UEE_e \tag{4.33}$$

$$OF_3 = Cost = Investment\ Cost + Operating\ Cost + UL \cdot \sum_{e=1}^{E} m_e \cdot UP_e \tag{4.34}$$

In these equations, *m* is the significant parameter of the *e-th* equipment, *E* is the total number of equipment, and *UEC, UEE* and *UP* are the unit embodied carbon factor, the unit embodied energy factor and the unit price of the *e-th* equipment, respectively. Examples of the significant parameters are the surface of a PV system or the rated power of a heat pump. In order to take into account for the useful life of each component and the variable value of the money along the life cycle of the building, the unit prices were multiplied by the Uniform Capital Recovery Factor (*UCRF*) of the investment, *i.e.* the annuity factor, that is employed to annualise an investment and is the reciprocal of the *USPWF*. The expression for the *UCRF* is shown in Eq. (4.35) [100]:

$$UCRF = \frac{i_{real} \cdot \left(1 + i_{real}\right)^n}{\left(1 + i_{real}\right)^n - 1} \tag{4.35}$$

where *n* is the year after the installation of the retrofit action and i_{real} is the real interest rate. The objective function in this step is the weighted sum of the normalised life cycle global warming potential, life cycle cumulative energy demand and annual cost, combined through the scalarization technique as in Eq. (4.36):

$$OF = w_{GWP} \cdot \frac{OF_1}{n_{GWP}} + w_{CED} \cdot \frac{OF_2}{n_{CED}} + w_{cost} \cdot \frac{OF_3}{n_{cost}} \tag{4.36}$$

where *w* are the weights for these objectives and *n* are the normalisation factors. These factors were introduced to sum quantities all expressed as pure numbers, since they had originally different units of measure.

4.2.2.2. Software tools

As well as for Step 1, some criteria were decided to select the best software to be used for the case studies. For this step, the following criteria were adopted:

- Research-oriented;
- Interoperability;
- Flexibility.

Regarding the optimisation software tool, although the study may have been performed using MOBO and EnergyPlus as well as for Step 1, the development of a programming code was preferred for a duplex reason. First, a more flexible approach was required, since the number of variables was much higher than in Step 1. Thus, as the assessment of the hourly energy demand, identified as the most time-consuming part of the simulations, was useless in this part of the study because it is fixed and imposed by the selection of the envelope features, this part was avoided using the energy demands as an input of the model. In this way, the optimisation process manages only the flows from each component as variables. Furthermore, the mathematical model was conceived to be highly generic, and this script was employed also for the buildings cluster optimisation, thus joining the bridges between these two parts of the project with a unique, flexible tool. Although MATLAB language was used in the present thesis, a freely available language as python may also be employed.

An exception to this criterion was done for the study regarding the residential case study in oceanic climate. This exception was necessary because the quasi-stationary method contained in Be18 generates average monthly outputs of energy demands, while the correct sizing of equipment for space heating and space cooling is usually performed considering the annual peak hour [87,101]. For this reason, this study was developed coupling MOBO and Be18 as well as it was done in Step 1. Furthermore, to show a different approach with respect to the other case studies, the dual step approach was avoided in this study, performing instead a whole building optimisation. This approach was preferred in this case because the quasi-stationary method of Be18 is much faster than the dynamic method of EnergyPlus, thus obtaining the results in a reasonable amount of time.

4.2.2.3. Optimisation process

The general process executed in this step is schematised in Fig. 4.12. In detail, using the outcomes of Step 1, a preliminary building model is developed on the BPS software, also including the dwellers' habits to model their contribution to the internal heat gains and the electricity demand profile. Based on these demands, on the climate and the experience of the analyst, the details of the optimisation problem are specified, setting the components that should be assessed, their life cycle impacts and costs, their efficiencies and describing their operation through additional constraints to the problem. The remaining constraints of the problem represent the fulfilment of each energy demand and, in general, an energy balance equation is specified for each energy vector.

The three objective functions of this step were combined using the scalarization technique [102]. The drawbacks related to this method, already explained in Section 2.3.1, were overcome formulating this mathematical problem as a linear problem. It is known that linear problems are inherently convex, thus every local minimum is also a global minimum. Nevertheless, writing a linear problem requires neglecting or simplifying some aspects of the real system’s behaviour.

Since this optimisation step was completely described using a MATLAB script explicitly reporting all the equations, the availability of a mathematical model allowed employing a different approach with respect to Step 1. The MATLAB Optimization Toolbox is equipped with several algorithms, able to satisfy almost every request. In the present case, the mathematical model depends on real and integer variables, where real variables mainly indicate energy flows and integer variables were employed for the storages and the synthesis variables. The presence of some integer variables in a linear model obliged employing the *intlingprog* MILP function. This MATLAB function is mainly based on the Branch and Bound algorithm, synthetically described in step 3 of Fig. 4.12 [103]. Furthermore, the MATLAB *intlingprog* function also implements a genetic algorithm to compare the solution with the result of the Branch and Bound. All these operations allow identifying rigorously the optimum of the problem, although each SOO can last up to one hour.

At the end of the process, the Pareto front was built and analysed to select the optimal equipment configuration. This operation was performed easily because the Pareto front in each study was composed of less than ten different solutions.

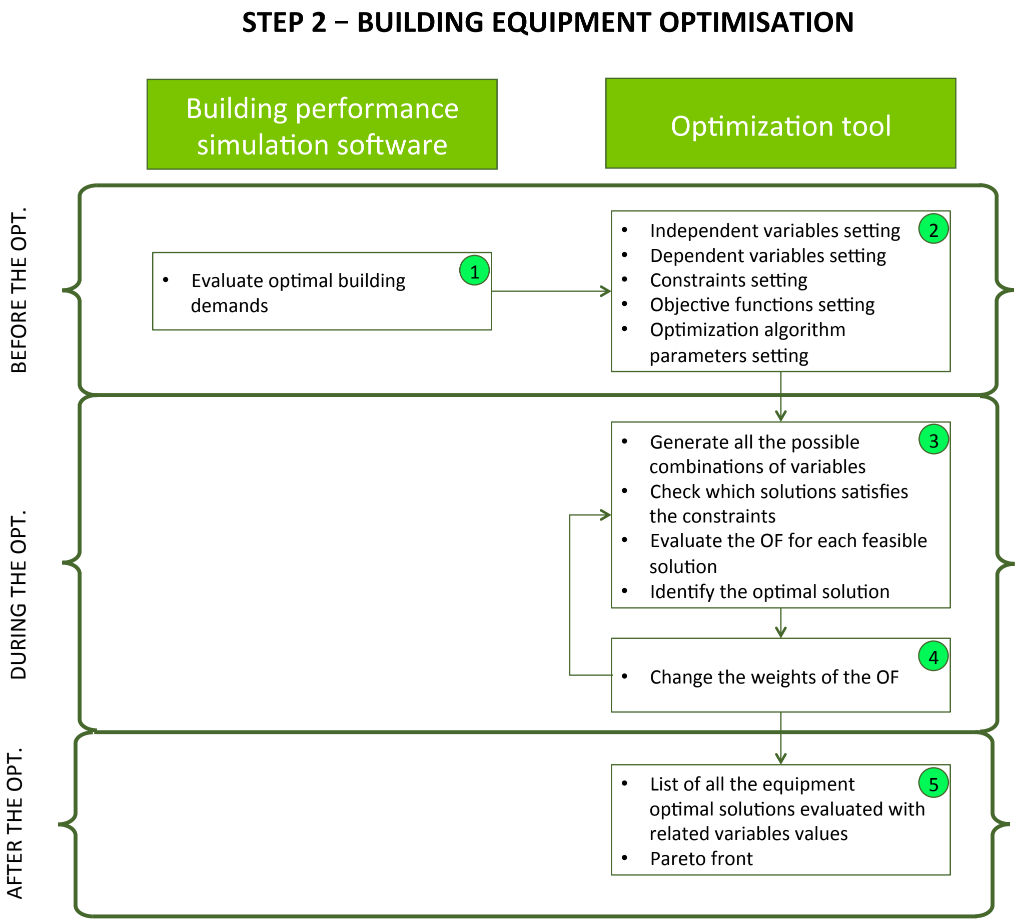

Fig. 4.12. Schematic of the equipment optimisation performed in Step 2

4.2.2.4. Mathematical model

The optimisation of the building technical equipment was performed according to a generic mathematical model known as *energy hub*. The concept of energy hub was defined during the mid-2000s [104] and subsequently deepened until it was completely formalised by Geidl in 2007 [105]. The definition of energy hubs describes them as "*entities consuming power at their input ports connected to, e.g. electrical distribution grids and natural gas infrastructures, and provide certain required energy services such as electricity, heating, cooling, compressed air, etc. at the output ports*" [105]. Although the mathematical framework was first conceived to be applied to microgrids, it is suitable for many energy systems applications, including buildings, collectively known as Multi-carrier Energy Systems (MES). Energy hub models may be used to manage energy carrier flows within a MES with sizes ranging from local to national levels. An energy hub may thus be considered as an interface between energy carrier suppliers and consumers, with network infrastructure in between. The input side is fed by electricity, natural gas and/or district heating, which are converted within the hub and transferred to the output port to meet the electricity, cooling or heating demands. An example of energy hub is shown in Fig. 4.13.

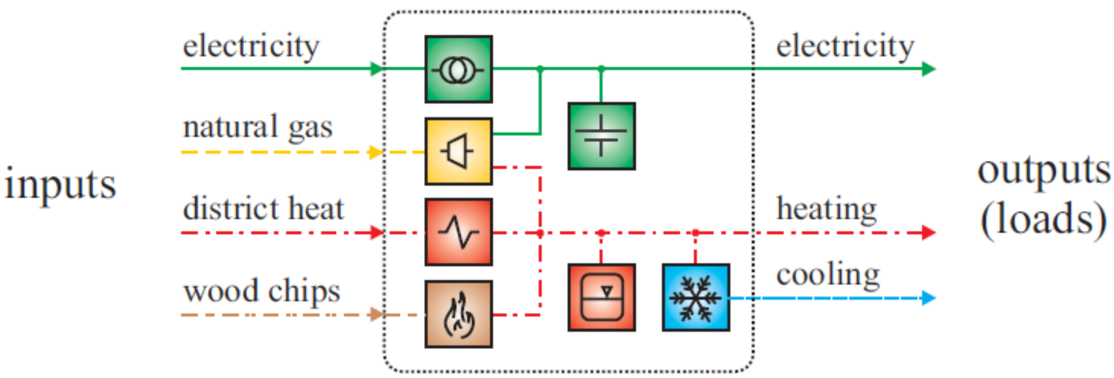

Fig. 4.13. Example of energy hub containing typical elements [106]

For the development of the energy hub model used in the present PhD research project, the following assumptions were done:

- Energy balances are evaluated in steady-state condition;
- Components efficiencies are independent on the load;
- Lines and networks losses are neglected while the energy losses in the system are considered only for the components through their efficiencies or coefficients of performance.

As every mathematical optimisation problem, this model is composed by parameters (input values that are kept constant), variables (values to be optimised), equality or inequality constraints (links between some of the variables, as energy and mass balances or components behaviour), lower and upper bounds (physical limits to value assumed by variables) and objective functions.

As already stated above, the parameters of the study are the building electricity, heating and cooling requirements, the features of each equipment and the objective functions coefficients (unit impact factors and unit prices). With specific reference to the unit prices of the equipment, a common approach in the technical community is to define an average value, *e.g.* 1500 €/kW$_p$ for the PV systems. This approach neglects scale factors since it is known that the unit price of components with a large size is much lower than the unit price of the same component with very lower size. This issue is quite important in optimisation studies since the optimal size of the component is unknown before the study and may vary in a large range. For this reason, the common strategy in optimisation studies is to employ a power law, as shown in Eq. (4.37):

$$Z_k = z_k \cdot \boldsymbol{S}_k^{\alpha_k} \tag{4.37}$$

where Z is the investment of the *k-th* component, z is a specific price, S is the size of the component and α is a parameter typically ranging between 0.4 and 0.8 [25]. The power law proved its advantages in many cases and became a standard in mechanical plants studies. Nevertheless, in order to keep the linearity of the problem, ensuring the uniqueness of the optimal solution, the investment cost for each *k-th* component was approximated as a linear function according to Eq. (4.38), as suggested in [107]:

$$Z_k = z_k \cdot \boldsymbol{S}_k^{\alpha_k} \cong C_k \cdot \boldsymbol{S}_k + C_{0,k} \cdot \boldsymbol{\delta}_k \tag{4.38}$$

In this equation, the unit price is replaced by the two cost factors C and C_0, while δ is the synthesis variable of the component. In this way, including this equation in the cost objective function, if the component is not selected $\delta = S = 0$ and the cost related to this component is not accounted for. The C and C_0 cost factors were determined through the least-squares method applied to market prices available on public reports or databases.

The first kind of constraints of the problem is the balance equations. Energy balances were set for each timestep for electrical energy (indicated with E in Eq. (4.39)) and for thermal energy (the balance of heating indicated with H in Eq. (4.40) and the balance of cooling indicated with F in Eq. (4.41)). Moreover, a mass balance was imposed for the supply of natural gas (indicated with NG in Eq. (4.42)). These equations combine the energy carrier from the main grid (subscript *grid*), the flows from and to the components to be installed, whose subscripts are explained in the dedicated sections, and the building energy requirements (subscript *req*). The term E_{sold} was introduced to include the purchase of PV power to the grid, while the terms H_{wasted} and F_{wasted} were introduced because the HP was modelled to produce both space heating and cooling simultaneously. The terms $E_{sto,ch}$, $E_{sto,disch}$, $H_{sto,ch}$ and $H_{sto,disch}$ indicate the charge (subscript *ch*) and the discharge (subscript *disch*) of electrical and thermal storage systems. The variable terms in the following equations were highlighted using a bold font.

$$\boldsymbol{E}_{grid}(t) - \boldsymbol{E}_{HP}(t) + \boldsymbol{E}_{PV}(t) - \boldsymbol{E}_{sold}(t) - \boldsymbol{E}_{sto,ch}(t) + \boldsymbol{E}_{sto,disch}(t) = E_{req}(t) \tag{4.39}$$

$$\boldsymbol{H}_{HP}(t) + \boldsymbol{H}_{NGB}(t) + \boldsymbol{H}_{STC}(t) - \boldsymbol{H}_{sto,ch}(t) + \boldsymbol{H}_{sto,disch}(t) - \boldsymbol{H}_{wasted}(t) = H_{req}(t) \tag{4.40}$$

$$\boldsymbol{F}_{HP}(t) - \boldsymbol{F}_{wasted}(t) = F_{req}(t) \tag{4.41}$$

$$NG_{grid}(t) = NG_{NGB}(t) \tag{4.42}$$

Further equality and inequality constraints were considered for each timestep, describing the behaviour of the heat pump, gas boiler, RES and storage, as in Eqn. (4.43) - (4.61).

HEAT PUMP (HP)

$$H_{HP}(t) = K_{HP,h} \cdot E_{HP}(t) \tag{4.43}$$

$$F_{HP}(t) = K_{HP,f} \cdot E_{HP}(t) \tag{4.44}$$

where H_{HP} and F_{HP} are the heating and cooling flows from the heat pump, respectively, E_{HP} is the corresponding absorbed electricity, $K_{HP,h}$ and $K_{HP,f}$ are the conversion coefficients from electricity to heating and from electricity to cooling, respectively, commonly known as Seasonal Coefficient Of Performance (SCOP) and Seasonal Energy Efficiency Ratio (SEER).

NATURAL GAS BOILER (NGB)

$$H_{NGB}(t) = K_{NGB} \cdot NG_{NGB}(t) \tag{4.45}$$

where H_{NGB} is the heating flow from the boiler, NG_{NGB} is the natural gas flowing into the boiler and K_{NGB} is the boiler efficiency.

PHOTOVOLTAIC (PV)

$$S_{PV} = K_{PV} \cdot I_{sun} \cdot I_{fract}(t) \cdot A_{PV} \cdot N_{PV} \tag{4.46}$$

where S_{PV} is the electricity output from the PV system in a day, K_{PV} is the conversion efficiency of the photovoltaic plant, I_{sun} is the daily average solar radiance availability, I_{fract} is the hourly fraction available of I_{sun}, A_{PV} is the surface of a single PV module and N_{PV} the number of modules to be installed. N_{PV} is thus both the synthesis and sizing variable related to the PV system.

SOLAR THERMAL COLLECTOR (STC)

$$S_{STC} = K_{STC} \cdot I_{sun} \cdot I_{fract}(t) \cdot A_{STC} \cdot N_{STC} \tag{4.47}$$

where S_{STC} is the energy output from the STC in a day, K_{STC} is the conversion efficiency of the solar collector, A_{STC} is the surface of a single STC collector and N_{STC} the number of collectors to be installed. N_{STC} is thus both the synthesis and sizing variable related to the STC system.

ELECTRICAL STORAGE (STO_{el})

$$E_{sto}(t+1) = E_{sto}(t) \cdot \left(1 - E_{sto,loss}\right) + K_{e,sto,ch} \cdot E_{sto,ch}(t+1) - E_{sto,disch}(t+1) / K_{e,sto,disch} \tag{4.48}$$

$$\boldsymbol{E}_{sto}(1) = \boldsymbol{E}_{sto}(end) \tag{4.49}$$

$$\boldsymbol{E}_{sto,ch}(t) \leq \boldsymbol{\delta}_{e,sto,ch}(t) \cdot Q_{e,sto,ch} \tag{4.50}$$

$$\boldsymbol{E}_{sto,disch}(t) \leq \boldsymbol{\delta}_{e,sto,disch}(t) \cdot Q_{e,sto,disch} \tag{4.51}$$

$$\boldsymbol{\delta}_{e,sto,ch}(t) + \boldsymbol{\delta}_{e,sto,disch}(t) \leq 1 \tag{4.52}$$

$$DoD \cdot \boldsymbol{S}_{e,sto} \leq \boldsymbol{E}_{sto}(t) \leq \boldsymbol{S}_{e,sto} \tag{4.53}$$

$$\boldsymbol{E}_{sto,ch}(t) \leq \boldsymbol{S}_{e,sto} \cdot (1 - DoD) \tag{4.54}$$

$$\boldsymbol{E}_{sto,disch}(t) \leq \boldsymbol{S}_{e,sto} \cdot (1 - DoD) \tag{4.55}$$

where E_{sto} *(t)* is the electrical energy stored in the device, $K_{e,sto,ch}$ and $K_{e,sto,disch}$ are the charge and discharge efficiencies of the electrical storage, respectively, $E_{sto,ch,}$ *(t)* and $E_{sto,disch,}$ *(t)* are the input and output electricity flows of the storage, respectively, $E_{sto.loss}$ is the self-discharge coefficient, assumed as a fraction of the stored electrical energy, $\delta_{e,sto,ch}$ *(t)* and $\delta_{e,sto,disch}$ *(t)* are Boolean variables indicating whether the electrical storage is charging or discharging at time *t*, respectively, $Q_{e,sto,ch}$ and $Q_{e,sto,disch}$ are upper limits to $E_{sto,ch,}$ *(t)* and $E_{sto,disch,}$ *(t)*, respectively, *DoD* is the Depth of Discharge of the electrical storage, and $S_{e,sto}$ is the capacity of the electrical storage.

THERMAL STORAGE (STO_{th})

$$\boldsymbol{H}_{sto}(t+1) = \boldsymbol{H}_{sto}(t) \cdot \left(1 - H_{sto,loss}\right) + K_{h,sto,ch} \cdot \boldsymbol{H}_{sto,ch}(t+1) - \boldsymbol{H}_{sto,disch}(t+1) / K_{h,sto,disch} \tag{4.56}$$

$$\boldsymbol{H}_{sto}(1) = \boldsymbol{H}_{sto}(end) \tag{4.57}$$

$$\boldsymbol{H}_{sto,ch}(t) \leq \boldsymbol{\delta}_{h,sto,ch}(t) \cdot Q_{h,sto,ch} \tag{4.58}$$

$$\boldsymbol{H}_{sto,disch}(t) \leq \boldsymbol{\delta}_{h,sto,disch}(t) \cdot Q_{h,sto,disch} \tag{4.59}$$

$$\boldsymbol{\delta}_{h,sto,ch}(t) + \boldsymbol{\delta}_{h,sto,disch}(t) \leq 1 \tag{4.60}$$

$$\boldsymbol{H}_{sto}(t) \leq \boldsymbol{S}_{h,sto} \tag{4.61}$$

where H_{sto} *(t)* is the thermal energy stored in the device, $K_{h,sto,ch}$ and $K_{h,sto,disch}$ are the charge and discharge efficiencies of the thermal storage, respectively, $H_{sto,ch,}$ *(t)* and $H_{sto,disch,}$ *(t)* are the input and output heating flows of the storage, respectively, $H_{sto.loss}$ is the self-discharge coefficient, assumed as a fraction of the stored thermal energy, $\delta_{h,sto,ch}$ *(t)* and $\delta_{h,sto,disch}$ *(t)* are Boolean variables that indicate whether the thermal storage is charging or discharging at time *t*, respectively, $Q_{h,sto,ch}$ and $Q_{h,sto,disch}$ are upper limits to $H_{sto,ch,}$ *(t)* and $H_{sto,disch,}$ *(t)*, respectively, and $S_{h,sto}$ is the capacity of the thermal storage.

Furthermore, synthesis variables were linked to the rated power of each component with the relationship shown in Eq. (4.62):

$$\boldsymbol{P_k} \leq \boldsymbol{\delta_k} \cdot Q_k \tag{4.62}$$

where Q_k is the upper bound to the available power (or capacity, for storages) of each component, usually set as a very high value. Through this equation, the rated power of the *k-th* component is automatically set to zero when its synthesis variable is null.

The mathematical model described so far was employed for the case studies related to the fictitious building and the existing detached house in the Mediterranean climate. As already stated in Section 4.2.2.2, the case study on the existing residential building in oceanic climate was performed as a whole building optimisation, *i.e.* envelope and equipment simultaneously optimised, using MOBO and Be18 as well as it was done for the Step 1. The related mathematical model included the following additional variables:

- PV system area;
- STC area;
- NGB rated power;
- District heating heat exchanger rated power (for a standard temperature difference);
- HP rated power.

The rated power of the components were modelled as discrete variables while the areas of the RES technologies were modelled as continuous variables. Boolean variables were also included as synthesis variables for each component. Since the indoor temperature never overcame 26 °C during some preliminary simulations, no cooling system design was evaluated in this optimisation study. Only one additional constraint was included to this model, related to solar technologies surface A_{PV} and A_{STC}, whose sum has to be lower than the available roof area A_{roof}, as in Eq. (4.63).

$$A_{PV} + A_{STC} \leq A_{roof} \tag{4.63}$$

4.2.3. Discussion on the proposed method for the optimisation of the performance of a single building

The previous sections illustrated how the holistic model for the multi-objective optimisation of the energy performance of a building was developed. The model can be applied to both design of new buildings and renovation of existing ones. Furthermore, the same approach is valid for any kind of building (residential, educational, industrial). On this regard, Kampelis et al. [108] proved how the same approach and renovation techniques can be applied to these three categories of buildings.

The main advantages of the model described so far lie in the combination of existing tools, most of them being free-of-charge, that are commonly employed both by researchers and design companies all over the world. The development of commercial software tools incorporating all the considerations described in this chapter may accelerate the current decarbonisation of the building sector, helping countries who signed international agreements on GHG emissions reduction and energy efficiency increase to attain their target. The employment of free-of-charge data may also help the development of commercial tools without requiring expensive investments for designers. The tools and the algorithms employed were accurately selected and compared, further improving the quality of the work.

Other researchers conducted similar studies employing free available tools for the optimisation of buildings. For example, Hollberg et al. [32,109–111] combined Rhinoceros 3D modeller and its graphical algorithm Grasshopper with EnergyPlus BPS through DIVA-For-Rhino or Honeybee plug-ins, using Galapagos, GOAT or Octopus plug-ins for the optimisation.

It is important to underline that nZEB or NZEB targets were not explicitly considered in this model because they represent special cases. Since the aim of this research project was to identify the best combination of alternatives for a building and its optimal energy demand according to a holistic point of view, it was preferred not to impose these minimum energy performance levels. Nevertheless, the method may be applied including a minimum level of use phase energy demand as an additional constraint.

The division of the optimisation in two steps should respect the common building design practice, where people with different background and expertise take care of the design of different aspects. Moreover, a multi-step approach allows the employment of different software tools in each step. In this way, each researcher or designer might employ his favourite tool. Multi-step approaches were successfully employed in other literature studies in the past. Ascione et al. [112] described a dual step method for the energy retrofit of a school. In detail, the first step aimed at minimising the heating and cooling loads and the discomfort hours, while the resulting Pareto Front was further optimised in the second step, minimising the LCC and the primary energy consumption to identify the best retrofit action. Lindberg et al. [113] developed a MILP mathematical optimisation model for the equipment of a zero-energy building, using fixed data of annual energy demand as input from a previous step. Gagnon et al. [98] employed a very similar approach, dedicating the first step to the envelope and the second step to the HVAC equipment, and compared the results with a whole-building optimisation on the same case study. Their work shows that the dual-step approach is effective in identifying the optimal solutions, although the whole-building optimisation required less computational time and found better solutions. Nevertheless, the authors underline that whole-building optimisation is much more complicated to implement.

The main limitation of the study is that the LCA analysis was conducted through the calculation of only two indicators, although they are the most commonly known. On this topic, the European standard providing guidelines on the LCA of buildings, EN 15978:2011, recommends assessing seven indicators describing environmental impacts, including the ozone depletion, the acidification for soil and water and the depletion of abiotic resources [114]. The selection of only two impacts derived from a balance between the optimality according to different criteria and the number of alternatives in the Pareto front, since the more are the OFs and the larger becomes the front because there are other solutions optimal according to the new criteria. On this regard, a new algorithm, maybe the first, for the efficient solution of multi-objective mixed integer problems with four objective functions was recently proposed in [115].

Other limitations of the study regard the lacking assessment of uncertainties on the input climate conditions or on the behaviour of the occupants, that are becoming hot topics in international studies on building physics [116–120]. Another improvement may lay on the assessment of the indoor comfort, since the pieces of equipment were optimised considering a fixed set-point temperature for winter and summer, neglecting adaptive models, and the assessment of the daylight was also neglected. Nevertheless, this choice was justified by the fact that the use phase energy demand was evaluated imposing a fixed set-point temperature, thus guaranteeing the comfort. Last, the economic analysis was based on the most employed cost terms, namely the investment, operating and maintenance costs, while the residual value of the investments after the end of the reference period or the disposal costs were neglected. Nevertheless, the philosophy driving the present project was the development of a simplified approach, as most of the optimisation models are. Otherwise, the resulting computational burden would be prohibitive. The method was conceived and its feasibility was proved through many case studies, showing that the optimal solutions effectively reduce all the objective functions simultaneously. Thus, the outcomes of the study should be considered as general guidelines for the decision-making, or preliminary results for more accurate building design or renovation project.

4.3. Building clusters performance optimisation

The development of the model for the building clusters optimisation was based on an approach typically employed for microgrids. This model was based on an energy hub formulation, allowing a compact structure to simulate a MES in a single optimisation study. Although the mathematical model developed in the present PhD project was largely based on existing equations and modelling techniques, its employment in an LCA study is original, to the best of author's knowledge. In detail, according to a literature review from 2017 on the smart grids environmental impacts [121], only one over one hundred and ninety-two studies involved LCA methodology to assess the impacts, and it was only related to home energy management systems. Furthermore, Salehi et al. [122] stated that their study, submitted on November 2018, was the first scientific paper on the environmental optimisation of MES, although they did not apply the LCA methodology.

The importance of including the clusters of buildings in the present study is related to the current transformation that the power systems are facing since the global warming pushed the introduction of distributed energy systems, mainly composed by RES plants. This aspect started the transition from a "vertically" to a "horizontally" integrated energy system, where the electricity is not produced only at the top level of the chain but at high, medium and low voltage levels [123]. Furthermore, the steeply increasing final energy demand of developing counties also pushed finding new ways to develop the energy infrastructures reliably and effectively [124]. Many studies and pilot projects show how the interaction between the energy networks, *i.e.* power, natural gas and district heating/cooling systems, can provide high flexibility to the energy system but also can be the origin of important energy efficiency interventions [125,126]. More in detail, the creation of MES should bring the following advantages [127]:

- Efficiency, deriving from the interaction among different components of the power system. For example, a region with a high wind power penetration and low energy demand might exploit the excess of wind energy in peak hours to charge the batteries of electric vehicles or to generate hydrogen and natural gas in power-to-gas plants;

- Reliability, because of the higher availability of energy sources. Thus, if loads are not constrained to be supplied by a unique source, they can choose the power source with the lowest cost;

- Flexibility, thanks to the increased freedom in supplying the loads, since, in a multi-source system, a polluting or costly energy carrier can be easily replaced with a more attractive energy source.

4.3.1. Optimisation process

The optimisation process and model are analogous to what already shown in Section 4.2.2. The MATLAB script inputs are the energy demands of the cluster, namely electricity, space heating, space cooling, DHW and freshwater. Based on these input parameters, the script simultaneously identifies the optimal combination of equipment (synthesis stage), their optimal rated sizes (design stage) and their optimal operating schedule during the analysed period (operation stage) that allow minimising the annualised costs, the life cycle equivalent emissions of carbon dioxide and the life cycle primary energy use. The electricity, space heating and space cooling demands were modelled as time-dependent values, thus one value per each time-step, while the DHW and freshwater demands were considered as daily requirements. This difference was included to assess also the possibility of exploiting the flexibility of the load to reduce the peak on the power network and to increase the efficiency of the whole power system.

In detail, the installation of the following components was considered: Natural Gas-fired Boiler (NGB), Electric Boilers (EB), Heat Pump (HP), Combined Heat and Power (CHP), Absorbing Chiller (AC), Photovoltaic (PV), Solar Thermal Collector (STC), electrical storage (STO_{el}) and thermal storage (STO_{th}). The HP provides both heating and cooling energy. Each component was schematised as one centralised system, although it may represent the equivalent of many smaller systems distributed over the cluster. For the flexibility services evaluation, the main power plant based on diesel generators (DG), a desalination system (DES) and a water storage (STO_{w}) were also included in the script and modelled as being composed of multiple units. Since the flexibility was assessed for an islanded microgrid, the power plant is alternative to the electricity provided by the main grid. The assumption that these components were already installed and amortised was included in the model, thus only their operating costs were assessed.

4.3.2. Mathematical model

As well as for the Step 2 of the single building optimisation model, the mathematical model for the optimisation of the cluster of buildings performance is a MILP problem, thus being composed by linear equations and real or integer variables. The real variables are the energy flows from the main networks and the equipment, while the integer variables are the synthesis variables for the equipment and the status variables for storages, for the DG and the DES systems.

The structure and the assumptions of the mathematical model were already explained in Section 4.2.2. The objective function is the weighted sum of the normalised life cycle global warming potential, life cycle cumulative energy demand and annual cost, combined through the scalarization technique as in Eq. (4.64). The three objectives were normalised in order to sum quantities all expressed as pure numbers, since they had originally different units of measure

$$OF = w_{GWP} \cdot \frac{OF_1}{n_{GWP}} + w_{CED} \cdot \frac{OF_2}{n_{CED}} + w_{cost} \cdot \frac{OF_3}{n_{cost}} \tag{4.64}$$

where w are the weights for these objectives, n are the normalisation factors and the expressions for OF_1, OF_2 and OF_3 are the second and third terms of Eqn. (4.32) – (4.34), repeated here below:

$$OF_1 = GWP = \sum_{e=1}^{E} m_e \cdot UEC_e + \sum_{f=1}^{F} \frac{l_f}{K_f} \cdot UEC_f \tag{4.32'}$$

$$OF_2 = CED = \sum_{e=1}^{E} m_e \cdot UEE_e + \sum_{f=1}^{F} \frac{l_f}{K_f} \cdot UEE_f \tag{4.33'}$$

$$OF_3 = \sum_{e=1}^{E} m_e \cdot UP_e + \sum_{f=1}^{F} \frac{l_f}{K_f} \cdot UP_f \tag{4.34'}$$

where the first summation of each equation is related to the purchase of the equipment and the second summation of each equation refers to the operation of the equipment. In detail, l is the amount of final energy produced by each *f-th* energy flow, K is the efficiency of each *f-th* component and F is the total number of energy flows. The contributions related to the maintenance of the equipment were neglected in this study, as well as the financial subsidies to energy efficiency and renewable energies.

Some differences were also introduced to the mathematical model shown in Eqn. (4.39) - (4.62). In detail, the mass and energy balance equations were modified to take into account for the power losses in the transformer of the substation feeding the cluster and for the additional flows related to CHP and AC. The variable terms in the following equations were highlighted using a bold font.

$$\left[\boldsymbol{E}_{grid}(t) + \boldsymbol{E}_{DG}(t)\right] \cdot \left(1 - K_{TR}\right) + \boldsymbol{E}_{CHP}(t) - \boldsymbol{E}_{HP}(t) + \boldsymbol{E}_{PV}(t) - \boldsymbol{E}_{sto,ch}(t) + \tag{4.65}$$

$$+\boldsymbol{E}_{\boldsymbol{sto,disch}}(t)-\boldsymbol{E}_{\boldsymbol{EB}}(t)-\boldsymbol{E}_{\boldsymbol{DES}}(t)=E_{req}(t)$$

$$\boldsymbol{H}_{\boldsymbol{CHP}}(t)+\boldsymbol{H}_{\boldsymbol{HP}}(t)+\boldsymbol{H}_{NGB}(t)+\boldsymbol{H}_{\boldsymbol{EB}}(t)+\boldsymbol{H}_{\boldsymbol{STC}}(t)-\boldsymbol{H}_{\boldsymbol{sto,ch}}(t)$$
$$+\boldsymbol{H}_{\boldsymbol{sto,disch}}(\boldsymbol{t})=H_{req}(\boldsymbol{t})+DHW_{req}(\boldsymbol{t}) \quad (4.66)$$

$$\boldsymbol{F}_{\boldsymbol{HP}}(t)+\boldsymbol{F}_{AC}(t)=F_{req}(t) \quad (4.67)$$

$$\boldsymbol{NG}_{\boldsymbol{grid}}(t)=\boldsymbol{NG}_{\boldsymbol{CHP}}(t)+\boldsymbol{NG}_{NGB}(t)+\boldsymbol{NG}_{AC}(t) \quad (4.68)$$

$$\sum_{t=1}^{24}\boldsymbol{DHW}_{\boldsymbol{req,flex,j}}(t)=DHW_{req} \quad (4.69)$$

$$\sum_{t=1}^{24}\boldsymbol{W}_{\boldsymbol{req,flex,j}}(t)=W_{req} \quad (4.70)$$

Furthermore, the following equations describing the operation of CHP and AC were included:

COMBINED HEAT AND POWER (CHP)

$$\boldsymbol{E}_{\boldsymbol{CHP}}(t)=K_{CHP,e}\cdot\boldsymbol{NG}_{\boldsymbol{CHP}}(t) \quad (4.71)$$

$$\boldsymbol{H}_{\boldsymbol{CHP}}(t)=K_{CHP,h}\cdot\boldsymbol{NG}_{\boldsymbol{CHP}}(t) \quad (4.72)$$

$$K_{CHP,e}+K_{CHP,h}<1 \quad (4.73)$$

where E_{CHP} is the electricity generated by CHP at time t, NG_{CHP} is the natural gas supply, H_{CHP} is the heat flow from the CHP, and $K_{CHP,e}$ and $K_{CHP,h}$ are the electrical and thermal efficiencies of the CHP.

ABSORBING CHILLER (AC)

$$\boldsymbol{F}_{\boldsymbol{AC}}(t)=K_{AC}\cdot\boldsymbol{NG}_{\boldsymbol{AC}}(t) \quad (4.74)$$

where F_{AC} is the cooling flow from the absorbing chiller, NG_{AC} is the natural gas flowing into the chiller and K_{AC} is the chiller efficiency. The chiller cannot be fed directly by heating energy in this model, because the value adopted for the efficiency refers to a high temperature heat source.

For the flexibility case study, the DG, DES and STO_w models were also included.

DIESEL GENERATORS (DG)

$$D_{\boldsymbol{DG}}=\sum_{t=1}^{24}\sum_{j=1}^{N_{DG}}\left[\frac{\boldsymbol{E}_{\boldsymbol{DG,j}}(t)}{K_{DG,j}(t)}\right] \quad (4.75)$$

where the electricity produced by each DG group is divided by its conversion efficiency K_{DG} to obtain the hourly diesel oil consumption, and then summed to the consumption of the other DG groups and to the daily hours to obtain the daily diesel oil consumption D_{DG}.

DESALINATION UNIT (DES)

$$\boldsymbol{W_{DES}} = -\boldsymbol{\delta_{DES}}(t) \cdot K_{DES} \cdot E_{unit} \tag{4.76}$$

where the freshwater produced by each DES unit, W_{DES}, that is modelled as constant, is given by the number of working units δ_{DES} multiplied by the electricity absorbed by each unit E_{unit} and by the conversion factor from electricity to purified water K_{DES}.

FRESHWATER STORAGE

$$\boldsymbol{W_{sto}}(t+1) = \boldsymbol{W_{sto}}(t) + \boldsymbol{W_{DES}}(t+1) - \boldsymbol{W_{req,flex}}(t+1) \tag{4.77}$$

$$\boldsymbol{W_{sto}}(1) = \boldsymbol{W_{sto}}(end) \tag{4.78}$$

$$\boldsymbol{W_{sto}}(t) \le \boldsymbol{S_{WSS}} \tag{4.79}$$

where W_{sto} is the freshwater in the storage, $W_{req,flex}$ is the daily freshwater demand of the cluster and S_{WSS} is the storage capacity.

The equations (4.46) and (4.47), describing the solar technologies energy production, were changed from equality into inequality constraints. This change was necessary to give some flexibility to the model, that otherwise would be too much constrained. This aspect derives from the modelling of the main plant and of the desalination system, whose electricity flows were modelled as step functions. In this way, if the storage system is not considered as optimal, the energy production from PV systems (the unique free energy flow in this model) is employed to balance the energy production and demands in Eq. (4.65).

4.3.3. Discussion on the proposed method for the optimisation of building clusters performance

The model for the optimisation of a cluster of buildings was based on a widespread approach, the energy hub, whose popularity increased rapidly form its introduction since it is accurate but its foundation are simple equations as energy balances evaluated in a steady-state condition. Furthermore, the linearity of the equations guarantees the uniqueness of the optimal solution.

The capacities of the model shown in this section were deeply tested, since the optimisations performed for the case studies involved several variables, with an order of magnitude ranging between 10^3 and 10^{38}! These optimisation studies were successfully conducted adopting some techniques to save computational resources. For example, as is common practice for sparse matrixes, *i.e.* matrixes with very few non-zero elements, the non-zero values were referred to through an indexing operation.

The inclusion of the LCA methodology in an energy hub formulation represents an original contribution of this project to the international literature, and also the assessment of flexibility services was rarely performed in energy hub models, although this is a very popular topic in the last few years.

The limit of the study is that the robustness of the optimal solutions on the input parameters was not assessed. As for the method for the single building optimisation, this part was neglected since the main aim of the study is to prove the feasibility of the methodology and to provide generic guidelines rather than effectively identify the optimal sizes of components. Nevertheless, the accuracy of input data was privileged, *e.g.* using linear extrapolations on market data instead of adopting an average unit price. Certainly, the results of this optimisation should be double-checked with a detailed simulation model implementing the rated sizes and the operation rules resulting from the optimisation, in order to evaluate the true values of the OFs and assess the saving.

4.4. Scientific literature contributions

Part of the work shown in this chapter was published in the following scientific papers:

JOURNAL ARTICLES

- Manfredi Crainz, Domenico Curto, Vincenzo Franzitta, Sonia Longo, Francesco Montana, Rossano Musca, Eleonora Riva Sanseverino, Enrico Telaretti, "Flexibility Services to Minimize the Electricity Production from Fossil Fuels. A Case Study in a Mediterranean Small Island", Energies, 2019, vol. 12(18), 3492.

INTERNATIONAL CONFERENCES PROCEEDINGS

- Giuseppe Attardo, Sonia Longo, Francesco Montana, Eleonora Riva Sanseverino, Quynh Thi Tu Tran and Gaetano Zizzo, "Urban Energy Hubs Economic Optimization and Environmental Comparison in Italy and Vietnam", IEEE 4th International Forum on Research and Technology for Society and Industry (RTSI), Palermo, 2018, pp. 1-6;
- Maurizio Cellura, Sonia Longo, Francesco Montana, Eleonora Riva Sanseverino, "Multi-Objective Building Envelope Optimization through a Life Cycle Assessment Approach", 2019 IEEE International Conference on Environment and Electrical Engineering and 2019 IEEE Industrial and Commercial Power Systems Europe (EEEIC / I&CPS Europe), Genoa, Italy, 2019, pp. 1-6;
- Nicoletta Cannata, Maurizio Cellura, Sonia Longo, Francesco Montana, Eleonora Riva Sanseverino, Quyen Le Luu, Ninh Quang Nguyen, "Multi-Objective Optimization of Urban Microgrid Energy Supply According to

Economic and Environmental Criteria", 2019 IEEE Milan PowerTech, Milan, Italy, 2019, pp. 1-6;

- Domenico Curto, Vincenzo Franzitta, Sonia Longo, Francesco Montana, Eleonora Riva Sanseverino, Enrico Telaretti, "Flexibility Services in a Mediterranean Small Island to Minimize Costs and Emissions Related to Electricity Production from Fossil Fuels", 20th IEEE Mediterranean Electrotechnical Conference (MELECON), Palermo, 2020, pp. 453-458.

NATIONAL CONFERENCE PROCEEDINGS

- Maurizio Cellura, Sonia Longo, Francesco Montana, Eleonora Riva Sanseverino, "Ottimizzazione Multi-Obiettivo delle Prestazioni Energetiche e Ambientali di un Edificio Residenziale", Atti del XIII Convegno della Rete Italiana LCA – VIII Convegno dell'Associazione Rete Italiana LCA (Proceedings of the XIII Conference of Italian LCA Network), Rome, Italy, 2019, pp. 1-10.

4.5. References

[1] Bahramian M, Yetilmezsoy K. Life cycle assessment of the building industry: an overview of two decades of research (1995–2018). Energy Build 2020;109917.

[2] Lasvaux S, Favre D, Périsset B, Bony J, Hildbrand C, Citherlet S. Life Cycle Assessment of Energy Related Building Renovation: Methodology and Case Study. Energy Procedia 2015;78:3496–501. doi:10.1016/j.egypro.2016.10.132.

[3] International Energy Agency (IEA). IEA Annex 31 - Energy Related Environmental Impact of Buildings n.d. http://www.iisbe.org/annex31/index.html (accessed March 25, 2020).

[4] International Energy Agency (IEA). IEA EBC Annex 56 - Cost-Effective Energy & CO2 Emissions Optimization in Building Renovation n.d. http://www.iea-annex56.org/ (accessed April 20, 2020).

[5] International Energy Agency (IEA). IEA EBC Annex 57 - Evaluation of Embodied Energy and CO2 Equivalent Emissions for Building Construction n.d. http://www.annex57.org/ (accessed March 25, 2020).

[6] European Parliament and Council. Directive (EU) 2018/844 of 30 May 2018 amending Directive 2010/31/EU on the energy performance of buildings and Directive 2012/27/EU on energy efficiency. 2018.

[7] United Nations. The Paris Agreement n.d. https://unfccc.int/process-and-meetings/the-paris-agreement/the-paris-agreement.

[8] Azari R, Abbasabadi N. Embodied energy of buildings: A review of data,

methods, challenges, and research trends. Energy Build 2018;168:225–35. doi:10.1016/j.enbuild.2018.03.003.

[9] International Energy Agency (IEA) EBC Annex 56. Life Cycle Assessment for Cost-Effective Energy and Carbon Emissions Optimization in Building Renovation. 2017.

[10] Krarti M, Ihm P. Evaluation of net-zero energy residential buildings in the MENA region. Sustain Cities Soc 2016;22:116–25.

[11] Harkouss F, Fardoun F, Biwole PH. Multi-objective optimization methodology for net zero energy buildings. J Build Eng 2018;16:57–71.

[12] Harkouss F, Fardoun F, Biwole PH. Optimal design of renewable energy solution sets for net zero energy buildings. Energy 2019;179:1155–75.

[13] Illankoon IMCS, Lu W. Optimising choices of 'building services' for green building: Interdependence and life cycle costing. Build Environ 2019;161:106247. doi:https://doi.org/10.1016/j.buildenv.2019.106247.

[14] Wang J, Yu C, Pan W. Relationship between operational energy and life cycle cost performance of high-rise office buildings. J Clean Prod 2020;262:121300. doi:https://doi.org/10.1016/j.jclepro.2020.121300.

[15] Li S, Lu Y, Kua HW, Chang R. The economics of green buildings: A life cycle cost analysis of non-residential buildings in tropic climates. J Clean Prod 2020;252:119771. doi:https://doi.org/10.1016/j.jclepro.2019.119771.

[16] Rabani M, Bayera Madessa H, Mohseni O, Nord N. Minimizing delivered energy and life cycle cost using Graphical script: An office building retrofitting case. Appl Energy 2020;268:114929. doi:https://doi.org/10.1016/j.apenergy.2020.114929.

[17] Schmidt M, Crawford RH. A framework for the integrated optimisation of the life cycle greenhouse gas emissions and cost of buildings. Energy Build 2018;171:155–67. doi:https://doi.org/10.1016/j.enbuild.2018.04.018.

[18] Robati M, McCarthy TJ, Kokogiannakis G. Integrated life cycle cost method for sustainable structural design by focusing on a benchmark office building in Australia. Energy Build 2018;166:525–37. doi:https://doi.org/10.1016/j.enbuild.2018.02.034.

[19] Shan X, Melina AN, Yang E-H. Impact of indoor environmental quality on students' wellbeing and performance in educational building through life cycle costing perspective. J Clean Prod 2018;204:298–309. doi:https://doi.org/10.1016/j.jclepro.2018.09.002.

[20] Yuan J, Nian V, Su B. Evaluation of cost-effective building retrofit strategies through soft-linking a metamodel-based Bayesian method and a life cycle cost assessment method. Appl Energy 2019;253:113573.

doi:https://doi.org/10.1016/j.apenergy.2019.113573.

[21] Kim D, Cho H, Koh J, Im P. Net-zero energy building design and life-cycle cost analysis with air-source variable refrigerant flow and distributed photovoltaic systems. Renew Sustain Energy Rev 2020;118:109508. doi:https://doi.org/10.1016/j.rser.2019.109508.

[22] German Federal Ministry of the Interior Building and Community. ÖKOBAUDAT Database 2019. https://www.oekobaudat.de/en/database/database-oekobaudat.html.

[23] European Union Joint Research Centre. European reference Life Cycle Database (ELCD) n.d. https://nexus.openlca.org/database/ELCD (accessed April 28, 2020).

[24] Molio Building Knowledge Center (in Danish "Molio Byggeriets Videnscenter"). Molio price database (in Danish) 2019. https://www.molio.dk/brug-molio-prisdata (accessed August 15, 2019).

[25] Bejan A, Tsatsaronis G, Moran M. Thermal Design and Optimization. John Wiley & Sons; 1995.

[26] Longo S, Montana F, Riva Sanseverino E. A review on optimization and cost-optimal methodologies in low-energy buildings design and environmental considerations. Sustain Cities Soc 2019;45:87–104.

[27] TRNSYS web page n.d. http://www.trnsys.com/ (accessed March 27, 2020).

[28] EQUA Simulation AB. IDA-ICE web page n.d. https://www.equa.se/en/ida-ice (accessed March 27, 2020).

[29] U.S. Department of Energy. EnergyPlus web page n.d. https://energyplus.net/ (accessed April 28, 2020).

[30] Gilles F, Bernard S, Ioannis A, Simon R. Decision-making based on network visualization applied to building life cycle optimization. Sustain Cities Soc 2017;35:565–73. doi:10.1016/j.scs.2017.09.006.

[31] Mazzeo D, Matera N, Cornaro C, Oliveti G, Romagnoni P, Santoli L De. EnergyPlus, IDA ICE and TRNSYS predictive simulation accuracy for building thermal behaviour evaluation by using an experimental campaign in solar test boxes with and without a PCM module. Energy Build 2020;212.

[32] Hollberg A, Ruth J. A Parametric Life Cycle Assessment Model for Façade Optimization. Build. Simul. Optim., 2014.

[33] DOE-2 web page n.d. http://doe2.com/doe2/.

[34] Crawley DB, Lawrie LK, Pedersen CO, Winkelmann FC. EnergyPlus: Energy Simulation Program. ASHRAE J 2000;42:49–56. doi:10.1.1.122.6852.

[35] American Society of Heating Refrigerating and Air-Conditioning Engineers. ASHRAE Handbook - Fundamentals. 2017.

[36] EnergyPlus source code n.d. https://github.com/NREL/EnergyPlus (accessed March 27, 2020).

[37] Danish Building Research Institute. Be18 2018. https://sbi.dk/beregningsprogrammet/Pages/Start.aspx (accessed March 29, 2020).

[38] International Organization for Standardization (ISO). ISO 13790:2008 - Energy performance of buildings. Calculation of energy use for space heating and cooling 2008.

[39] Mathworks. MATLAB web page n.d. https://www.mathworks.com/products/matlab.html (accessed March 22, 2020).

[40] GenOpt web page n.d. https://simulationresearch.lbl.gov/GO/ (accessed March 27, 2020).

[41] modeFRONTIER web page n.d. http://www.esteco.com/modefrontier (accessed March 27, 2020).

[42] MOBO web page n.d. http://ibpsa-nordic.org/tools.html (accessed March 27, 2020).

[43] MLE+ web page n.d. http://www.madhurbehl.com/mleplus.html (accessed March 15, 2020).

[44] jEPlus+EA web page n.d. http://www.jeplus.org/wiki/doku.php?id=docs:jeplus_ea:start (accessed March 27, 2020).

[45] Opt-E-Plus web page n.d. https://www.nrel.gov/tech_deployment/pdfs/45620.pdf (accessed March 27, 2020).

[46] EQUA Simulation AB. IDA ESBO web page n.d. https://www.equa.se/en/esbo (accessed March 15, 2020).

[47] BEopt web page n.d. https://beopt.nrel.gov/ (accessed March 27, 2020).

[48] BCVTB web page n.d. https://simulationresearch.lbl.gov/bcvtb/FrontPage (accessed March 15, 2020).

[49] Palonen M, Hamdy M, Hasan A. MOBO A New Software for Multi-Objective Building Performance Optimization. 13th Conf Int Build Perform Simul Assoc 2013:2567–74.

[50] Niemelä T, Kosonen R, Jokisalo J. Cost-optimal energy performance renovation measures of educational buildings in cold climate. Appl Energy 2016;183:1005–

20. doi:10.1016/j.apenergy.2016.09.044.

[51] Pal SK, Takano A, Alanne K, Siren K. A life cycle approach to optimizing carbon footprint and costs of a residential building. Build Environ 2017;123:146–62. doi:10.1016/j.buildenv.2017.06.051.

[52] Pal SK, Takano A, Alanne K, Palonen M, Sirén K. A multi-objective life cycle approach for optimal building design: A case study in Finnish context. J Clean Prod 2017;143:1021–35. doi:10.1016/j.jclepro.2016.12.018.

[53] Niemelä T, Kosonen R, Jokisalo J. Cost-effectiveness of energy performance renovation measures in Finnish brick apartment buildings. Energy Build 2017;137:60–75. doi:10.1016/j.enbuild.2016.12.031.

[54] Niemelä T, Levy K, Kosonen R, Jokisalo J. Cost-optimal renovation solutions to maximize environmental performance, indoor thermal conditions and productivity of office buildings in cold climate. Sustain Cities Soc 2017;32:417–34. doi:10.1016/j.scs.2017.04.009.

[55] Niemelä T, Kosonen R, Jokisalo J. Energy performance and environmental impact analysis of cost-optimal renovation solutions of large panel apartment buildings in Finland. Sustain Cities Soc 2017;32:9–30. doi:10.1016/j.scs.2017.02.017.

[56] Wang C, Kilkis S, Tjernström J, Nyblom J, Martinac I. Multi-objective Optimization and Parametric Analysis of Energy System Designs for the Albano University Campus in Stockholm. Procedia Eng 2017;180:621–30. doi:10.1016/j.proeng.2017.04.221.

[57] Manrique Delgado B, Cao S, Hasan A, Sirén K. Multiobjective optimization for lifecycle cost, carbon dioxide emissions and exergy of residential heat and electricity prosumers. Energy Convers Manag 2017;154:455–69. doi:10.1016/j.enconman.2017.11.037.

[58] Belafi Z, Hong T, Reith A. Smart building management vs. intuitive human control—Lessons learnt from an office building in Hungary. Build Simul 2017;10:811–28. doi:10.1007/s12273-017-0361-4.

[59] Hirvonen J, Sirén K. A novel fully electrified solar heating system with a high renewable fraction - Optimal designs for a high latitude community. Renew Energy 2018;127:298–309. doi:10.1016/j.renene.2018.04.028.

[60] Rehman H ur, Hirvonen J, Sirén K. Influence of technical failures on the performance of an optimized community-size solar heating system in Nordic conditions. J Clean Prod 2018;175:624–40. doi:10.1016/j.jclepro.2017.12.088.

[61] Manrique Delgado B, Kotireddy R, Cao S, Hasan A, Hoes PJ, Hensen JLM, et al. Lifecycle cost and CO2 emissions of residential heat and electricity prosumers in Finland and the Netherlands. Energy Convers Manag 2018;160:495–508. doi:10.1016/j.enconman.2018.01.069.

[62] Harkouss F, Fardoun F, Biwole PH. Passive design optimization of low energy buildings in different climates. Energy 2018;165:591–613.

[63] Hirvonen J, ur Rehman H, Sirén K. Techno-economic optimization and analysis of a high latitude solar district heating system with seasonal storage, considering different community sizes. Sol Energy 2018;162:472–88. doi:10.1016/j.solener.2018.01.052.

[64] Sankelo P, Jokisalo J, Nyman J, Vinha J, Sirén K. Cost-optimal energy performance measures in a new daycare building in cold climate. Int J Sustain Energy 2019;38:104–22. doi:10.1080/14786451.2018.1448398.

[65] Arabzadeh V, Jokisalo J, Kosonen R. A cost-optimal solar thermal system for apartment buildings with district heating in a cold climate. Int J Sustain Energy 2019;38:141–62. doi:10.1080/14786451.2018.1505725.

[66] Wang C, Martinac I, Magny A. Multi-objective robust optimization of energy systems for a sustainable district in Stockholm. Build. Simul. Conf. 2015, 2015, p. 2010–7.

[67] Bionda D, Kräuchi P, Plüss I, Schröcker M. Simulation of the thermal performance of translucent phase change materials and whole-building energy implications. 10th Conf. Adv. Build. Ski., 2015. doi:10.13140/RG.2.1.1729.4806.

[68] Hasan A, Vesanen T, Jung N, Holopainen R. Automated optimum geometry generation of a building for the minimization of heating and cooling energy demands. Build. Simul. Optim. Conf. 2016, 2016.

[69] Bionda D, Kräuchi P, Plüss I, Schröcker M. Building energy simulation of the thermal performance of translucent PCM exposed to different climates. Status-Seminar «Forschen für den Bau im Kontext von Energ. und Umwelt», 2016. doi:10.13140/RG.2.2.35357.51683.

[70] Niemelä T, Kosonen R, Jokisalo J. Cost-Effective Measures For Energy Improvement Of 1980'S Detached Houses In Cold Climate. Build. Simul. Optim. Conf. 2016, 2016.

[71] Niemelä T, Vuolle M, Kosonen R, Jokisalo J, Salmi W, Nisula M. Dynamic simulation methods of heat pump systems as a part of dynamic energy simulation of buildings. Build. Simul. Optim. Conf. 2016, 2016.

[72] Pal SK, Takano A, Alanne K, Siren K. Integrating architectural and energy viewpoint for a multi objective optimization during early design stage. Build. Simul. Optim. Conf. 2016, 2016, p. 2008–13.

[73] Wang C, Martinac I, Magny A. Multi-objective optimization of energy system designs for the Albano university campus in Stockholm. YRSB16, 2016. doi:10.1016/j.proeng.2017.04.221.

[74] Kayo G, Hasan A, Martinac I, Lahdelma R. Optimal Planning Tool For Nearly

Zero Energy District, 2016.

[75] Harkouss F, Fardoun F, Biwole PH. Multi-objective decision making optimization of a residential net zero energy building in cold climate. 2017 Sensors Networks Smart Emerg. Technol., 2017.

[76] Panagiotidou M, Aye L. Comparison of Multi-objective Optimisation Tools for Building Performance Simulation with TRNSYS 18. Build. Simul. Optim. Conf. 2018, 2018.

[77] Harkouss F, Biwole PH, Fardoun F. Passive designs and renewable energy systems optimization of a net zero energy building in Embrun/France. ICCGE 2018, 2018. doi:10.1088/1755-1315/154/1/012009.

[78] Phdungsilp A. Modeling urban energy flows at macro and district levels: towards a sustainable urban metabolism. 2015.

[79] Niikko A. Kuntien kiinteistönhoidon resurssien mitoituksen optimointi (Optimization of the building maintenance resources in municipalities). 2015.

[80] Stenberg S-Å. Tietokonesalien hukkalämmön hyödyntämismahdollisuuksien teknis-taloudellinen optimointi (Technical and economical optimization of data center waste heat utilization). 2015.

[81] Höglund P. Impact of future usage patterns on the insulation demand for office buildings in Stockholm. 2016.

[82] Wang C. Optimal Design of District Energy Systems : a Multi- Objective Approach. 2016.

[83] Sankelo P. Optimal production and use of solar electricity in municipal nearly Zero Energy service buildings. 2016.

[84] Linse M. An Investigation of Cost-Efficient Solutions in Order to Meet the Energy Requirements in Multi-Family Buildings. 2016.

[85] Sihvonen S. Optimization of demand response control strategies in Finnish city-owned buildings. 2017.

[86] Harkouss F. Conception optimale de bâtiments à énergie nette nulle sous différents climats (Optimal design of net zero energy buildings under different climates). 2018.

[87] European Committee for Standardization (CEN). EN 12831:2003 - Heating systems in buildings. Method for calculation of the design heat load 2003.

[88] International Organization for Standardization (ISO). ISO 6946:2007 - Building components and building elements. Thermal resistance and thermal transmittance. Calculation method 2007.

[89] International Organization for Standardization (ISO). ISO 10077-1:2006 - Thermal performance of windows, doors and shutters. Calculation of thermal transmittance. Part 1: General 2006.

[90] International Organization for Standardization (ISO). ISO 13370:2007 - Thermal performance of buildings. Heat transfer via the ground. Calculation methods 2007.

[91] Deb K, Pratab S, Agarwal S, Meyarivan T. A Fast and Elitist Multiobjective Genetic Algorithm: NGSA-II. IEEE Trans Evol Comput 2002;6:182–97. doi:10.1109/4235.996017.

[92] Hamdy M, Palonen M, Hasan A. Implementation of Pareto-Archive NSGA-II Algorithms to a nearly-Zero-Energy Building Optimization Problem. First Build. Simul. Optim. Conf., Loughborough Uni., UK: IBPSA-England; 2012.

[93] Deb K, Tiwari S. Omni-optimizer: A Procedure for Single and Multi-objective Optimization. In: Coello Coello CA, Hernández Aguirre A, Zitzler E, editors. Int. Conf. Evol. Multi-Criterion Optim. EMO 2005, Berlin, Heidelberg: Springer; 2005, p. 47–61.

[94] Chehouri A, Younes R, Perron J, Ilinca A. A Constraint-Handling Technique for Genetic Algorithms using a Violation Factor. J Comput Sci 2016;12:350–62.

[95] Mühlenbein H. How genetic algorithms really work: Mutation and hillclimbing. Proc. 2nd Int. Conf. Parallel Probl. Solving from Nat. (PPSN ’92), Brussels (Belgium): 1992, p. 15–25.

[96] Palonen M, Hasan A. MOBO Beta 0.3b Manual Version 1.4 2014.

[97] Eiben ÁE, Smith JE. Introduction to Evolutionary Computing. 2nd ed. Natural Computing Series, Springer-Verlag; 2015.

[98] Gagnon R, Gosselin L, Decker] S [Armand. Performance of a sequential versus holistic building design approach using multi-objective optimization. J Build Eng 2019;26:100883. doi:https://doi.org/10.1016/j.jobe.2019.100883.

[99] Ascione F, Bianco N, Iovane T, Mauro GM, Napolitano DF, Ruggiano A, et al. A real industrial building: Modeling, calibration and Pareto optimization of energy retrofit. J Build Eng 2020;29.

[100] Short W, Packey DJ, Holt T. A manual for the economic evaluation of energy efficiency and renewable energy technologies. 1995. doi:NREL/TP-462-5173.

[101] Spitler JD. Load Calculation Applications Manual. Second Edi. American Society of Heating, Refrigerating and Air-Conditioning Engineers; 2014.

[102] Ehrgott M. A discussion of scalarization techniques for multiple objective integer programming. Ann Oper Res 2006;147:343–60. doi:10.1007/s10479-006-0074-z.

[103] Sioshansi R, Conejo A. Optimization in Engineering. Models and Algorithms. Springer Nature; 2017. doi:10.1007/978-3-319-56769-3.

[104] Favre-Perrod P. A vision of future energy networks. 2005 IEEE Power Eng. Soc. Inaug. Conf. Expo. Africa, 2005, p. 13–7. doi:10.1109/PESAFR.2005.1611778.

[105] Geidl M. Integrated Modeling and Optimization of Multi-Carrier Energy Systems. PhD Thesis - Swiss Federal Institute of Technology (ETH), Zurich, 2007. doi:10.3929/ethz-a-005377890.

[106] Geidl M, Koeppel G, Favre-Perrod P, Klöckl B, Andersson G, Fröhlich K. The Energy Hub – A Powerful Concept for Future Energy Systems. Third Annu. Carnegie Mellon Conf. Electr. Ind., 2007.

[107] Piacentino A, Barbaro C, Cardona F, Gallea R, Cardona E. A comprehensive tool for efficient design and operation of polygeneration-based energy μgrids serving a cluster of buildings. Part I: Description of the method. Appl Energy 2013;111:1204–21. doi:10.1016/j.apenergy.2012.11.078.

[108] Kampelis N, Gobakis K, Vagias V, Kolokotsa D, Standardi L, Isidori D, et al. Evaluation of the performance gap in industrial, residential & tertiary near-Zero energy buildings. Energy Build 2017;148:58–73. doi:https://doi.org/10.1016/j.enbuild.2017.03.057.

[109] Hollberg A, Ruth J. Parametric performance evaluation and optimization based on life cycle demands. 8th Energy Forum Adv. Build. Ski., Bressanone, Italy: 2013.

[110] Hollberg A, Ruth J. LCA in architectural design—a parametric approach. Int J Life Cycle Assess 2016;21:943–60. doi:10.1007/s11367-016-1065-1.

[111] Klüber N, Hollberg A, Ruth J. Life cycle optimized application of renewable raw materials for retrofitting measures. World Sustain. Build. 2014, Barcelona, Spain: 2014, p. 1–7.

[112] Ascione F, Bianco N, De Masi RF, Mauro GM, Vanoli GP. Energy retrofit of educational buildings: Transient energy simulations, model calibration and multi-objective optimization towards nearly zero-energy performance. Energy Build 2017;144:303–19. doi:10.1016/j.enbuild.2017.03.056.

[113] Byskov K, Doorman G, Fischer D, Korpås M, Ånestad A, Sartori I. Methodology for optimal energy system design of Zero Energy Buildings using mixed-integer linear programming. Energy Build 2016;127:194–205. doi:10.1016/j.enbuild.2016.05.039.

[114] European Committee for Standardization (CEN). EN 15978:2011 - Sustainability of construction works. Assessment of environmental performance of buildings. Calculation method 2011.

[115] Burachik RS, Kaya CY, Rizvi MM. Algorithms for generating pareto fronts of

multi-objective integer and mixed-integer programming problems. ArXiv 2019:1–23.

[116] Carlucci S, Simone] M [De, Firth SK, Kjærgaard MB, Markovic R, Rahaman MS, et al. Modeling occupant behavior in buildings. Build Environ 2020;174:106768. doi:https://doi.org/10.1016/j.buildenv.2020.106768.

[117] Oldewurtel F, Parisio A, Jones CN, Gyalistras D, Gwerder M, Stauch V, et al. Use of model predictive control and weather forecasts for energy efficient building climate control. Energy Build 2012;45:15–27. doi:https://doi.org/10.1016/j.enbuild.2011.09.022.

[118] Tian W, Wilde] P [de. Uncertainty and sensitivity analysis of building performance using probabilistic climate projections: A UK case study. Autom Constr 2011;20:1096–109. doi:https://doi.org/10.1016/j.autcon.2011.04.011.

[119] Hu S, Yan D, Azar E, Guo F. A systematic review of occupant behavior in building energy policy. Build Environ 2020;175:106807. doi:https://doi.org/10.1016/j.buildenv.2020.106807.

[120] Du J, Pan W, Yu C. In-situ monitoring of occupant behavior in residential buildings – a timely review. Energy Build 2020;212:109811. doi:https://doi.org/10.1016/j.enbuild.2020.109811.

[121] Moretti M, Djomo SN, Azadi H, May K, Vos] K [De, Passel] S [Van, et al. A systematic review of environmental and economic impacts of smart grids. Renew Sustain Energy Rev 2017;68:888–98. doi:https://doi.org/10.1016/j.rser.2016.03.039.

[122] Salehi J, Namvar A, Gazijahani FS. Scenario-based Co-Optimization of neighboring multi carrier smart buildings under demand response exchange. J Clean Prod 2019;235:1483–98. doi:https://doi.org/10.1016/j.jclepro.2019.07.068.

[123] Arnone D, Bertoncini M, Paternò G, Rossi A, Ippolito MG, Riva Sanseverino E. Smart Multi-carrier Energy System: Optimised Energy Management and Investment Analysis. 2016 IEEE Int. Energy Conf., 2016, p. 1–6. doi:10.1109/ENERGYCON.2016.7513926.

[124] Cannata N, Cellura M, Longo S, Montana F, Riva Sanseverino E, Luu QL, et al. Multi-Objective Optimization of Urban Microgrid Energy Supply According to Economic and Environmental Criteria. 2019 IEEE Milan PowerTech, 2019, p. 1–6.

[125] Jia Y, Mi Z, Zhang W, Liu L. Optimal operation of multi-energy systems in distributed energy network considering energy storage. 2017 IEEE Conf. Energy Internet Energy Syst. Integr., 2017, p. 1–6. doi:10.1109/EI2.2017.8245261.

[126] Drauz SR, Spalthoff C, Würtenberg M, Kneikse TM, Braun M. A modular approach for co-simulations of integrated multi-energy systems: Coupling multi-energy grids in existing environments of grid planning operation tools. 2018

Work. Model. Simul. Cyber-Physical Energy Syst., 2018, p. 1–6. doi:10.1109/MSCPES.2018.8405395.

[127] Crainz M, Curto D, Franzitta V, Longo S, Montana F, Musca R, et al. Flexibility Services to Minimize the Electricity Production from Fossil Fuels. A Case Study in a Mediterranean Small Island. Energies 2019;12. doi:10.3390/en12183492.

Chapter Five – Case studies on single building optimisation

5.1. Introduction

This section describes the case studies optimising the energy performance of a single building. Although this topic was often assessed in the existing scientific literature, the methodological approach integrating the life cycle impact and the costs related to the project was hardly investigated. The application of the method should help decision-makers and designers at identifying the best available techniques to effectively save energy and reduce the carbon footprint of the building sector, considering the buildings one-by-one.

The case studies presented in this thesis assessed two different scales of buildings, namely single-floor single-family houses and a multi-story residential building. In detail, the first study tested the method on a cuboidal fictitious building with a square floor area, simulated in the Mediterranean climate of Palermo. The second case study involves an existing 3-storeys residential building located in Denmark (oceanic climate) hosting 24 families, while the last case study describes an existing single-family detached house in Palermo. All these cases involve the renovation of buildings. In addition to the different size and climate, a different approach was adopted for the use phase energy performance simulation. In detail, the two-step approach using different software tools described in Chapter 4 was adopted for the case studies in Palermo, also involving a preliminary 3D modelling phase and the adoption of a dynamic BPS (EnergyPlus). Since the adoption of a detailed dynamic calculation is often disregarded in Danish context, the energy rating software Be18 was employed both for envelope and equipment optimisation, since its adoption is mandatory. This case was also the unique involving a whole building optimisation study, although an envelope optimisation was also performed.

The studies did not take into account the attainment of the nearly zero-energy level stated by the EU, since the aim of the project is to support the policymakers in their decisions rather than just comply with the current regulations. Furthermore, each member state of the EU decided a national limit for the nZEBs, preventing the comparability among the countries. Nevertheless, the method illustrated in this thesis may be easily expanded including the nZEB level as an additional constraint to be satisfied.

Regarding the LCA analysis, since all the case studies involve renovations rather than the design of new buildings, the assessed life cycle modules are B4 and B6. The module B4 was assessed including the production (modules A1-A3) and end-of-life (modules C3-C4) of the interventions, while B6 is the energy use in the operating phase, assessed by the BPS. All the parameters employed in these studies are secondary data, although they are representative of the national context of each case study.

5.2. Fictitious building in Mediterranean climate

The first case study was focused on a fictitious building with a simple structure and shape. This study was developed to verify the feasibility of the dual-step method illustrated in the previous chapter and show how the algorithm works. Thus, a simplified shape was preferred in order to avoid that shape-related features affect the results. The analysis was performed optimising the building's performance in the climatic condition of Palermo, the capital city of Sicily, Italy (Mediterranean climate).

5.2.1. Case study description

The case study involves the renovation of a simplified cuboid-shaped building with a flat roof. The building has 10 m of length and width and 3.5 m height. There are 8 windows, 2 in each orientation, with a total surface of 24 m^2. It should represent a single-family detached house with a single floor. The illustration of this house is provided in Fig. 5.1 and Fig. 5.2. It is assumed that the owner decides to improve the energy performance of the building to reduce his energy bills and to save energy. In the AS-IS scenario (previously the renovation), it was assumed that the energy demand was totally covered through electricity and natural gas from the main grids, using an old gas boiler with an efficiency of 0.85 and an air conditioner with SEER = 2.5 to be replaced with new ones or with other technologies. The estimated annual electricity and natural gas demands are 11,362 kWh and 10,840 kWh, respectively.

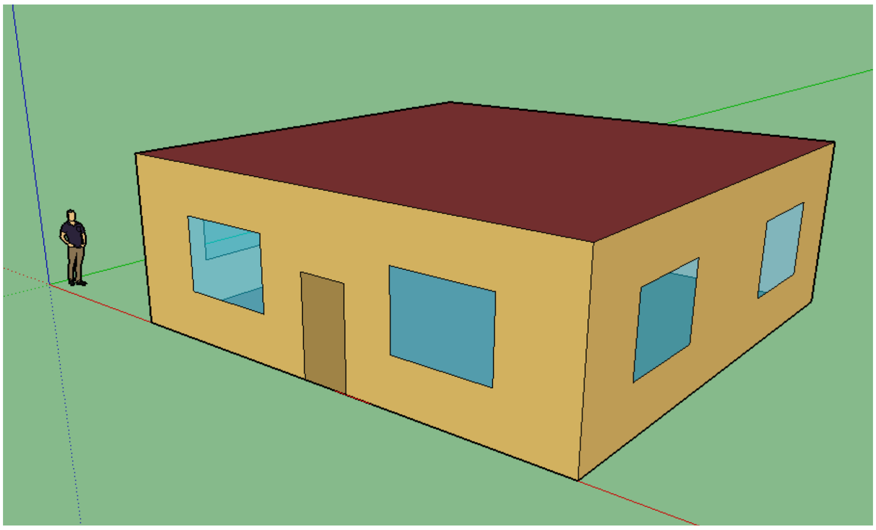

Fig. 5.1. Front view of the model in SketchUp Make 2017 of the fictitious building case study

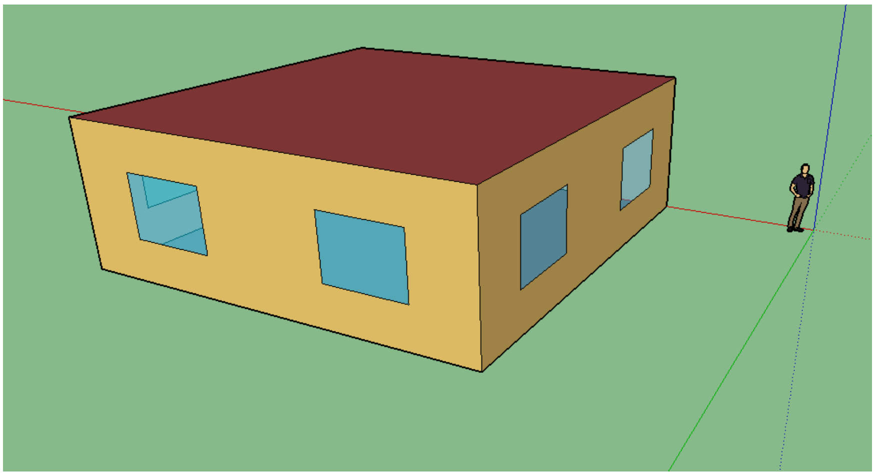

Fig. 5.2. Back view of the model in SketchUp Make 2017 of the fictitious building case study

5.2.2. Step 1 input data

In order to obtain reliable data on the district energy requirements, the 3D building model was developed on SketchUp Make 2017. The thermal features of the main components of the building are described in Table 5.1.

Table 5.1. Thermal features of the main components of the fictitious building model

Component	Layer 1 (outside)	Layer 2	Layer 3	Layer 4	Layer 5
Exterior Wall	M: Bricks T: 102 mm D: 1920 kg/m^3 C: 0.89 W/(m K)	M: Heavyweight concrete blocks T: 203 mm D: 2240 kg/m^3 C: 1.95 W/(m K)	M: Insulation board T: 50 mm D: 43 kg/m^3 C: 0.03 W/(m K)	M: Air space R: 0.15 m^2 K/W	M: Gypsum board T: 19 mm D: 800 kg/m^3 C: 0.16 W/(m K)
Exterior Roof	M: Lightweight concrete blocks T: 102 mm D: 1280 kg/m^3 C: 0.53 W/(m K)	M: Air space R: 0.18 m^2 K/W	M: Acoustic tile T: 19 mm D: 368 kg/m^3 C: 0.06 W/(m K)	-	-
Exterior Floor	M: Insulation board T: 50 mm D: 43 kg/m^3 C: 0.03 W/(m K)	M: Heavyweight concrete blocks T: 203 mm D: 2240 kg/m^3 C: 1.95 W/(m K)	-	-	-
Exterior Door	M: Metal surface T: 0,8 mm D: 7824 kg/m^3 C: 45.3 W/(m K)	M: Insulation board T: 25 mm D: 43 kg/m^3 C: 0.03 W/(m K)	-	-	-
Exterior Window	M: Clear glass T: 3 mm C: 0.9 W/(m K)	Gas gap Gas: Air Thickness: 13 mm	M: Clear glass T: 3 mm C: 0.9 W/(m K)	-	-

M: Material; T: Thickness; D: Density; C: Thermal Conductivity; R: Thermal Resistance

Internal gains (*i.e.* occupants, lighting and electric equipment) were neglected in Step 1, as the target is to focus on the building's envelope. The infiltration rate was calculated according to the equation of Coblenz and Achenbach (Eq. (5.1)) [1]:

$$Infiltration = I_{design} \cdot F_{schedule} \cdot \left(A + B \cdot |T_{zone} - T_{odb}| + C \cdot u_w + D \cdot u_w^2 \right) \tag{5.1}$$

where I_{design} is the design value of air changes per hour, $F_{schedule}$ is the schedule set for the infiltration rate, T_{zone} is the hourly zone temperature (°C), T_{odb} is the outdoor air dry-bulb temperature (°C), u_w is the wind speed and A, B, C and D are the extrapolation coefficients. The values for I_{design}, the extrapolation coefficients (suggested by ASHRAE), and $F_{schedule}$ adopted for the simulations are shown in Table 5.2:

Table 5.2. Parameters employed for the simulation of heat gains for infiltration in the fictitious building

Parameter	Value
I_{design}	0.1 h^{-1}
A	0.606
B	0.03636 K^{-1}
C	0.1177 s/m
D	0 s^2/m^2
$F_{schedule}$	
January	0.71
February	0.89
March	0.84
April	0.97
May	1.00
June	0.91
July	0.78
August	0.76
September	0.78
October	0.80
November	0.62
December	0.61

The annual energy performance simulation on EnergyPlus is based on a standard weather file, usually embedded in the simulation software for the most common cities, while for other cities can be found online. These files contain the standard annual average values of the main physical quantities describing the climate with an hourly detail, as dry bulb outdoor temperature, relative humidity, direct and diffuse normal solar radiation, wind speed, and wind direction. The weather file for Palermo was downloaded from the typical meteorological year files generator developed by the EU Commission [2], and is related to the city centre conditions. It was noticed that the file available on the EnergyPlus website [3] presented two anomalous temperature values during winter that caused a huge peak in the heating demand.

The input file for EnergyPlus, the BPS employed in this study, was created using the Euclid plug-in for SketchUp. The building operating final energy demand was obtained by fixing indoor setpoint temperatures equal to 20 °C for the heating season and 26 °C for the cooling season, and employing an ideal HVAC plant with infinite rated power and unitary efficiency. In this way, technology's performance does not affect the results.

To calculate the annual energy performance of the house, the *Conduction Transfer Function* algorithm was applied to the *Heat Balance Method* [4,5], with a third-order backward difference algorithm for the air node. *DOE-2* and *TARP* algorithms were selected for the convective heat transfer simulation between the building and the outside environment and between the building and the indoor environment, respectively [1]. The resulting annual operating final energy demand is 5188.28 MJ for space heating and 20,092.35 MJ for space cooling. Since EnergyPlus suggests using 10 minutes as timestep for the simulations, the operating final energy demand was calculated using 10 minutes, 30 minutes and 1 hour as timestep. The resulting annual final energy for heating and cooling changed up to about 1%, with respect to the demand obtained with 10 minutes as timestep. Thus, 1 hour was adopted as a timestep for the optimisation, with a deriving saving in the total computational time (about 5 seconds per each building simulation).

The variables selected for the optimisation are the thicknesses of three insulation materials to be installed on two different kinds of surface and the thicknesses of two construction materials. In detail, the installation of rock wool, glass wool or Expanded Polystyrene (EPS) insulation boards was considered for external walls and roof, while additional layers of hollow bricks or concrete were considered to increase the thermal mass of the external walls. The increase of thermal mass on the roof was neglected to avoid structural problems. Excluding concrete layer thickness, modelled as a continuous variable, each variable can assume six or seven values, selected from commercial sizes, in order to reach up to about 15 cm for insulation materials and 50 cm for thermal mass materials. The minimum value was set equal to 10^{-5} since it is the minimum allowed by EnergyPlus, while a value equal to zero would cause errors in the simulation. Assuming that the concrete can be schematised to have 501 values (from 0 to 500 mm), the search space is thus composed of $(7^4) \cdot (6^3) \cdot 501 = 259{,}826{,}616$ building configurations. The thicknesses and thermal features of the materials used for the renovation are shown in Table 5.3.

Since it is a renovation study, the impacts and costs were assessed as differential values between the new configuration and the existing structure; in this way, only the new components were considered in the calculations, neglecting the impacts and costs related to the previous structure.

Unit impact factors for GWP and EE of the materials employed in this study were not assessed directly but drawn from the Environmental Product Declarations (EPD) of representative materials from the Italian or European contexts. Values are shown in Table 5.4, referred to the Declared Unit (DU). In detail, the DU of insulation materials is a 1-m^2 board having a thickness that guarantees a thermal resistance of 1 m^2 K/W, according to the Product Category Rules (PCR) 2014:13 on insulation materials, while the DU for the construction materials is 1000 kg of material.

Unit costs of the materials employed in this study were drawn from Italian catalogues of large do-it-yourself shops. The absolute cost values of at least 4 alternatives for each material were referred to the unit surface and the unit thickness, and then obtained through a least-squares regression. They only take into account the cost of material, neglecting the labour cost. Values are shown in Table 5.5.

Impacts and costs related to the maintenance of building were neglected, because the reference life of the building, assumed to be 60 years, was close or equal to the useful life of the materials for the renovation.

For this study, the multi-objective genetic NSGA II algorithm was selected [6], as it is one of the most employed and performing one [7,8]. The optimisation algorithm parameters were set equal to values suggested by the optimisation tool, and are reported in Table 5.6. The entire search space, composed of over 259 million alternatives, was investigated through only 16·126 = 2016 building configurations, with an enormous time-saving. The computational time on a standard office personal computer was equal to about 20 minutes.

Table 5.3. Insulation materials properties for the fictitious building optimisation

Intervention	Physical and Thermal Properties			
	Thickness	Thermal Conductivity	Density	Specific Heat Capacity
	[m]	[W/(m·K)]	[kg/m^3]	[J/(kg·K)]
Exterior wall additional insulation with rock wool	0.00001, 0.051, 0.076, 0.092, 0.133, 0.152 (6 values)	0.0368	38.5	800
Exterior wall additional insulation with glass wool	0.00001, 0.025, 0.05, 0.075, 0.1, 0.125, 0.15 (7 values)	0.0320	30.0	800
Exterior wall additional insulation with EPS	0.00001, 0.025, 0.05, 0.075, 0.1, 0.125, 0.15 (7 values)	0.0363	15.9	1500
Roof additional insulation with rock wool	0.00001, 0.051, 0.076, 0.092, 0.133, 0.152 (6 values)	0.0368	38.5	800
Roof additional insulation with glass wool	0.00001, 0.025, 0.05, 0.075, 0.1, 0.125, 0.15 (7 values)	0.0320	30.0	800
Roof additional insulation with EPS	0.00001, 0.025, 0.05, 0.075, 0.1, 0.125, 0.15 (7 values)	0.0363	15.9	1500
Exterior wall additional thermal mass with hollow bricks	0.00001, 0.25, 0.3, 0.38, 0.44, 0.5 (6 values)	0.89	1920	790
Exterior wall additional thermal mass with concrete	0.00001 – 0.50 (continuous)	1.95	2240	900

Table 5.4. Unit impact factors for GWP and EE and useful life of components for the fictitious building optimisation

Material	Unit EGWP	Unit EE	Useful Life
	[kg $CO_{2,eq}$/DU]	[MJ/DU]	[years]
Rock wool insulation boards	6.60	137.41	60
Glass wool insulation boards	2.09	54.35	50
EPS insulation boards	5.35	98.93	60
Hollow bricks	283.00	7300.00	60
Concrete	327.00	3663.00	60

Table 5.5. Unit prices of components for the fictitious building optimisation

Material	**Unit Price**
	[€/m^3]
Rock wool insulation boards	98.54
Glass wool insulation boards	91.17
EPS insulation boards	143.66
Hollow bricks	93.46
Concrete	110.20

Table 5.6. NSGA II parameters adopted for the fictitious building envelope optimisation

Parameter	**Value**
Population size	16
Generations	126
Mutation rate	0.1
Crossover rate	0.9

5.2.3. Step 1 results

The optimisation of the building performance allowed to obtain the set of optimal retrofit interventions constituting the four-dimensional Pareto front of the problem [9]. The output of the study is shown through two-dimensional graphs in Fig. 5.3 – Fig. 5.8, where red squares indicate all the 2016 building configurations evaluated in the optimisation (dominated solutions) and the blue line interpolates the optimal solutions, identifying the Pareto front. Since four objective functions were employed, only a part of the Pareto front can be visualized in each graph.

The Operating Energy Consumption is clearly a conflicting objective with respect to the other three functions, thus a Pareto-like distribution is identifiable in Fig. 5.3, Fig. 5.4 and Fig. 5.5; on the opposite, since EE, EGWP and Investment Cost objective functions were calculated with analogous formulas in this study, these quantities result as non-conflicting objectives, as shown in Fig. 5.6, Fig. 5.7 and Fig. 5.8. Furthermore, two quasi-linear trends can be clearly identified between EE and EGWP in Fig. 5.8.

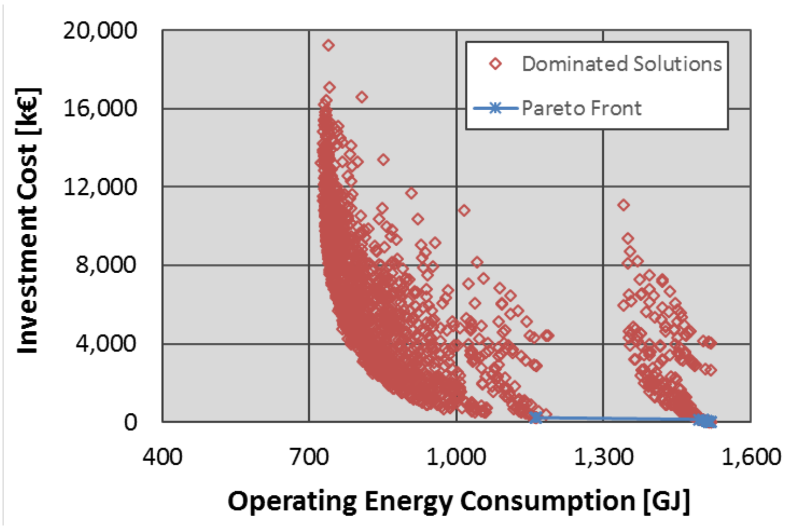

Fig. 5.3. Investment cost against operating energy consumption for the fictitious building in Step 1

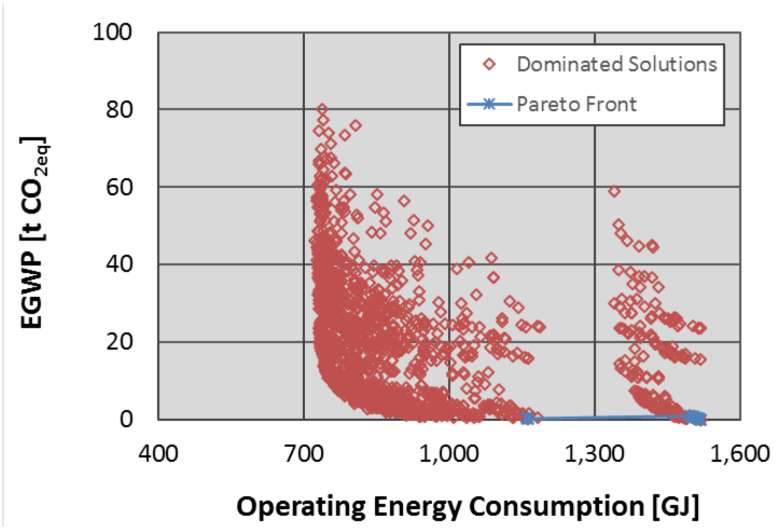

Fig. 5.4. Embodied GWP against operating energy consumption for the fictitious building in Step 1

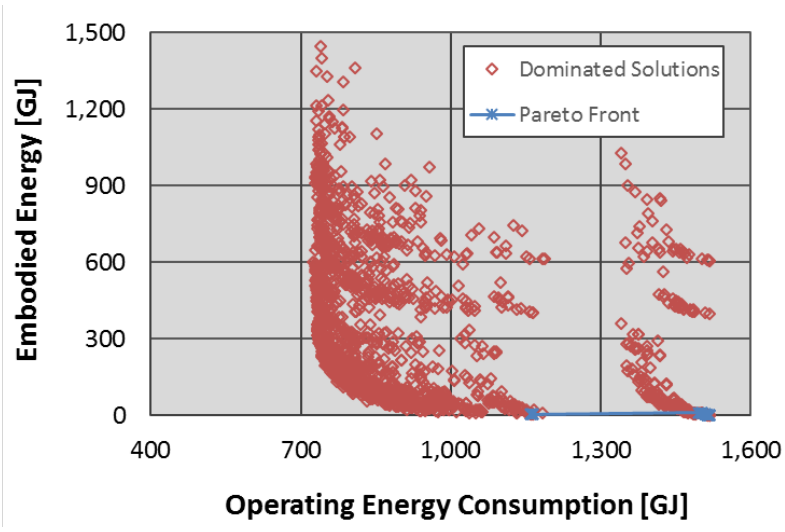

Fig. 5.5. Embodied Energy against operating energy consumption for the fictitious building in Step 1

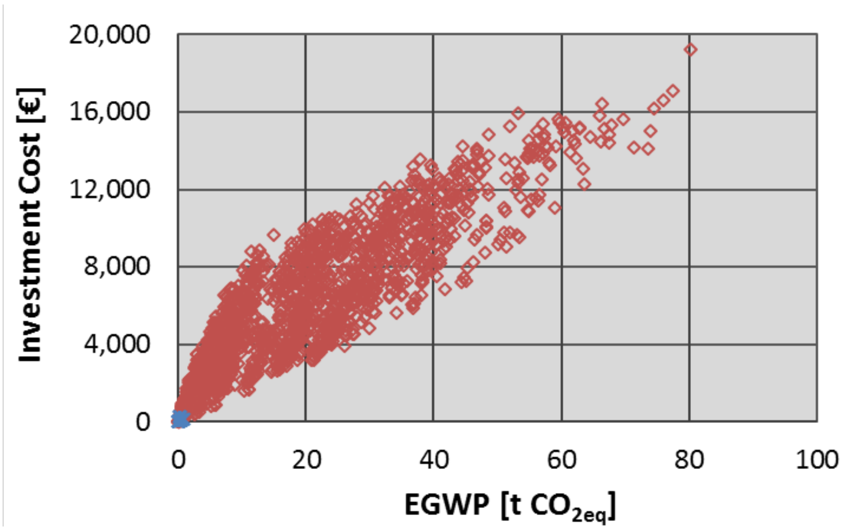

Fig. 5.6. Investment cost against embodied GWP for the fictitious building in Step 1

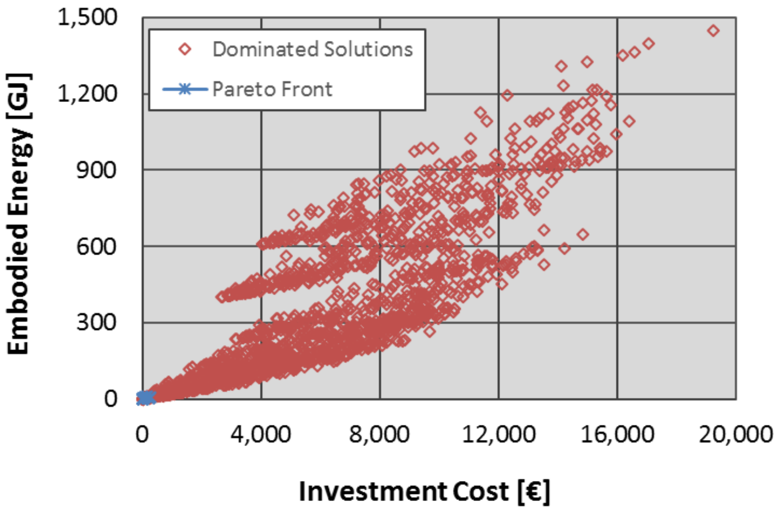

Fig. 5.7. Embodied energy against investment cost for the fictitious building in Step 1

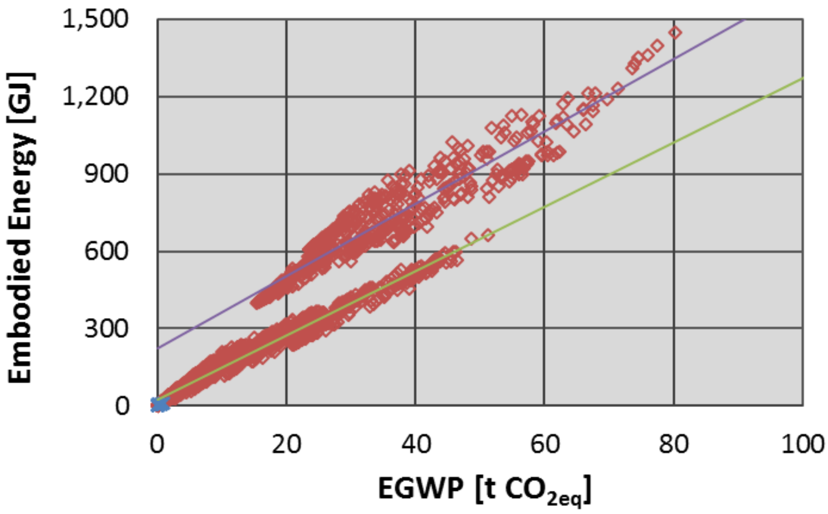

Fig. 5.8. Embodied energy against embodied GWP for the fictitious building in Step 1

Table 5.7 illustrates the values assumed by the objective functions in the solutions of the Pareto front and the corresponding values of variables; analysing this table, it is possible to state that operating energy consumption and investment costs are the real conflicting objectives in this study. Table 5.8 compares the objective functions at the extreme solutions[1] with the range obtained in all the 2016 solutions of the optimisation. Although it is a multi-objective optimisation, the compromise solutions in the Pareto front have very low values of EE, EGWP and Investment Cost with respect to the range. Furthermore, since GWP, EE and Investment Cost are non-conflicting objectives, their extreme solutions overlap.

Regarding the optimal interventions, the optimisation converged to ten retrofit solutions. In these solutions, the external walls were never insulated, while regarding the massive materials' layers, bricks were never adopted, preferring small amounts of concrete (between 0 and 0.012 m). The insulation of the roof was considered in three out of ten solutions, adopting the lowest available thickness (0.025 m), while in the others no insulation was considered. These solutions may be justified considering that the pre-retrofit envelope already had a very high thermal performance. Notwithstanding the optimisation identified a certain amount of compromise solutions, the values of thicknesses of the materials are quite concentrated in a limited portion of the feasibility space, allowing the designer or the customer, that is usually more interested into economic aspects, to select the cheapest solution without impacting significantly on final energy consumption. On the opposite, the solution with minimum operating energy consumption for air conditioning shows that, with an economic expenditure lower than 1000 € (including labour costs), the final energy demand can be reduced from 1518 GJ to 1160 GJ (- 24%). EGWP related to the optimal retrofit interventions is always lower than 1 ton of $CO_{2\text{-eq}}$.

Table 5.7. Objective functions of the Pareto front for the fictitious building optimisation in Step 1 using a heat map (green: positive; light yellow: intermediate; red: negative)

Operating Energy Consumption	Embodied Global Warming Potential	Embodied Energy	Investment Cost	Concrete Thickness	Glass Wool Thickness
[MJ]	[kg $CO_{2\text{-eq}}$]	[MJ]	[€]	[m]	[m]
1,159,874	329	6,116	253	0.002	0.025
1,161,540	206	4,744	235	0.001	0.025
1,163,874	166	4,287	229	0	0.025
1,495,356	982	11,015	148	0.012	0.000
1,501,479	696	7,815	105	0.008	0.000
1,502,290	655	7,357	99	0.008	0.000
1,509,450	329	3,700	50	0.004	0.000
1,513,290	166	1,871	26	0.002	0.000
1,515,188	84	957	13	0.001	0.000
1,518,304	0	0	0	0.000	0.000

[1] The concept of extreme solutions was explained in Section 2.3

Table 5.8. Objective functions at extreme solutions and variability range for the fictitious building optimisation in Step 1

	Operating Energy Consumption	**GWP**	**EE**	**Investment Cost**
	[GJ]	**[kg $CO_{2\text{-eq}}$]**	**[MJ]**	**[€]**
Operating Energy Consumption extreme solution	1160	329	6116	253
GWP, EE and Investment Cost extreme solution	1518	0	0	0
Range	724 – 1518	0 – 80,205	0 – 1.5 · 10^6	0 – 19,200

An example of the improvement of the solutions from one generation to the following is provided in Fig. 5.9. At the beginning of the simulation, random solutions are assessed (population 1, blue spots). With population 25 (light blue spots), some optimal solution was identified, while the Pareto front (population 126, dark red spots), is completely assessed at about population 100 (values are it is behind population 126).

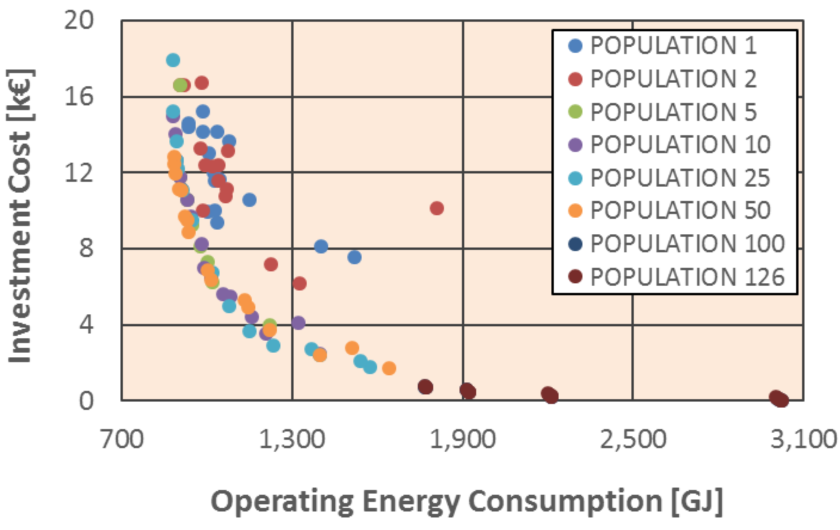

Fig. 5.9. Progress in the generations for the fictitious building in Step 1

The selection of the optimal envelope for the building renovation was performed with the utopia point criterion. Excluding the solutions with null or negligible retrofit actions (< 1 cm of concrete layer and no insulation), the solution with the lower Euclidean distance from the origin of the axes is the solution shown in the third row of Table 5.7, having 2.5 cm of insulation of the roof with glass wool and no additional concrete layer on the external walls. This building configuration has very low Use Phase Energy Consumption (very close to the minimum) and intermediate values of impacts and costs.

5.2.4. Step 2 input data

For the second step of the optimisation, the final energy demands during the standard years of the building are the most important input. To gather these data, the optimal building configuration identified during the Step 1 was simulated the standard behaviour of the occupants, introducing schedules to describe the thermal and electrical loads due to occupants, lighting, electrical equipment, and ventilation, that are provided in Table 5.9 – Table 5.13.

Table 5.9. Occupants presence (relative values related to 4 people)

OCCUPANTS NUMBER	Weekdays	Weekend
00:00 → 01:00	1	0.5
01:00 → 07:00	1	1
07:00 → 08:00	0.75	1
08:00 → 11:00	0	1
11:00 → 12:00	0	0
12:00 → 13:00	0.25	0
13:00 → 14:00	0.75	1
14:00 → 15:00	0.5	1
15:00 → 16:00	0.5	1
16:00 → 18:00	0.5	0.5
18:00 → 19:00	0.75	0
19:00 → 20:00	1	1
20:00 → 21:00	1	1
21:00 → 23:00	1	0
23:00 → 24:00	1	0.5

Table 5.10. Thermal Loads due to the Occupants Activity [W] (values from [10]*)*

OCCUPANTS ACTIVITY	Weekdays	Weekend
00:00 → 01:00	80	100
01:00 → 06:00	80	80
06:00 → 07:00	95	80
07:00 → 08:00	140	80
08:00 → 09:00	0	95
09:00 → 10:00	0	140
10:00 → 11:00	0	120
11:00 → 12:00	0	0
12:00 → 13:00	230	0
13:00 → 14:00	140	120
14:00 → 15:00	140	80
15:00 → 16:00	140	120
16:00 → 18:00	140	120
18:00 → 19:00	170	0
19:00 → 20:00	158	120
20:00 → 21:00	140	120
21:00 → 23:00	120	0
23:00 → 24:00	80	80

Table 5.11. Fraction of Sensible Thermal Loads due to the Lighting System with Reference to the Maximum Load (400 W)

LIGHTING	Weekdays	Weekend
00:00 → 06:00	0.00	0.00
06:00 → 07:00	0.15	0.00
07:00 → 08:00	0.15	0.00
08:00 → 10:00	0.00	0.18
10:00 → 18:00	0.00	0.00
18:00 → 19:00	0.67	0.00
19:00 → 20:00	0.67	0.15
20:00 → 21:00	0.67	0.67
21:00 → 22:00	1.00	0.00
22:00 → 23:00	0.67	0.00
23:00 → 24:00	0.00	0.80

Table 5.12. Sensible Thermal Loads due to Electric Equipment [W]

EQUIPMENT	Weekdays	Weekend
00:00 → 06:00	552.00	552.00
06:00 → 08:00	1457.75	552.00
08:00 → 10:00	552.00	1457.75
10:00 → 11:00	552.00	1552.00
11:00 → 12:00	552.00	552.00
12:00 → 13:00	1902.00	552.00
13:00 → 14:00	1052.00	1252.00
14:00 → 15:00	1052.00	552.00
15:00 → 16:00	552.00	1052.00
16:00 → 17:00	1052.00	1052.00
17:00 → 18:00	552.00	1052.00
18:00 → 19:00	1402.00	552.00
19:00 → 20:00	1902.00	1552.00
20:00 → 21:00	1052.00	2572.00
21:00 → 22:00	1617.00	552.00
22:00 → 23:00	1552.00	552.00
23:00 → 24:00	552.00	1052.00

Table 5.13. Fraction of Windows Opening for Ventilation, Influencing Sensible and Latent Thermal Loads, with Reference to the Maximum Windows Surface [%]

VENTILATION	Weekdays	Weekend
00:00 → 06:00	0.00	0.00
06:00 → 08:00	0.10	0.00
08:00 → 09:00	0.00	0.10
09:00 → 10:00	0.00	0.30
10:00 → 11:00	0.00	0.10
11:00 → 12:00	0.00	0.00
12:00 → 13:00	0.30	0.00
13:00 → 14:00	0.40	0.40
14:00 → 15:00	0.00	0.00
15:00 → 16:00	0.00	0.20
16:00 → 18:00	0.00	0.10
18:00 → 19:00	0.10	0.00
19:00 → 20:00	0.30	0.10
20:00 → 21:00	0.30	0.30
21:00 → 24:00	0.00	0.00

The performance of the building with the optimised envelope and these schedules was simulated, obtaining the energy demand for electricity, space heating and space cooling with hourly detail during the standard year shown in Fig. 5.10. Although the sizing of HVAC components is usually performed using a different approach, based on very conservative assumptions, the annual energy demand with hourly detail from the EnergyPlus simulation was employed to identify the optimal size of the equipment

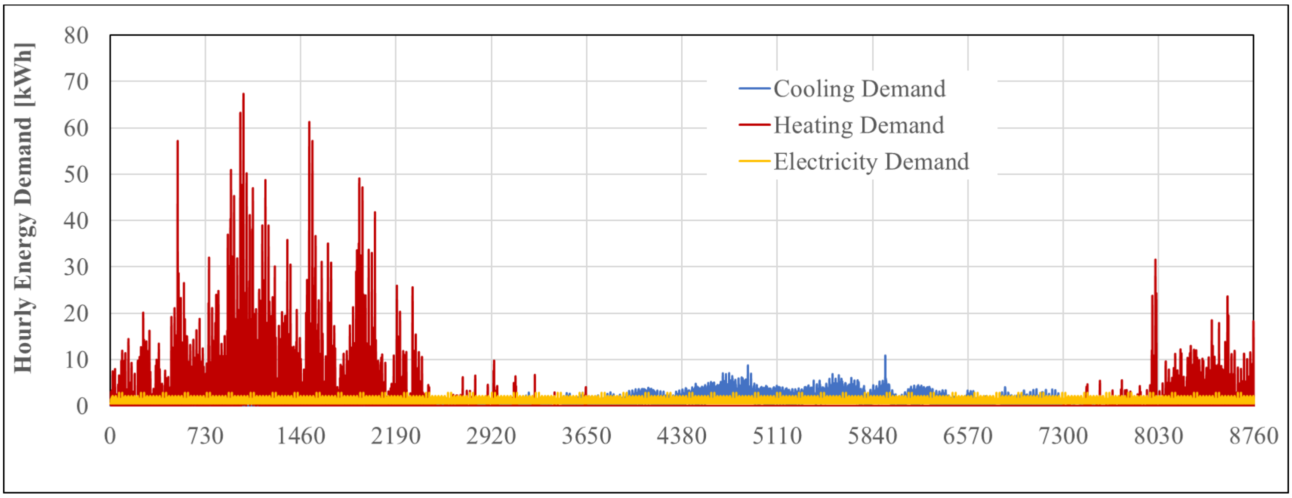

Fig. 5.10. Annual energy demands of the fictitious building with optimised envelope

Since these hourly values are expressed in kWh, their numerical value is equal to the power requested by the building in kW. Although the electrical power demand never exceeds 3.3 kW, that is the standard capacity of the electricity meter in domestic applications, and the space cooling demand is unusually high for a building with these dimensions, the space heating demand often exceeds 35 kW, that is the most common rated power of domestic boilers in Italy. Thus, in order to avoid oversizing of the heating equipment, an upper bound to the power equal to 35 kW was imposed, with a resulting discomfort in the heating season for a limited number of hours. A recap of these considerations is provided in Table 5.14. No thermal discomfort considerations were developed in this study.

Table 5.14. Annual final energy demands of the building and upper bound to the power

	Annual Final Energy Demand [kWh/y]	**Peak [kW]**	**Limit [kW]**	**Discomfort Hours [#]**
Cooling Demand	6702	10.9	11.0	0
Heating Demand	9526	65.9	35.0	31
Electricity Demand	8681	2.8	3.3	0

For this case study, the optimisation assessed to install the following equipment:

RES	**HVAC**	**STORAGE**
• Photovoltaic panel (PV)	• Gas boiler (NGB)	• Li-ions electrical (STO_{el})
• Solar thermal collector (STC)	• Heat pump / air conditioner (HP)	• Sensible thermal (STO_{th})

The variables for the MOO problem are synthesis, design and operation variables for the RES, HVAC and Storage equipment listed above. It was further assumed that the existing gas boiler is old and inefficient and that the owner also wants to replace it. The optimisation was performed according to the scheme shown in Fig. 5.11.

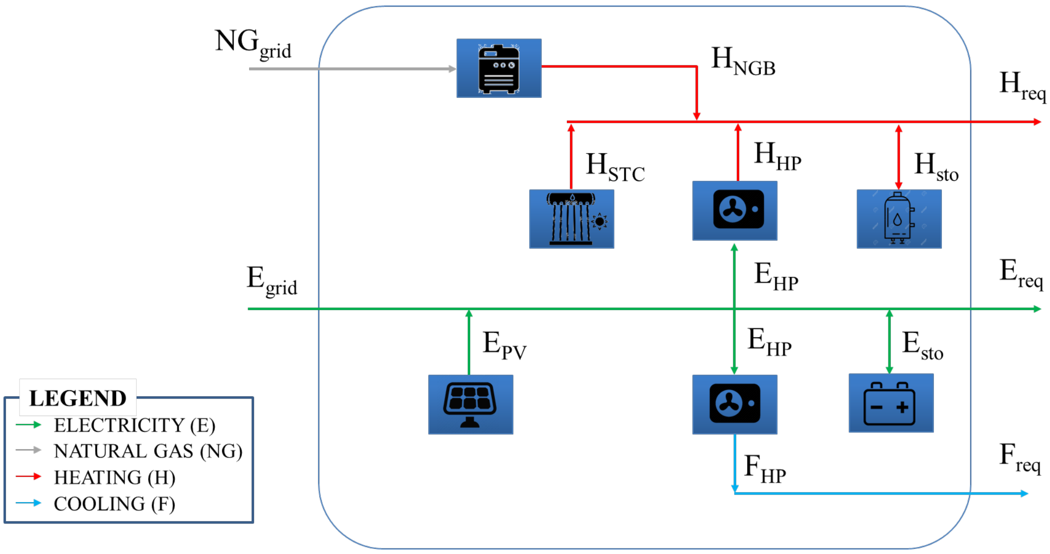

Fig. 5.11. Reference scheme for the energy hub model describing the fictitious building

The hourly demand was employed as input for the MATLAB script for the single building optimisation. Nevertheless, the use of annual data with hourly detail in the optimisation would have required 8760 values for each energy flow of the hub, with a consequent enormous computational burden for the computer. Since this level of accuracy was considered to be excessive for an optimisation problem, where relations are usually simplified in order to attain the optimal solution, the standard year was simplified using four equivalent hours for each day, reducing the number of operation variables for each component to 1460. The problem was thus composed of 6 synthesis variables (one variable for each component), 6 design variables indicating the size of each component, 2·1460 variables for the electricity and gas networks, 2·1460 variables for the energy flowing into HVAC, 2·1460 variables for the energy flowing out from RES systems, and 2·5·1460 variables indicating the status of the storage systems. The total number of variables in this case study was 23,372, while with 24 daily hours the problem would be composed of 140,172 variables.

Since the roof of the house is flat, the PV and STC modules should have a minimum spacing to avoid self-shading phenomena. In order to identify the maximum available rooftop surface, the dimensions of a PV and a STC commercial module were collected. From Fig. 5.10 it is evident that the thermal demand is higher than the electricity demand. For this reason, the available surface, equal to a square with 10 m length, thus a surface of 100 m^2 was shared between PV and STC in a proportion of 40% and 60%, respectively. Thus, a surface of $10 \cdot 4 = 40$ m^2 is available for PV system and $10 \cdot 6 = 60$ m^2 is available for STC.

The distance between the rows was calculated setting the tilt angle equal to 40°, close to the local latitude as is common practice, and considering that the day of the year with maximum self-shading risk is on the winter solstice when the declination is equal to -23.45°. With these input data, the necessary spacing between the modules was calculated, as shown in Table 5.15.

Table 5.15. Minimum distance between rows of solar technologies for the fictitious building

	PV	**STC**
Length (L)	1.65 m	1.987 m
Width	0.992 m	1.27 m
Length projected on the horizontal plane	L·cos(40) = 1.264 m	L·cos(40) = 1.522 m
Minimum distance between rows	L·sin(40)/tan(23.45) = 2.445 m	L·sin(40)/tan(23.45) = 2.944 m

Using these measures, it is possible to install three rows of PV modules with four modules in each row ($N_{PV,max}$ = 12 modules, $A_{PV,max}$ = 19.642 m^2) and two rows of STC with four collectors in each row ($N_{STC,max}$ = 8 modules, $A_{STC,max}$ = 20.188 m^2). Although different configurations of the systems may allow higher exploitation of solar technologies, it was assumed that not the whole surface was available and that the rooftop may not be able to handle the structural load of a higher number of modules.

A value of annual average solar radiation available on the city, necessary for the calculation of RES technologies energy production, was evaluated as the average value from the hourly solar radiation available on the weather file, summing direct and diffuse components, obtaining a value of 6.71 kWh/(m^2 day).

Technical parameters as conversion efficiencies in the components, assumed to be constant, were collected from technical and market reports, and are available in Table 5.16. The cost functions were also drawn from representative reports of the country, and a linear trend for each component was extrapolated through the least-squares method according to Eq. (4.37) in Chapter 4. These values are available in Table 5.17.

The values adopted for the embodied impacts of the equipment are average values from international literature, while data on electricity and gas in the Italian context were drawn from an LCA database. These parameters are shown in Table 5.18. The progressive decarbonisation of the Italian electricity mix in the close future was neglected in the embodied impacts of the electricity, as well as the progressive escalation of prices for both energy carriers. Environmental benefits related to the electricity produced through the PV system and sold to the grid were not included in the analysis, considering only the related economic convenience.

Table 5.16. Technical parameters of the equipment for the fictitious building optimisation

Parameter	Value
Transformer efficiency	99% [11]
Heat pump SCOP	4.1 [12]
Heat pump SEER	5.7 [12]
Heat pump useful life	15 years [13]
Natural gas boiler efficiency	90.1% [12]
Natural gas boiler useful life	24 years [13]
Photovoltaic module efficiency	17.11% [12]
Photovoltaic Balance of Plant efficiency	95% [11]
Photovoltaic system dimensions	$1.65 \cdot 0.992$ m^2 [12]
Photovoltaic system max available surface	19.642 m^2
Photovoltaic system useful life	25 years [12]
Solar thermal collector zero-loss efficiency	79.7% [12]
Solar thermal collector first order heat loss coefficient	3.18 $W/(m^2\ K)$ [12]
Solar thermal collector second order heat loss coefficient	0.008 $W/(m^2\ K^2)$ [12]
Solar thermal collector average efficiency (ΔT = 30 °C)	69.4%
Solar thermal collector dimensions	$1.987 \cdot 1.27$ m^2 [12]
Solar thermal collector max available surface	20.188 m^2
Solar thermal collector useful life	15 years [14]
Electrical storage charging efficiency	97% [11]
Electrical storage discharging efficiency	97% [11]
Electrical storage Depth of Discharge	20% [11]
Electrical storage useful life	7 years [15]
Thermal storage charging efficiency	100% [16]
Thermal storage discharging efficiency	100% [16]
Thermal storage self-discharge coefficient	0.01 kWh/h [16]
Thermal storage useful life	15 years [16]

Table 5.17. Economic parameters of the energy carriers and equipment for the fictitious building optimisation

Parameter	Value
Electrical energy final user price	0.207 €/kWh [17]
Natural gas final user price	0.767 €/kWh [18]
Heat pump first order investment cost	106 €/kW_{cool} [12]
Heat pump zero-th order investment cost	596 € [12]
Natural gas boiler first order investment cost	52 €/kW [12]
Natural gas boiler zero-th order investment cost	114 € [12]
Photovoltaic system first order investment cost	527 €/unit [12]
Photovoltaic system zero-th order investment cost	0 € [12]
Solar thermal collector first order investment cost	600 €/unit [12]
Solar thermal collector zero-th order investment cost	0 € [12]
Electrical storage first order investment cost	165 €/kWh [12]
Electrical storage zero-th order investment cost	2974 € [12]
Thermal storage first order investment cost	36 €/kWh [12]
Thermal storage zero-th order investment cost	77 € [12]
Real interest rate	5.00% [19]

Table 5.18. LCA impact factors of the energy carriers and equipment for the fictitious building optimisation

Item	GWP	CED
Electricity from the Italian grid	0.7089 kg $CO_{2\text{-eq}}$/kWh [20]	11.8 MJ/kWh [20]
Natural gas from the Italian grid	0.0369 kg $CO_{2\text{-eq}}$/kWh [20]	4.1203 MJ/kWh [20]
Manufacture of heat pumps	239.4 kg $CO_{2\text{-eq}}$/kW [21]	1250.4 MJ /kW [21]
Manufacture of gas boilers	19.5 kg $CO_{2\text{-eq}}$/kW [21–23]	92.65 MJ /kW [21]
Operation of gas boilers	0.264 kg $CO_{2\text{-eq}}$/kWh [22]	0.00 MJ /kWh
Manufacture of photovoltaic systems	88.04 kg $CO_{2\text{-eq}}/m^2$ [24]	1619 MJ/m^2 [25]
Manufacture of solar collectors	0.3245 kg $CO_{2\text{-eq}}/m^2$ [26]	39.55 MJ/m^2 [26]
Manufacture of electric storages	76.284 kg $CO_{2\text{-eq}}$/kWh [27]	540 MJ/kWh [27]
Manufacture of thermal storages	8.14 kg $CO_{2\text{-eq}}$/kWh [21]	145.297 MJ/kWh [21]

5.2.5. Step 2 results

The MOO problem was solved using the scalarization technique and a MILP algorithm. The Pareto front was obtained changing the weighs to the three objectives, and the worst values of each OF were adopted as normalisation factors. It is clear that, in this case, the CED and GWP have the same trend, thus introducing these two OF in a three-objective optimisation means somehow to overweigh the LCA aspects. This is proved by the fact that minimising CED and GWP with different weights without taking into account for the costs, the optimal solutions were the same, and even with cost weights up to 0.5 the solutions had the same LCA impact, although the costs were reduced. The values of the OF obtained with the different weighs are provided in Table 5.19, using a coloured background when the values are equal. Due to this aspect, only three different solutions were obtained with w_{cost} from 0 to 0.75, and the Pareto front was populated densifying the values of w_{cost}.

Table 5.19. Optimal values of the OF and related weights for the fictitious building optimisation

SCENARIO	w_{cost}	w_{CED}	w_{GWP}	Annualised Cost	CED	GWP
				€/year	MJ	kg $CO_{2\text{-eq}}$
MIN COST	1.000	0.000	0.000	1,339	2,214,900	132,870
COST >>>>> GWP, NO CED	0.950	0.000	0.050	1,342	2,026,831	121,582
COST >>>> GWP, NO CED	0.870	0.000	0.130	1,363	1,878,755	112,708
COST >>> GWP, NO CED	0.833	0.000	0.167	1,388	1,735,260	104,116
COST >> GWP, NO CED	0.750	0.000	0.250	1,422	1,608,478	96,534
COST > CED, NO GWP	0.667	0.333	0.000	1,422	1,608,478	96,534
COST > GWP, NO CED	0.667	0.000	0.333	1,422	1,608,478	96,534
COST > CED = GWP	0.500	0.250	0.250	1,512	1,478,433	88,880
COST = GWP, NO CED	0.500	0.000	0.500	1,512	1,478,433	88,880
COST = CED, NO GWP	0.500	0.000	0.500	1,512	1,478,433	88,880
CED > COST, NO GWP	0.333	0.667	0.000	1,512	1,478,433	88,880
BALANCED	0.333	0.333	0.333	1,512	1,478,433	88,880
GWP > COST, NO CED	0.333	0.000	0.667	1,512	1,478,433	88,880
MIN CED	0.000	1.000	0.000	2,034	1,478,433	88,880
CED > GWP, NO COST	0.000	0.667	0.333	2,034	1,478,433	88,880
GWP > CED, NO COST	0.000	0.333	0.667	2,034	1,478,433	88,880
MIN GWP	0.000	0.000	1.000	2,034	1,478,433	88,880

Although many more combinations of weights were tried, the optimal solutions were the same as the ones shown in Table 5.19. The three 2D Pareto fronts are shown in Fig. 5.12, where a linear extrapolation between CED and GWP in optimal compromise solutions was highlighted. In these graphs, the solutions with green background in Table 5.19 were excluded, since it is possible to obtain exactly the same CED and GWP values with a lower cost.

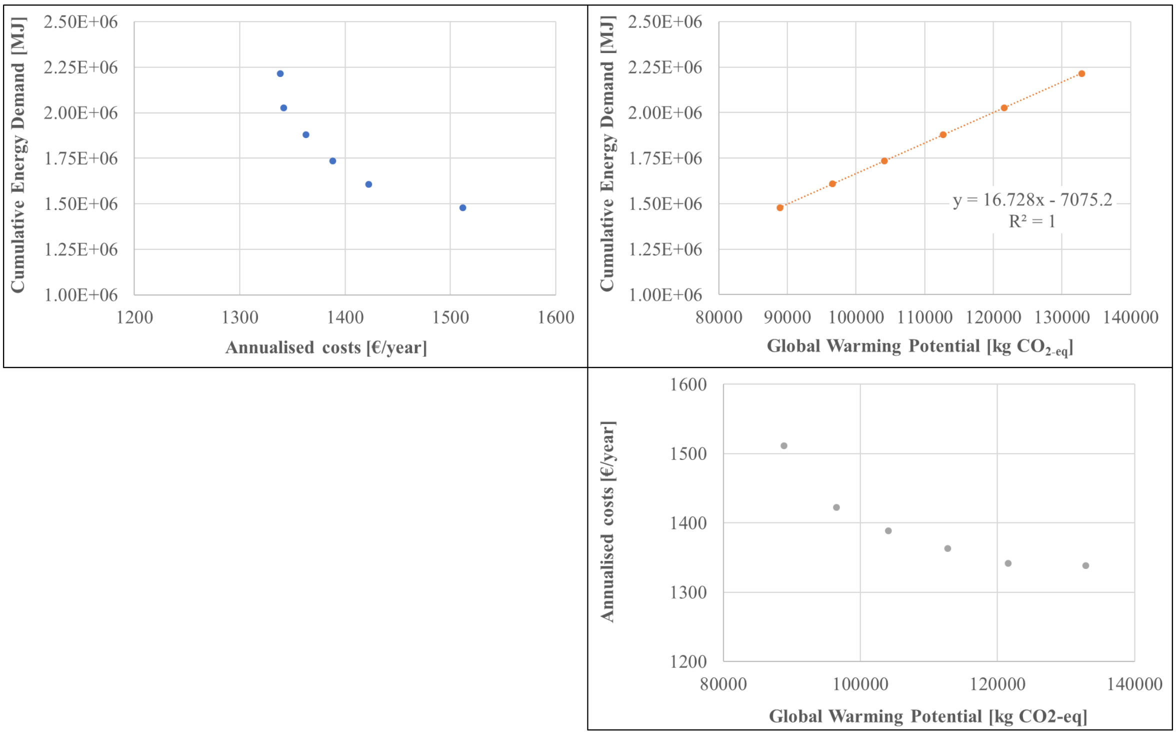

Fig. 5.12. 2D Pareto fronts for the Step 2 of the fictitious building optimisation

Regarding the optimal values of the variables, *i.e.* the equipment sizing, NGB and STO_{el} were never selected, while PV was always selected with maximum possible size, allowing to cover most of the electricity demand and proving that this technology is both cost-optimal and environmentally-optimal. The thermal technologies showed a clear trend in the sizing process, with a higher size of HP with higher values of w_{cost} and higher sizes of STC and STO_{th} for lower values of w_{cost}, that become fixed after w_{cost} = 0.5. Nevertheless, the size of thermal storage becomes unacceptable for the solutions with high weight to the LCA impacts. The electricity demand from the grid increases depending on the HP size. The optimal sizes of the components are shown in Table 5.20.

In order to identify the best combination of equipment sizes and operation, the values of impacts and costs related to the optimal envelope renovation were added to the six solutions of the Pareto front resulting from the Step 2 optimisation. Using the utopia point criterion, as already done for Step 1, the best compromise solution was identified as the one described in the rows with a grey background in Table 5.19 and Table 5.20. The resulting values of the objective functions are recapped in Table 5.21, together with the economic, energy and carbon payback times [28]. The renovation is highly convenient from all the points of view, with energy and carbon payback times being lower than one year.

Table 5.20. Optimal values of the variables and related weights for the fictitious building optimisation

	N_{PV}	N_{STC}	P_{HP}	$V_{sto,th}$	E_{grid}
	#	#	kW	m^3	kWh/year
MIN COST	12	3	6.5	1.26	3,097.70
COST >>>>> GWP, NO CED	12	4	6	1.33	2,832.37
COST >>>> GWP, NO CED	12	5	5	3.48	2,420.94
COST >>> GWP, NO CED	12	6	4.5	3.48	2,420.94
COST >> GWP, NO CED	12	7	4	5.21	2,242.00
COST > CED, NO GWP	12	7	4	5.21	2,242.00
COST > GWP, NO CED	12	7	4	5.21	2,242.00
COST > CED = GWP	12	8	2.6	14.46	2,058.25
COST = GWP, NO CED	12	8	2.6	14.46	2,058.25
COST = CED, NO GWP	12	8	2.6	14.46	2,058.25
CED > COST, NO GWP	12	8	2.6	14.46	2,058.25
BALANCED	12	8	2.6	14.46	2,058.25
GWP > COST, NO CED	12	8	2.6	14.46	2,058.25
MIN CED	12	8	2.6	14.46	2,058.25
CED > GWP, NO COST	12	8	2.6	14.46	2,058.25
GWP > CED, NO COST	12	8	2.6	14.46	2,058.25
MIN GWP	12	8	2.6	14.46	2,058.25

Table 5.21. Optimal values of the objective functions and payback times for the fictitious building optimisation

	Economic criterion	*Energy criterion*	*Carbon criterion*
Embodied - Envelope	229 €	4287 MJ	166 kg $CO_{2\text{-eq}}$
Embodied - Equipment	57,488 €	63,417 MJ	3486 kg $CO_{2\text{-eq}}$
Operating (over 60 years)	27,846 €	1,587,339 MJ	95,372 kg $CO_{2\text{-eq}}$
TOT	85,562 €	1,655,043 MJ	99,023 kg $CO_{2\text{-eq}}$
Operating in AS-IS scenario (over 60 years)	639,956 €	10,724,006 MJ	507,322 kg $CO_{2\text{-eq}}$
Payback Time	5.66 years	0.44 years	0.53 years

5.3. Real building in oceanic climate

The second case study was developed on an existing residential building located in the village of Hvalsø (Denmark), 55 km west of Copenhagen. It is a 3-storeys residential building, being part of a complex of three buildings collectively known as *Traneparken*. This small district was renovated in 2012 mainly because the thermal envelope was run down, but also energy efficiency interventions were integrated. The complex was already analysed in the past by the researchers of the Danish Building Research Institute of the Aalborg University Copenhagen, who also participated in the renovation. The study, developed during the external stay in Copenhagen, allowed gathering a practical experience on the renovation of buildings and on typical techniques from cold climates. Furthermore, one of the aims of this study is to compare the retrofit solutions selected during the renovation occurred in 2012 with the outcomes of the optimisation study, although no minimum legal requirement was considered in the study.

5.3.1. Case study description

The selected building (Traneparken Block B) has a heated floor area of 2048 m^2, with a total of 24 flats, and before the refurbishment was composed of a typical '60s construction made up of prefabricated reinforced concrete sandwich elements with insulation material. The roof is made up of a fibre cement board and was insulated, while the floor has a concrete layer and an insulation layer. Windows were double-glazed with a *U*-value of 1.8 W/(m^2 K). The building plan area is rectangular, with the main axis oriented along the East-West direction, and has a Window to Wall Ratio (WWR) equal to 0.18 and a surface over volume ratio equal to 0.31 m^2/m^3. Although the three blocks are quite close, no mutual shading was considered in the building energy modelling. In Fig. 5.13, the Traneparken complex is shown with the indication of the three blocks. Main components' area with their thermal transmittance *U* and main thermal bridges length and linear thermal transmittance ψ are provided in Table 5.22.

Fig. 5.13. Satellite view of the blocks of Traneparken complex

Table 5.22. Main geometrical and thermal features of the real Danish building optimisation

Element	Features	Area [m²]	U [W/m²·K]
Exterior concrete walls	Concrete sandwich, 50 mm mineral wool insulation	1047.67	0.66
Roof	14-degree slope, fibre cement cladding, 185 mm insulation	682.62	0.20
Exterior light walls	Light board, 45 mm insulation	330.55	0.70
Basement walls	Concrete, no insulation	363.84	1.00
Basement floor	100 mm expanded clay aggregate insulation	730.80	0.40
Shared floor slab between staircase and basement	Concrete deck, no insulation	48.18	1.30
Shared walls between apartments and staircase	Light weight concrete, no insulation	482.91	1.20
Staircase windows	2-layer glazing	85.83	2.40
Flats windows	2-layer glazing	298.27	2.40
Thermal bridges		**Length [m]**	**ψ [W/m·K]**
Façade / windows, doors		860.00	0.03
Foundation / basement wall		149.20	0.50

The building space heating and DHW requirements are fulfilled by district heating through a 200-kW plate heat exchanger, with three 300 l tanks for DHW storage. There is no space cooling system installed, and the flats are ventilated by a mechanical exhaust system which, extracted air from bathrooms, toilets and kitchens. There are energy-saving light bulbs in all indoor lamps on the stairways, equipped with automatic switch-off controls based on presence sensors. Outdoor lighting has automatic daylight switch-off.

After the renovation, the building envelope was improved with the interventions described in Table 5.23. Furthermore, a demand-controlled balanced mechanical ventilation system with heat recovery was installed for the flats' ventilation, and a 33 kW_p PV system was installed on the rooftop facing the South. Through these interventions, the annual energy demand of the building was reduced from 166.4 kWh/(m^2 y) to 77.2 kWh/(m^2 y). This allowed the annual economic expense related to energy bills to decrease from 66,700 € to 45,500 €.

Table 5.23. Structural interventions during the renovation of the real Danish building

Element	Intervention	Old U-value [W/m²·K]	New U-value [W/m²·K]
Exterior Walls	190 mm additional insulation and new brick layer	0.66	0.15
External light walls	285 mm additional insulation and new brick layer	0.70	0.11
Basement walls	250 mm additional insulation light-weight concrete blocks 100 mm extra insulation (plinth)	1.00	0.25
Roof	250 mm additional insulation on extended roof construction	0.20	0.09
Windows	3-layer glazing	2.40	0.80

5.3.2. Input data

The energy simulation of this building was entirely developed in Be18, that is based on the quasi-steady state monthly averaged balance described in the ISO 13790:2008 international standard [29]. This method is simplified with respect to the dynamic simulation with hourly detail performed by EnergyPlus. For example, the preliminary 3D modelling of the building is not required, as well as the weather file and the exact list of materials composing each opaque surface. This last information is necessary in EnergyPlus to calculate the dynamic thermal characteristics of each building component, influencing the heat transfer when a transient calculation method is employed. The list of the thermal transmittance of the components used in this study is shown in Table 5.22.

The simulation model was subject to validation, namely the fine-tuning of model parameters aimed at approaching actual measurements. In detail it was possible to compare the annual energy consumption for heating and DHW both before and after the actual renovation, ensuring that the optimisation could be applied to a reliable simulation model. The validation was based on the measurement of the total consumption of the district heating supplying the building, and then split in heating and DHW contributions based on the individual heat meters. The measurements were further degree-day corrected for comparison with the calculated consumption. Since the comparison proved a quite large difference, the models were calibrated according to the occupants behaviour parameters. The key quantities were the indoor temperature, measured to be approximately 22 °C instead of 20 °C, and the ventilation rate, equal to 0.34 $l/s/m^2$ on average instead of the value of 0.30 $l/s/m^2$ recommended by standards. This operation was illustrated with more details in [30,31].

Taking as a reference the renovation occurred in 2012, the interventions on the building envelope for the Step 1 involved additional insulation on the external concrete walls, the light walls, the basement walls and the roof, new cladding on the external walls, the basement walls and the roof, and the replacement of the glazed surfaces on windows, balconies and staircase. Different windows glazing and frames according to the orientation were also investigated. The physical and thermal properties of these materials are shown in Table 5.24 and Table 5.25. Furthermore, the complete set of interventions is described in Table 5.26, together with the LCA and economic parameters employed for the optimisation [32]. To identify the search space it is necessary to evaluate the number of possible alternatives, given by the number of possible alternatives for each variable elevated to the number of variables. For example, there are nine possible insulation thicknesses for external walls and three materials, thus $9^3 = 729$ variables related to the possibility of increasing the insulation thickness in external walls. Considering the number of variables assessed in this study, the search space is composed of $(9^6) \cdot (8^3) \cdot (2^{64}) = 5.84 \cdot 10^{17}$ buildings.

The correct development of Step 2 was prevented by the fact that using an energy rating tool based on the quasi-steady state method, the energy demand of the optimal building envelope was available with an average monthly detail. This level of detail was unacceptable; thus, a different and more practical approach was adopted. In detail, as well as for Step 1, the equipment optimisation was performed on Be18 & MOBO. The upper bound of the rated power of the heating components was set equal to 55 kW, namely the size of the heat exchanger installed in the building before the renovation, that would be for sure sufficient also for the building with optimised envelope. Since there is not a predictable link between the energy produced and the rated power using this approach, the actual fulfilling of the air conditioning demand of the building was checked after the simulations. Since the space cooling demand was equal to zero, no cooling equipment was considered. Furthermore, since the same software environment was employed for envelope and equipment optimisation, a whole building optimisation was performed instead of the dual step approach.

The additional variables of the problem are the PV system area, the STC area, the NGB rated power, the HP rated power, and the district heating heat exchanger rated power (for a standard temperature difference). The areas of solar technologies were modelled as continuous variables while the remaining equipment sizes were considered as discrete variables. The rooftop area available for the solar technologies installation is equal to 220 m^2, thus both of the system's areas were bounded between 0 and 220 m^2, while Boolean variables were also included for each component to set the constraints. Since the building has a tilted roof, no spacing to avoid self-shading was required in this case. Considering the number of additional variables, the search space is composed of $(9^6) \cdot (8^3) \cdot (2^{68}) \cdot 8 \cdot (12^3) = 8.98 \cdot 10^{20}$ buildings. The LCA and economic parameters for the OFs describing the components are in Table 5.27, while the parameters related to the energy carriers are shown in Table 5.28 [32]. Since projections on the impacts of electricity and district heating due to the different energy mix in Denmark were also available [33], these projections were included in the analysis. The economic analysis was performed in Danish Coronas, although the final results were also converted in euros.

Table 5.24. Insulation materials properties for the real Danish building optimisation

Insulation		**Physical and thermal properties**		
		Thickness	**Range**	**Thermal conductivity**
		[m]	**[m]**	**[W/(m·K)]**
Exterior concrete walls	Mineral wool	0.050	0 - 0.4	0.034
	Cellulose	0.050	0 - 0.4	0.040
	EPS	0.050	0 - 0.4	0.038
Exterior light walls	Mineral wool	0.050	0.09 - 0.44	0.034
	Cellulose	0.050	0.09 - 0.44	0.040
	EPS	0.050	0.09 - 0.44	0.038
Roof	Mineral wool	0.050	0 - 0.4	0.042
	Cellulose	0.050	0 - 0.4	0.040
Basement wall	EPS	0.050	0 - 0.4	0.038

Table 5.25. Glazing properties for the real Danish building optimisation

Windows and glazing	**Physical and thermal properties**	
	Thermal transmittance	**Solar energy transmittance**
	[W/(m²·K)]	**-**
Windows with double-glazing	1.1	0.44
Window with triple-glazing	0.8	0.38
New balconies with single-glazing	4.7	0.60
New balconies with double-glazing	1.1	0.44
New balconies with triple-glazing	0.8	0.38
Staircase window with single-glazing	4.7	0.60
Staircase window double-glazing	1.1	0.44
Staircase window triple-glazing	0.8	0.38

Table 5.26. Envelope related parameters for the real Danish building optimisation

Envelope interventions		LCA Parameters (A and C Phases)			Economic Parameters	
		Embodied Energy	Embodied GWP	Service Life	Investment + Labour Cost excluding VAT	
		[kWh]	[kg CO_{2-eq}]	[y]	[DKK/m]	[DKK]
Insulation	Mineral wool on exterior walls	1563	3.90	80	1062.60	75.72
	Cellulose on exterior walls	2.56	0.35	60	1649.20	54.65
	EPS on exterior walls	22.31	5.78	80	778.04	68.91
	Mineral wool on roof	15.63	3.90	50	449.45	58.56
	Cellulose on roof	2.56	0.35	40	514.85	66.08
	EPS on basement walls	22.31	5.78	80	778.04	68.91
Cladding	Bricks on exterior walls	294.36	58.19	80	0.00	1085.99
	Slate + supporting construction on exterior walls	108.90	17.95	120	0.00	804.78
	Fibre cement board + supporting construction on exterior walls	55.14	9.77	60	0.00	690.64
	Aluminium board + supporting construction on exterior walls	452.55	92.36	60	0.00	460.95
	Fibre cement board on roof	85.39	11.69	40	0.00	489.29
	Ceramic roof tiles on roof	123.00	23.04	60	0.00	642.16
	Bituminous membrane on roof	308.09	46.45	20	0.00	587.54
	Zinc (double standing seam) on roof	324.62	28.11	50	0.00	1577.73
	Light weight concrete blocks on basement walls	112.64	32.21	80	0.00	590.50
Windows frames and glazing	Windows with double-glazing	132.97	37.79	25	0.00	1411.54
	Windows with triple-glazing	199.45	56.68	25	0.00	1711.54
	Windows with PVC frame and double-glazing	431.14	125.09	50 (frame)	0.00	2268.14
	Windows with PVC frame and triple-glazing	497.62	143.98	50 (frame)	0.00	2437.25
	Windows with aluminium frame and double-glazing	639.56	136.65	60 (frame)	0.00	4186.12
	Windows with aluminium frame and triple-glazing	706.05	155.54	60 (frame)	0.00	4494.01
	Windows with wood frame and double-glazing	659.94	69.93	50 (frame)	0.00	2899.61
	Windows with wood frame and triple-glazing	726.43	88.83	50 (frame)	0.00	4074.29
Balcony and staircase glazing	Single-glazing	50.08	13.70	50	0.00	390.66
	Double-glazing	132.97	37.79	25	0.00	1411.54
	Triple-glazing	199.45	56.68	25	0.00	1711.54

Table 5.27. Service equipment related parameters for the real Danish building optimisation

Equipment	LCA Parameters			Economic Parameters			Service Life
	Embodied Energy	Embodied GWP	Functional Unit	Investment + Labour Cost excluding VAT		Functional Unit	
	[MJ]	[kg CO_{2-eq}]	-	[DKK/FU]	[DKK]	-	[years]
PV system	5054.430	316.150	1 m^2	2498.60	0.00	1 m^2	30
Solar thermal collector	1841.178	105.492	1 m^2	6645.19	7066.53	1 m^2	30
District heating heat exchanger	69.360	5.051	1 kW	1781.94	0.00	1 kW	30
Natural gas boiler	18,802.320	1330.570	1 unit	1186.88	0.00	1 kW	30
Heat pump	4780.435	341.070	1 kW	10,567.47	0.00	1 kW	30

Table 5.28. Energy carriers related parameters for the real Danish building optimisation

Service	LCA Parameters (A phase)				Economic Parameters	
	Primary Energy	GWP	Lower Heating Value	Functional Unit	Supply Cost excluding VAT	
	[MJ]	[kg CO_{2-eq}]	[kWh/kg]	-	[DKK]	[DKK / kW]
Electricity from the grid - 2015	6.380	0.352	-	1 kWh	2.20	-
Electricity from the grid - 2020	6.060	0.201	-	1 kWh	-	-
Electricity from the grid - 2025	5.870	0.169	-	1 kWh	-	-
Electricity from the grid - 2035	5.170	0.031	-	1 kWh	-	-
Electricity from the grid - 2050	4.220	0.024	-	1 kWh	-	-
Electricity to the grid	0.000	0.000	-	1 kWh	0.26	
District heating from the grid - 2015	0.694	0.187	-	1 kWh	0.40	0.30
District heating from the grid - 2020	0.680	0.112	-	1 kWh	-	-
District heating from the grid - 2025	0.720	0.101	-	1 kWh	-	-
District heating from the grid - 2035	0.460	0.072	-	1 kWh	-	-
District heating from the grid - 2050	0.310	0.058	-	1 kWh	-	-
Natural gas from the grid	3.888	0.239	15.18	1 kWh	5.49	-

Since four MOO algorithms are available in MOBO, a comparison between their performance was done, also with different settings of the parameters, in order to identify the most suitable one. The performance of these algorithms was compared through the number of the resulting feasible solutions and optimal compromise solutions (Pareto front), as reported in Table 5.29, and through the visualisation of the resulting bi-dimensional Pareto fronts, shown in Fig. 5.14. According to these results, the Omni-Optimizer algorithm was selected, using 200 generations and 40 individuals for each generation, while the crossover rate was set equal to 0.9.

Table 5.29. Comparison of the performance of MOO algorithms for the real Danish building optimisation

	Population	***Generations***	***Alternatives***	***Feasible solutions***	***Pareto front***
aNSGA II	16	200	3200	768	252
aNSGA II	40	200	8000	2267	379
NSGA II	40	200	8000	2434	381
Omni-Optimizer	40	200	8000	2986	491
Omni-Optimizer	16	500	8000	2150	267

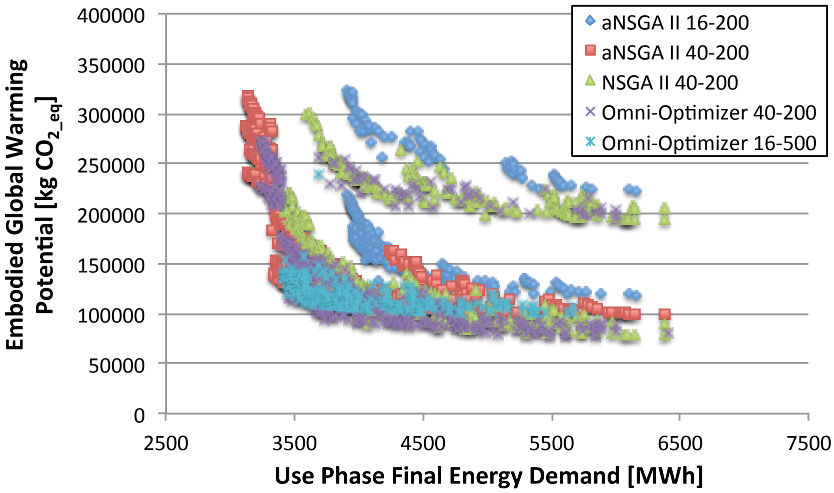

Fig. 5.14. Comparison of bi-dimensional Pareto fronts for the real Danish building optimisation

5.3.3. Step 1 results

The optimisation of the building envelope allowed identifying 2986 feasible solutions, while the related Pareto front is composed by 491 compromise solutions. Fig. 5.15 – Fig. 5.20 show all the feasible solutions (blue rhombi), the Pareto front (green triangles), the extreme solutions (red squares) and the best compromise solution (orange circle), using the six possible combinations of the four objective functions. From the analysis of these pictures, the Pareto front results to be split into three regions, with each region including at least one of the extreme solutions. The quasi-linear trend in the graph relating EGWP and EE indicates that these functions are concurrent objectives also in this case study; for this reason, the extreme solutions minimising these OFs are very close.

The best compromise solution was identified adopting the utopia point distance to the Pareto front, selecting the building configuration with the lowest Euclidean distance. The main features of this solution, together with the other seven with very low Euclidean distance, are reported in Table 5.30. The solutions were listed with decreasing Euclidean distance from the left to the right. The roof was not further insulated in most of these solutions, while the external and basement walls were equipped with an additional insulation layer, most commonly with cellulose, whose thickness ranges between 10 and 30 cm. Fibre cement was selected as the cladding material in each alternative, both for walls and roof, and double-glazing was considered for apartment and staircase windows in both orientations, while no glazing is the most adopted solution for the balconies. Although it seems to be counter-intuitive, the windows frames are usually composed of different materials according to the orientation, *i.e.* PVC for South-oriented windows and wood for North-oriented windows. This difference may be explained because the glazed surface in the South-oriented wall is almost the double of the North-oriented one. This aspect should be linked to the performance indicators in Table 5.26, where the wood frames have the lowest EGWP and PVC framed windows have the lowest investment cost and EE.

Table 5.30. Comparison of the main features of the best compromise solutions for the envelope optimisation of the real Danish building

# of solution	1196	1469	1739	1541	1277	1532	1750	1383
Concrete walls insulation material	Cellulose	Cellulose	EPS	Cellulose	Cellulose	Cellulose	Cellulose	Cellulose
Light walls insulation material	Cellulose	Mineral wool	Cellulose	Mineral wool	Mineral wool	Cellulose	Cellulose	Cellulose
Roof insulation material	No insulation	Cellulose	No insulation	Cellulose	Cellulose	No insulation	No insulation	No insulation
External walls insulation thickness	0.25 m	0.10 m	0.10 m	0.20 m	0.25 m	0.20 m	0.10 m	0.25 m
Light walls insulation thickness	0.34 m	0.24 m	0.19 m	0.14 m	0.14 m	0.44 m	0.14 m	0.14 m
Basement walls insulation thickness	0.10 m	0.20 m	0.20 m	0.05 m	0.20 m	0.10 m	0.30 m	0.30 m
Roof insulation thickness	-	0.40 m	-	0.35 m	0.10 m	-	-	-
External walls cladding material	Fibre-cement	Fibre-cement	Fibre-cement	Fibre-cement	Fibre-cement	Fibre-cement	Fibre-cement	Fibre-cement
Roof cladding material	Fibre-cement	Fibre-cement	Fibre-cement	Fibre-cement	Fibre-cement	Fibre-cement	Fibre-cement	Fibre-cement
Balcony glazing	Single glazing	No glazing	No glazing	No glazing	No glazing	No glazing	No glazing	No glazing
Staircase glazing	Double glazing	Double glazing	Double glazing	Double glazing	Double glazing	Double glazing	Double glazing	Double glazing
North façade windows glazing	Double glazing	Double glazing	Double glazing	Double glazing	Double glazing	Double glazing	Double glazing	Double glazing
South façade windows glazing	Double glazing	Double glazing	Double glazing	Double glazing	Double glazing	Double glazing	Double glazing	Double glazing
South façade windows frame	PVC	PVC	PVC	PVC	PVC	PVC	PVC	PVC
North façade windows frame	Wood	Wood	Wood	Wood	Wood	Wood	Wood	PVC

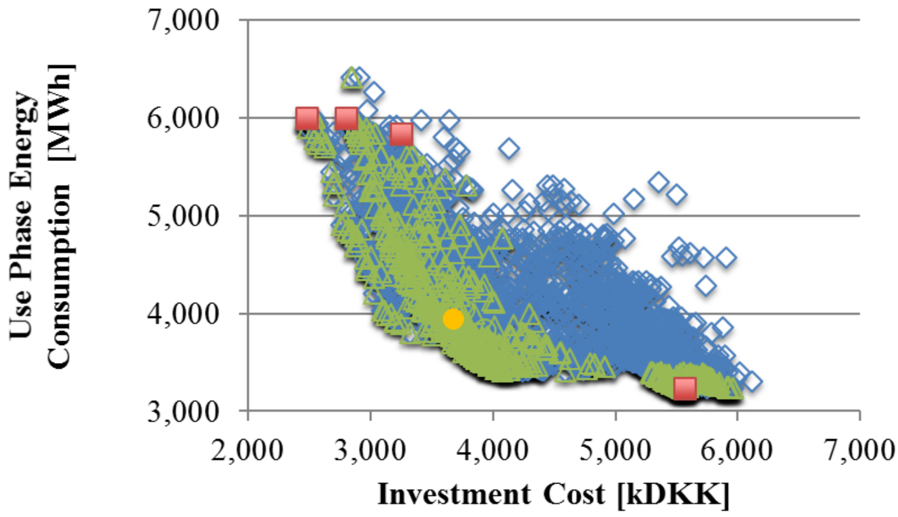

Fig. 5.15. Investment cost against use phase energy consumption for the real Danish building in Step 1

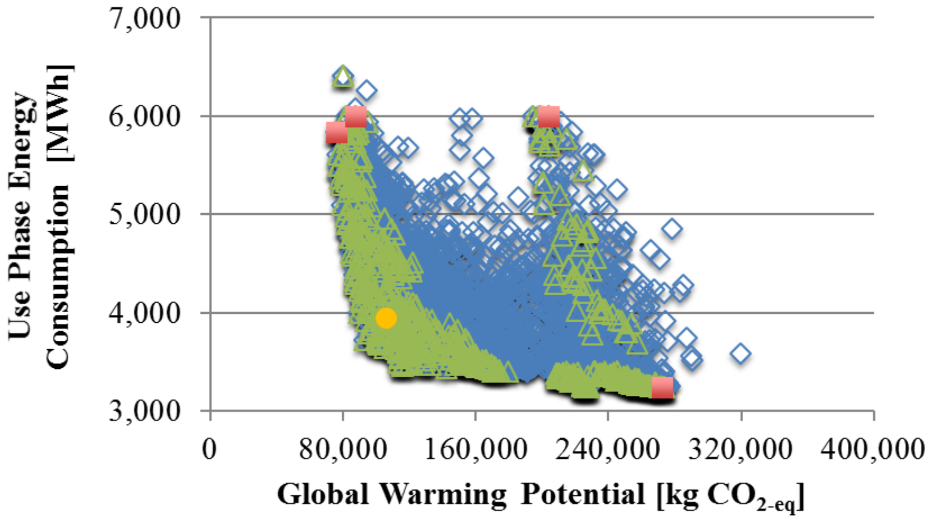

Fig. 5.16. Embodied GWP against use phase energy consumption for the real Danish building in Step 1

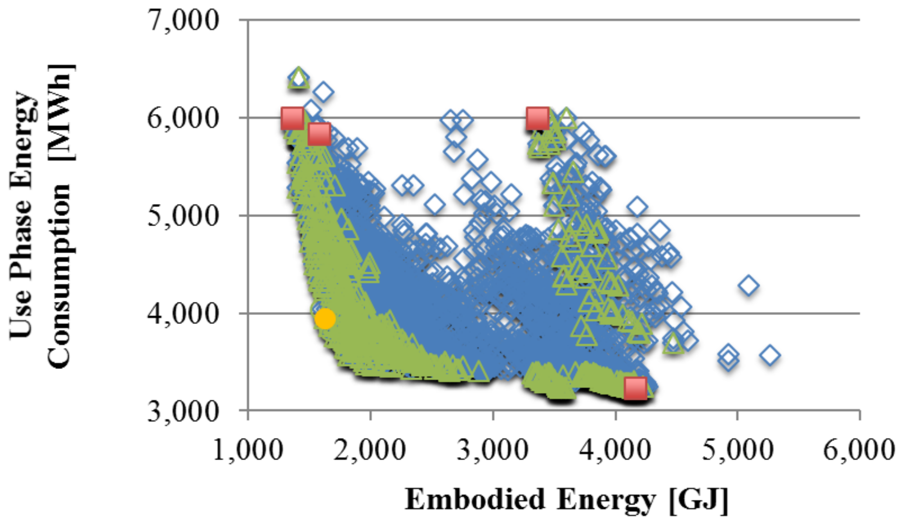

Fig. 5.17. Embodied energy against use phase energy consumption for the real Danish building in Step 1

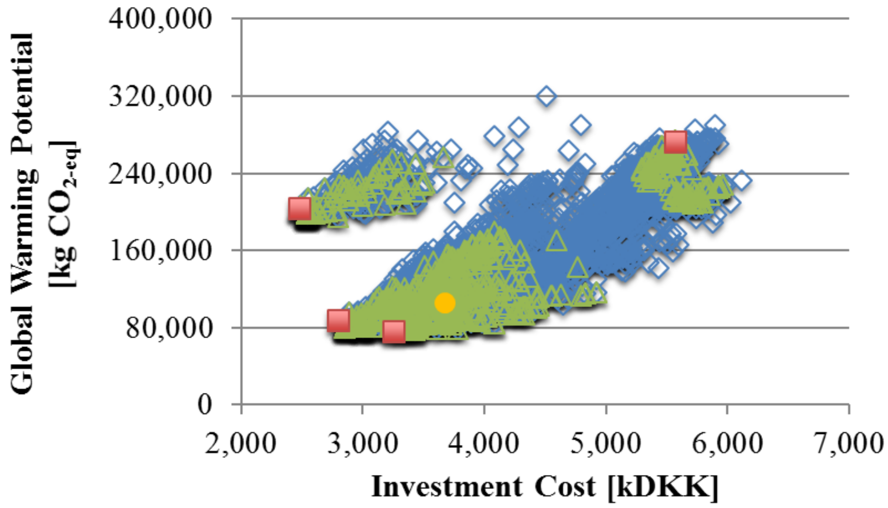

Fig. 5.18. Investment cost against embodied GWP for the real Danish building in Step 1

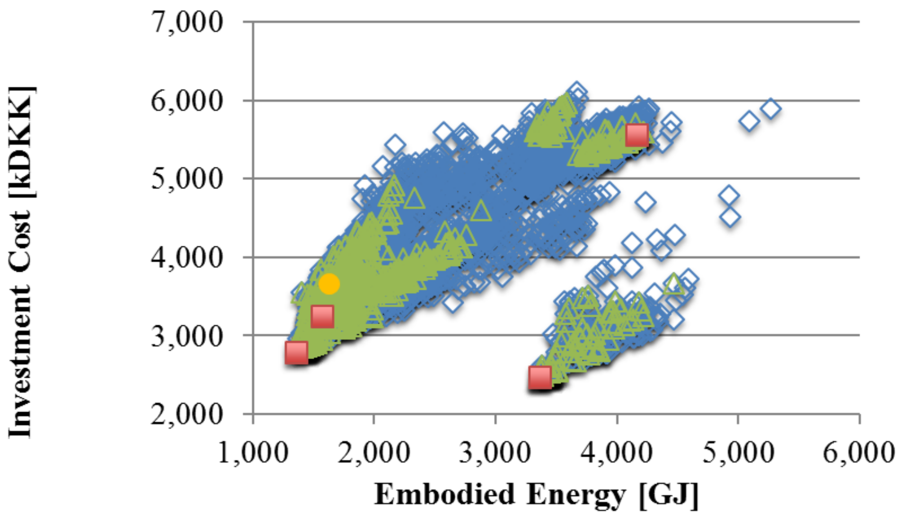

Fig. 5.19. Embodied energy against investment cost for the real Danish building in Step 1

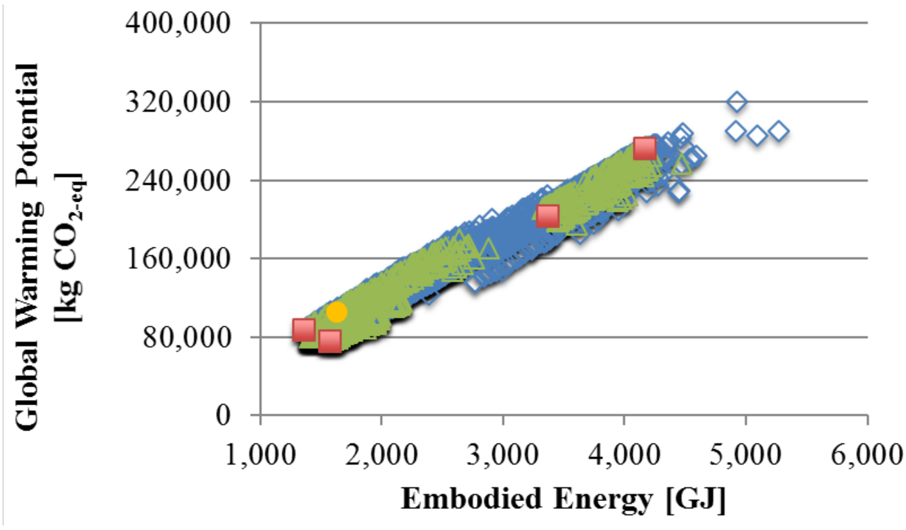

Fig. 5.20. Embodied energy against embodied GWP for the real Danish building in Step 1

For these optimal solutions, the annual final energy demand ranges between 76.5 and 83.7 kWh/m^2/y. These figures are quite close to the value resulting from the renovation occurred in 2012, *i.e.* 77.2 kWh/m^2/y. The solution with the minimum Euclidean distance, identified as the best compromise solution, has an investment cost of 3,672,627 DKK (about 500 k€), the EGWP of the interventions is 105.9 tons of $CO_{2\text{-}eq}$ and the EE is equal to 1625 GJ. The features of this solution are in the last column of Table 5.30. The relative contribution of insulation, cladding and transparent materials to the three "embodied" objective functions is shown in Fig. 5.21.

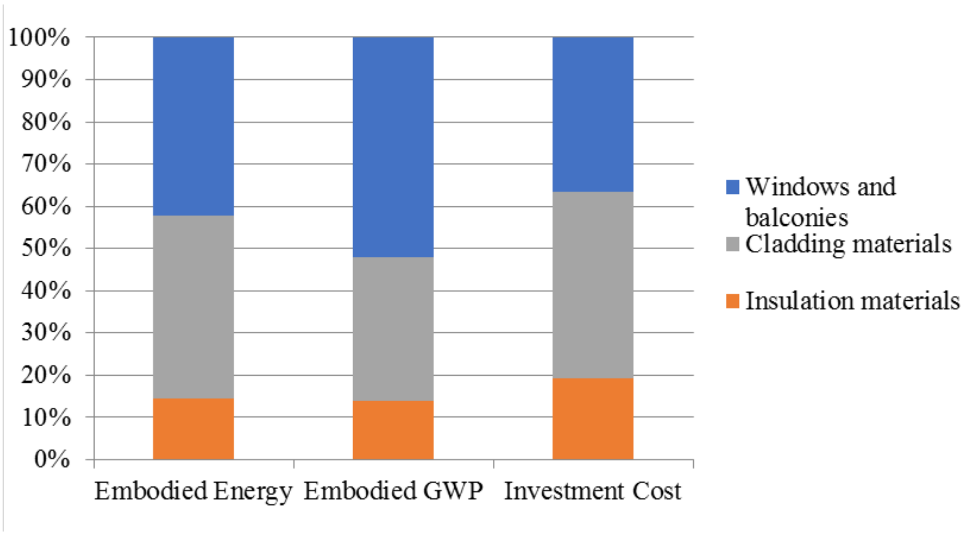

Fig. 5.21. Share of embodied impacts and investment cost for the three groups of envelope interventions for the optimal solution of the real Danish building in Step 1

5.3.4. Whole building optimisation results

The simultaneous optimisation of the envelope and the equipment of the building allowed identifying 744 feasible solutions and the related Pareto front was composed of only 8 compromise solutions. As for the previous case, the optimisation study was repeated with many algorithms and combinations of parameters, but the number of feasible solutions in this case study was always limited. Even in this case, the Omni-Optimizer algorithm with 200 generations and 40 people in each generation was the best performing. An overview of the resulting OFs values of this optimisation run is provided in Fig. 5.22 - Fig. 5.24, where are illustrated the feasible solutions (blue rhombi) and the Pareto front (orange squares), also highlighting the extreme solutions (grey triangles).

Differently from the first study, where the use phase energy demand was clearly conflicting with embodied impacts and investment costs, each objective function in this optimisation is composed of a term related to the construction materials and a term related to the operation of the building. This aspect highlights and extends to the whole life cycle the quasi-linear trend in the graph relating GWP and CED, while the conflict between the other objectives becomes less evident. Furthermore, all of the feasible solutions are concentrated in a relatively concentrated region of the search space, suggesting that the optimisation algorithm converged to this minimum region.

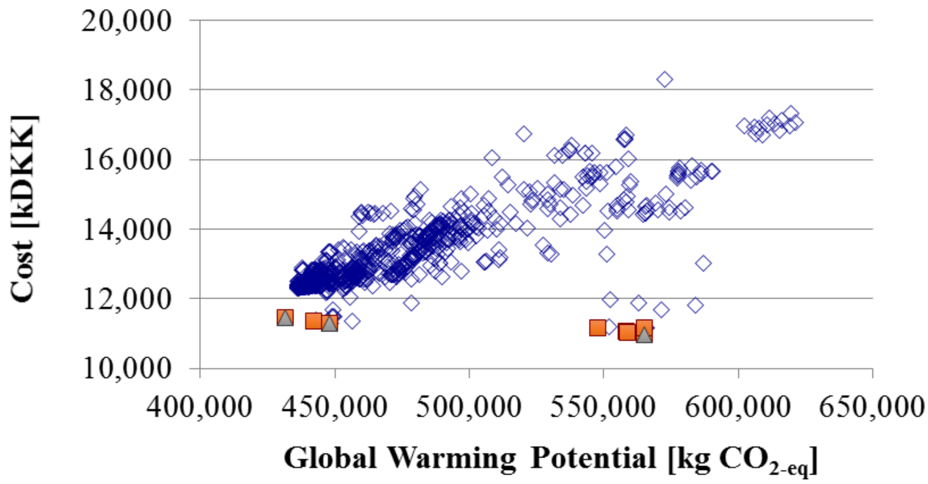

Fig. 5.22. Costs against GWP for the real Danish building in the whole building optimisation

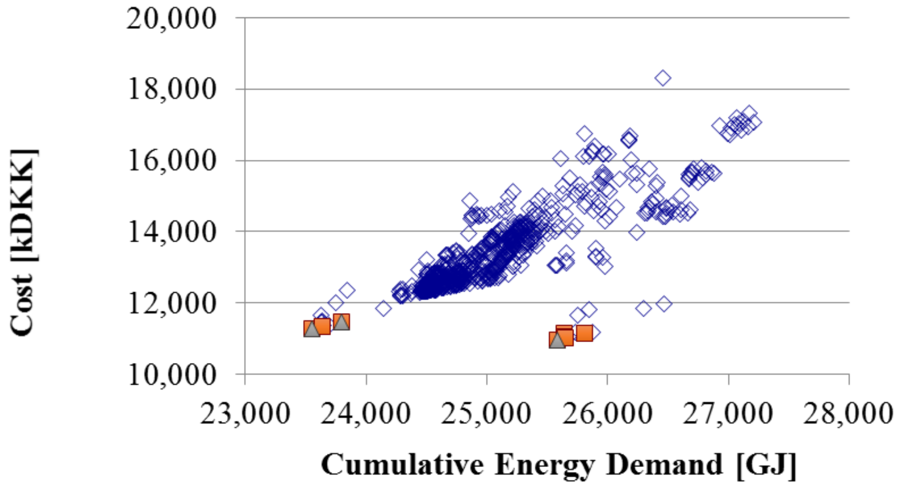

Fig. 5.23. Costs against CED for the real Danish building in the whole building optimisation

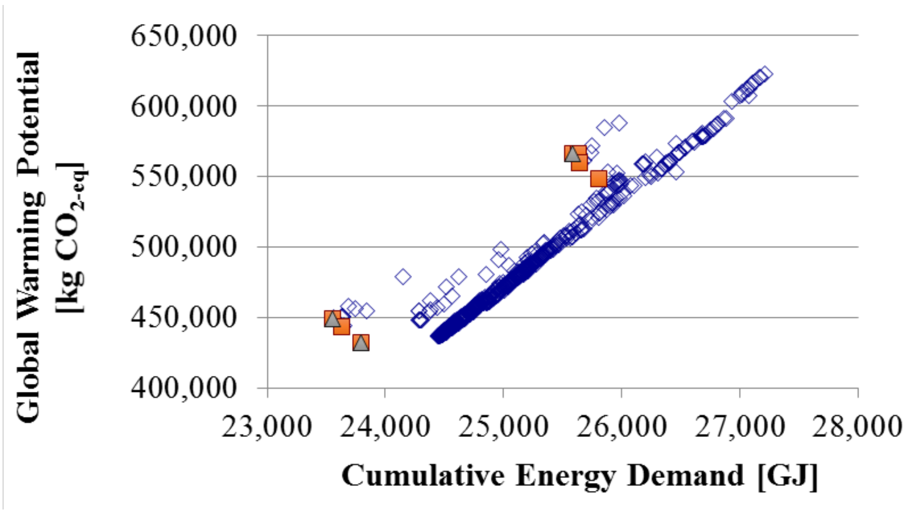

Fig. 5.24. GWP against CED for the real Danish building in the whole building optimisation

The Pareto front is made up of only eight solutions; these alternatives' features are listed in Table 5.31, ordered with decreasing Euclidean distance from the left to the right. The best compromise solution was identified adopting the utopia point distance to the Pareto front, selecting the building configuration with the lowest Euclidean distance. These building solutions have very similar features, with null additional insulation layers and the same glazing for each component. The difference is in the cladding material, that does not influence the thermal performance, since these materials have large ventilated air cavities, thus the thermal transmittance of the envelope is the same for each building solution. The walls cladding is most commonly aluminium-based in the solutions, because it is the cheapest solution, although having the highest environmental impact, and only tiles appear among the optimal roof cladding solutions. Fibre-cement, the best material selected in the envelope optimisation, is however selected in some solutions for the walls cladding. As in the previous case, PCV is often preferred for South-oriented windows while North-oriented window frames are usually composed of wood. Even the variables related to the equipment are very similar, selecting PV only in one solution and basing the heating system on district heating, disregarding the installation of solar collectors or recurring to natural gas. This result may be due to the low values of average solar radiation available in Denmark and to the high values of specific impacts and cost of the natural gas.

Table 5.31. Comparison of the main features of the best compromise solutions for the whole building optimisation of the real Danish building

# of solution	**8**	**1**	**5**	**2**	**6**	**12**	**15**	**19**
Concrete walls insulation	No insulation	No insulation	No insulation	No insulation	No insulation	No insulation	No insulation	No insulation
Light walls insulation	No insulation	No insulation	No insulation	No insulation	No insulation	No insulation	No insulation	No insulation
Roof insulation	No insulation	No insulation	No insulation	No insulation	No insulation	No insulation	No insulation	No insulation
Basement walls insulation	No insulation	No insulation	No insulation	No insulation	No insulation	No insulation	No insulation	No insulation
External walls cladding material	Aluminium	Aluminium	Aluminium	Aluminium	Aluminium	Fibre cement	Fibre cement	Fibre cement
Roof cladding material	Tiles	Tiles	Tiles	Tiles	Tiles	Tiles	Tiles	Tiles
Balcony glazing	No glazing	No glazing	No glazing	No glazing	No glazing	No glazing	No glazing	No glazing
Staircase glazing	Double glazing	Double glazing	Double glazing	Double glazing	Double glazing	Double glazing	Double glazing	Double glazing
North wall windows glazing	Double glazing	Double glazing	Double glazing	Double glazing	Double glazing	Double glazing	Double glazing	Double glazing
South wall windows glazing	Double glazing	Double glazing	Double glazing	Double glazing	Double glazing	Double glazing	Double glazing	Double glazing
North wall windows frame	Aluminium	PVC	Wood	Wood	Wood	PVC	Wood	Wood
South wall windows frame	PVC	PVC	PVC	PVC	Wood	PVC	PVC	Wood
PV surface [m^2]	0	1.93	0	0	0	0	0	0
Solar collectors surface [m^2]	0	0	0	0	0	0	0	0
Heating technology	District heating	District heating	District heating	District heating	District heating	District heating	District heating	District heating

The best compromise solution is also the solution with minimum GWP (solution 19 in Table 5.31). For this alternative, GWP is equal to 432 tons of $CO_{2\text{-eq}}$, CED is equal to 23,800 GJ, and the investment cost is 11,435,000 DKK (about 1.500 k€), related to the reference period of 50 years. The relative contribution of embodied and operating terms to each objective function is shown in Fig. 5.25. The embodied contributions are related only to the envelope components, since no renovation on equipment was selected for this solution.

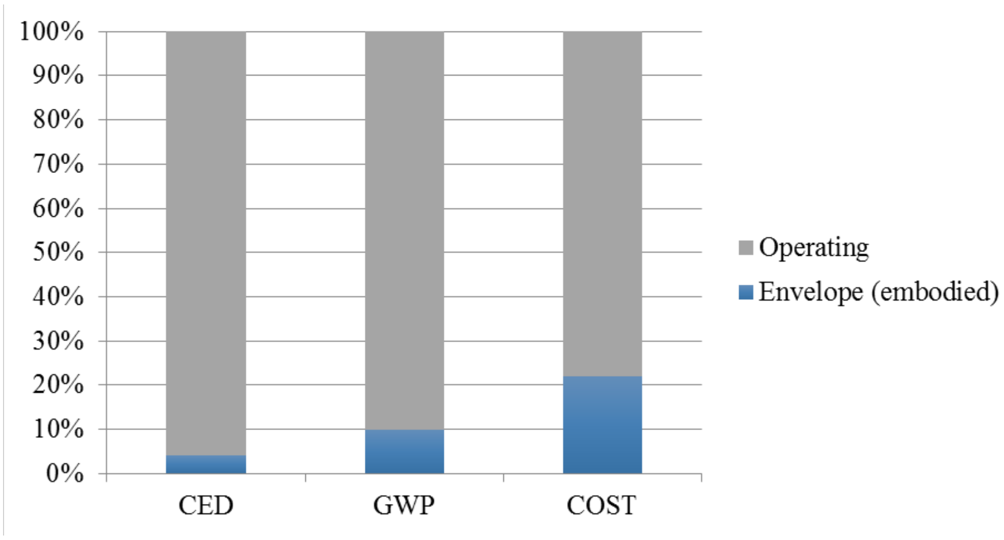

Fig. 5.25. Share of embodied impacts and investment cost for the three groups of envelope interventions for the optimal solution of the whole building optimisation of the real Danish building

5.4. Real building in Mediterranean climate

The last case study on the optimisation of a single building was concentrated on the renovation of an existing single-family detached house in Palermo. The building was analysed in a previous project by the Department of Engineering of the University of Palermo because of its representativeness of the local building sector. In this way, the results obtained in this study may be extended to many similar houses in the same city and region.

5.4.1. Case study description

The building has a unique floor, with a base area of 119,80 m^2 including two bedrooms, one bathroom, a kitchen and a living room. The living room is newer and higher than the rest of the building, with 4.2 m against 2.9 m of the other rooms. There are six windows and two doors, and both of the two entrances of the house communicate with a porch. The floor plan is shown in Fig. 5.26 while the other sketches of the house are reported in Fig. 5.27 - Fig. 5.30. The main geometrical and thermal features of the envelope are listed in Table 5.32. The space heating and DHW production are provided through an LPG boiler with efficiency equal to 0.89, while the space-cooling requirement is fulfilled with an air conditioner with SEER = 3.3 [34].

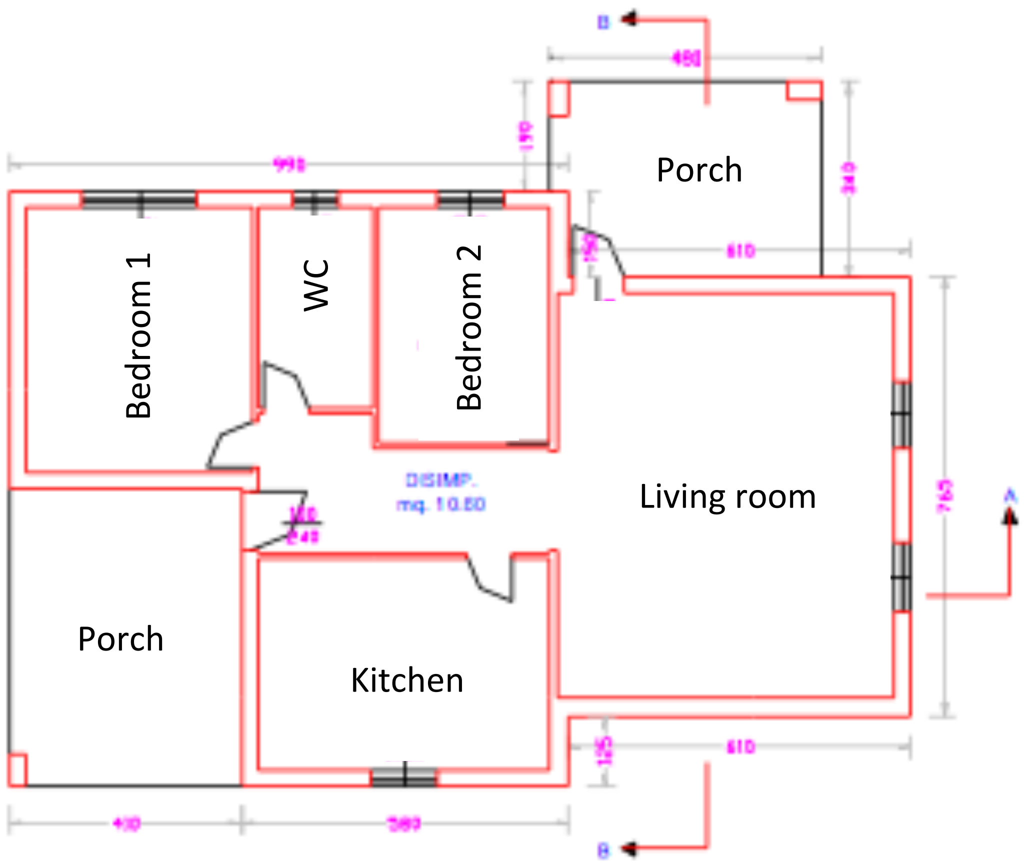

Fig. 5.26. Floor plan of the real Italian building case study

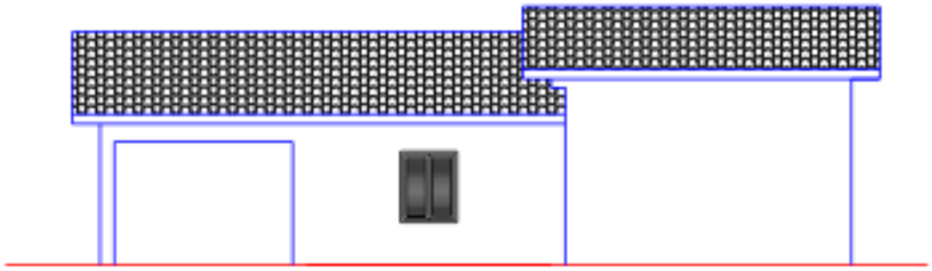

Fig. 5.27. Sketch of the North-East view of the real Italian building case study

Fig. 5.28. Sketch of the North-West view of the real Italian building case study

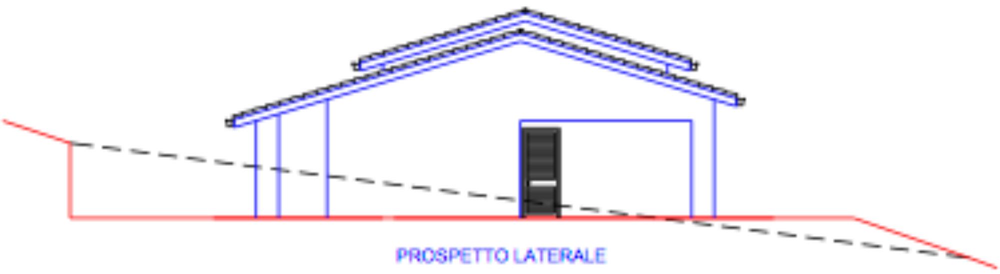

Fig. 5.29. Sketch of the South-East view of the real Italian building case study

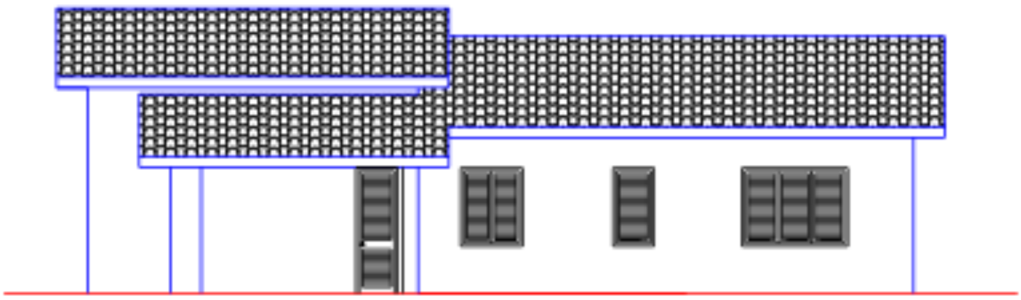

Fig. 5.30. Sketch of the South-West view of the real Italian building case study

Table 5.32. Main geometric and thermal features of the envelope of the real Italian building case study

Component	Layer 1 (outside)	Layer 2	Layer 3	Layer 4	Layer 5	Layer 6
Exterior Wall	M: Lime mortar plaster T: 0.025 m D: 1400 kg/m3 C: 0.70 W/(m K)	M: Perforated bricks T: 0.120 m D: 800 kg/m3 C: 2.58 W/(m K)	M: Foam vermiculite T: 0.020 m D: 120 kg/m3 C: 0.08 W/(m K)	M: Air cavity T: 0.030 m	M: Perforated bricks T: 0.080 m D: 800 kg/m3 C: 2.50 W/(m K)	M: Lime mortar plaster T: 0.0250 m D: 1400 kg/m3 C: 0.70 W/(m K)
Interior Wall	M: Lime mortar plaster T: 0.025 m D: 1400 kg/m^3 C: 0.70 W/(m K)	M: Perforated bricks T: 0.080 m D: 800 kg/m3 C: 2.50 W/(m K)	M: Lime mortar plaster T: 0.025 m D: 1400 kg/m3 C: 0.70 W/(m K)	-	-	-
Exterior Roof	M: Clay roof tiles cover T: 0.030 m D: 1000 kg/m3 C: 0.20 W/(m K)	M: Wooden structure T: 0.025 m D: 450 kg/m3 C: 0.12 W/(m K)	M: Air cavity T: 0.090 m	M: Light concrete block T: 0.200 m D: 641 kg/m3 C: 0.20 W/(m K)	M: Lime mortar plaster T: 0.025 m D: 1400 kg/m3 C: 0.70 W/(m K)	-
Exterior Floor	M: Ventilated air cavity T: 0.200 m C: 1.50 W/(m K)	M: Reinforced concrete T: 0.150 m D: 1900 kg/m3 C: 1.06 W/(m K)	M: Plasters T: 0.020 m D: 2300 kg/m3 C: 1.00 W/(m K)	-	-	-
Exterior Door	M: Metal surface T: 0,8 mm D: 7824 kg/m^3 C: 45.3 W/(m K)	M: Insulation board T: 25 mm D: 43 kg/m^3 C: 0.03 W/(m K)	-	-	-	-
Exterior Window	M: Clear glass T: 4 mm C: 0.9 W/(m K)	Gas gap Gas: Air Thickness: 13 mm	M: Clear glass T: 4 mm C: 0.9 W/(m K)	-	-	-

M: Material; T: Thickness; D: Density; C: Thermal Conductivity; R: Thermal Resistance

5.4.2. Step 1 input data

Starting from the information reported above, a 3D model in SketchUp Make 2017 was created. The porches were not included as thermal zones and their roofs were modelled as shading objects. As for the first case study, the input file for EnergyPlus was created using the Euclid plug-in for SketchUp. Internal gains (*i.e.* occupants, lighting and electric equipment) were neglected in Step 1, as the target is to focus on the building's envelope. The infiltration rate was calculated according to the equation of Coblenz and Achenbach, already shown in Eq. (5.1). The values for I_{design} and the extrapolation coefficients (suggested by ASHRAE) adopted for the simulations for all of the thermal zones are shown in Table 5.2. The values for $F_{schedule}$ were set equal to 1 for the whole year. The building operating final energy demand was obtained by fixing indoor setpoint temperatures to 20 °C for the heating season and 26 °C for the cooling season, and employing an ideal HVAC plant with infinite rated power and unitary efficiency. In this way, technology's performance does not affect the results.

To calculate the annual energy performance of the house, the *Conduction Transfer Function* algorithm was applied to the *Heat Balance Method* [4,5], with a third-order backward difference algorithm for the air node. *DOE-2* and *TARP* algorithms were selected for the convective heat transfer simulation between the building and the outside environment and between the building and the indoor environment, respectively [1]. For the energy performance simulation, the weather file for the exact location of the analysed building was downloaded from the typical meteorological year files generator developed by the EU [2].

Table 5.33. Parameters employed for the simulation of heat gains for infiltration in the real Italian building case study

Parameter	Value
I_{design}	0.1 h^{-1}
A	0.606
B	0.03636 K^{-1}
C	0.1177 s/m
D	0 s^2/m^2

Before the optimisation, a preliminary assessment was performed to investigate the change in accuracy and in the computational burden with a higher number of thermal zones. The configurations compared in this phase, together with the annual final energy demand and the duration of the simulations are shown in Table 5.34.

Table 5.34. Comparison of performance between different models of the real Italian building case study

	Heating demand relative difference	**Cooling demand relative difference**	**Computation time**
6 zones (one for each room + corridor)	0,00%	0,00%	14 – 20 s
2 zones (one for the living room and one for the rest)	-0,52%	-6,73%	13 – 14 s
1 zone (one for the whole building)	-3,37%	-8,04%	9 – 18 s

In detail, although a higher number of thermal zones should cause a higher detail in results but even a higher computational burden, the simulations for the building with six thermal zones lasted only four seconds on average more than the building with a unique zone in this case. For this reason, the building model with each of the six rooms modelled as a different thermal zone was selected. The front and back views of the model are shown in Fig. 5.31 - Fig. 5.32. Simulating the building with the features described above, the resulting annual operating final energy demand is 30,628 MJ for space heating and 1531 MJ for space cooling.

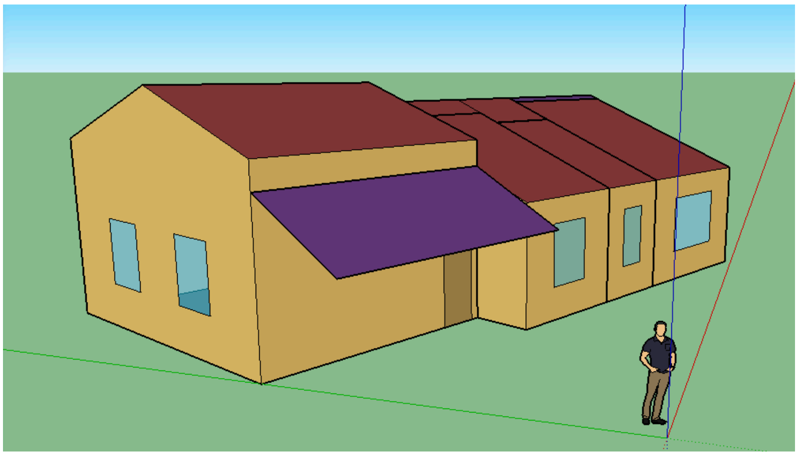

Fig. 5.31. Front view of the model in SketchUp Make 2017 of the real Italian building case study

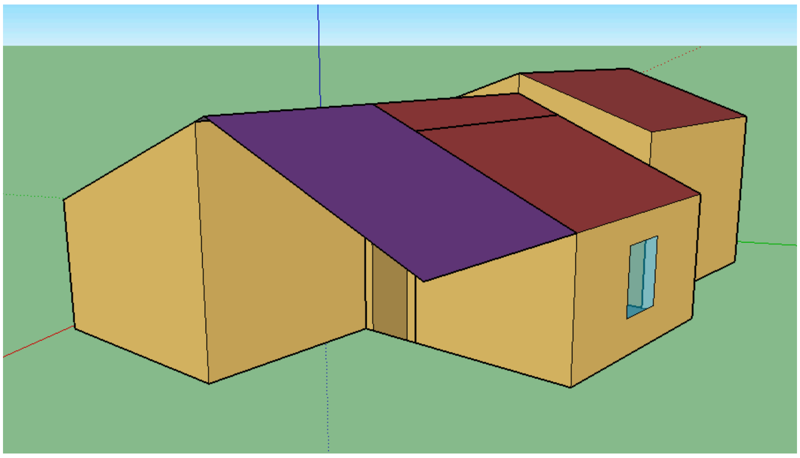

Fig. 5.32. Back view of the model in SketchUp Make 2017 of the real Italian building case study

The proposed renovation interventions for the envelope are the insulation of the external walls, the roof and the ground floor (on the inside), additional thermal mass of the external walls and the replacement of the windows.

In order to further differentiate the interventions, different values were allowed for insulation and thermal mass thicknesses of the external walls and windows with different orientation. Furthermore, the installation of 3 different insulation materials, 2 different thermal mass materials and 6 different kinds of windows was investigated. The number of alternatives for each variable was reduced with respect to the previous case studies, since high thicknesses of insulation or thermal mass were never selected in the Pareto front. Considering the total number of possible combinations, shown in Table 5.35, the search space of this problem is composed of $(2^{36}) \cdot (4^{18}) \cdot (401^{4}) = 1.22 \cdot 10^{32}$ building configurations.

Table 5.35. Number of alternatives for each variable and search space calculation

Intervention	Alternatives	Materials	Number of Surfaces	Combinations
Insulation boards	4	3	6	$4^{18} = 6.87 \cdot 10^{10}$
Boolean variables for insulation boards	2	3	6	$2^{18} = 2.62 \cdot 10^{5}$
Concrete	401	1	4	$401^{4} = 2.59 \cdot 10^{10}$
Boolean variables for window frames	2	3	3 (no windows on East walls)	$2^{9} = 512$
Boolean variables for window glazing	2	3	3 (no windows on East walls)	$2^{9} = 512$
TOT				$\mathbf{1.22 \cdot 10^{32}}$

The thermal properties of the opaque retrofit materials are reported in Table 5.36, while data on windows glazing and frames are in Table 5.37. The unit impact factors for GWP and EE of the materials employed in this study were not assessed directly but drawn from the EPD of representative materials from the Italian or European contexts. Unit costs of the materials were drawn from Italian catalogues of large do-it-yourself shops, extrapolating the values through the least-squares method from at least 4 alternatives for each material. These values are shown in Table 5.38, with the impacts referred to the DU. The thermal properties in Table 5.36 come from the same EPDs used for the impact assessment. Replacements were considered only for window glazing since the service life of the other components was equal or almost equal to the reference life of the building, assumed to be 60 years.

Table 5.36. Opaque materials properties for the real Italian building optimisation

Material	Available thicknesses	Density	Specific Heat Capacity	Thermal Conductivity
	[m]	[kg/m^3]	[J/(kg·K)]	[W/(m·K)]
EPS insulation boards	10^{-5}; 0.025; 0.050; 0.075	15.9	1500	0.0363
Rockwool insulation boards	10^{-5}; 0.051; 0.076; 0.092	38.5	800	0.0368
Glass wool insulation boards	10^{-5}; 0.025; 0.050; 0.075	30.0	800	0.0320
Concrete	From 10^{-5} to 0.2 with 0.001 step	2240.0	900	1.9500

Table 5.37. Glazing properties for the real Italian building optimisation [10]

Window	**Thermal Transmittance**	**SHGC**
	[W/(m^2·K)]	**[-]**
Double glazing, aluminium frame	3.31	0.64
Double glazing, wood frame	2.86	0.57
Double glazing, PVC frame	2.58	0.57
High performing double glazing, aluminium frame	2.75	0.55
High performing double glazing, wood frame	2.34	0.49
High performing double glazing, PVC frame	2.07	0.49
Triple glazing, aluminium frame	2.56	0.49
Triple glazing, wood frame	2.22	0.47
Triple glazing, PVC frame	1.98	0.47

Table 5.38. Unit impacts and costs for the interventions on the real Italian building optimisation

Window	**Embodied Energy**	**Global Warming Potential**	**Investment Costs**	**Service Life**
EPS insulation boards	98.93 MJ/m^2	5.35 kg $CO_{2\text{-}eq}$/m^2	143.66 €/m^3	60 years
Rockwool insulation boards	137.41 MJ/m^2	6.60 kg $CO_{2\text{-}eq}$/m^2	98.54 €/m^3	60 years
Glass wool insulation boards	54.35 MJ/m^2	2.09 kg $CO_{2\text{-}eq}$/m^2	91.17 €/m^3	50 years
Concrete layer	3663 MJ/ton	327 kg $CO_{2\text{-}eq}$/ton	110.20 €/m^3	60 years
Double glazing, aluminium frame	427.5 MJ/m^2 (glazing) + 121.77 MJ/kg (frame)	29.8 kg $CO_{2\text{-}eq}$/m^2 (glazing) + 7.26 kg $CO_{2\text{-}eq}$/kg (frame)	153.05 €/m^2	25 years (glazing) 60 years (frame)
Double glazing, wood frame	427.5 MJ/m^2 (glazing) + 2618 MJ/kg (frame)	29.8 kg $CO_{2\text{-}eq}$/m^2 (glazing) + 109 kg $CO_{2\text{-}eq}$/kg (frame)	349.81 €/m^2	25 years (glazing) 60 years (frame)
Double glazing, PVC frame	427.5 MJ/m^2 (glazing) + 73 MJ/kg (frame)	29.8 kg $CO_{2\text{-}eq}$/m^2 (glazing) + 5.04 kg $CO_{2\text{-}eq}$/kg (frame)	136.09 €/m^2	25 years (glazing) 60 years (frame)
High performing double glazing, aluminium frame	724.6 MJ/m^2 (glazing) + 121.77 MJ/kg (frame)	51 kg $CO_{2\text{-}eq}$/m^2 (glazing) + 7.26 kg $CO_{2\text{-}eq}$/kg (frame)	153.05 €/m^2	25 years (glazing) 60 years (frame)
High performing double glazing, wood frame	724.6 MJ/m^2 (glazing) + 2618 MJ/kg (frame)	51 kg $CO_{2\text{-}eq}$/m^2 (glazing) + 109 kg $CO_{2\text{-}eq}$/kg (frame)	349.81 €/m^2	25 years (glazing) 60 years (frame)
High performing double glazing, PVC frame	724.6 MJ/m^2 (glazing) + 73 MJ/kg (frame)	51 kg $CO_{2\text{-}eq}$/m^2 (glazing) + 5.04 kg $CO_{2\text{-}eq}$/kg (frame)	136.09 €/m^2	25 years (glazing) 60 years (frame)
Triple glazing, aluminium frame	753.5 MJ/m^2 (glazing) + 121.77 MJ/kg (frame)	50.3 kg $CO_{2\text{-}eq}$/m^2 (glazing) + 7.26 kg $CO_{2\text{-}eq}$/kg (frame)	153.05 €/m^2	25 years (glazing) 60 years (frame)
Triple glazing, wood frame	753.5 MJ/m^2 (glazing) + 2618 MJ/kg (frame)	50.3 kg $CO_{2\text{-}eq}$ /m^2 (glazing) + 109 kg $CO_{2\text{-}eq}$ /kg (frame)	349.81 €/m^2	25 years (glazing) 60 years (frame)
Triple glazing, PVC frame	753.5 MJ/m^2 (glazing) + 73 MJ/kg (frame)	50.3 kg $CO_{2\text{-}eq}$/m^2 (glazing) + 5.04 kg $CO_{2\text{-}eq}$/kg (frame)	136.09 €/m^2	25 years (glazing) 60 years (frame)

5.4.3. Step 1 results

For this study, the multi-objective genetic Omni-Optimizer algorithm was selected, using a crossover rate equal to 0.9 and a mutation rate equal to 0.00893. Although the best combination of population size and generations suggested by MOBO was 16 and 126, respectively, an attempt with 50 generations was done, in order to verify how the solutions might improve after 50 generations. Several optimisation runs were performed (at least five) using the same combination. The results were compared in terms of the number of solutions (Table 5.39) and of the goodness of the Pareto front solutions (Fig. 5.33). As one may expect, the solutions obtained using 126 generations are much more than using 50 generations, and the related Pareto fronts are even better. The unexpected aspect is that the solutions are much better, as shown in Fig. 5.33. Another interesting aspect is that the algorithm took different paths in each of the eleven runs, since, comparing all of the 6656 feasible and non-duplicate solutions from each run, no further duplicates were found. These solutions were investigated in order to identify the new resulting Pareto front, that was composed of 31 compromise building configurations, all of them being identified with 126 generations. The Euclidean distance of these solutions was calculated, identifying the best compromise solution.

Table 5.39. Comparison of the number of solutions with different algorithm parameters for the real Italian building optimisation

Optimization	**# of theoretic solutions**	**# of effective, feasible and non-duplicate solutions**	**# of elements in the Pareto front**
Omni-Optimizer 16 50_run 1	800	363	4
Omni-Optimizer 16 50_run 2	800	239	8
Omni-Optimizer 16 50_run 3	800	183	18
Omni-Optimizer 16 50_run 4	800	265	14
Omni-Optimizer 16 50_run 5	800	215	9
Omni-Optimizer 16 50_run 6	800	264	23
Omni-Optimizer 16 126_run 1	2016	1066	13
Omni-Optimizer 16 126_run 2	2016	1064	6
Omni-Optimizer 16 126_run 3	2016	1084	11
Omni-Optimizer 16 126_run 4	2016	937	10
Omni-Optimizer 16 126_run 5	2016	976	9

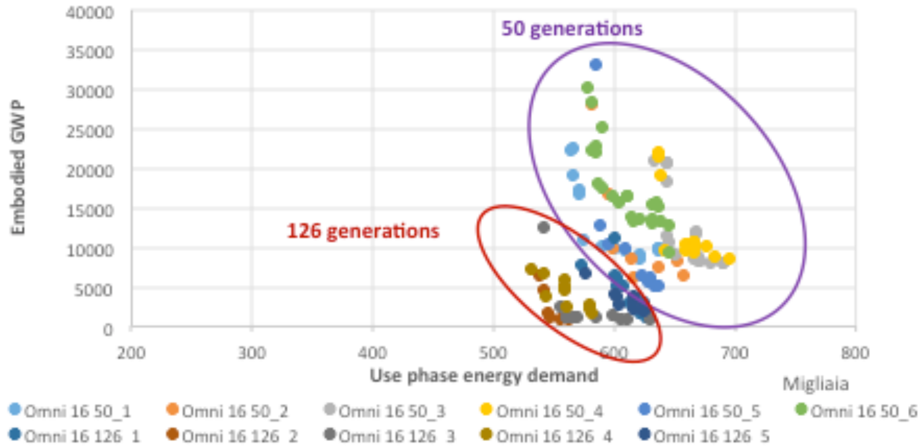

Fig. 5.33. Comparison of the solutions in the Pareto front with different algorithm parameters for the real Italian building optimisation

The six graphs correlating the four objective functions are provided in Fig. 5.34 – Fig. 5.39, showing all the 6656 feasible solutions, the Pareto front, the extreme solutions (minima) and the best compromise. It is possible to see how the search space close to the Pareto front was deeply investigated and that, as in the previous cases, the trend between EE and EGWP is almost linear, with a high value of the coefficient of determination. Furthermore, in this case, a quasi-linear trend can be identified even between EE and investment cost and between investment cost and EGWP.

For the successive analysis of the study, the results from the optimisation run where the best compromise was identified, *i.e.* the fourth run of the Omni-Optimizer algorithm with 126 generations, were employed. In detail, the main features from the eight solutions of the Pareto front with lower Euclidean distance are shown in Table 5.40, with decreasing Euclidean distance from the left to the right. The most common solutions did not consider the envelope insulation, apart from the East-oriented walls, while the additional thermal mass seem to be installed without a specific logic, with higher values on the West oriented walls. All the solutions have the same windows features, although each orientation has different properties than the others. The solutions in the last four columns have very similar features and Euclidean distance, and were considered for the Step 2. Nevertheless, since solution 456 is almost equal to 263 and 490 is almost the same of 515, only the envelopes of the solutions 263 and 515 were further optimised. In detail, referring to the output of the envelope optimisation, the investment costs are equal to 4516 € and 4228 €, respectively for 263 and 515, the embodied energy is 31.9 GJ and 22.2 GJ, respectively, and the embodied GWP is 2410 kg $CO_{2\text{-eq}}$ and 1678 kg $CO_{2\text{-eq}}$, respectively.

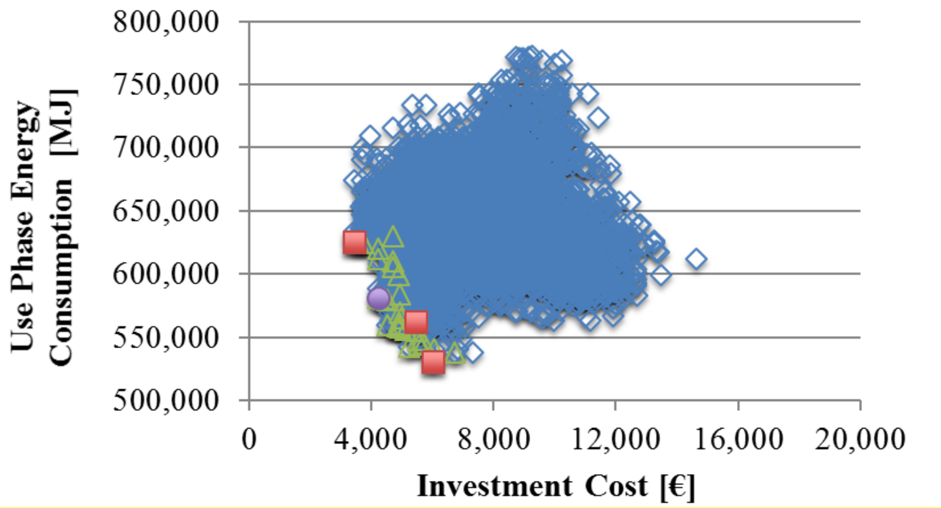

Fig. 5. 34. Investment cost against use phase energy consumption for the real Italian building in Step 1

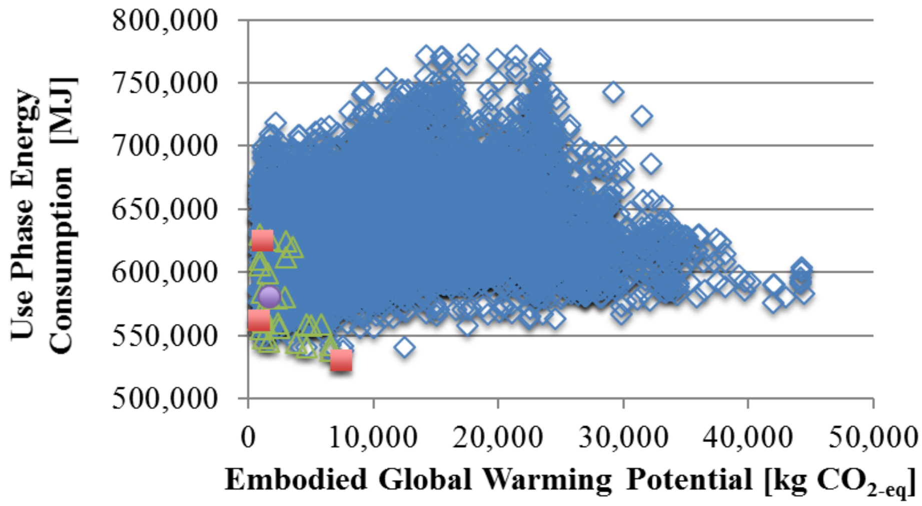

Fig. 5.35. Embodied GWP against use phase energy consumption for the real Italian building in Step 1

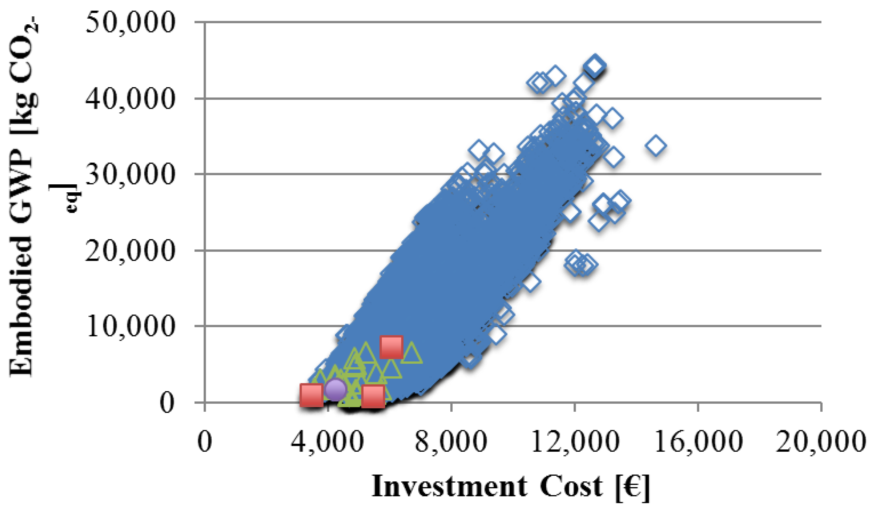

Fig. 5.36. Investment cost against embodied GWP for the real Italian building in Step 1

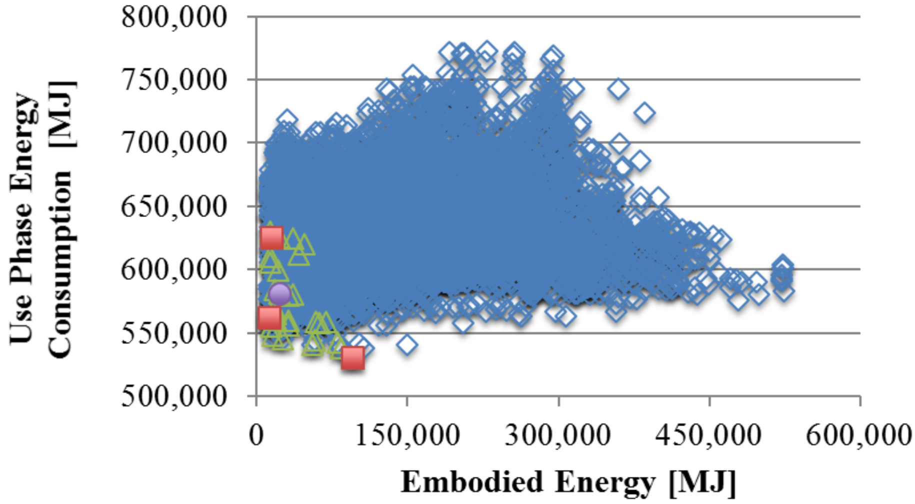

Fig. 5.37. Embodied energy against use phase energy consumption for the real Italian building in Step 1

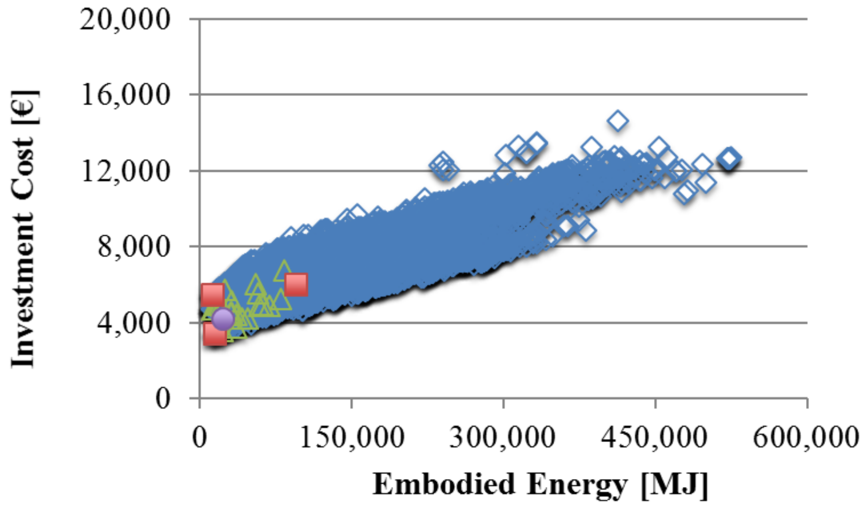

Fig. 5.38. Embodied energy against investment cost for the real Italian building in Step 1

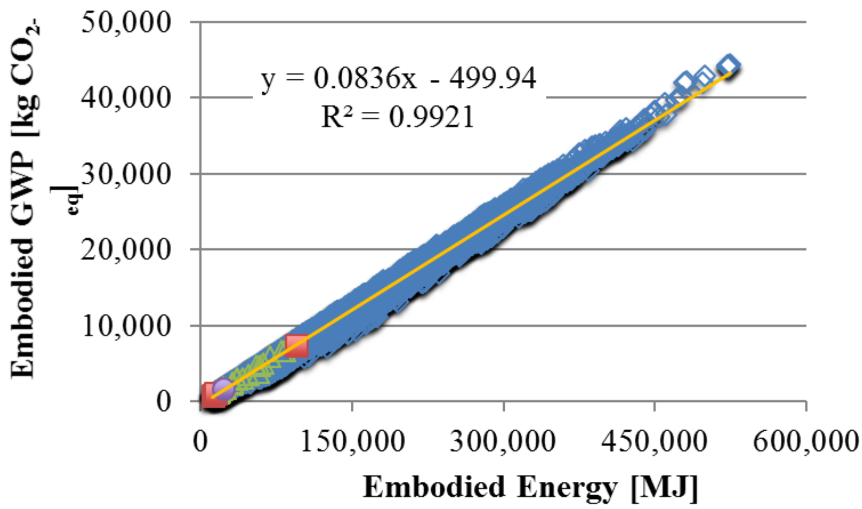

Fig. 5.39. Embodied energy against embodied GWP for the real Italian building in Step 1

Table 5.40. Comparison of the main features of the best compromise solutions for the envelope optimisation of the real Italian building

SOLUTION #	217	262	255	259	456	490	263	515
Air conditioning final demand [MWh/y]	2.52	2.59	2.58	2.58	2.68	2.69	2.59	2.69
North walls insulation material	Glass wool	No insulation	No insulation	No insulation	No insulation	No insulation	No insulation	No insulation
West walls insulation material	EPS	No insulation	No insulation	No insulation	No insulation	No insulation	No insulation	No insulation
South walls insulation material	Glass wool	No insulation	No insulation	No insulation	No insulation	No insulation	No insulation	No insulation
East walls insulation material	No insulation	No insulation	Glass wool	Glass wool	EPS	No insulation	EPS	No insulation
Roof insulation material	No insulation	No insulation	No insulation	No insulation	No insulation	No insulation	No insulation	No insulation
Floor insulation material	No insulation	No insulation	No insulation	No insulation	No insulation	No insulation	No insulation	No insulation
North walls insulation thick. [m]	0.075	0	0	0	0	0	0	0
West walls insulation thickness [m]	0.075	0	0	0	0	0	0	0
South walls insulation thick. [m]	0.075	0	0	0	0	0	0	0
East walls insulation thickness [m]	0	0	0.075	0.075	0.05	0	0.05	0
Roof insulation thickness [m]	0	0	0	0	0	0	0	0
Floor insulation thickness [m]	0	0	0	0	0	0	0	0
North wall windows glazing	High performing double glazing	High performing double glazing	High performing double glazing	High performing double glazing	High performing double glazing	High performing double glazing	High performing double glazing	High performing double glazing
West wall windows glazing	Triple glazing	Triple glazing	Triple glazing	Triple glazing	Triple glazing	Triple glazing	Triple glazing	Triple glazing
South wall windows glazing	Triple glazing	Triple glazing	Triple glazing	Triple glazing	Triple glazing	Triple glazing	Triple glazing	Triple glazing
North wall windows frame	Wood	Wood	Wood	Wood	Wood	Wood	Wood	Wood
West wall windows frame	PVC	PVC	PVC	PVC	PVC	PVC	PVC	PVC
South wall windows frame	Aluminium	Aluminium	Aluminium	Aluminium	Aluminium	Aluminium	Aluminium	Aluminium
North walls concrete thickness [m]	0.009	0.002	0.005	0.002	0.014	0.009	0.014	0.014
West walls concrete thickness [m]	0.057	0.151	0.132	0.107	0.007	0.057	0.007	0.007
South walls concrete thickness [m]	0.001	0.014	0.001	0.014	0.014	0.001	0.014	0.001
East walls concrete thickness [m]	0.004	0.004	0.004	0.004	0	0.004	0.004	0.004

5.4.4. Step 2 input data

The final energy demand of the buildings obtained in the previous step was estimated including the aspects that were previously neglected, as internal gains due to the occupants, their DHW requirement, the electric equipment, the lighting, and the ventilation. In order to get reliable data on the use profile of the building, these schedules were based on a questionnaire administered to the inhabitants of the house and on the energy bills. The same schedules were adopted for both of the buildings, and the values employed in this study are shown in Table 5.41 – Table 5.47.

Table 5.41. Occupants presence (relative values related to 3 people)

OCCUPANTS NUMBER	Weekdays	Weekend
00:00 → 08:00	1	1
08:00 → 22:00	0.6	0.933
22:00 → 24:00	1	1

Table 5.42. Thermal loads due to the occupants activity [W] (values from [10]*)*

OCCUPANTS ACTIVITY	Weekdays	Weekend
00:00 → 01:00	80	100
01:00 → 06:00	80	80
06:00 → 07:00	95	80
07:00 → 08:00	140	80
08:00 → 09:00	0	95
09:00 → 10:00	0	140
10:00 → 11:00	0	120
11:00 → 12:00	0	0
12:00 → 13:00	230	0
13:00 → 14:00	140	120
14:00 → 15:00	140	80
15:00 → 16:00	140	120
16:00 → 18:00	140	120
18:00 → 19:00	170	0
19:00 → 20:00	158	120
20:00 → 21:00	140	120
21:00 → 23:00	120	0
23:00 → 24:00	80	80

Table 5.43. Domestic hot water thermal load

DHW	Values
Daily DHW requirement	40.3 L/people/day
Annual energy requirement	2307 kWh/year
Schedule of the water heater	Always on

Table 5.44. Lighting system maximum power

Thermal Zone	Maximum lighting power
Living room	105 W
Bathroom	45 W
Bedroom 1	45 W
Bedroom 2	75 W
Kitchen	105 W
Corridor	30 W

Table 5.45. Fraction of sensible thermal loads due to the lighting system with reference to the maximum load

LIGHTING	Weekdays	Weekend
00:00 → 06:00	0.00	0.00
06:00 → 07:00	0.15	0.00
07:00 → 08:00	0.15	0.00
08:00 → 10:00	0.00	0.18
10:00 → 18:00	0.00	0.00
18:00 → 19:00	0.67	0.00
19:00 → 20:00	0.67	0.15
20:00 → 21:00	0.67	0.67
21:00 → 22:00	1.00	0.00
22:00 → 23:00	0.67	0.00
23:00 → 24:00	0.00	0.80

Table 5.46. Sensible Thermal Loads due to Electric Equipment [W]

EQUIPMENT	Weekdays	Weekend
00:00 → 06:00	552.00	552.00
06:00 → 08:00	1457.75	552.00
08:00 → 10:00	552.00	1457.75
10:00 → 11:00	552.00	1552.00
11:00 → 12:00	552.00	552.00
12:00 → 13:00	1902.00	552.00
13:00 → 14:00	1052.00	1252.00
14:00 → 15:00	1052.00	552.00
15:00 → 16:00	552.00	1052.00
16:00 → 17:00	1052.00	1052.00
17:00 → 18:00	552.00	1052.00
18:00 → 19:00	1402.00	552.00
19:00 → 20:00	1902.00	1552.00
20:00 → 21:00	1052.00	2572.00
21:00 → 22:00	1617.00	552.00
22:00 → 23:00	1552.00	552.00
23:00 → 24:00	552.00	1052.00

Table 5.47. Fraction of windows opening for ventilation, influencing sensible and latent thermal loads, with reference to the windows surface [%]

VENTILATION	Weekdays	Weekend
00:00 → 06:00	0.00	0.00
06:00 → 08:00	0.10	0.00
08:00 → 09:00	0.00	0.10
09:00 → 10:00	0.00	0.30
10:00 → 11:00	0.00	0.10
11:00 → 12:00	0.00	0.00
12:00 → 13:00	0.30	0.00
13:00 → 14:00	0.40	0.40
14:00 → 15:00	0.00	0.00
15:00 → 16:00	0.00	0.20
16:00 → 18:00	0.00	0.10
18:00 → 19:00	0.10	0.00
19:00 → 20:00	0.30	0.10
20:00 → 21:00	0.30	0.30
21:00 → 24:00	0.00	0.00

Simulating the performance of the buildings with the optimised envelope and these schedules, the final energy requirements for electricity, space heating and space cooling during the standard year were evaluated with hourly detail. Although there are some differences, both of these annual trends are shown in Fig. 5.40, since the differences cannot be appreciated with the adopted scale. This low difference is due to the limited differences in the interventions between the two building configurations. These values were employed for the second step to identify the optimal rated power of the equipment. Although the values for space heating and cooling highly overcome the classical rated power of domestic technical systems, it is well known that an energy calculation based on the energy assessment provides different results from a calculation based on the power flows. Nevertheless, these values were employed as an indication of the annual energy demand, imposing an upper limit when the trends were higher than typical rated power for domestic equipment, namely 35 kW for space heating and 6 kW for space cooling. In this way, the oversizing of the equipment was prevented.

Furthermore, in order to avoid the divergence of the simulation, the hourly demands were aggregated in groups of equivalent hours composed of the sum of the demands in each group of hours. This operation simplified the calculation, reducing the computational burden and ensuring to obtain a solution in a few seconds on a standard office computer. The total number of variables of this problem is equal to 5846, while with 24 daily hours the problem would be composed of 140,172 variables.

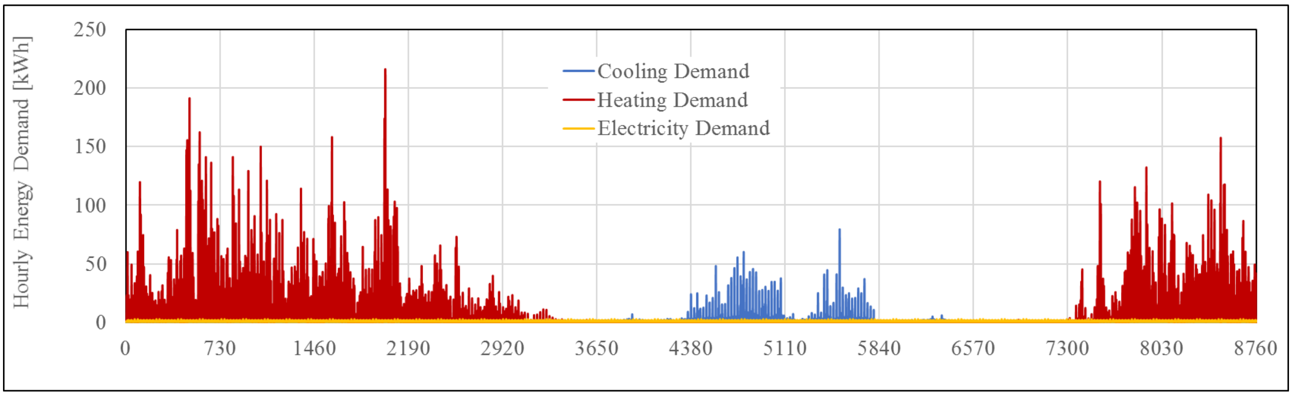

Fig. 5.40. Annual energy demands of the real Italian building with the optimised envelope

As for the fictitious building case study, the optimisation performed in the second step of this case study was performed according to the scheme shown in Fig. 5.11, thus assessing the installation of the six components here below:

RES	HVAC	STORAGE
• Photovoltaic panel (PV)	• Gas boiler (NGB)	• Li-ions electrical (STO_{el})
• Solar thermal collector (STC)	• Heat pump / air conditioner (HP)	• Sensible thermal (STO_{th})

The variables for the problem refer to the synthesis, design and operation stages of these components. Since it was assumed that the existing gas boiler was old and inefficient, the installation of a new boiler was considered.

For the calculation of the average annual solar radiation to be employed to evaluate the RES production, the average hourly values of direct and diffuse components were drawn from the weather file, obtaining a value equal to 6.78 kWh/(m^2 day). No spacing to avoid self-shading among the systems was required in this case study, since the building has a tilted roof. The installation of solar systems was supposed on the South-oriented fraction of the roof, having a total area of 76.56 m^2, where the porches were excluded to avoid structural problems. The shorter part of the roof, namely the roof over the living room, was dedicated to PV installation. With 3.88 m · 5.95 m = 23.09 m^2, up to 3 rows of 3 PV modules may be installed (9 modules), covering 14.73 m^2. The larger part of the South-oriented roof, covering the bedrooms and the bathroom, was instead dedicated to the STC system. This part of the roof has a surface of 5.57 m · 9.6 m = 53.47 m^2, that may be covered with 4 rows of 4 collectors (16 collectors), that thus would cover about 40.38 m^2. The larger part of the roof was dedicated to thermal energy production since the space heating demand is much higher than the electricity demand, as in Fig. 5.40.

The technical parameters describing the equipment, as conversion efficiencies or the dimensions of the solar technologies, were assumed to be constant in order to keep the linearity of the problem. A collection of Italian technical and market reports was performed to get representative data of the country, where both technical and economic data were available. The technical parameters are reported in Table 5.48, while the cost parameters for the economic objective function are available in Table 5.49. The values adopted for the embodied impacts of the equipment are average values from international literature, while data on electricity and gas in the Italian context were drawn from an LCA database. These parameters are shown in Table 5.50. Environmental benefits related to the electricity produced through the PV system and sold to the grid were not included in this study, and only the economic convenience of the reduced purchase of electricity from the national grid was considered.

Regarding the trend of the embodied impacts of the electricity, the Italian policy on the decarbonisation of the electricity mix in the close future is still not consolidated. In detail, the current national energy and climate plan states that Italy will phase-out its coal-fired thermal power plants within 2025 [35], although combined cycle gas turbines will be exploited to replace them, in order to guarantee the safety of the national power system. Thus, a constant value equal to the current impacts was considered. Even the escalation of prices in the life cycle for both electricity and natural gas was neglected in the study.

Table 5.48. Technical parameters of the equipment for the real Italian building optimisation

Parameter	**Value**
Transformer efficiency	99% [11]
Heat pump SCOP	4.1 [12]
Heat pump SEER	5.7 [12]
Heat pump useful life	15 years [13]
Natural gas boiler efficiency	90.1% [12]
Natural gas boiler useful life	24 years [13]
Photovoltaic module efficiency	17.11% [12]
Photovoltaic Balance of Plant efficiency	95% [11]
Photovoltaic system dimensions	$1.65 \cdot 0.992$ m^2 [12]
Photovoltaic system max available surface	19.642 m^2
Photovoltaic system useful life	25 years [12]
Solar thermal collector zero-loss efficiency	79.7% [12]
Solar thermal collector first order heat loss coefficient	3.18 W/(m^2 K) [12]
Solar thermal collector second order heat loss coefficient	0.008 W/(m^2 K^2) [12]
Solar thermal collector average efficiency (ΔT = 30 °C)	69.4%
Solar thermal collector dimensions	$1.987 \cdot 1.27$ m^2 [12]
Solar thermal collector max available surface	20.188 m^2
Solar thermal collector useful life	15 years [14]
Electrical storage charging efficiency	97% [11]
Electrical storage discharging efficiency	97% [11]
Electrical storage Depth of Discharge	20% [11]
Electrical storage useful life	7 years [15]
Thermal storage charging efficiency	100% [16]
Thermal storage discharging efficiency	100% [16]
Thermal storage self-discharge coefficient	0.01 kWh/h [16]
Thermal storage useful life	15 years [16]

Table 5.49. Economic parameters of the energy carriers and equipment for the real Italian building optimisation

Parameter	Value
Electrical energy final user price	0.207 €/kWh [17]
Natural gas final user price	0.767 €/kWh [18]
Heat pump first order investment cost	106 €/kW_{cool} [12]
Heat pump zero-th order investment cost	596 € [12]
Natural gas boiler first order investment cost	52 €/kW [12]
Natural gas boiler zero-th order investment cost	114 € [12]
Photovoltaic system first order investment cost	527 €/unit [12]
Photovoltaic system zero-th order investment cost	0 € [12]
Solar thermal collector first order investment cost	600 €/unit [12]
Solar thermal collector zero-th order investment cost	0 € [12]
Electrical storage first order investment cost	165 €/kWh [12]
Electrical storage zero-th order investment cost	2974 € [12]
Thermal storage first order investment cost	36 €/kWh [12]
Thermal storage zero-th order investment cost	77 € [12]
Real interest rate	5.00% [19]

Table 5.50. LCA impact factors of the energy carriers and equipment for the real Italian building optimisation

Item	GWP	CED
Electricity from the Italian grid	0.7089 kg $CO_{2\text{-}eq}$/kWh [20]	11.8 MJ/kWh [20]
Natural gas from the Italian grid	0.0369 kg $CO_{2\text{-}eq}$/kWh [20]	4.1203 MJ/kWh [20]
Manufacture of heat pumps	239.4 kg $CO_{2\text{-}eq}$/kW [21]	1250.4 MJ /kW [21]
Manufacture of gas boilers	19.5 kg $CO_{2\text{-}eq}$/kW [21–23]	92.65 MJ /kW [21]
Operation of gas boilers	0.264 kg $CO_{2\text{-}eq}$/kWh [22]	-
Manufacture of photovoltaic systems	88.04 kg $CO_{2\text{-}eq}/m^2$ [24]	1619 MJ/m^2 [25]
Manufacture of solar collectors	0.3245 kg $CO_{2\text{-}eq}/m^2$ [26]	39.55 MJ/m^2 [26]
Manufacture of electric storages	76.284 kg $CO_{2\text{-}eq}$/kWh [27]	540 MJ/kWh [27]
Manufacture of thermal storages	8.14 kg $CO_{2\text{-}eq}$/kWh [21]	145.297 MJ/kWh [21]

5.4.5. Step 2 results

The problem to identify the optimal synthesis, design and operation of the building technical systems was solved using the scalarization technique and a MILP algorithm. Since the scalarization technique converts a MOO in a SOO, many combinations of weights of the OFs were employed to completely identify the Pareto front, while the worst values of each OF were adopted as normalisation factors. The values of the OF obtained with the different weighs are provided in Table 5.51, using a coloured background to highlight when the values are equal. Although many more combinations of weights were tried, the optimal solutions were the same of the ones shown in Table 5.51, thus these twelve values make up the whole Pareto front of this study. Investigating the table a quasi-proportional trend between CED and GWP may be identified for this application, although this link does not occur in each situation. It is also evident that, for each combination of weighs, envelope # 263 has very higher performance, since the higher insulation level positively influences the operation of the equipment during the life cycle.

Table 5.51. Optimal values of the OFs and related weights for the real Italian building optimisation in the Step 2

SCENARIO	w_{cost}	w_{CED}	w_{GWP}	**Envelope # 263**			**Envelope # 515**		
				Annualised Cost	**CED**	**GWP**	**Annualised Cost**	**CED**	**GWP**
				€/year	**MJ**	**kg CO_{2-eq}**	**€/year**	**MJ**	**kg CO_{2-eq}**
MIN COST	1.000	0.000	0.000	2185.52	2,838,170	170,424	2213.71	2,925,058	175,644
COST >>>>> GWP, NO CED	0.995	0.000	0.005	2185.52	2,837,115	170,362	2213.89	2,883,201	173,160
COST >>>> GWP, NO CED	0.870	0.000	0.130	2185.76	2,782,707	167,132	2213.89	2,883,201	173,160
COST >>> GWP, NO CED	0.833	0.000	0.167	2189.61	2,758,683	165,714	2213.89	2,883,201	173,160
COST >> GWP, NO CED	0.750	0.000	0.250	2191.57	2,746,837	165,015	2217.51	2,861,330	171,869
COST > CED, NO GWP	0.667	0.333	0.000	2191.57	2,746,837	165,015	2217.51	2,861,330	171,869
COST > GWP, NO CED	0.667	0.000	0.333	2191.57	2,746,837	165,015	2217.51	2,861,330	171,869
COST > CED = GWP	0.500	0.250	0.250	2207.77	2,722,670	163,615	2246.86	2,816,319	169,261
COST = ENE, NO GWP	0.500	0.000	0.500	2216.12	2,711,997	163,000	2259.74	2,799,750	168,305
CED > COST, NO GWP	0.333	0.667	0.000	2286.10	2,628,675	158,205	2335.56	2,709,592	163,118
BALANCED	0.333	0.333	0.333	2346.62	2,585,456	155,772	2419.81	2,649,004	159,704
GWP > COST, NO CED	0.333	0.000	0.667	2375.38	2,566,647	154,718	2454.64	2,626,198	158,426
GWP >> COST, NO CED	0.250	0.000	0.750	2375.38	2,566,647	154,718	2674.68	2,506,613	151,807
GWP >>> COST, NO CED	0.200	0.000	0.800	2654.63	2,429,374	147,177	2792.44	2,461,957	149,413
GWP >>>> COST, NO CED	0.010	0.000	0.990	2654.63	2,429,374	147,177	2792.44	2,461,957	149,413
MIN GWP	0.000	0.000	1.000	3176.80	2,429,374	147,177	3314.61	2,461,957	149,413
GWP > CED, NO COST	0.000	0.333	0.667	3176.80	2,429,374	147,177	3314.61	2,461,957	149,413
CED > GWP, NO COST	0.000	0.667	0.333	3176.80	2,429,374	147,177	3314.61	2,461,957	149,413
MIN CED	0.000	1.000	0.000	3176.80	2,429,374	147,177	3314.61	2,461,957	149,413

Looking at the equipment features, shown in Table 5.52, NGB and STO_{el} were never selected, just like in the fictitious case study, while both PV and STC were installed in every alternative with the maximum possible size. This aspect confirms that the installation of solar RES technologies in Mediterranean climate would be very convenient from each of the points of view considered in this study, and, since the upper bound was always selected, a higher surface would likely be required, at least in some cases. Last, the HP and STO_{th} sizes showed an inverse trend, with a higher power from HP being cost-optimal while higher volumes of STO_{th} being preferred to minimise the impacts. Nevertheless, although a very high upper bound was considered for the STO_{th} volume, values higher than 10 m^3 look hard to be effectively installed in a single-family house, mainly for encumbrance reasons. The building with the envelope from the optimisation solution # 515 has always slightly higher sizes, justifying the higher costs and impacts in Table 5.51.

Table 5.52. Optimal values of the variables and related weights for the real Italian building optimisation

	N_{PV}	N_{STC}	P_{HP}		$V_{sto,th}$		E_{grid}	
	263 & 515	***263 & 515***	***263***	***515***	***263***	***515***	***263***	***515***
	#	#	kW	kW	m^3	m^3	kWh	kWh
MIN COST	9	16	6.4	6.6	4.51	4.88	3985	4108
COST >>>>> GWP, NO CED	9	16	6.4	6.6	4.55	6.52	3984	4049
COST >>>> GWP, NO CED	9	16	6.2	6.6	6.69	6.52	3907	4049
COST >>> GWP, NO CED	9	16	6.2	6.6	8.13	6.52	3873	4049
COST >> GWP, NO CED	9	16	6.2	6.4	8.85	7.85	3857	4018
COST > CED, NO GWP	9	16	6.2	6.4	8.85	7.85	3857	4018
COST > GWP, NO CED	9	16	6.2	6.4	8.85	7.85	3857	4018
COST > CED = GWP	9	16	6.2	6.4	11.93	13.48	3822	3954
COST = ENE, NO GWP	9	16	6.2	6.4	13.45	13.48	3807	3931
CED > COST, NO GWP	9	16	5.3	6.4	25.94	29.36	3689	3803
BALANCED	9	16	5.3	6.4	35.63	42.86	3628	3718
GWP > COST, NO CED	9	16	5.3	6.4	40.16	48.35	3601	3685
GWP >> COST, NO CED	9	16	5.3	4.7	40.16	82.12	3601	3516
GWP >>> COST, NO CED	9	16	2.3	2.5	82.45	99.44	3407	3452
GWP >>>> COST, NO CED	9	16	2.3	2.5	82.45	99.44	3407	3452
MIN GWP	9	16	2.3	2.5	82.45	99.44	3407	3452
GWP > CED, NO COST	9	16	2.3	2.5	82.45	99.44	3407	3452
CED > GWP, NO COST	9	16	2.3	2.5	82.45	99.44	3407	3452
MIN CED	9	16	2.3	2.5	82.45	99.44	3407	3452

In order to identify the best combination of the envelope, the equipment sizes and operation, the values of impacts and costs related to the optimal envelope renovation were added to the impacts and costs of the alternatives shown in Table 5.51, identifying the impacts and costs related to the life cycle of the building (the annual costs were projected to the reference life of 60 years). The OFs of the resulting 23 solutions are shown in Table 5.54. These values were processed to identify the global Pareto front of the case study, since some of the solutions dominated the others, with the result that the Pareto front is composed only by the solutions with envelope # 263 excluding the one minimising the impacts, *i.e.* the first eleven columns of Table 5.54. The solutions are graphically represented with three 2D Pareto fronts in Fig. 5.41, where a linear extrapolation between CED and GWP in optimal compromise solutions was performed, reporting the coefficient of determination.

Table 5.53. Optimal values of the OFs for the real Italian building optimisation over the reference life

SCENARIO	**Cost**	**CED**	**GWP**
	€	**MJ**	**kg $CO_{2\text{-eq}}$**
Envelope # 263, minimum COST	135,647	2,870,105	172,834
Envelope # 263, COST >>>>> GWP, NO CED	135,647	2,869,050	172,772
Envelope # 263, COST >>>> GWP, NO CED	135,661	2,814,642	169,542
Envelope # 263, COST >>> GWP, NO CED	135,892	2,790,618	168,124
Envelope # 263, COST > GWP, NO CED	136,010	2,778,772	167,425
Envelope # 263, COST > CED = GWP	136,982	2,754,605	166,025
Envelope # 263, COST = ENE, NO GWP	137,483	2,743,932	165,410
Envelope # 263, CED > COST, NO GWP	141,682	2,660,610	160,615
Envelope # 263, BALANCED	145,313	2,617,391	158,182
Envelope # 263, GWP > COST, NO CED	147,039	2,598,582	157,128
Envelope # 263, GWP >>> COST, NO CED	163,794	2,461,309	149,587
Envelope # 263, minimum GWP & CED	195,124	2,461,309	149,587
Envelope # 515, minimum COST	137,050	2,947,220	177,322
Envelope # 515, COST >>> GWP, NO CED	137,061	2,905,363	174,838
Envelope # 515, COST > GWP, NO CED	137,278	2,883,493	173,547
Envelope # 515, COST > CED = GWP	139,039	2,838,482	170,939
Envelope # 515, COST = ENE, NO GWP	139,812	2,821,913	169,983
Envelope # 515, CED > COST, NO GWP	144,361	2,731,754	164,796
Envelope # 515, BALANCED	149,416	2,671,167	161,382
Envelope # 515, GWP > COST, NO CED	151,506	2,648,361	160,104
Envelope # 515, GWP >> COST, NO CED	164,709	2,528,776	153,485
Envelope # 515, GWP >>> COST, NO CED	171,774	2,484,120	151,091
Envelope # 515, minimum GWP & CED	203,104	2,484,120	151,091

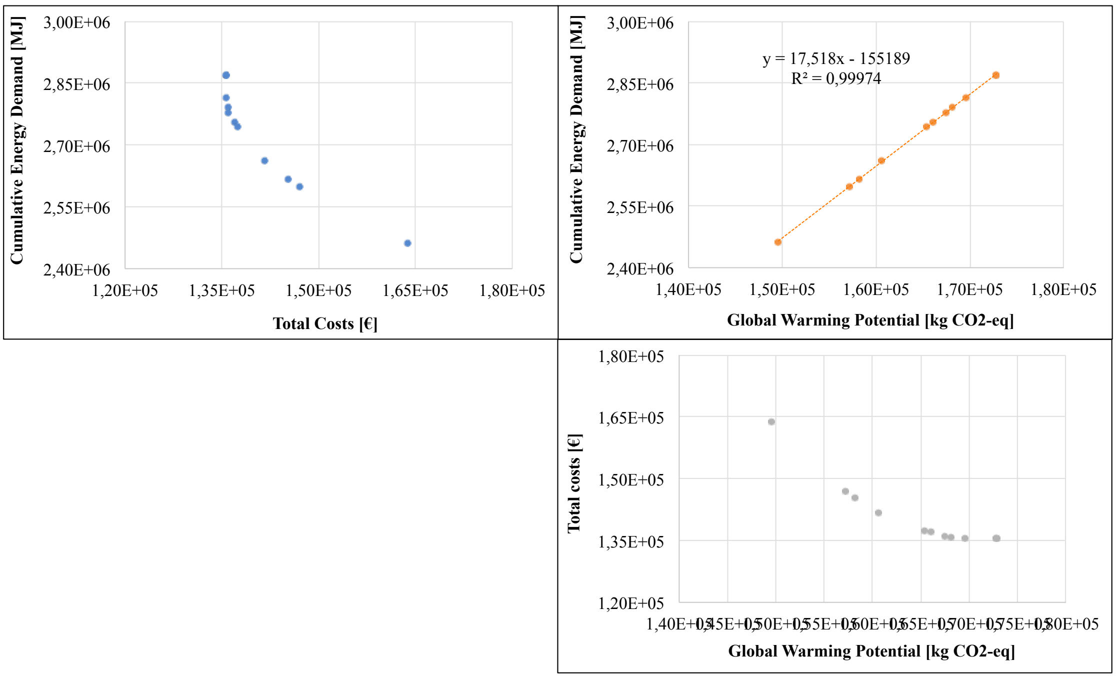

Fig. 5.41. 2D Pareto fronts for the Step 2 of the real Italian building optimisation

The last phase of this case study was the identification of the best compromise solution, performed using the utopia point criterion. The alternative to effectively implement for the building renovation is the solution with envelope from solution # 263 and labelled as “GWP > COST, NO CED“ in Table 5.54 and in Table 5.52. The resulting values of the objective functions are recapped in Table 5.54, together with the economic, energy and carbon payback times. Although this is a compromise solution between the three OFs, the renovation is highly convenient from all the points of view, since all the payback times are lower than 4 years.

Table 5.54. Optimal values of the objective functions and payback times for the real Italian building optimisation

	Economic criterion	***Energy criterion***	***Carbon criterion***
Embodied - Envelope	4516 €	31,935 MJ	2410 kg $CO_{2\text{-}eq}$
Embodied - Equipment	97,793 €	337,426 MJ	19,685 kg $CO_{2\text{-}eq}$
Operating (over 60 years)	44,730 €	2,229,222 MJ	135,033 kg $CO_{2\text{-}eq}$
TOT	147,039 €	2,598,582 MJ	157,128 kg $CO_{2\text{-}eq}$
Operating in AS-IS scenario (over 60 years)	1,814,766 €	15,989,122 MJ	495,435 kg $CO_{2\text{-}eq}$
Payback Time	3.47 years	1.61 years	3.68 years

5.5. Scientific literature contributions

Part of the work shown in this chapter was published in the following scientific papers:

JOURNAL ARTICLES

- Francesco Montana, Kai Kanafani, Kim B. Wittchen, Harpa Birgisdottir, Sonia Longo, Maurizio Cellura, Eleonora Riva Sanseverino, “Multi-objective optimization of building life cycle performance. A housing renovation case study in Northern Europe”, Sustainability, 2020, vol. 12(18), 7807.

BOOK CHAPTERS

- Francesco Montana, Sonia Longo, Harpa Birgisdottir, Maurizio Cellura, Rolf Frischknecht, Francesco Guarino, Benedek Kiss, Bruno Peuportier, Thomas Recht, Eleonora Riva Sanseverino, Zsuzsa Szalay, “Multi-criteria oriented optimization of building energy performances: the Annex 72 IEA-EBC experience”, in “Energy Systems Evaluation”, Ed. Springer, 2020, *in press*.

INTERNATIONAL CONFERENCE PROCEEDINGS

- Maurizio Cellura, Sonia Longo, Francesco Montana, Eleonora Riva Sanseverino, "Multi-Objective Building Envelope Optimization through a Life Cycle Assessment Approach", 2019 IEEE International Conference on Environment and Electrical Engineering and 2019 IEEE Industrial and Commercial Power Systems Europe (EEEIC / I&CPS Europe), Genoa, Italy, 2019, pp. 1-6.

NATIONAL CONFERENCE PROCEEDINGS

- Maurizio Cellura, Sonia Longo, Francesco Montana, Eleonora Riva Sanseverino, "Ottimizzazione Multi-Obiettivo delle Prestazioni Energetiche e Ambientali di un Edificio Residenziale", Atti del XIII Convegno della Rete Italiana LCA – VIII Convegno dell'Associazione Rete Italiana LCA (Proceedings of the XIII Conference of Italian LCA Network), Rome, Italy, 2019, pp. 1-10.

5.6. References

[1] U.S. Department of Energy. EnergyPlus v8.9.0 Documentation - Engineering Reference 2018:1–1715.

[2] European Union Joint Research Centre. Typical meteorological year files generator n.d. https://ec.europa.eu/jrc/en/PVGIS/tools/tmy (accessed April 28, 2020).

[3] U.S. Department of Energy. EnergyPlus web page n.d. https://energyplus.net/ (accessed April 28, 2020).

[4] Delcroix B, Kummert M, Daoud A, Hiller M. Conduction Transfer Functions in TRNSYS Multizone Building Model: Current Implementation, Limitations and Possible Improvements. Fifth Natl. Conf. IBPSA-USA, 2012, p. 219–26.

[5] Crawley DB, Lawrie LK, Pedersen CO, Winkelmann FC. EnergyPlus: Energy Simulation Program. ASHRAE J 2000;42:49–56. doi:10.1.1.122.6852.

[6] Deb K, Pratab S, Agarwal S, Meyarivan T. A Fast and Elitist Multiobjective Genetic Algorithm: NGSA-II. IEEE Trans Evol Comput 2002;6:182–97. doi:10.1109/4235.996017.

[7] Hamdy M, Nguyen A-T, Hensen JLM. A performance comparison of multi-objective optimization algorithms for solving nearly-zero-energy-building design problems. Energy Build 2016;121:57–71. doi:10.1016/j.enbuild.2016.03.035.

[8] Longo S, Montana F, Riva Sanseverino E. A review on optimization and cost-optimal methodologies in low-energy buildings design and environmental considerations. Sustain Cities Soc 2019;45:87–104.

[9] Deb K. Multi-Objective Optimization Using Evolutionary Algorithms. John

Wiley Sons, LTD 2001:497.

[10] American Society of Heating Refrigerating and Air-Conditioning Engineers. ASHRAE Handbook - Fundamentals. 2017.

[11] Attardo G, Longo S, Montana F, Riva Sanseverino E, Tran QTT, Zizzo G. Urban Energy Hubs Economic Optimization and Environmental Comparison in Italy and Vietnam. 2018 IEEE 4th Int. Forum Res. Technol. Soc. Ind., 2018, p. 1–6.

[12] Enel X web page n.d. https://www.enelxstore.com/it/it/prodotti/.

[13] ASHRAE. ASHRAE Equipment Life Expectancy chart. n.d.

[14] Fan J, Chen Z, Furbo S, Perers B, Karlsson B. Efficiency and lifetime of solar collectors for solar heating plants. Proc. ISES Sol. World Congr. 2009, 2009, p. 331–40.

[15] Smith K, Saxon A, Keyser M, Lundstrom B, Cao Z, Roc A, et al. Life Prediction Model for Grid- Connected Li-ion Battery Energy Storage System Preprint. 2017 Am. Control Conf., 2017, p. 1–6.

[16] Cannata N, Cellura M, Longo S, Montana F, Riva Sanseverino E, Luu QL, et al. Multi-Objective Optimization of Urban Microgrid Energy Supply According to Economic and Environmental Criteria. 2019 IEEE Milan PowerTech, 2019, p. 1–6.

[17] ARERA. Andamento del prezzo dell’energia elettrica per il consumatore domestico tipo in maggior tutela. Average value in 2019 n.d. https://www.arera.it/it/dati/eep35.htm (accessed April 21, 2020).

[18] ARERA. Andamento del prezzo del gas naturale per un consumatore domestico tipo in regime di tutela n.d. https://www.arera.it/it/dati/gp27new.htm (accessed April 21, 2020).

[19] Biancardi A. The cost of capital in the energy and water sectors in Italy 2016.

[20] European Union Joint Research Centre. European reference Life Cycle Database (ELCD) n.d. https://nexus.openlca.org/database/ELCD (accessed April 28, 2020).

[21] Beccali M, Cellura M, Longo S, Nocke B, Finocchiaro P. LCA of a solar heating and cooling system equipped with a small water – ammonia absorption chiller. Sol Energy 2012;86:1491–503. doi:10.1016/j.solener.2012.02.010.

[22] Zhang D, Evangelisti S, Lettieri P, Papageorgiou LG. Optimal design of CHP-based microgrids: Multiobjective optimisation and life cycle assessment. Energy 2015;85:181–93. doi:10.1016/j.energy.2015.03.036.

[23] Gulotta TM, Guarino F, Cellura M, Lorenzini G. A Constructal Law optimization of a boiler inspired by Life Cycle thinking. Therm Sci Eng Prog 2018;6:380–7. doi:10.1016/j.tsep.2018.01.008.

[24] Schaefer H, Hagedorn G. Hidden energy and correlated environmental characteristics of P.V. power generation. Renew Energy 1992;2:0–7.

[25] Fukurozaki SH, Zilles R, Sauer IL. Energy Payback Time and CO2 Emissions of 1.2 kWp Photovoltaic Roof-Top System in Brazil. Int J Smart Grid Clean Energy 2013;2:164–169.

[26] Gökulu O, Kadırgan F, Kadırgan MAN. Life cycle assessment (LCA) of a solar selective surface produced by continuous process and solar flat collectors 2016;135:284–90. doi:10.1016/j.solener.2016.05.049.

[27] Mcmanus MC. Environmental consequences of the use of batteries in low carbon systems: The impact of battery production. Appl Energy 2012;93:288–95. doi:10.1016/j.apenergy.2011.12.062.

[28] Asdrubali F, Ballarini I, Corrado V, Evangelisti L, Grazieschi G, Guattari C. Energy and environmental payback times for an NZEB retrofit. Build Environ 2018. doi:10.1016/j.buildenv.2018.10.047.

[29] International Organization for Standardization (ISO). ISO 13790:2008 - Energy performance of buildings. Calculation of energy use for space heating and cooling 2008.

[30] Rose J, Thomsen KE, Mørck OC, Gutierrez MSM, Jensen SØ. Refurbishing blocks of flats to very low or nearly zero energy level–technical and financial results plus co-benefits. Energy Build 2019;184:1–7. doi:https://doi.org/10.1016/j.enbuild.2018.11.051.

[31] Rose J, Thomsen KE, Mørck OC, Gutierrez MSM, Jensen SØ. Energirenovering af Traneparken. 2017.

[32] German Federal Ministry of the Interior Building and Community. ÖKOBAUDAT Database 2019. https://www.oekobaudat.de/en/database/database-oekobaudat.html.

[33] COWI consulting. Nye emissionsfaktorer for el og fjernvarme. 2016.

[34] Beccali M, Cellura M, Fontana M, Longo S, Mistretta M. Energy retrofit of a single-family house: Life cycle net energy saving and environmental benefits. Renew Sustain Energy Rev 2013;27:283–93. doi:10.1016/j.rser.2013.05.040.

[35] Italian Government. Integrated National Energy and Climate Plan. 2019.

Chapter Six – Case studies on building clusters optimisation

6.1. Introduction

This section describes the case studies developed on clusters of buildings. The extension of the methodological framework developed in this thesis to the cluster level was performed since the current trend of research in building physics is to analyse many buildings instead of a single one, in order to investigate further possibilities to attain energy savings.

The scientific interest in the investigation of the energy performance of building clusters arises from many points of view [1]:

- It is possible to predict the demand of many buildings with more accuracy since the load peaks and valleys of a single customer tend to be mitigated in the cluster;
- The transformation from a vertically integrated to a horizontally integrated power system started the diffusion of distributed energy systems and the development of microgrids and smart grids, that may be considered as clusters of buildings exchanging power and data on their behaviour;
- Designing zero-energy districts is easier than designing zero-energy buildings since the single building in the cluster does not have to meet the zero balance;
- From a practical point of view, it is easier to find adequate spaces to install the RES and HVAC systems

It is possible to find several definitions related to the concept of building clusters or buildings communities according to different perspectives, but there is not a univocal description of clusters' features in the literature. Furthermore, it is not clear if the energy consumers in a cluster are residential, commercial or industrial users. Vigna et al. reviewed some definitions in 2018 in order to develop a new and comprehensive one: "a building cluster identifies a group of buildings interconnected to the same energy infrastructure, such that the change of behaviour/energy performance of each building affects both the energy infrastructure and the other buildings of the whole cluster" [2]. This definition is mainly based on building interconnection, without specifying whether it is a physical and/or market relation, and even the dimension of the cluster is not specified. In detail, a physical interconnection may allow, for example, a PV system installed on the rooftop of a building to also supply other buildings in the cluster, while a market relation may be exploited to aggregate the cluster providing flexibility services to the grid. The energy flexibility in a building could be defined as "the ability of demand-side installations to respond to power systems requirements for ramping up or down using on-site storage capabilities, increasing or decreasing electricity consumption patterns whilst maintaining acceptable indoor comfort bandwidth during a specific period of time" [3]. The energy flexibility of buildings is commonly considered as a way to mitigate peak loads in power systems, deferring investments in the grid capacity in the future. Depending on the kind of consumers making up the cluster (residential, commercial or industrial), different levels of energy flexibilities may be provided to the grid. Residential and commercial buildings may supply flexibility services adjusting the HVAC systems use, shifting of plug-loads and charging electric vehicles [4], while industrial buildings may set their daily or weekly schedules according to the distribution system operator requests.

The proof of the current interest on the topics of the clusters of buildings and the energy flexibility from the international scientific community is the increasing number of working groups of the IEA EBC. In detail, IEA Annex 60 [5] and IEA Annex 63 [6] focus their activities on building clusters and energy communities, IEA Annex 83 analyses the positive energy districts, also including flexibility services, while IEA Annex 67 [7] and IEA Annex 82 [8] mainly investigate the flexibility integration in buildings and clusters to save energy and decarbonise the economy.

For what above, the case studies presented in this thesis assessed two different scales of building cluster, namely an urban district and a small island. In the first study, the optimisation of synthesis, design and operation stages of the components aimed at fulfilling the urban district energy requirements was investigated, while in the second study, including residential and industrial customers, also the flexibility of these kinds of buildings was assessed and optimised. Another difference between these two case studies lays on the energy demands estimation: a BPS was employed for the urban district, while the island energy demands were derived from an extensive literature investigation and review.

As already shown in Chapter 4, the optimisation of the clusters of buildings was performed developing an energy hub model in MATLAB environment, simulating the districts as islanded microgrids. This kind of model allows a compact formulation but high reliability and flexibility, and a linear formulation was employed, as in most of energy hub studies. The linearity has the major advantage of ensuring the uniqueness of the solution since the problem is said to be intrinsically convex, so that a local minimum is also a global minimum. The drawback to be paid is that, since none of the physical phenomena is effectively linear, some simplifications had to be introduced in the model, as is often done in optimisation studies. This aspect was mainly faced in the second case study, where the flexibility service was aimed at ensuring the local thermal power plant to operate at maximum efficiency, with the thermal efficiency depending on the load instead of being constant, thus introducing a non-linearity in the problem.

A difference in the approach between the case studies on single buildings and clusters of buildings was also introduced. In detail, since the results on single buildings optimisation clearly highlighted that GWP and CED are non-conflicting objectives, only the cost and the GWP were minimised in these case studies, although the CED was also assessed.

6.2. Urban district in a developed and a developing country in warm climate

This case study describes the multi-objective optimisation of the life cycle impacts and costs of a fictitious urban district. The variables of the problem relate to the simultaneous synthesis, design and operation of the equipment aimed at fulfilling the district's electricity, heating and cooling demands, which are considered as fixed values.

Moreover, a comparison between two cities in different economic and environmental contexts is provided, confronting the Italian and Vietnamese scenarios. The selection of the Vietnamese context was driven by the availability of detailed data provided by the researchers of the Vietnam Academy of Science and Technology. In detail, the two cities (Palermo and Hanoi) were selected since they have both warm climates but belong to different socio-economic contexts. In this way, the different average prices of energy and equipment and the different electricity production technological mix implied important differences in the results.

The comparison of climates was performed according to the widely employed Köppen–Geiger climate classification system [9]. In detail, this system assigns the world climates to one of five main climate groups divided depending on the seasonal precipitation and temperature trends. Each group is further described with one or two subgroups indicating the seasonal precipitation and the average temperature. Each group or subgroup is specified through a letter. According to the most updated data available [10], Hanoi is classified as "Cwa" (mild temperate climate with dry Winter and hot Summer), while Palermo is classified as "Csa" (mild temperate climate with dry and hot Summer). Both of these cities have thus a mild temperate climate and a hot Summer season, where the term "temperate" indicates that the mean temperature is below 18 °C and above -3 °C during the coldest month of the year.

6.2.1. Case study description

The fictitious urban district was assumed to be composed by 35 two-floor detached houses, with each house having four dwellings and being equipped with a car box. An example of this kind of district may be a set of terraced houses. The illustration of one of these houses is provided in Fig. 6.1 and Fig. 6.2. In the AS-IS scenario (previously the retrofit), the energy demand was assumed to be totally covered through electricity and natural gas from the main grids.

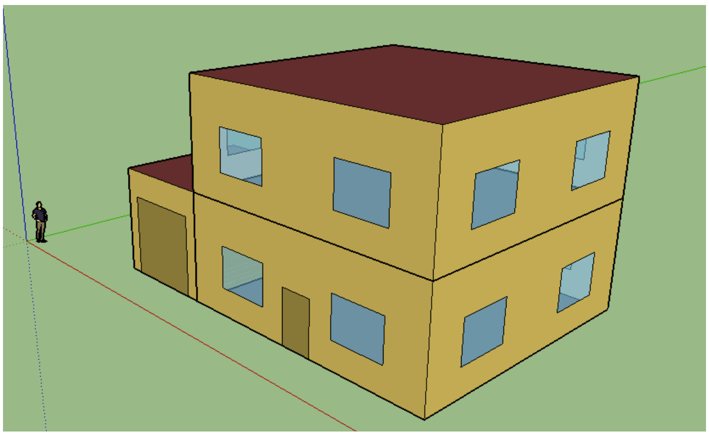

Fig. 6.1. Front view of the model in SketchUp Make 2017 of one of the detached houses

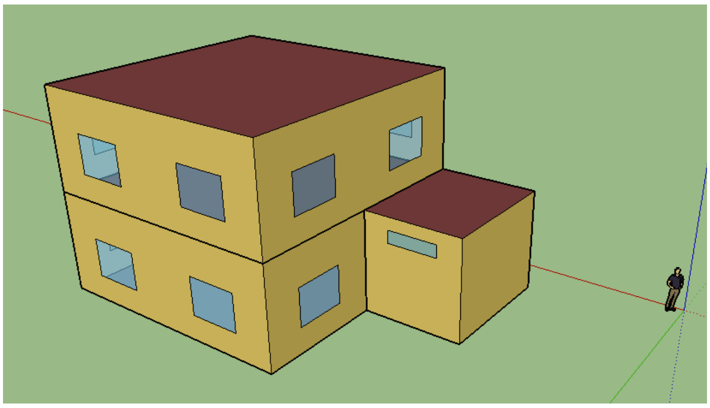

Fig. 6.2. Back view of the model in SketchUp Make 2017 of one of the detached houses

In order to save energy and costs, it is supposed that the district dwellings want to investigate the possibility of satisfying their demands through the installation of the following components: natural gas boiler (NGB), replacing the existing ones currently installed in each building; heat pumps (HP) for space heating and cooling; a cogeneration system (CHP) for electricity and heating production; absorbing chiller for space cooling production through waste heat; electricity and heating production through PV and solar thermal collectors (STC); electrical and thermal energy storage systems (STO_{el} and STO_{th}) to improve the exploitation of energy from RES system, decoupling energy production and consumption periods. The objective is the simultaneous minimisation of the annual costs and the equivalent GHG emissions. The optimisation model of the cluster was developed with reference to Fig. 6.3, where the labels on the energy flows use the same nomenclature of the equations in Chapter 3.

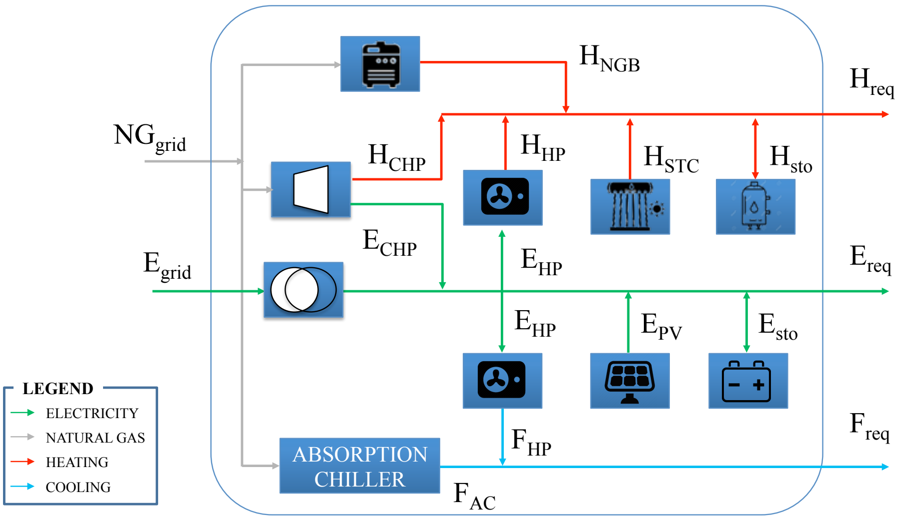

Fig. 6.3. Reference scheme for the energy hub model describing the fictitious urban district building cluster

6.2.2. Input data

To obtain reliable data on the district energy requirements, the model of a single building was developed on SketchUp Make 2017 and its annual electricity, heating and cooling demands were obtained simulating the building model on EnergyPlus 8.7 with an hourly detail using Palermo and Hanoi's climates. The weather file for Palermo was downloaded from the typical meteorological year files generator developed by the EU [11], while the weather file for Hanoi was downloaded from the EnergyPlus website [12]. In the simulation, the garage was assumed to be a non-heated zone, while ground and first floor set-point temperatures were set equal to 20 °C for space heating and 26 °C for space cooling. A multiplier for the indoor temperature equal to 5 was included in both ground and first floors, simulating the thermal capacity of the furniture. The thermal features of the main components of the building are described in Table 6.1, while the schedules representing the thermal loads due to occupants, lighting, electrical equipment, and ventilation are provided in Table 6.2 - Table 6.5.

The infiltration rate was calculated according to the equation of Coblenz and Achenbach (Eq. (6.1)) [14]:

$$Infiltration = I_{design} \cdot F_{schedule} \cdot \left(A + B \cdot \left| T_{zone} - T_{odb} \right| + C \cdot u_w + D \cdot u_w^2 \right) \tag{6.1}$$

where I_{design} is the design value of air changes per hour, $F_{schedule}$ is the schedule set for the infiltration rate, T_{zone} is the hourly zone temperature (°C), T_{odb} is the outdoor air dry-bulb temperature (°C), u_w is the wind speed and A, B, C and D are the extrapolation coefficients. The values for I_{design}, the extrapolation coefficients (suggested by ASHRAE), and Fschedule adopted for the simulations are shown in Table 6.6.

Table 6.1. Thermal features of the main components of the building model

Component	Layer 1 (outside)	Layer 2	Layer 3
Exterior Wall	Bricks Thickness: 102 mm Density: 1920 kg/m^3 Conductivity: 0.89 W/(m K)	Heavyweight concrete Thickness: 350 mm Density: 2240 kg/m^3 Conductivity: 1.95 W/(m K)	Gypsum board Thickness: 19 mm Density: 800 kg/m^3 Conductivity: 0.16 W/(m K)
Exterior Roof	I06 R-30 Thickness: 244 mm Density: 19.2 kg/m^3 Conductivity: 0.05 W/(m K)	Lightweight concrete Thickness: 102 mm Density: 1280 kg/m^3 Conductivity: 0.53 W/(m K)	Gypsum board Thickness: 19 mm Density: 800 kg/m^3 Conductivity: 0.16 W/(m K)
Exterior Floor	Natural stones Thickness: 60 mm Density: 2000 kg/m^3 Conductivity: 1.5 W/(m K)	Concrete blocks Thickness: 203 mm Density: 800 kg/m^3 Conductivity: 1.11 W/(m K)	Wood layer Thickness: 25 mm Density: 608 kg/m^3 Conductivity: 0.15 W/(m K)
Interior Floor	Concrete blocks Thickness: 203 mm Density: 800 kg/m^3 Conductivity: 1.11 W/(m K)	Wood layer Thickness: 25 mm Density: 608 kg/m^3 Conductivity: 0.15 W/(m K)	-
Exterior Door	Wood layer Thickness: 25 mm Density: 608 kg/m^3 Conductivity: 0.15 W/(m K)	-	-
Exterior Window	Clear glass Thickness: 3 mm Conductivity: 0.9 W/(m K)	Gas gap Gas: Air Thickness: 13 mm	Clear glass Thickness: 3 mm Conductivity: 0.9 W/(m K)

Table 6.2. Fraction of Thermal Loads due to the Occupants Presence and Activity with Reference to the Maximum Load (4 occupants and 315 W/m^2, absolute values from [13]*)*

OCCUPANTS	Ground floor - Weekdays	Ground floor - Weekend	First floor - Weekdays	First floor - Weekend
00:00 → 01:00	0.00	0.00	0.51	0.32
01:00 → 06:00	0.00	0.00	0.51	0.51
06:00 → 07:00	0.22	0.00	0.38	0.51
07:00 → 08:00	0.67	0.00	0.00	0.51
08:00 → 09:00	0.00	0.22	0.00	0.38
09:00 → 10:00	0.00	0.89	0.00	0.00
10:00 → 11:00	0.00	0.76	0.00	0.00
11:00 → 12:00	0.00	0.00	0.00	0.00
12:00 → 13:00	0.37	0.00	0.00	0.00
13:00 → 14:00	0.67	0.76	0.00	0.00
14:00 → 15:00	0.00	0.00	0.44	0.51
15:00 → 16:00	0.00	0.38	0.44	0.38
16:00 → 18:00	0.00	0.38	0.44	0.00
18:00 → 19:00	0.37	0.00	0.44	0.00
19:00 → 20:00	0.57	0.38	0.44	0.00
20:00 → 21:00	0.89	0.89	0.00	0.00
21:00 → 23:00	0.00	0.00	0.76	0.00
23:00 → 24:00	0.00	00.32	0.51	0.00

Table 6.3. Fraction of Sensible Thermal Loads due to the Lighting System with Reference to the Maximum Load (150 W)

LIGHTING	Ground floor - Weekdays	Ground floor - Weekend	First floor - Weekdays	First floor - Weekend
00:00 → 01:00	0.00	0.00	0.00	0.15
01:00 → 06:00	0.00	0.00	0.00	0.00
06:00 → 07:00	0.15	0.00	0.07	0.00
07:00 → 08:00	0.15	0.00	0.33	0.00
08:00 → 09:00	0.00	0.18	0.00	0.15
09:00 → 10:00	0.00	0.18	0.00	0.12
10:00 → 11:00	0.00	0.00	0.00	0.00
11:00 → 12:00	0.00	0.00	0.00	0.00
12:00 → 13:00	0.00	0.00	0.00	0.00
13:00 → 14:00	0.00	0.00	0.00	0.00
14:00 → 15:00	0.00	0.00	0.00	0.00
15:00 → 16:00	0.00	0.00	0.00	0.00
16:00 → 18:00	0.00	0.00	0.00	0.00
18:00 → 19:00	0.67	0.00	0.00	0.00
19:00 → 20:00	0.67	0.15	0.00	0.00
20:00 → 21:00	0.67	0.67	0.00	0.00
21:00 → 22:00	1.00	0.00	0.00	0.00
22:00 → 23:00	0.67	0.00	0.00	0.00
23:00 → 24:00	0.00	00.80	0.00	0.00

Table 6.4. Sensible Thermal Loads due to Electric Equipment [W]

EQUIPMENT	Ground floor - Weekdays	Ground floor - Weekend	First floor - Weekdays	First floor - Weekend
00:00 → 01:00	552.00	552.00	0.00	500.00
01:00 → 06:00	552.00	552.00	0.00	0.00
06:00 → 07:00	1457.75	552.00	0.00	0.00
07:00 → 08:00	1457.75	552.00	675.00	0.00
08:00 → 09:00	552.00	1457.75	0.00	0.00
09:00 → 10:00	552.00	1457.75	0.00	0.00
10:00 → 11:00	552.00	1552.00	0.00	0.00
11:00 → 12:00	552.00	552.00	0.00	0.00
12:00 → 13:00	1902.00	552.00	0.00	0.00
13:00 → 14:00	1052.00	1252.00	0.00	0.00
14:00 → 15:00	1052.00	552.00	130.00	0.00
15:00 → 16:00	552.00	1052.00	130.00	500.00
16:00 → 17:00	1052.00	1052.00	130.00	0.00
17:00 → 18:00	552.00	1052.00	130.00	0.00
18:00 → 19:00	1402.00	552.00	500.00	0.00
19:00 → 20:00	1902.00	1552.00	400.00	0.00
20:00 → 21:00	1052.00	2572.00	0.00	0.00
21:00 → 22:00	1617.00	552.00	0.00	0.00
22:00 → 23:00	1552.00	552.00	0.00	0.00
23:00 → 24:00	552.00	1052.00	0.00	0.00

Table 6.5. Fraction of Windows Opening for Ventilation, Influencing Sensible and Latent Thermal Loads, with Reference to the Maximum Windows Surface [%]

VENTILATION	Ground floor - Weekdays	Ground floor - Weekend	First floor - Weekdays	First floor - Weekend
January to May				
00:00 → 01:00	0.00	0.00	0.00	0.10
01:00 → 06:00	0.00	0.00	0.00	0.00
06:00 → 07:00	0.10	0.00	0.10	0.00
07:00 → 08:00	0.10	0.00	0.30	0.00
08:00 → 09:00	0.00	0.10	0.00	0.10
09:00 → 10:00	0.00	0.30	0.00	0.30
10:00 → 11:00	0.00	0.10	0.00	0.00
11:00 → 12:00	0.00	0.00	0.00	0.00
12:00 → 13:00	0.30	0.00	0.10	0.00
13:00 → 14:00	0.40	0.40	0.10	0.00
14:00 → 15:00	0.00	0.00	0.40	0.10
15:00 → 16:00	0.00	0.20	0.40	0.10
16:00 → 17:00	0.00	0.10	0.40	0.10
17:00 → 18:00	0.00	0.10	0.40	0.10
18:00 → 19:00	0.10	0.00	0.40	0.10
19:00 → 20:00	0.30	0.10	0.30	0.00
20:00 → 21:00	0.30	0.30	0.00	0.00
21:00 → 22:00	0.00	0.00	0.10	0.00
22:00 → 23:00	0.00	0.00	0.10	0.00
23:00 → 24:00	0.00	0.00	0.00	0.00
June to August				
00:00 → 01:00	0.60	0.60	0.80	1.00
01:00 → 06:00	0.60	0.60	0.80	1.00
06:00 → 07:00	0.20	0.60	0.40	1.00
07:00 → 08:00	0.20	0.60	0.50	1.00
08:00 → 09:00	0.00	0.30	0.00	0.40
09:00 → 10:00	0.00	0.30	0.00	0.40

10:00 → 11:00	0.00	0.30	0.00	0.00
11:00 → 12:00	0.00	0.00	0.00	0.00
12:00 → 13:00	0.30	0.00	0.10	0.00
13:00 → 14:00	0.40	0.40	0.10	0.00
14:00 → 15:00	0.00	0.00	0.80	0.60
15:00 → 16:00	0.00	0.30	0.80	0.60
16:00 → 17:00	0.00	0.30	0.80	0.60
17:00 → 18:00	0.00	0.30	0.80	0.60
18:00 → 19:00	0.30	0.00	0.80	0.00
19:00 → 20:00	0.60	0.30	0.80	0.00
20:00 → 21:00	0.60	0.30	0.80	0.00
21:00 → 22:00	0.60	0.00	0.80	0.00
22:00 → 23:00	0.60	0.00	0.80	0.00
23:00 → 24:00	0.60	0.60	0.80	1.00
September to December				
00:00 → 01:00	0.00	0.00	0.00	0.10
01:00 → 06:00	0.00	0.00	0.00	0.00
06:00 → 07:00	0.10	0.00	0.10	0.00
07:00 → 08:00	0.10	0.00	0.30	0.00
08:00 → 09:00	0.00	0.10	0.00	0.10
09:00 → 10:00	0.00	0.30	0.00	0.30
10:00 → 11:00	0.00	0.10	0.00	0.30
11:00 → 12:00	0.00	0.00	0.00	0.00
12:00 → 13:00	0.30	0.00	0.10	0.00
13:00 → 14:00	0.40	0.40	0.10	0.00
14:00 → 15:00	0.00	0.00	0.40	0.10
15:00 → 16:00	0.00	0.20	0.40	0.10
16:00 → 17:00	0.00	0.10	0.40	0.10
17:00 → 18:00	0.00	0.10	0.40	0.10
18:00 → 19:00	0.10	0.00	0.40	0.00
19:00 → 20:00	0.30	0.10	0.30	0.00
20:00 → 21:00	0.30	0.30	0.00	0.00
21:00 → 22:00	0.00	0.00	0.10	0.00
22:00 → 23:00	0.00	0.00	0.10	0.00
23:00 → 24:00	0.00	0.00	0.00	0.00

Table 6.6. Parameters employed for the simulation of heat gains for infiltration

Parameter	Value
I_{design}	0.1 h^{-1}
A	0.606
B	0.03636 K^{-1}
C	0.1177 s/m
D	0 s^2/m^2
$F_{schedule}$	
January	0.71
February	0.89
March	0.84
April	0.97
May	1.00
June	0.91
July	0.78
August	0.76
September	0.78
October	0.80
November	0.62
December	0.61

Simulating the building model described so far allowed obtaining the electricity, space heating and space cooling demands of a single building of the cluster. The energy demands of the district were assumed to be proportional to that of the single building, neglecting simultaneity factors. Nevertheless, the use of annual data with hourly detail in the optimisation would have required 8760 values for each energy flow of the hub, with a consequent enormous computational burden for the computer. Optimising the hourly operation of the 8 components assessed in this study (one for each kind), this problem should evaluate 157,696 variables, with the equality constraints matrix having 52,568 rows and 157,696 columns (61.8 GB of memory) and the inequality constraints matrix having 113,888 rows and 157,696 columns (133.8 GB of memory). Since this huge level of memory was not available and since this level of accuracy was considered to be excessive for an optimisation problem, where relations are usually simplified to attain the optimal solution, four representative standard days, one for each season, were used as input of the optimisation problem. This led to 96 values for each energy flow, allowing each optimisation to be solved in a few minutes. In detail, the problem is composed by 8 synthesis variables (one variable for each component), 6 design variables indicating the size of each component, because the synthesis and design variables for the RES system coincide, 2·96 variables for the electricity and gas networks, 4·96 variables for the energy flowing into NGB, HP, CHP and AC, 2·96 variables for the energy flowing out from RES systems, and 2·5·96 variables indicating the status of the storage systems. The total number of variables in this case study was 1742. The standard days were obtained as the average of the demands in the days of each season. The trends of the resulting energy demands are shown in Fig. 6.4 – Fig. 6.8. Since the electricity demand only depends on the lighting and the internal equipment, it is the same for both Italian and Vietnamese scenarios.

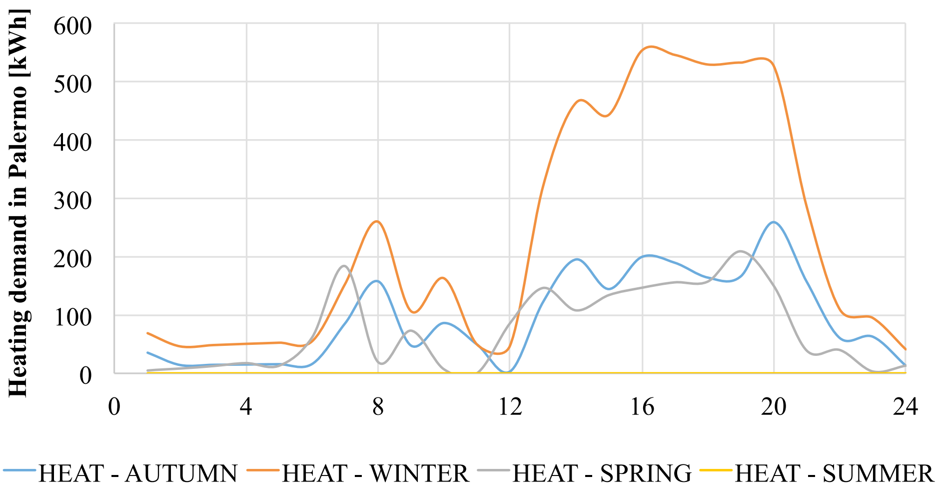

Fig. 6.4. Heating demand for Palermo's climate in the four standard seasonal days

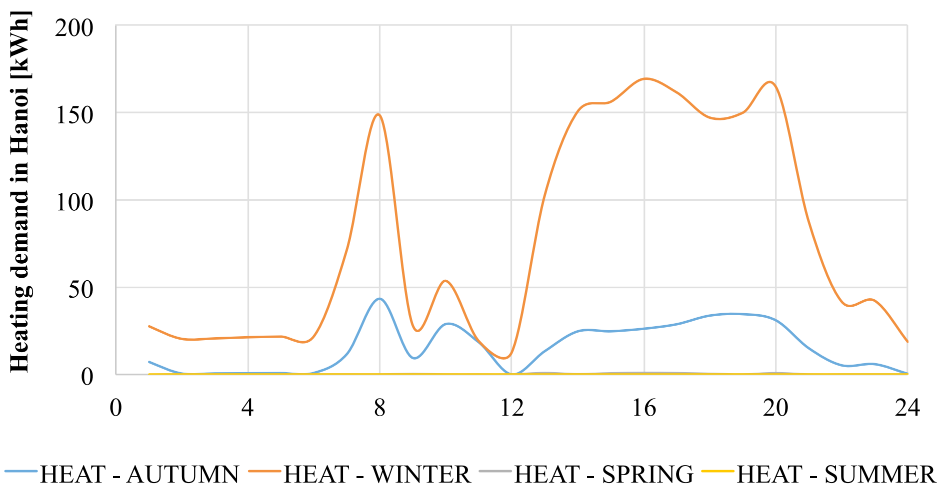

Fig. 6.5. Heating demand for Hanoi's climate in the four standard seasonal days (trends for Spring and Summer are overlapped)

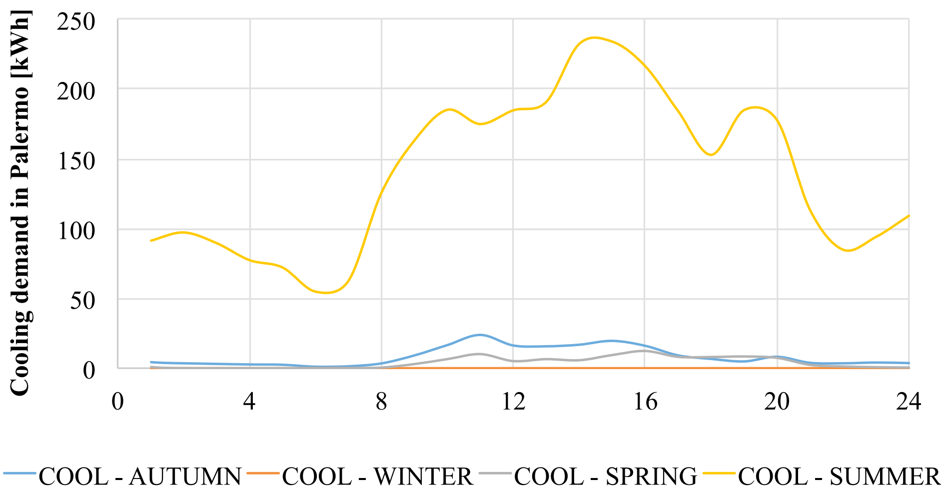

Fig. 6.6. Cooling demand for Palermo's climate in the four standard seasonal days

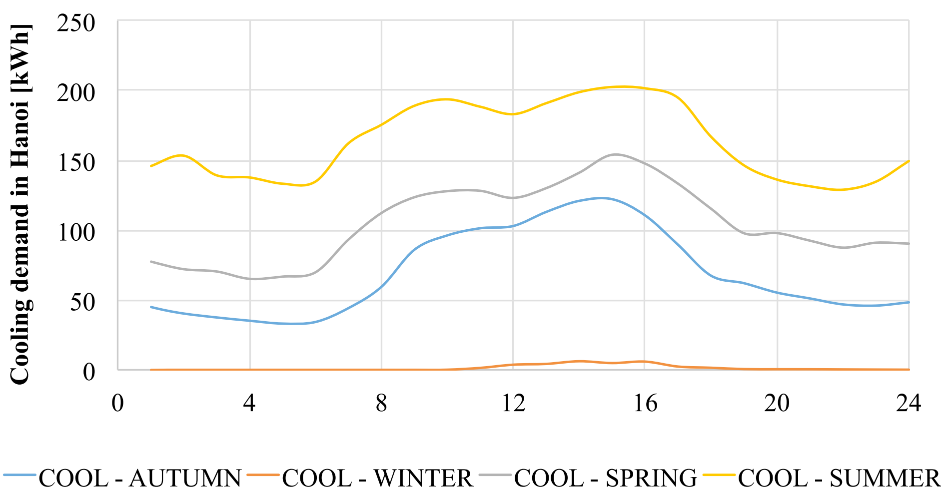

Fig. 6.7. Cooling demand for Hanoi's climate in the four standard seasonal days

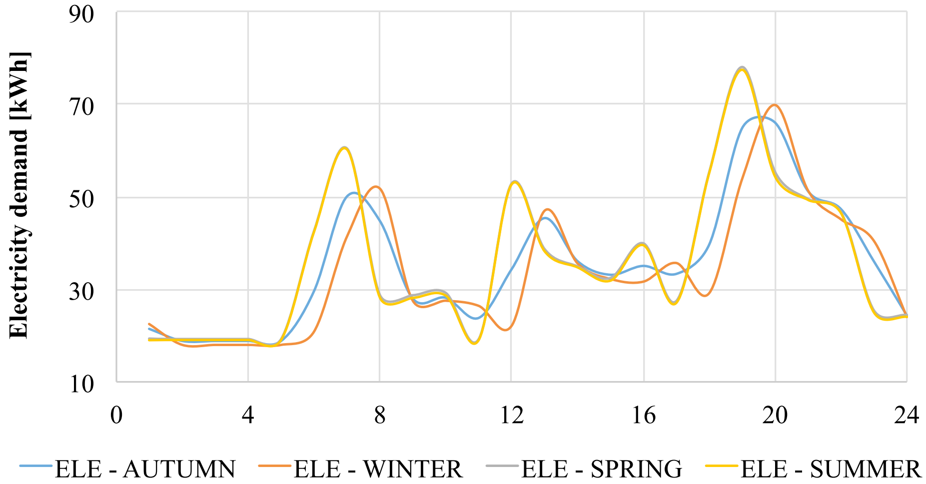

Fig. 6.8. Electricity demand for Palermo's and Hanoi's climates in the four standard seasonal days trends for Spring and Summer are overlapped)

These energy demands, assumed to be fixed, were used as input for the optimisation model as the target to be fulfilled in the design of the equipment.

A value of annual average solar radiation available on the city, necessary for the calculation of RES technologies energy production, was evaluated as the average value from the hourly solar radiation available on the weather file, summing direct and diffuse components, obtaining a value of 6.01 kWh/(m^2 day) for Palermo and 4.83 kWh/(m^2 day) for Hanoi.

Technical parameters as conversion efficiencies in the components, assumed to be constant and equal in both geographical contexts, were collected form technical and market reports, and are available in Table 6.7. The cost functions were also drawn from representative reports of the two countries, and a linear trend for each component was extrapolated through the least-squares method according to Eq. (3.37) in Chapter 3. These values are available in Table 6.8.

Table 6.7. Technical parameters of the equipment for the fictitious district optimisation

Parameter	**Value**
Transformer efficiency	99% [15]
Cogenerator electrical efficiency	36.5% [16]
Cogenerator thermal efficiency	53.9% [16]
Cogenerator useful life	20 years [17]
Heat pump SCOP	4.1 [18]
Heat pump SEER	5.7 [18]
Heat pump useful life	15 years [17]
Natural gas boiler efficiency	90.1% [18]
Natural gas boiler useful life	24 years [17]
Gas-fired absorbing chiller SEER	1.3 [19]
Gas-fired absorbing chiller useful life	23 years [17]
Photovoltaic module efficiency	17.11% [18]

Parameter	Value
Photovoltaic Balance of Plant efficiency	95% [15]
Photovoltaic system dimensions	$1.65 \cdot 0.992\ m^2$ [18]
Photovoltaic system max available surface	1000 m^2
Photovoltaic system useful life	25 years [18]
Solar thermal collector zero-loss efficiency	79.7% [18]
Solar thermal collector first-order heat loss coefficient	3.18 $W/(m^2\ K)$ [18]
Solar thermal collector second-order heat loss coefficient	0.008 $W/(m^2\ K^2)$ [18]
Solar thermal collector average efficiency (ΔT = 30 °C)	69.4%
Solar thermal collector dimensions	$1.987 \cdot 1.27\ m^2$ [18]
Solar thermal collector max available surface	1000 m^2
Solar thermal collector useful life	15 years [20]
Electrical storage charging efficiency	97% [15]
Electrical storage discharging efficiency	97% [15]
Electrical storage Depth of Discharge	20% [15]
Electrical storage self-discharge coefficient	0.01 kWh/h [15]
Electrical storage useful life	7 years [21]
Thermal storage charging efficiency	100% [15]
Thermal storage discharging efficiency	100% [15]
Thermal storage self-discharge coefficient	0.01 kWh/h [15]
Thermal storage useful life	15 years [22]

Table 6.8. Economic parameters of the energy carriers and equipment for the fictitious district optimisation in the Italian and Vietnamese scenarios

Parameter	*Italian scenario*	*Vietnamese scenario*
Electrical energy wholesale price	0.076 \$/kWh [23]	0.116 \$/kWh [24]
Natural gas wholesale price	0.029 \$/kWh [23]	0.094 \$/kWh [25]
Cogenerator first order investment cost	854.570 $\$/kW_{el}$ [16]	1000 $\$/kW_{el}$ [26]
Cogenerator zero-th order investment cost	165668.605 \$ [16]	0 \$ [26]
Heat pump first order investment cost	123.44 $\$/kW_{cool}$ [18]	993.077 $\$/kW_{cool}$ [22]
Heat pump zero-th order investment cost	693.411 \$ [18]	-1933.820 \$ [22]
Natural gas boiler first order investment cost	60.523 \$/kW [18]	138.677 \$/kW [22]
Natural gas boiler zero-th order investment cost	132.006 \$ [18]	0 \$ [22]
Gas-fired absorbing chiller first order investment cost	147.337 \$/kW [19]	147.337 \$/kW [19]
Gas-fired absorbing chiller zero-th order investment cost	62033.721 \$ [19]	62033.721 \$ [19]
Photovoltaic system first order investment cost	1366.142 $\$/kW_p$ [18]	1400 $\$/kW_p$ [22]
Photovoltaic system zero-th order investment cost	3055.583 \$ [18]	0 \$ [22]
Solar thermal collector first order investment cost	208.605 \$/kW [18]	208.605 \$/kW [22]
Solar thermal collector zero-th order investment cost	0 \$ [18]	0 \$ [22]
Electrical storage first order investment cost	191.35 \$/kWh [18]	89.529 \$/kWh [22]
Electrical storage zero-th order investment cost	3457.723 \$ [18]	80.576 \$ [22]
Thermal storage first order investment cost	29.685 \$/kWh [18]	29.685 \$/kWh [18]
Thermal storage zero-th order investment cost	3189.045 \$ [18]	3189.045 \$ [18]
Real interest rate	5.00% [27]	6.25% [28]

The values adopted for the embodied impacts of the equipment are average values from international literature since no considerable differences are expected. These parameters are shown in Table 6.9.

Table 6.9. LCA impact factors of the equipment for the fictitious district optimisation in the Italian and Vietnamese scenarios

Parameter	Value
GWP of the manufacture of cogenerators	4290 kg $CO_{2\text{-}eq}$/kW [29]
GWP of the operation of cogenerators	0.225 kg $CO_{2\text{-}eq}$/kWh [29]
GWP of the manufacture of heat pumps	239.4 kg $CO_{2\text{-}eq}$/kW [30]
GWP of the manufacture of gas boilers	25 kg $CO_{2\text{-}eq}$/kW [29–31]
GWP of the operation of gas boilers	0.264 kg $CO_{2\text{-}eq}$/kWh [29]
GWP of the manufacture of gas-fired absorbing chillers	146.42 kg $CO_{2\text{-}eq}$/kW [30]
GWP of the operation of gas-fired absorbing chillers	0.203 kg $CO_{2\text{-}eq}$/kWh [29]
GWP of the manufacture of photovoltaic systems	3.5 kg $CO_{2\text{-}eq}$/kW [32]
GWP of the manufacture of solar collectors	0.434 kg $CO_{2\text{-}eq}$/kW [33]
GWP of the manufacture of electric storages	76.284 kg $CO_{2\text{-}eq}$/kWh [34]
GWP of the manufacture of thermal storages	8.14 kg $CO_{2\text{-}eq}$/kWh [30]
CED of the manufacture of heat pumps	1250.4 MJ /kW [30]
CED of the manufacture of gas boilers	92.65 MJ /kW [30]
CED of the manufacture of gas-fired absorbing chillers	2338.167 MJ/kW [30]
CED of the manufacture of photovoltaic systems	9464.21 MJ/kW [35]
CED of the manufacture of solar collectors	56.95 MJ/kW [33]
CED of the manufacture of electric storages	540 MJ/kWh [34]
CED of the manufacture of thermal storages	145.297 MJ/kWh [30]

The main difference in LCA impacts lies in the different energy mixes of the two countries. In detail, as shown in Fig. 6.9, the electricity production in Vietnam is still mainly based on coal-fired power plants, although there is also a large share of hydropower, while Italian electricity is mainly produced in combined cycle gas turbines power plants, that are usually more efficient and less impacting.

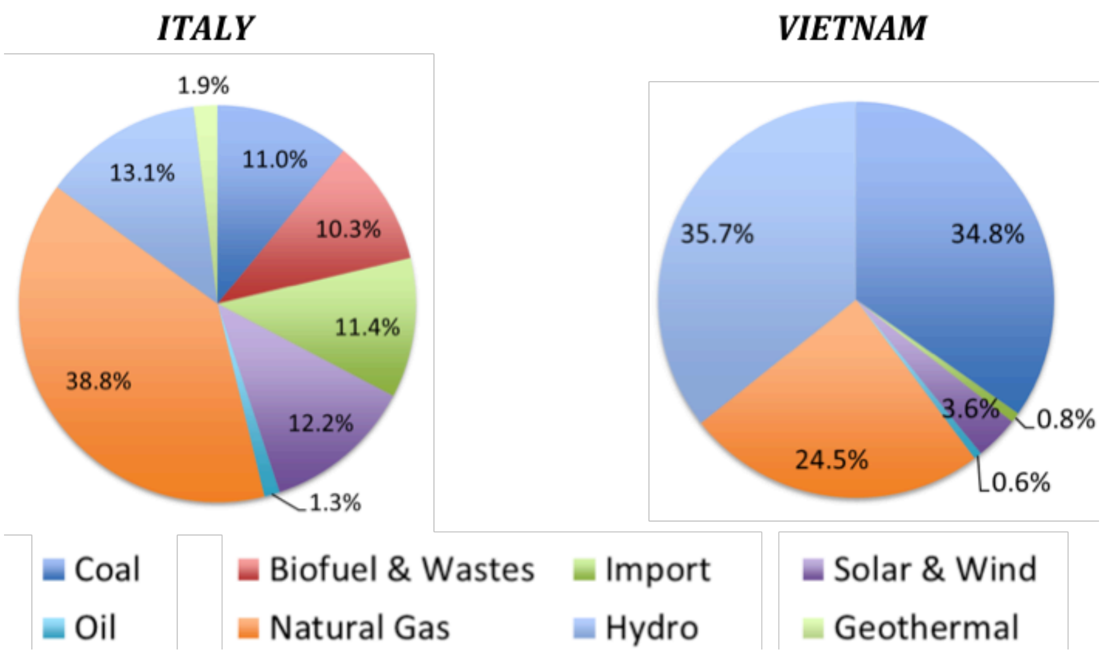

Fig. 6.9. Electricity production mix in Italy [36] *and in Vietnam* [37] *in 2016*

Although the impacts related to electricity production in Italy, as well as most of the Western countries, is available on international databases, no reliable LCA data for the Vietnamese electricity mix were available. Thus, for sake of equality, an estimation of the average CO_2 equivalent emissions of the electricity in Italy and Vietnam were calculated with reference to the methodology developed by the Italian Higher Institute for Environmental Protection and Research (Istituto Superiore per la Protezione e la Ricerca Ambientale, ISPRA), shown in [38]. In detail, the following approach was adopted:

- Collection of data on the electricity production of each country, with details on the energy sources and technologies;
- Conversion of the electricity production into annual equivalent emissions using the average equivalent emission factors from the ISPRA report for the coal, oil and gas-fired power plants. These emission factors take into account the greenhouse effect related to carbon dioxide, methane and nitrogen oxides;
- Calculation of the average specific emission factors for that country dividing the annual equivalent emissions in each country by the total electricity generated in that year.

This approach provides for sure a very rough estimation of the true $CO_{2\text{-eq}}$ emissions of the electricity sectors in Italy and Vietnam since the effect of only the main GHG was considered and only the influence of the use phase of the power plants (electricity production) was considered. Nevertheless, this approach seems the best available to keep the comparability between the two countries. For the CED calculation, since no other approach was identified, the CED for the electricity produced in Italy was drawn from the ELCD database, and the CED for the electricity produced in Vietnam was scaled to the former value according to the ration between the GHG emission factors. Since no LCA data for the natural gas from the grid in Vietnam were also available, the CED was set equal to the lower heating value of the fuel, while the GWP was neglected, considering only the emissions related to the combustion. These data are shown in Table 6.10.

Table 6.10. LCA impact factors of the energy carriers for the fictitious district optimisation in the Italian and Vietnamese scenarios

Parameter	***Italian scenario***	***Vietnamese scenario***
Electricity unit GHG emission factor	325 gCO_2/kWh	513 gCO_2/kWh
Electricity unit CED factor	11.8 MJ/kWh	18.63 MJ/kWh
Natural Gas unit CED factor	2.77E-1 MJ/kWh	2.77E-1 MJ/kWh

6.2.3. Results

The optimisation model allowed obtaining a set of optimal solutions according to the cost and environmental criteria for the two selected locations. Since the scalarization technique adopted for this study converts a MOO is an SOO problem, the Pareto front was identified changing the weights assigned to the two OFs (cost and GWP functions), in order to cover the whole interval between w_{cost} = 0 (environmental optimisation) and w_{cost} = 1 (economic optimisation). Since this is a two-objective optimisation with two conflicting objectives, the worst value of each OF can be identified minimising the other one. Thus, the environmental and economic optimisations were first performed, to gather the worst value of each OF to be used as normalisation factors in the subsequent optimisations.

The Pareto fronts for the Italian and Vietnamese contexts are depicted in Fig. 6.10. The most evident outcome that can be derived is that the optimal solutions in the Italian scenario are both less impacting and cheaper thanks to the higher penetration of renewable energy sources in the electricity production mix. Another evidence is that these fronts are made up of a limited number of solutions, although 17 optimisations were performed for each context. The Italian scenario presents 12 alternatives, although only 5 are visualised in Fig. 6.10, while the 10 Vietnamese scenario related solutions are much more concentrated. It is relatively easy to identify the best compromise solution in these Pareto fronts since a negligible rising in emissions causes huge economic saving in both scenarios. In general terms, having few compromise solutions helps the decision-maker in the identification of the compromise solution to be realized.

Regarding the components' sizes, a comparison between the cost-optimal and the carbon optimal solutions is provided in Table 6.11 and Table 6.12 for the Italian and Vietnamese scenarios, respectively. It is possible to state that some technologies are independent on the optimisation criterion, as the CHP, HP and STC. In detail, CHP is never selected, while HP's and STC's sizes have very high values. In the Italian context, PV and storages are strongly recommended to minimise the greenhouse effect, disregarding the NGB, that is much cheaper than STC instead. In the Vietnamese context, it is economically convenient to store the heating energy from the boiler, while it is environmentally advantageous to use the heating from the boiler to feed the absorbing chiller.

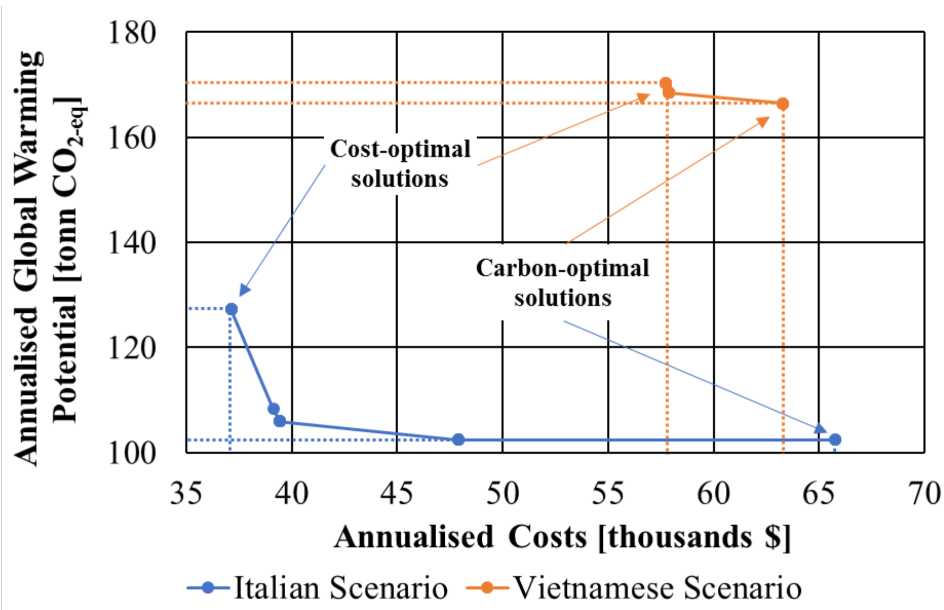

Fig. 6.10. Pareto fronts for the Italian and Vietnamese scenarios

Table 6.11. Cost-optimal and carbon-optimal sizes of equipment and corresponding objective functions values in the Italian context

Quantity	***COST-OPT***	***CARB-OPT***
PV plant [kW_p]	86	124
Cogenerator [kW_{el}]	0	0
Heat Pump [kW_{cool}]	169	169
NG Boiler [kW_{th}]	286	110
Absorbing Chiller [kW_{cool}]	0	0
Solar Collector [kW_{th}]	503	503
Electrical Storage [kWh_{el}]	0	353
Thermal Storage [kWh_{th}]	1,933	3,617
Annualized costs for the cluster [k$/year]	**37**	**66**
Annualized carbon emissions for the cluster [tons CO_2-eq/year]	**127**	**102**
Annualized primary energy demand for the cluster [MJ/year]	**3.14E6**	**2.79E6**

Table 6.12. Cost-optimal and carbon-optimal sizes of equipment and corresponding objective functions values in the Vietnamese context

Quantity	***COST-OPT***	***CARB-OPT***
PV plant [kW_p]	100	100
Cogenerator [kW_{el}]	0	0
Heat Pump [kW_{cool}]	146	146
NG Boiler [kW_{th}]	72	58
Absorbing Chiller [kW_{cool}]	0	163
Solar Collector [kW_{th}]	0	0
Electrical Storage [kWh_{el}]	173	254
Thermal Storage [kWh_{th}]	3,941	2,561
Annualized costs for the cluster [k$/year]	**58**	**63**
Annualized carbon emissions for the cluster [tons CO_2-eq/year]	**170**	**166**
Annualized primary energy demand for the cluster [MJ/year]	**5.11E+06**	**4.30E+06**

In order to verify the robustness of the solution to the number of time steps, the equivalent hours of each seasonal day were progressively reduced from 24 to 12, 6 and 4. Using as a reference the value of the OFs with 24 hours, the percentage variation was plotted in Fig. 6.11. All these values are higher than the 80% of the original result, that may be considered as the same order of magnitude of the errors introduced in the model through the linearization and the steady-state energy and mass balances. Thus, the number of equivalent hours may be successfully reduced without excessively compromising the result of the optimisation.

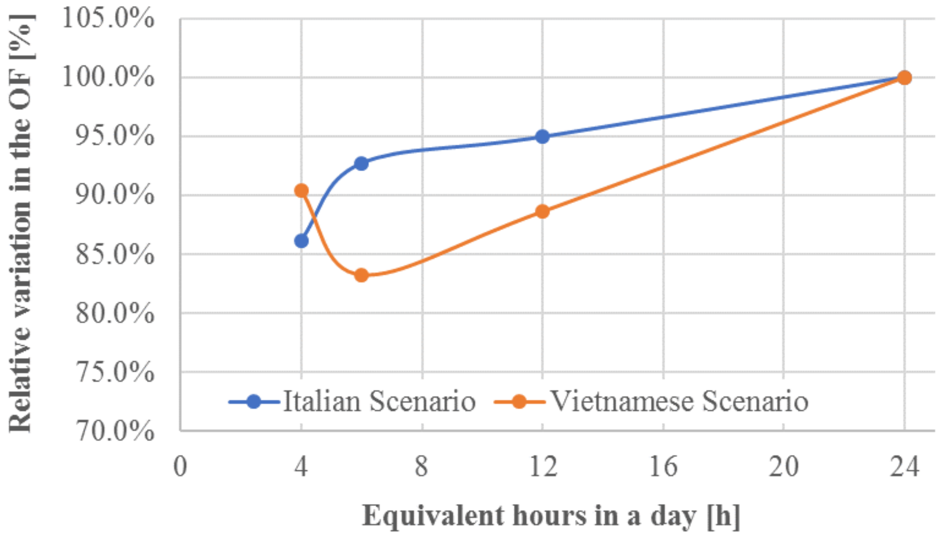

Fig. 6.11. Relative variation in the objective function depending on the number of equivalent hours

6.3. Small island in Mediterranean climate

This case study describes the multi-objective optimisation of the life cycle impacts and costs of the island of Pantelleria. The variables of the problem relate to the simultaneous synthesis, design and operation of the equipment aimed at fulfilling the district's electricity, space heating and cooling demands, DHW and freshwater. Since the island is distant from the mainland, all these demands have to be satisfied locally, so that it is an actual electric island. This case study allowed testing the limits of the assumptions behind the energy hub model, since it neglects the transport losses that might become significant in a case study as big as an island. The local distribution system operator company provided most of the information employed for this case study. The company soon proved to be available to cooperate in research projects and to receive the indications from this study to adapt their business, demonstrating how the importance behind this kind of studies is perceived at industrial level.

6.3.1. Case study description

Pantelleria is an island located in the Strait of Sicily, at about 65 km east of the Tunisia coasts in the Mediterranean Sea. With an extension of roughly 84.5 km^2, it is the largest between the fourteen small islands belonging to Sicily. The territory is mountainous and has a volcanic origin. The position of the island in the Strait of Sicily is shown in Fig. 6.12, where also a map of the available solar radiation is provided, while a satellite view of the island is shown in Fig. 6.13. Pantelleria is a national park, mainly due to the preservation of the landscape and the typical constructions, the

"Dammusi", datable to about 835 AD. This aspect strongly limited the installation of RES systems in the island in the past, until the Italian government emitted a decree on 14 February 2017 promoting renewable energies in small islands. The decree sets specific targets for each island; in detail, the target for Pantelleria is the installation of 2720 kW of electricity from RES plants and 3,130 m^2 of STC [39]. These targets may be easily attained, since the RES installation potential in Pantelleria is very high, covering solar, wind, geothermal and biomasses [40]. In detail, according to the World Solar Atlas, the global solar radiation on the horizontal plane in Pantelleria is about 1865 kWh/m^2 [41].

To date, the thermal RES systems installed in the island are 281.89 m^2 of STC, while the electricity is produced by 2 small wind turbines with a total capacity of 32 kW, and by many PV plants with different rated sizes, covering loads of both private customers and big loads as a school, the hospital and the airport, with a cumulated peak power equal to 647.5 kW [42]. Furthermore, the island hosts a prototype for the production of electricity from wave energy with a rated size of 3.2 kW since 2015 [43].

Fig. 6.12. Map with the average solar radiation indicating the position of Pantelleria [41]

Fig. 6.13. Satellite view of Pantelleria

Neglecting these RES plants, the current electricity generation system of Pantelleria is mainly based on eight diesel oil generators with a cumulated installed power of about 25 MW, that is largely oversized if compared to the average demand, ranging between 2 and 8 MW. The diesel oil consumption related to the electricity production in Pantelleria was over 8,000 tons in 2018 and were used to generate 36.5 GWh.

The electricity in Pantelleria is produced, distributed and sold by a vertically integrated company. Given the difficulties in managing this small islanded system, the Italian government recognizes an incentive to the electric company, that in 2015 accounted for more than 9 million € [44]. Regarding the thermal uses, the natural gas or district heating/cooling infrastructures are absent, forcing the local population to fulfil their air conditioning and DHW demands mainly through electric boilers or air-to-air heat pumps.

The study aims at investigating the potential of energy saving and reduction of the environmental impacts related to the optimal management of the local power plant and to the installation of RES and storage systems. Furthermore, since the electric company and the management of the local desalination (DES) unit aim at cooperating, the study also assessed the energy flexibility potential of the local DES plant for the production of freshwater. Another step forward was included, assessing also the flexibility of the domestic users through the optimal management of the Electric Resistance Water Heaters (ERWH).

6.3.2. Input data

In order to optimise the energy system of Pantelleria, several data were collected on both local production and demand. A complete overview of the data collection is available in [44], while an extract being reported here for the necessities of this thesis. Regarding the energy production, the rated sizes of the eight thermal generators composing the local power plant and the cumulated RES capacity is summarised in Table 6.13. It is possible to see that the current RES capacity is negligible to thermal power.

Table 6.13. Rated capacity of generation units in Pantelleria

Generation units	Rated power [kW]	Rated power [%]
Diesel generator 1	1,250	5%
Diesel generator 2	5,040	20%
Diesel generator 3	3,070	12%
Diesel generator 4	2,920	11%
Diesel generator 5	3,089	12%
Diesel generator 6	2,648	10%
Diesel generator 7	1,760	7%
Diesel generator 8	5,220	20%
RES	682.7	3%
TOT Diesel generators	*24,997*	*97%*
TOT Diesel + RES	*25,679.7*	*100%*

Regarding the energy demand, all the main final uses can be related to power consumption, while LPG is often employed for cooking. The power load may be equally split among residential demand, services and offices demand, and industrial demand. The annual trend of power consumption has a strong variation, mainly due to the tourists increasing the local population up to 135%, with the peak being during summer. The electrical company of the island provided the power generated by the thermal generators as monthly standard days with hourly detail. Data are available in Table 6.14 and were plotted in Fig. 6.14. Since the RES generation on the island is limited, this trend can be considered as an optimal estimation of the island electricity demand. The maximum power demand occurs in August, because of the massive presence of tourists, while the month with minimum demand is May, as tourists' presence is not relevant and there is no need of air conditioning. Since space heating and cooling, DHW and freshwater demands are all fulfilled through electricity, no further demand trends were collected. The hourly detail was considered to be an adequate timestep for the optimisation, thus twelve optimisations on the monthly standard days were performed.

Table 6.14. Power generated in the monthly standard days by thermal generation groups in Pantelleria

Hour	Jan	Feb	Mar	Apr	May	Jun	Jul	Aug	Sep	Oct	Nov	Dec
00:00	3,532	2,598	2,783	2,094	2,573	2,954	3,274	4,509	4,038	2,647	2,853	2,710
01:00	2,382	1,895	2,213	1,597	2,321	2,641	2,961	4,344	3,834	3,347	2,069	1,960
02:00	2,281	1,696	2,014	1,299	2,131	2,601	2,879	3,944	3,533	3,098	2,055	1,952
03:00	2,182	1,796	1,920	1,264	1,972	2,449	2,784	3,662	3,640	2,997	2,001	1,970
04:00	2,232	1,846	1,871	1,279	1,722	2,499	2,716	3,293	3,328	3,047	1,965	1,854
05:00	2,231	1,946	1,819	1,352	1,631	2,489	2,476	3,248	3,433	3,047	1,973	1,862
06:00	2,432	2,046	2,264	1,561	1,418	2,453	2,375	3,399	3,632	3,147	2,349	2,264
07:00	2,840	2,146	2,426	2,150	1,322	2,854	2,625	3,502	3,470	2,953	2,196	2,406
08:00	2,532	3,248	3,175	2,496	1,746	3,255	3,536	3,969	4,023	3,218	2,795	3,015
09:00	2,718	3,296	2,861	2,545	2,819	3,386	3,690	4,751	4,185	3,495	2,896	3,256
10:00	2,790	2,986	2,963	2,966	2,864	3,269	3,901	5,064	4,010	3,697	2,951	3,150
11:00	2,575	3,038	2,871	2,604	2,653	3,176	3,910	4,693	4,234	3,498	2,854	2,935
12:00	2,561	3,098	2,870	2,555	2,438	3,314	3,819	4,496	4,285	3,496	2,854	2,999
13:00	2,415	3,096	2,784	2,519	2,439	3,285	3,926	4,462	4,735	3,593	2,951	3,305
14:00	2,615	2,791	2,658	2,394	2,338	2,986	3,740	4,207	4,685	3,693	2,801	3,009
15:00	2,925	2,769	2,605	2,416	2,153	3,050	3,39	3,993	4,733	3,343	2,849	2,804
16:00	2,865	2,920	2,639	2,292	2,141	3,191	3,451	3,894	4,634	3,292	2,776	3,552
17:00	3,635	3,096	2,681	2,545	2,147	3,543	3,546	4,111	4,974	3,493	3,158	3,709
18:00	4,120	3,696	2,783	2,651	2,414	3,558	3,673	4,193	5,337	3,793	3,813	4,059
19:00	4,438	4,298	3,639	2,696	2,742	3,716	3,775	4,997	5,533	4,393	3,835	4,239
20:00	4,723	4,398	4,440	3,517	2,838	3,988	3,828	5,927	5,837	3,793	4,135	4,511
21:00	4,421	4,248	4,469	3,696	3,249	4,441	4,428	6,854	5,438	3,493	3,928	4,145
22:00	3,871	3,846	3,769	3,254	3,204	4,141	3,981	5,622	4,888	3,193	3,834	3,906
23:00	3,375	2,998	3,529	2,480	2,689	3,841	3,696	5,051	4,533	2,793	3,431	3,349

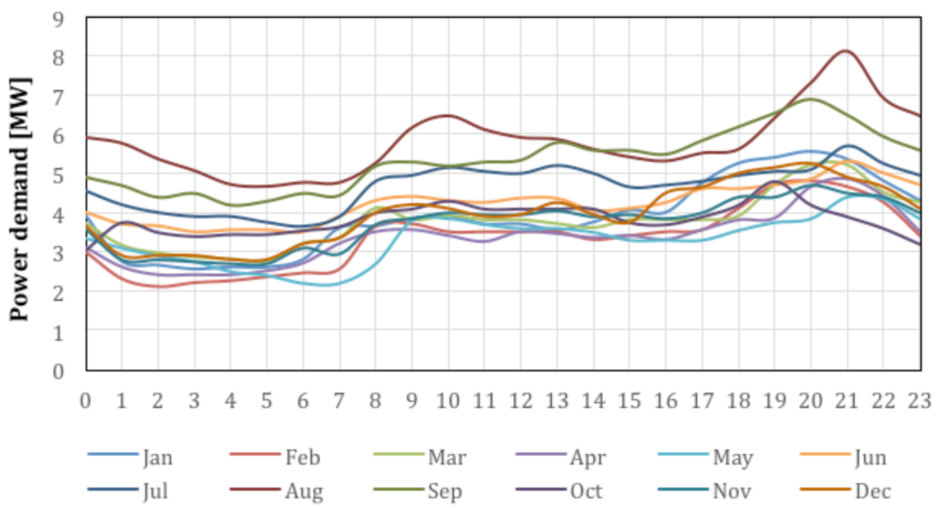

Fig. 6.14. Hourly trend of power generated in the monthly standard days by thermal generation groups in Pantelleria

Further investigating the electricity demand to identify the targets of the flexibility services, the highest contributions were ascribed to DHW production and the DES plant, requiring about 3800 MWh and 3300 MWh every year, respectively. In detail, the high share for DHW is related to the widespread diffusion of ERWH, while the DES system has to produce about 870,000 m^3 of freshwater annually to cover the demand of the residents and tourists. The electricity demand of both of these loads was considered for the flexibility services, setting a daily requirement to be fulfilled and letting the optimiser decide when each equipment had to be operated. In detail, the optimisation assumes the availability of remotely controlled ERWH, since this technology is already available on the market [44].

The daily power consumption related to DHW and freshwater production in each month was estimated from literature data. In detail, the power demand for DHW was estimated from data available on the Sustainable Energy Action Plan of the island [45], while the freshwater demand was estimated from the DES monthly power consumption, provided by the company, and using an average conversion factor between electricity demand and freshwater production equal to 0.25 m^3/kWh, as suggested by the company. The values adopted for DHW and freshwater daily requirements are provided in Table 6.15. A uniform distribution of these demands over each hour of the month was assumed. In this way, a daily target to be satisfied was identified, and the island power demand was reduced, removing the fraction required for DHW and DES, thus including the electricity and space conditioning uses and was modelled as a fixed quantity.

Table 6.15. DHW and freshwater daily demands in monthly standard days

Month	***DHW demand [kWh] (Authors elaborations on*** [45]***)***	***Freshwater demand [m³]***
January	8,470	2,300
February	9,325	2,100
March	8,515	2,100
April	9,661	2,500
May	9,677	2,500
June	11,849	2,700
July	12,537	3,100
August	15,827	3,450
September	12,203	2,650
October	9,342	1,600
November	9,239	1,500
December	8,463	1,950

For the exploitation of flexibility services, a storage system for both the demands (DHW and freshwater) was necessary. Thus, since the ERWH are inherently hot water storages, these components were modelled as Hot Water Storage Systems (HWSS) having a power flow in input. For the DES system, an interview to the company allowed to know that the plant dispatches the freshwater produced to a Water Storage System (WSS) 5,000 m^3 capacity.

According to this analysis of the existing energy system of Pantelleria, the reference schematic employed the cluster model in the AS-IS scenario is shown in Fig. 6.15. As for the previous case, a unique component for each technology was modelled, representing the equivalent of many analogous components widespread for the island. The unique exception to this assumption was done for the power plant, where all the eight Diesel Generators (DG) were modelled. Although the technology for space heating and cooling does not influence the results of the present analysis, the presence of a heat pump (HP) in the scheme was assumed. The TO-BE scenario, involving the installation of PV, STC and Electricity Storage System (ESS) and the flexibility of DES and HWSS (Fig. 6.16), aims at identifying the optimal combination of components (synthesis stage), their optimal sizes (design stage) and their optimal operating schedule (operation stage) minimising the annualised costs and the GHG equivalent emissions for meeting the energy demand in Pantelleria.

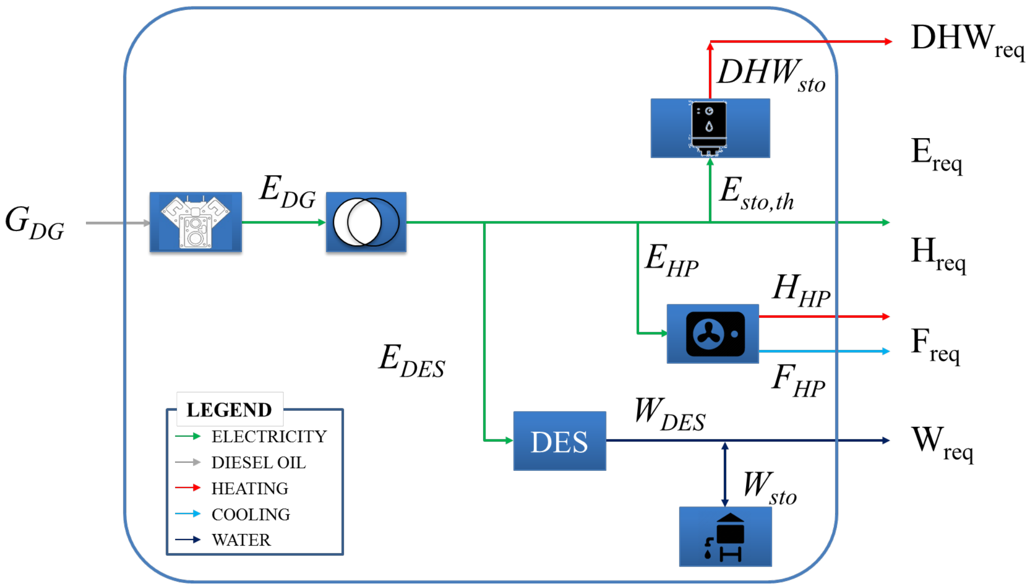

Fig. 6.15. Schematic of the energy system of Pantelleria in the AS-IS scenario

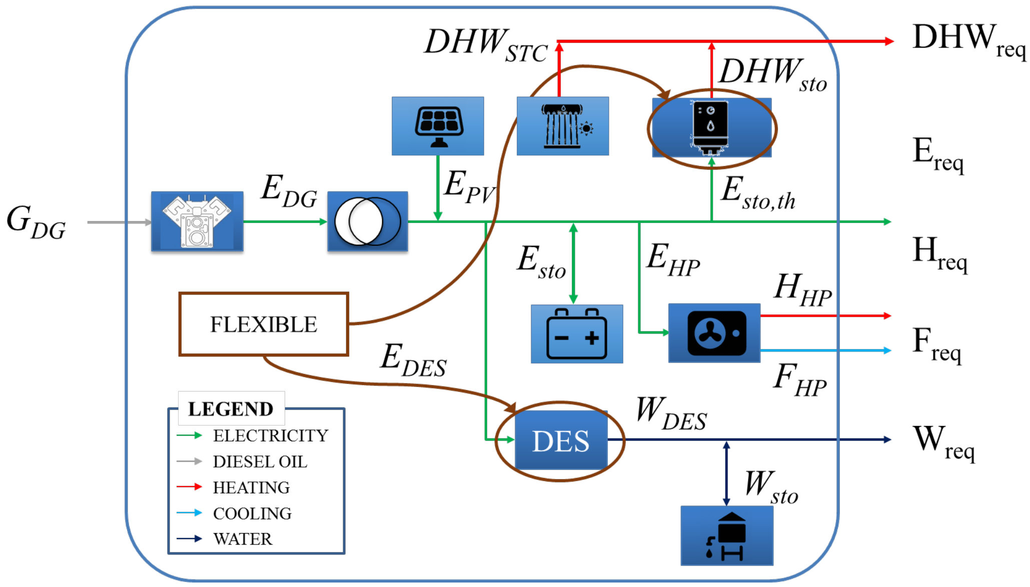

Fig. 6.16. Schematic of the energy system of Pantelleria in the TO-BE scenario

Since DG, DES and HWSS are already installed, it is assumed that they are already suitable for meeting the peak load. Thus, only the operation stage of these components was investigated. A different approach was adopted for the WSS, assuming that the DES flexibility may benefit from a higher capacity. The space heating and cooling equipment were neglected. Furthermore, it is worth to underline that the thermal storage, a necessary component for the STC systems, is assumed to be already available exploiting the existing electrical boilers.

Since the installation of renewable technologies is subjected to constraints due to landscape preservation, the maximum available surface to be used as upper bound for the optimisation problem was estimated according to the methodology shown in [46]. In detail, the surface of rooftops in residential buildings was estimated from satellite pictures in this reference to be equal to about 246,000 m^2, that is reduced by 40% to take into account for the necessary distance from edges and by a further 25% due to the reduced surface availability for antennas or water tanks, obtaining about 110,846 m^2 available. For the availability in industrial buildings, 4500 m^2 available from rooftops and shelters were estimated. This total surface was split as 76,900 m^2 available for PV and 38,450 m^2 dedicated to STC installation.

For the average solar radiation, the monthly average solar radiation was calculated from the hourly annual data from the JRC Typical Meteorological Year generator [11], and the resulting values are provided in Table 6.16. The solar radiation trend was assumed to follow a daily sinusoidal path, with sunrise at 7 a.m. and sunset at 6 p.m.

Table 6.16. Average solar radiation in monthly standard days

Month	**Average solar radiation [kWh/(m^2 day)]**
January	3.74
February	6.08
March	6.08
April	7.13
May	9.05
June	10.18
July	10.03
August	9.44
September	7.61
October	6.31
November	5.25
December	3.93

Most of the efficiencies of the equipment were assumed to be constants, in order to keep the linearity of the problem, adopting reasonable average values. Nevertheless, since one of the aims of the study was to optimise the operation of diesel generators, the efficiency variation at a partial load of these components was taken into account. To reach this aim, the true efficiency trend, estimated through data provided by the company, was simplified assuming four average values in four regions. The estimated efficiency variation with load and the average values are shown in Fig. 6.17. A recap of the technical parameters employed for the study, describing the performance of the components, is provided in Table 6.17.

Regarding the objective functions, the annualised cost and GWP for the operation of the island were minimised, while the annualised CED was also assessed. Costs and impacts related to the maintenance were not included in the economic objective function, since they are assumed to be negligible for the new equipment and to be independent on the optimisation for diesel generators. To assess the total cost for the community, even subsidies to RES and the remuneration for the flexibility service from DES and HWSS were ignored. The unit cost of the gas oil was provided by the company, while average values for the other costs and impacts from the literature were employed for the other terms. The parameters adopted for the economic objective function are shown in Table 6.18, while the LCA unit impact factors are reported in Table 6.19.

It is worth to mention that, in this study, the economic optimisation is also oriented to the reduction of greenhouse gases emissions and primary energy use during the running phase of the system, since every action aims at reducing the diesel generators consumption, increasing its efficiency through the flexibility of DES and DHW storages or replacing part of its generation through renewables.

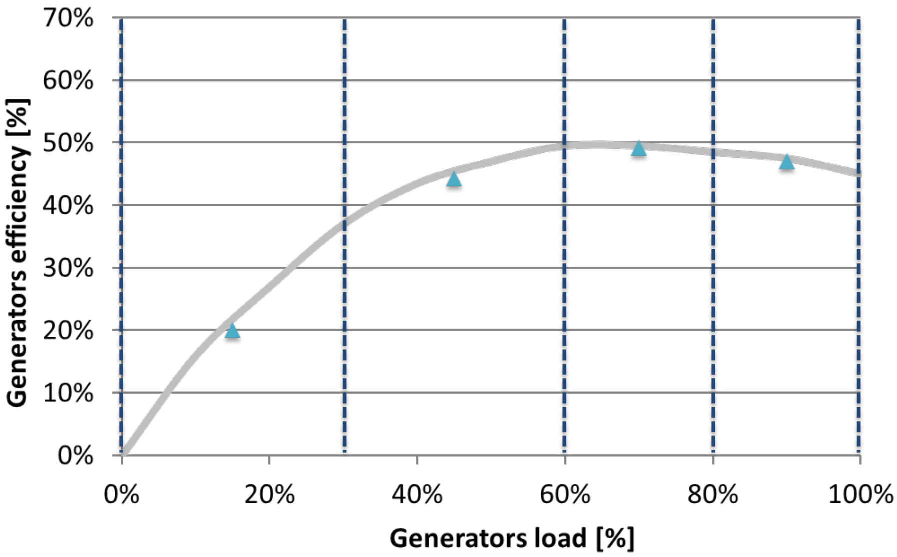

Fig. 6.17. Diesel generators efficiency vs. load estimated trend and piecewise averaging

Table 6.17. Technical parameters employed for the optimisation of the energy system of Pantelleria

Parameter	Value
Diesel generators efficiency at part load between 0% and 30%	20.0% [44]
Diesel generators efficiency at part load between 30% and 60%	44.3% [44]
Diesel generators efficiency at part load between 60% and 80%	49.2% [44]
Diesel generators efficiency at part load between 80% and 100%	47.0% [44]
Freshwater storage initial available capacity	5000 m^3 [44]
Lower heating value of diesel oil	41.025 MJ/kg [44]
Transformer efficiency	99% [44]
Electricity consumption for the production of one cube meter of freshwater	4 kWh/ m^3 [44]
Electricity consumption per each desalination unit	200 kW [44]
Photovoltaic module efficiency	17.11% [18]
Photovoltaic Balance of Plant efficiency	95% [44]
Photovoltaic system dimensions	$1.65 \cdot 0.992$ m^2 [18]
PV maximum available area	76,900 m^2
Solar thermal collector zero-loss efficiency	79.7% [18]
Solar thermal collector first-order heat loss coefficient	3.18 W/(m^2 K) [18]
Solar thermal collector second-order heat loss coefficient	0.008 W/(m^2 K^2) [18]
Solar thermal collector average efficiency (ΔT = 30 °C)	69.4%
Solar thermal collector dimensions	$1.987 \cdot 1.27$ m^2 [18]
Solar collector maximum available area	38,450 m^2
Electrical storage charging efficiency	97% [15]
Electrical storage discharging efficiency	97% [15]
Electrical storage Depth of Discharge	20% [15]
Electricity storage size upper bound	10,000 kWh
DHW storage charging efficiency	95% [44]
DHW storage discharging efficiency	100% [44]
DHW storage self-discharge rate (thermal losses)	1%/h [44]

Table 6.18. Economic parameters employed for the optimisation of the energy system of Pantelleria

Parameter	Value
Diesel generators operating cost (diesel oil supply cost)	650 €/m^3 [44]
PV system investment cost	527 € [18]
STC investment cost	650 € [18]
Investment cost of electrical storage	165 €/kWh [18]
Investment cost of electrical storage	2974 € [18]
Electrical storage first order investment cost	165 €/kWh
Electrical storage zero-th order investment cost	2974 €
Water storage system investment cost	450 €/m^3 [44]
Real interest rate in the Italian energy sector	5% [27]
Useful life of PV system	25 years [18]
Useful life of STC	15 years [20]
Useful life of electrical storage	7 years [21]
Useful life of water storage	25 years [44]
Capital recovery factor of PV system	0.071
Capital recovery factor of STC	0.096
Capital recovery factor of electrical storage	0.173
Capital recovery factor of water storage	0.071

Table 6.19. LCA impact factors employed for the optimisation of the energy system of Pantelleria

Parameter	Value
Diesel generators operating GWP	0.225 kg $CO_{2,eq}$/kWh [29]
Photovoltaic system embodied GWP	3.5 kg $CO_{2,eq}$/kW [32]
Solar thermal collector embodied GWP	0.3245 kg $CO_{2,eq}/m^2$ [33]
Lithium-ion electricity storage embodied GWP	21.19 kg $CO_{2,eq}$/MJ [34]
Photovoltaic system embodied energy	1619 MJ/m^2 [35]
Solar thermal collector embodied energy	39.55 MJ/m^2 [33]
Lithium-ion electricity storage embodied energy	540 MJ/kWh [34]

As already stated, the standard operating year was simulated with 12 monthly standard days with an hourly detail. Thus, the number of simulated operating hours is 288, with a total number of 12,674 continuous variables and 867 discrete variables. The continuous variables are related to the power flows from renewables and storages, while the discrete variables are the power flows from the diesel generators, the power consumption of the DES unit and the status of the electrical storage. Considering upper and lower bounds of the discrete variables, the search space of this problem is composed of $1.3 \cdot 10^{382}$ alternative combinations. Since this search space would lead to a prohibitive computational time, the problem was solved in this way:

- Run the twelve monthly optimisations, obtaining optimal solutions for synthesis, design, and operation of each variable in each standard monthly day;
- Compare the optimal sizes of equipment and select the most common;
- Extend the results to the whole year repeating the optimisation by fixing the most common optimal sizes.

The optimisation problem was thus simplified, reducing the size of the problem to 1,058 continuous variables and 75 discrete variables, with $4.5 \cdot 10^{38}$ combinations for each optimisation. Although the solution obtained through this approach is a sub-optimal solution to the problem, simulations showed that results change by less than 9%. Since the objective functions are non-conflicting, the identification of the Pareto front was not required. Instead, the simulations were repeated minimising only the annual cost or the annual GWP, with results being quite similar.

6.3.3. Results

6.3.3.1. Economic optimisation

The annual cost minimisation shows that the installation of PV, STC and ESS in Pantelleria would be highly profitable. PV size ranges between 4.8 and 9.7 MW, with smaller sizes being installed during summer standard days when solar radiation is higher. The DES unit is consequently activated mainly during the peak hours of PV production. STC systems are also massively installed, covering almost totally the DHW demand, with HWSS being hardly employed. The ESS optimal size often exceeds 7.8

MWh and is equal to the upper bound between May and October. Instead, the combination of low solar radiation and relatively low demands in November, December and January makes the direct consumption of the PV electricity more convenient. The installation of further water storage capacity was always ignored.

Since all of these components appear to be cost-optimal, the highest values of the optimal sizes of PV, STC and ESS, equal to 9.7 MW, 3230 m^2 and 10 MWh, respectively, were selected as optimal. Repeating the optimisations with these fixed values, the annual cost for the operation of the system was reduced from 6.2 M€/year to 3.5 M€/year (43% of reduction), including the annualized installation cost for equipment. The corresponding annualized equivalent GHG emissions were also highly reduced, decreasing from 25 Mtons of $CO_{2\text{-eq}}$/year in the AS-IS scenario (for the diesel generators operation) to 6.4 Mtons of $CO_{2\text{-eq}}$/year (74% of reduction). The annualised primary energy consumption was also highly reduced. Using data from 2018 for the AS-IS scenario, 8115 tons of gas oil were burned in the power plant, corresponding to 332,934 GJ/year of primary energy. In the cost-optimal scenario, the annual CED was equal to 105,024 GJ/year (-68%), with 100,579 GJ/year being related to the power plant operation. In the following Fig. 6.18 – 6.29, the twelve daily trends of the main power flows in the island are shown.

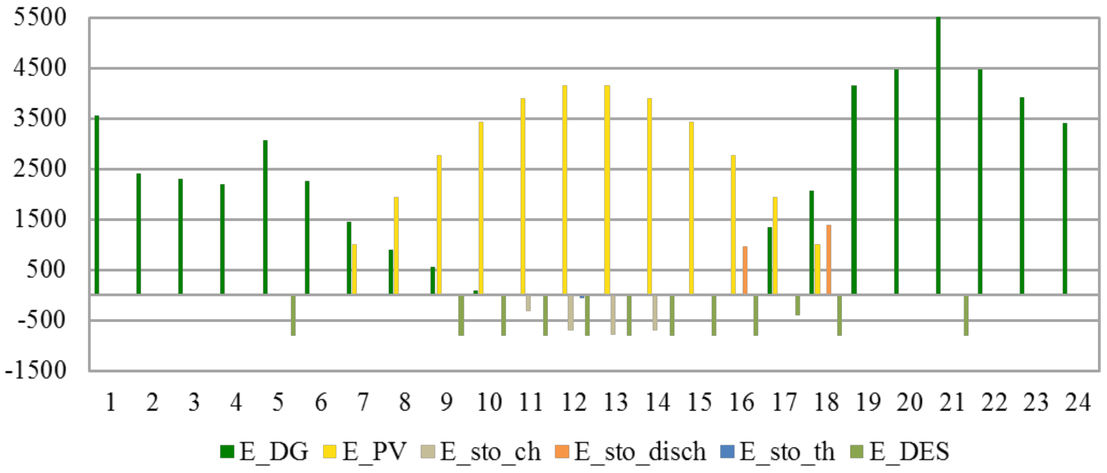

Fig. 6.18. Power flows in the standard day of January for the cost-optimal solution

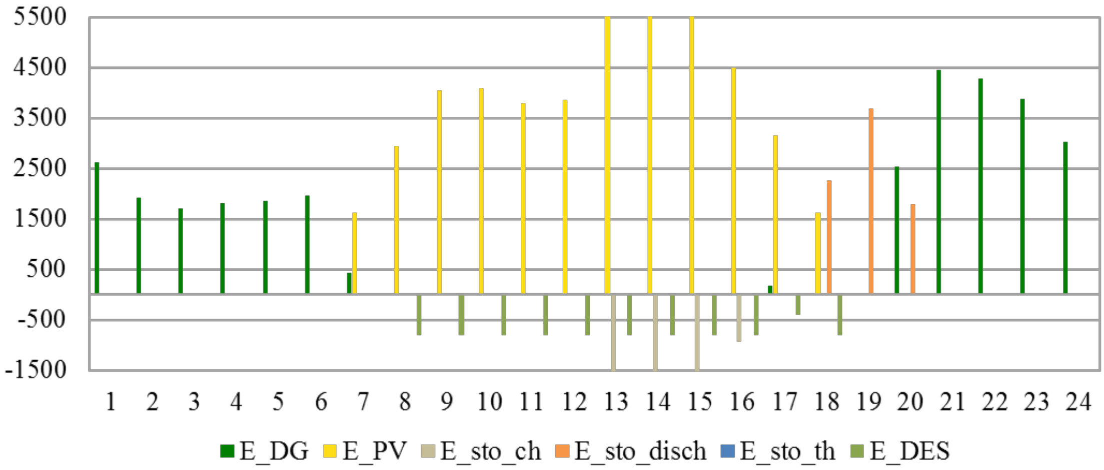

Fig. 6.19. Power flows in the standard day of February for the cost-optimal solution

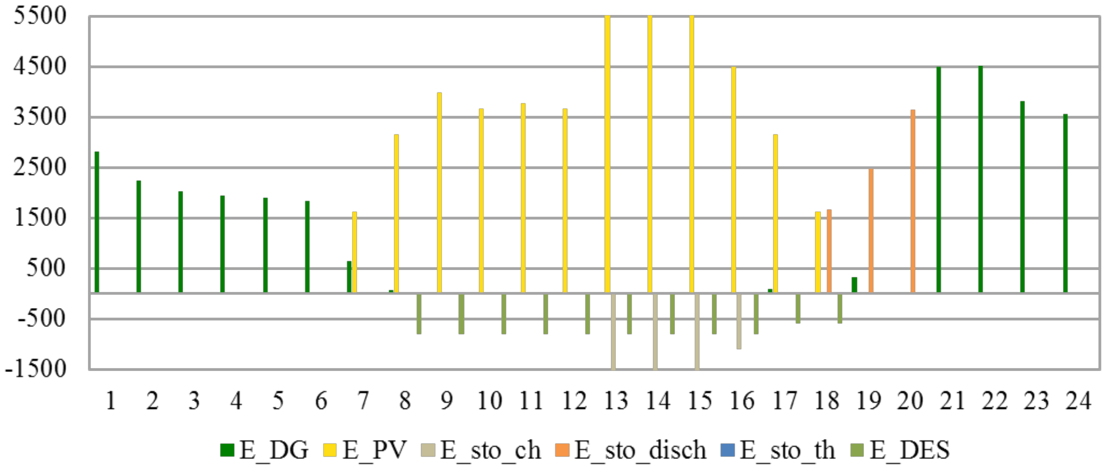

Fig. 6.20. Power flows in the standard day of March for the cost-optimal solution

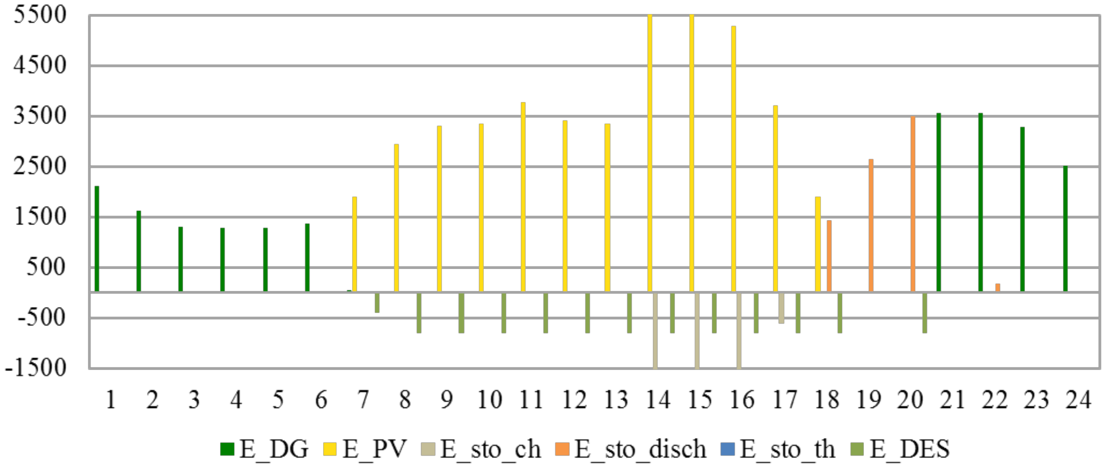

Fig. 6.21. Power flows in the standard day of April for the cost-optimal solution

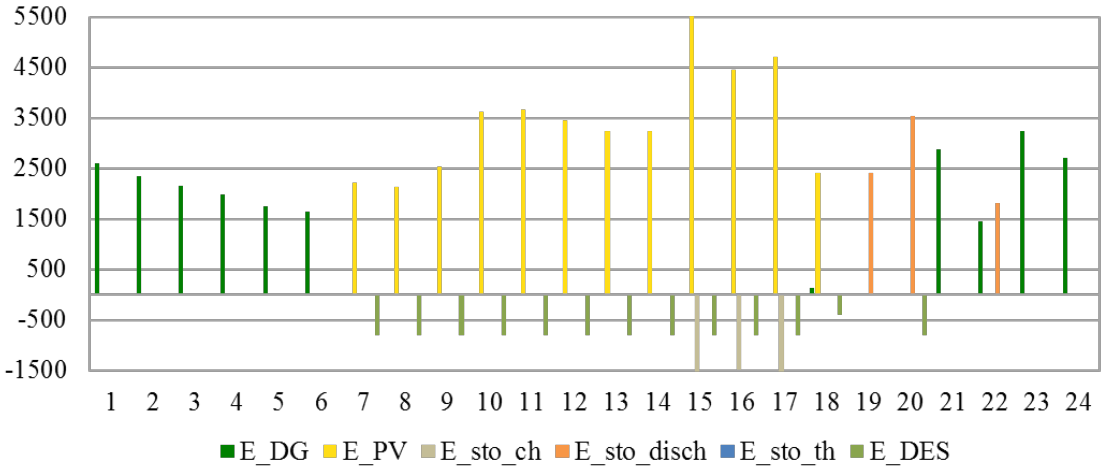

Fig. 6.22. Power flows in the standard day of May for the cost-optimal solution

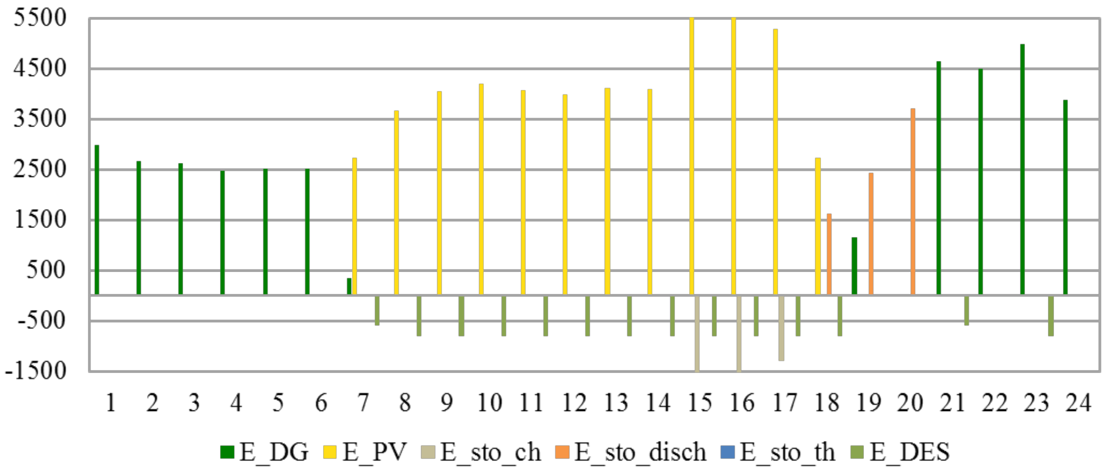

Fig. 6.23. Power flows in the standard day of June for the cost-optimal solution

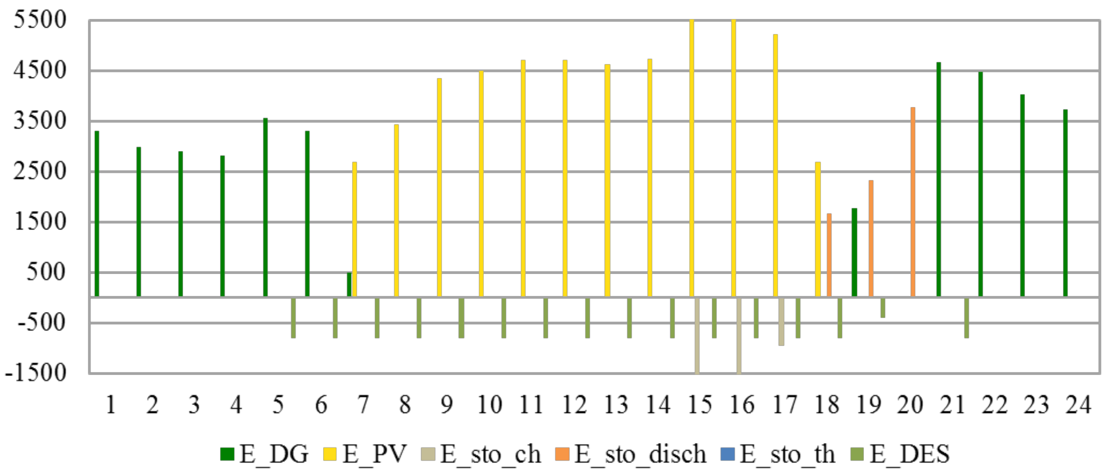

Fig. 6.24. Power flows in the standard day of July for the cost-optimal solution

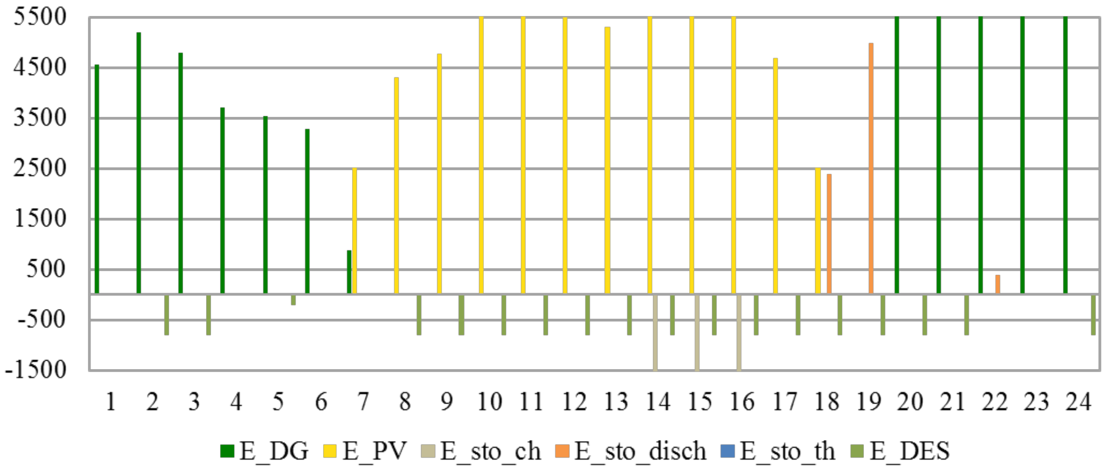

Fig. 6.25. Power flows in the standard day of August for the cost-optimal solution

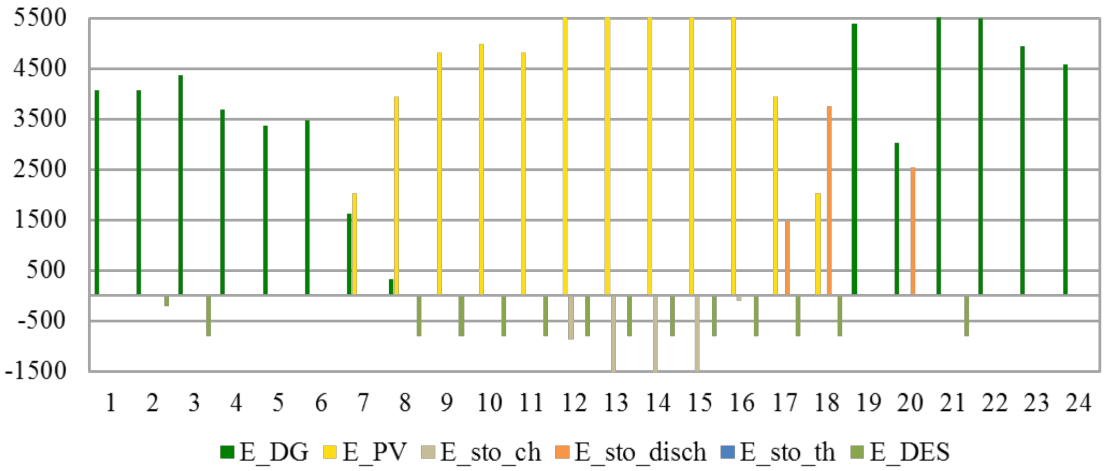

Fig. 6.26. Power flows in the standard day of September for the cost-optimal solution

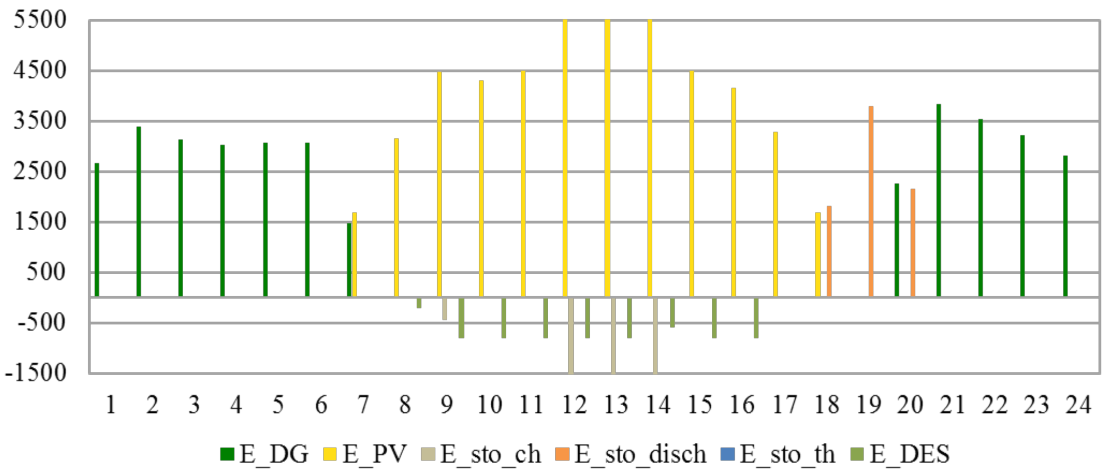

Fig. 6.27. Power flows in the standard day of October for the cost-optimal solution

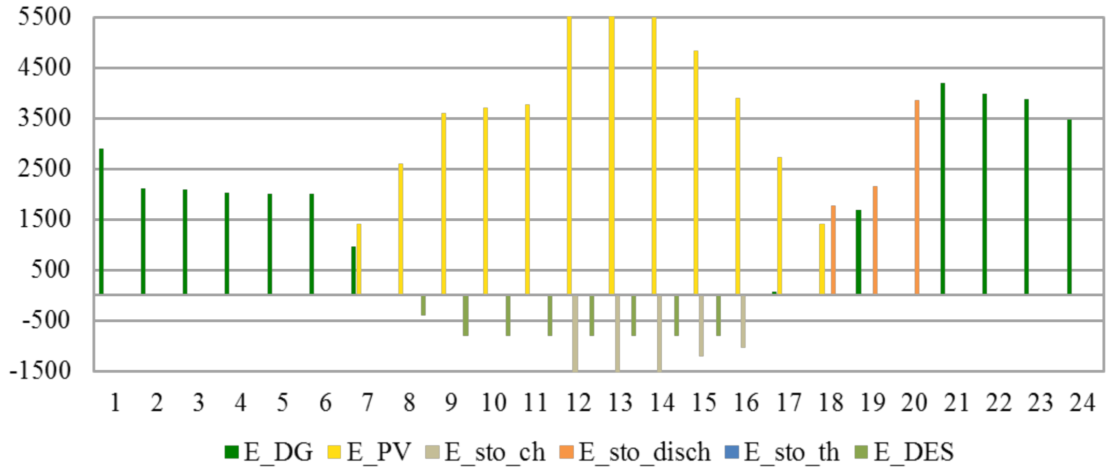

Fig. 6.28. Power flows in the standard day of November for the cost-optimal solution

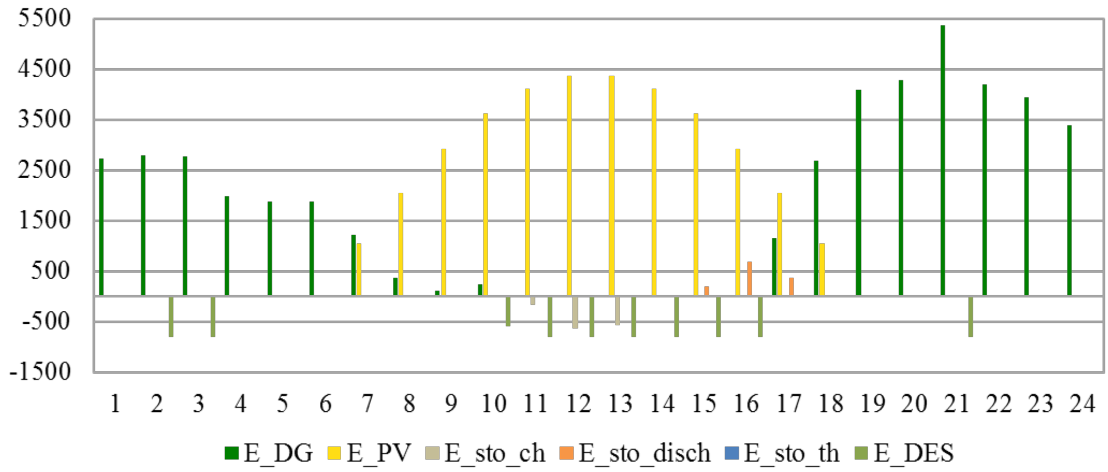

Fig. 6.29. Power flows in the standard day of December for the cost-optimal solution

6.3.3.2. Environmental optimisation

The minimisation of the annualised equivalent GHG emissions of the energy system of Pantelleria converged to an unexpected optimal solution. In detail, for the fulfilling of the DHW requirement, the installation of the STC was disregarded in favour of the employment of the HWSS, that is fed during the day through the electricity produced by PV, as well as the DES unit. Consequently, the optimal sizes of PV and ESS were almost always equal to the upper bounds, equal to 13.2 MW and 10 MWh, respectively. This solution may seem unusual since solar heating is often considered as an easy and "green" way to produce DHW.

Among the twelve optimisations, the optimal sizes were different only in May, when the low electrical load does not justify a massive PV installation, and in January and December, when the solar radiation is minimum. Thus, the optimisations in these three months were repeated with fixed component sizes. The resulting annual emissions, equal to 25 Mtons of $CO_{2\text{-eq}}$/year in the AS-IS scenario for the diesel oil combustion, were reduced to 6.1 Mtons of $CO_{2\text{-eq}}$/year (75% of reduction), also including the embodied impacts of the PV and ESS. Similarly, the annual CED was reduced from 332,934 GJ/year to 101,185 GJ/year, resulting in a reduction equal to 70%. Since the reduction of the impacts is strictly related to the diesel generators operation, the annualized cost decreased from 6.2 M€/year to 3.8 M€/year (39% of reduction).

The twelve daily trends of the main power flows in the carbon-optimised island are shown in Fig. 6.30 – 6.41.

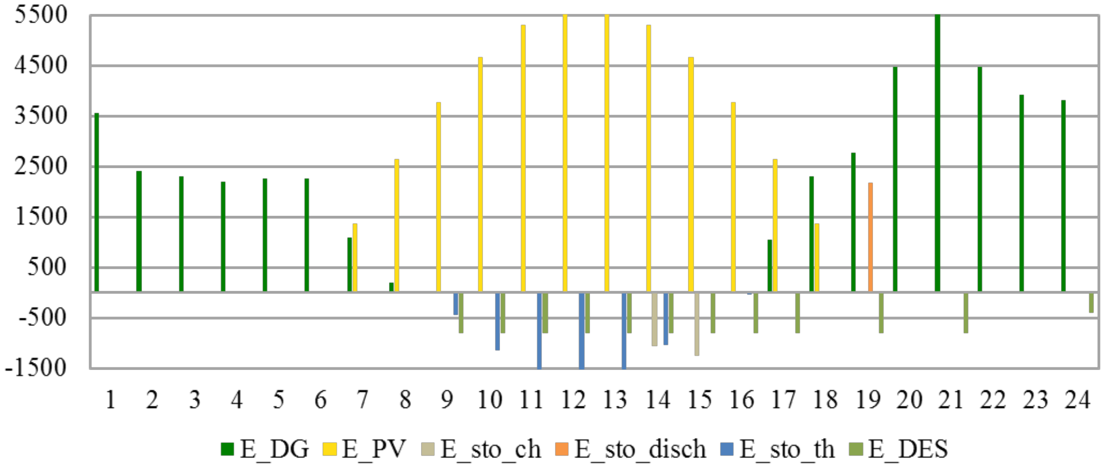

Fig. 6.30. Power flows in the standard day of January for the environmentally-optimal solution

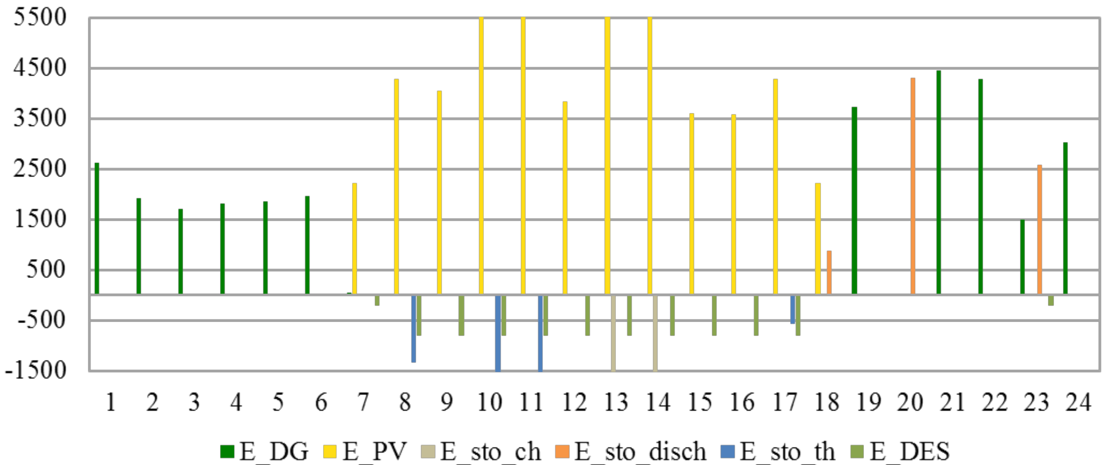

Fig. 6.31. Power flows in the standard day of February for the environmentally-optimal solution

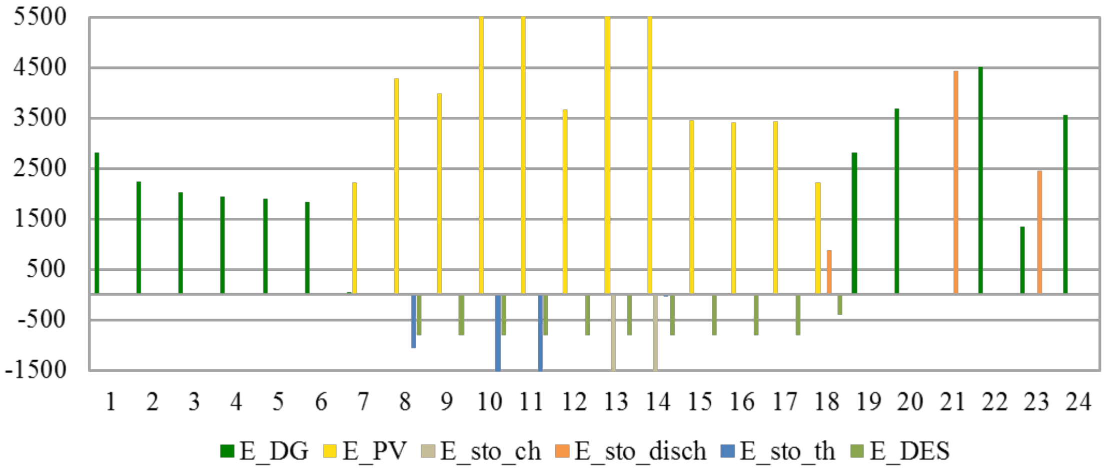

Fig. 6.32. Power flows in the standard day of March for the environmentally-optimal solution

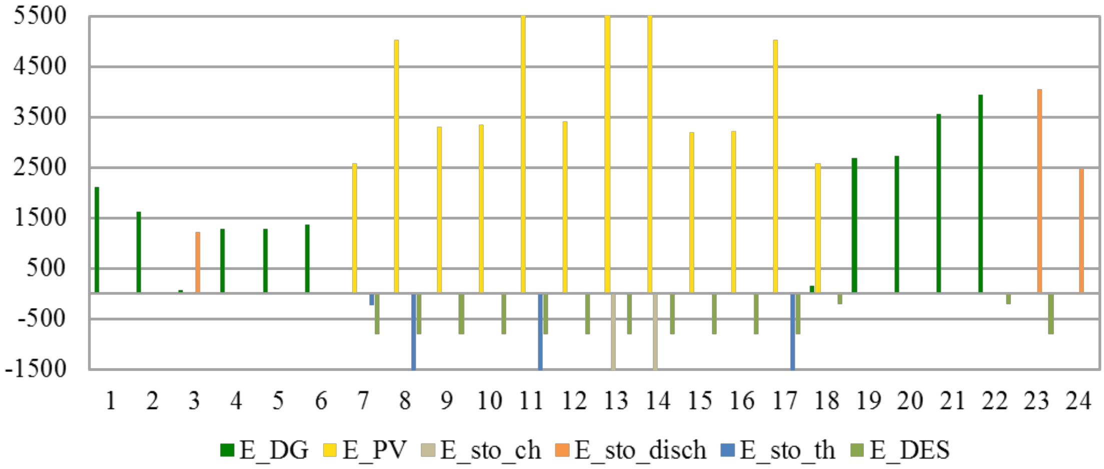

Fig. 6.33. Power flows in the standard day of April for the environmentally-optimal solution

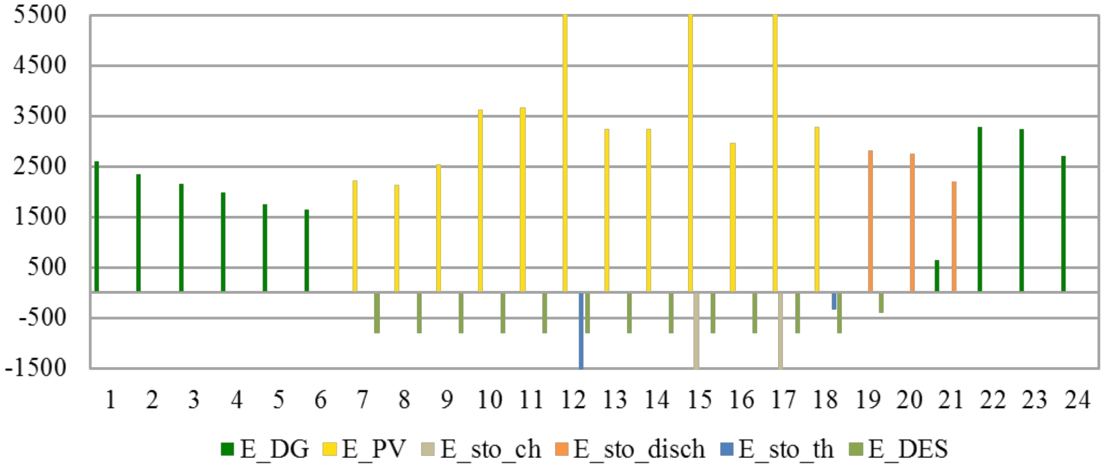

Fig. 6.34. Power flows in the standard day of May for the environmentally-optimal solution

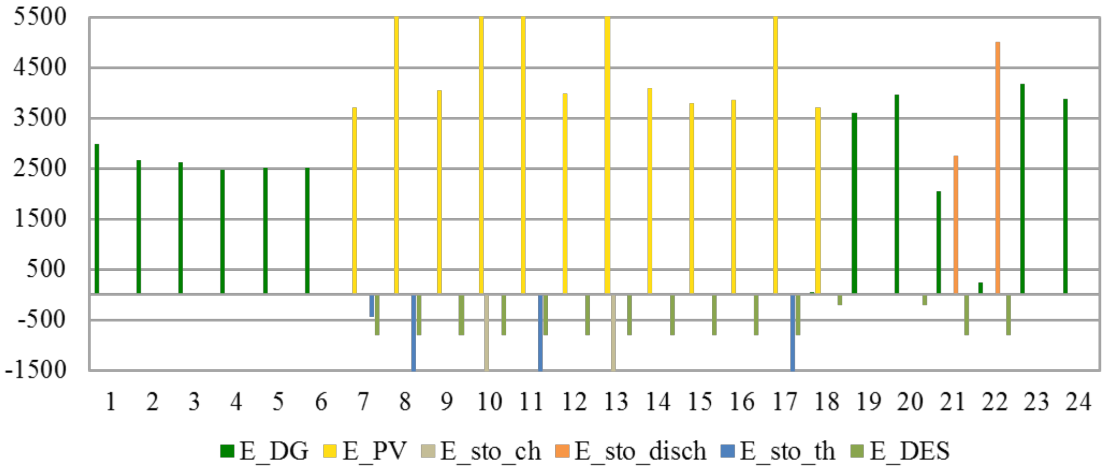

Fig. 6.35. Power flows in the standard day of June for the environmentally-optimal solution

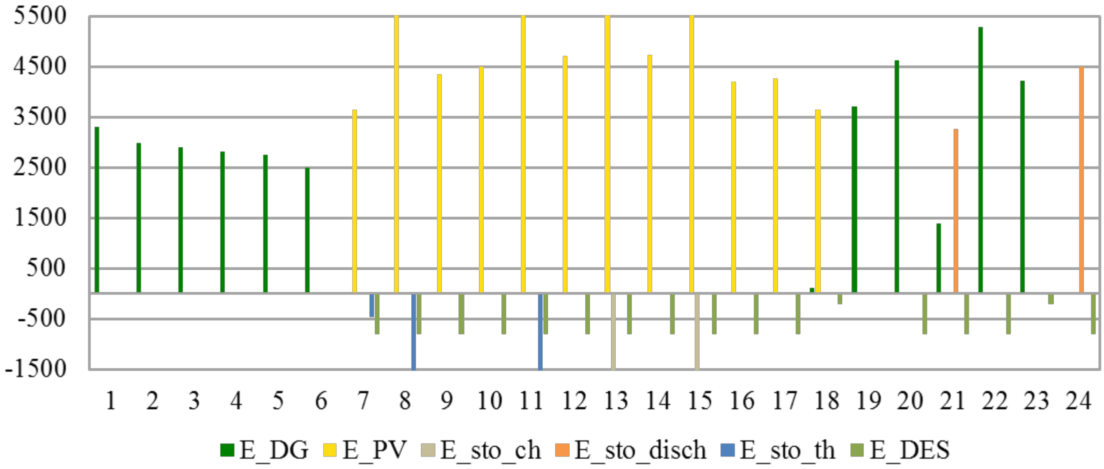

Fig. 6.36. Power flows in the standard day of July for the environmentally-optimal solution

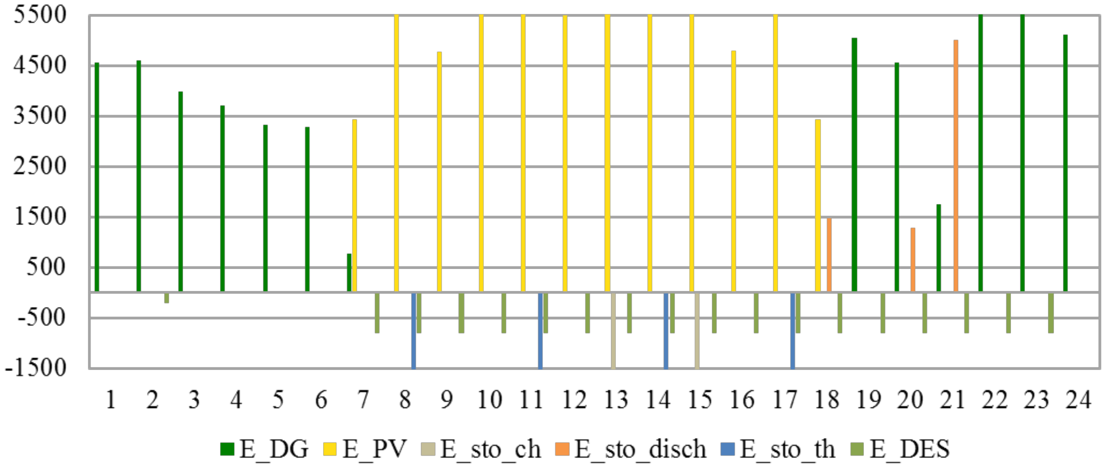

Fig. 6.37. Power flows in the standard day of August for the environmentally-optimal solution

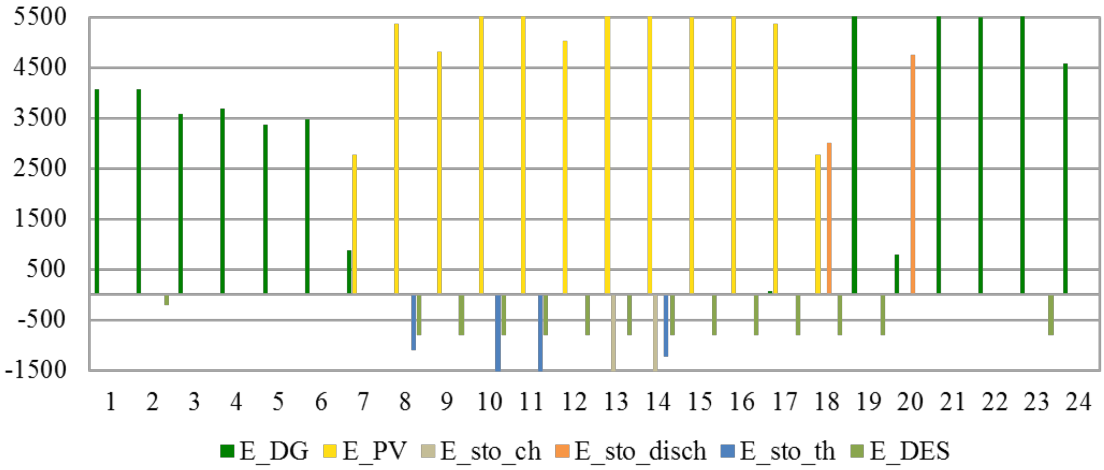

Fig. 6.38. Power flows in the standard day of September for the environmentally-optimal solution

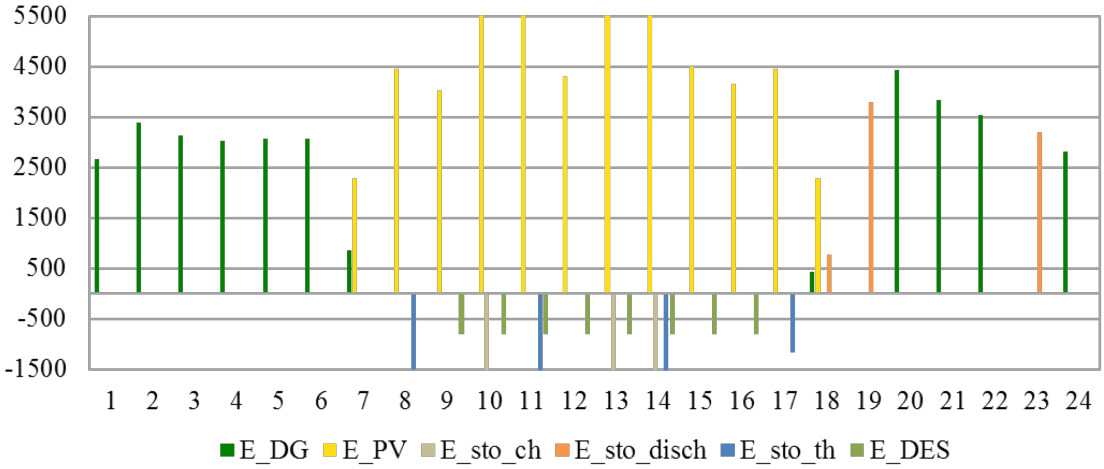

Fig. 6.39. Power flows in the standard day of October for the environmentally-optimal solution

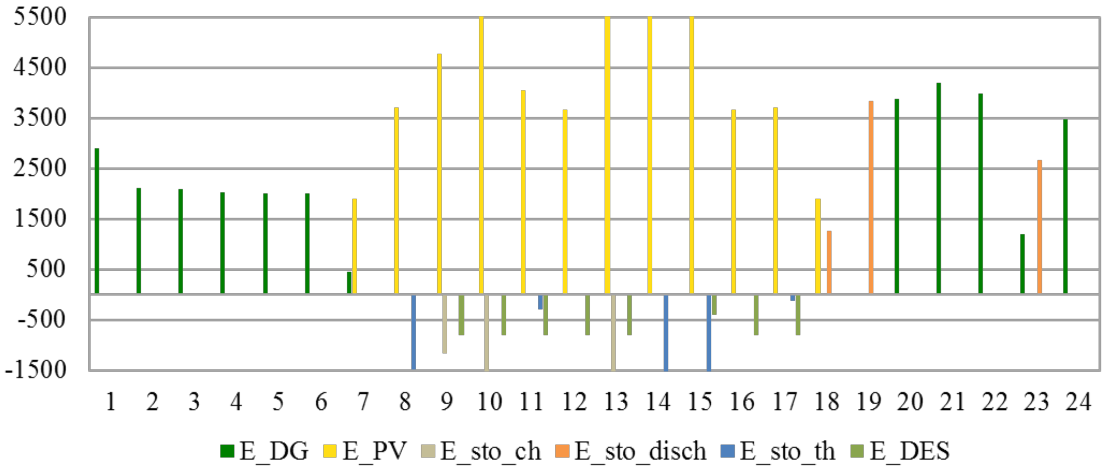

Fig. 6.40. Power flows in the standard day of November for the environmentally-optimal solution

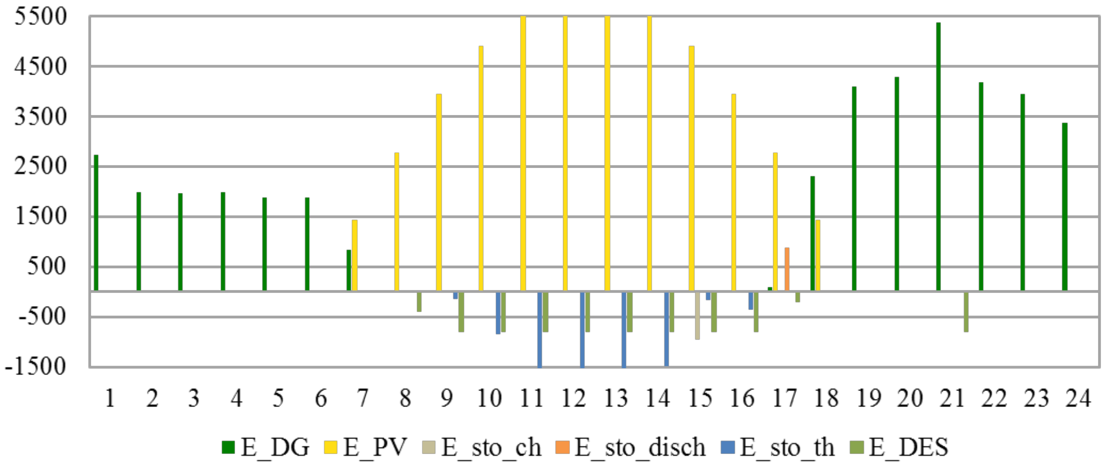

Fig. 6.41. Power flows in the standard day of December for the environmentally-optimal solution

6.4. Scientific literature contributions

Part of the work shown in this chapter was published in the following scientific papers:

JOURNAL ARTICLES

- Manfredi Crainz, Domenico Curto, Vincenzo Franzitta, Sonia Longo, Francesco Montana, Rossano Musca, Eleonora Riva Sanseverino, Enrico Telaretti, "Flexibility Services to Minimize the Electricity Production from Fossil Fuels. A Case Study in a Mediterranean Small Island", Energies, 2019, vol. 12(18), 3492.

INTERNATIONAL CONFERENCES PROCEEDINGS

- Giuseppe Attardo, Sonia Longo, Francesco Montana, Eleonora Riva Sanseverino, Quynh Thi Tu Tran and Gaetano Zizzo, "Urban Energy Hubs Economic Optimization and Environmental Comparison in Italy and Vietnam", IEEE 4th International Forum on Research and Technology for Society and Industry (RTSI), Palermo, 2018, pp. 1-6;
- Nicoletta Cannata, Maurizio Cellura, Sonia Longo, Francesco Montana, Eleonora Riva Sanseverino, Quyen Le Luu, Ninh Quang Nguyen, "Multi-Objective Optimization of Urban Microgrid Energy Supply According to Economic and Environmental Criteria", 2019 IEEE Milan PowerTech, Milan, Italy, 2019, pp. 1-6;
- Domenico Curto, Vincenzo Franzitta, Sonia Longo, Francesco Montana, Eleonora Riva Sanseverino, Enrico Telaretti, "Flexibility Services in a Mediterranean Small Island to Minimize Costs and Emissions Related to

Electricity Production from Fossil Fuels", 20th IEEE Mediterranean Electrotechnical Conference (MELECON), Palermo, 2020, pp. 453-458.

6.5. References

[1] IEA EBC Annex 67. Literature review on energy flexibility definitions and indicators for building clusters. 2018.

[2] Vigna I, Pernetti R, Pasut W, Lollini R. New domain for promoting energy efficiency: Energy Flexible Building Cluster. Sustain Cities Soc 2018;38:526–33. doi:https://doi.org/10.1016/j.scs.2018.01.038.

[3] Mishra S, Koduvere H, Palu I, Kuhi-Thalfeldt R, Rosin A. Assessing demand side flexibility with renewable energy resources. 2016 IEEE 16th Int. Conf. Environ. Electr. Eng., 2016, p. 1–6. doi:10.1109/EEEIC.2016.7555546.

[4] IEA EBC Annex 67. User needs, motivation and barriers for application of Energy Flexibility in Buildings. 2017.

[5] International Energy Agency (IEA). IEA EBC Annex 60 - New generation computational tools for building and community energy systems based on the Modelica and Functional Mockup Interface standards n.d. http://www.iea-annex60.org (accessed April 26, 2020).

[6] International Energy Agency (IEA). IEA EBC Annex 63 - Implementation of energy strategies in communities – Putting energy in urban planning processes n.d. http://annex63.iea-ebc.org/ (accessed April 28, 2020).

[7] International Energy Agency (IEA). IEA EBC Annex 67 - Energy Flexible Buildings n.d. http://www.annex67.org/ (accessed April 28, 2020).

[8] International Energy Agency (IEA). IEA EBC Annex 82 - Energy Flexible Buildings Towards Resilient Low Carbon Energy Systems n.d. https://www.iea-ebc.org/projects/project?AnnexID=82 (accessed April 28, 2020).

[9] Köppen W. Klassifikation der Klimate nach Temperatur, Niederschlag und Jahresablauf. Petermanns Geogr Mitt 1918;64.

[10] Peel MC, Finlayson BL, McMahon TA. Updated world map of the Köppen-Geiger climate classification. Hydrol Earth Syst Sci 2007;11:1633–44. doi:10.5194/hess-11-1633-2007.

[11] European Union Joint Research Centre. Typical meteorological year files generator n.d. https://ec.europa.eu/jrc/en/PVGIS/tools/tmy (accessed April 28, 2020).

[12] U.S. Department of Energy. EnergyPlus web page n.d. https://energyplus.net/ (accessed April 28, 2020).

[13] American Society of Heating Refrigerating and Air-Conditioning Engineers. ASHRAE Handbook - Fundamentals. 2017.

[14] U.S. Department of Energy. EnergyPlus v8.9.0 Documentation - Engineering Reference 2018:1–1715.

[15] Attardo G, Longo S, Montana F, Riva Sanseverino E, Tran QTT, Zizzo G. Urban Energy Hubs Economic Optimization and Environmental Comparison in Italy and Vietnam. 2018 IEEE 4th Int. Forum Res. Technol. Soc. Ind., 2018, p. 1–6.

[16] IRCI Impianti ed Energia web page n.d. https://www.ircispa.com/.

[17] ASHRAE. ASHRAE Equipment Life Expectancy chart. n.d.

[18] Enel X web page n.d. https://www.enelxstore.com/it/it/prodotti/.

[19] Piacentino A, Barbaro C, Cardona F, Gallea R, Cardona E. A comprehensive tool for efficient design and operation of polygeneration-based energy μgrids serving a cluster of buildings. Part I: Description of the method. Appl Energy 2013;111:1204–21. doi:10.1016/j.apenergy.2012.11.078.

[20] Fan J, Chen Z, Furbo S, Perers B, Karlsson B. Efficiency and lifetime of solar collectors for solar heating plants. Proc. ISES Sol. World Congr. 2009, 2009, p. 331–40.

[21] Smith K, Saxon A, Keyser M, Lundstrom B, Cao Z, Roc A, et al. Life Prediction Model for Grid- Connected Li-ion Battery Energy Storage System Preprint. 2017 Am. Control Conf., 2017, p. 1–6.

[22] Cannata N, Cellura M, Longo S, Montana F, Riva Sanseverino E, Luu QL, et al. Multi-Objective Optimization of Urban Microgrid Energy Supply According to Economic and Environmental Criteria. 2019 IEEE Milan PowerTech, 2019, p. 1–6.

[23] Italian Energy Markets Manager (GME) web page n.d. http://www.mercatoelettrico.org/.

[24] Vietnam Electricity web page n.d. http://en.evn.com.vn/d6/gioi-thieu-d/RETAIL-ELECTRICITY-TARIFF-9-28-252.aspx.

[25] Vietstock web page n.d. https://vietstock.vn/2018/01/thang-02-2018-gas-giam-20000-dongbinh-768-581118.htm.

[26] Dapice D. Counting all of the Costs: Choosing the Right Mix of Electricity Sources in Vietnam to 2025. 2017.

[27] Biancardi A. The cost of capital in the energy and water sectors in Italy 2016.

[28] Trading economics web page n.d. https://tradingeconomics.com/vietnam/interest-rate.

[29] Zhang D, Evangelisti S, Lettieri P, Papageorgiou LG. Optimal design of CHP-based microgrids: Multiobjective optimisation and life cycle assessment. Energy 2015;85:181–93. doi:10.1016/j.energy.2015.03.036.

[30] Beccali M, Cellura M, Longo S, Nocke B, Finocchiaro P. LCA of a solar heating and cooling system equipped with a small water – ammonia absorption chiller. Sol Energy 2012;86:1491–503. doi:10.1016/j.solener.2012.02.010.

[31] Gulotta TM, Guarino F, Cellura M, Lorenzini G. A Constructal Law optimization of a boiler inspired by Life Cycle thinking. Therm Sci Eng Prog 2018;6:380–7. doi:10.1016/j.tsep.2018.01.008.

[32] Schaefer H, Hagedorn G. Hidden energy and correlated environmental characteristics of P.V. power generation. Renew Energy 1992;2:0–7.

[33] Gökulu O, Kadırgan F, Kadırgan MAN. Life cycle assessment (LCA) of a solar selective surface produced by continuous process and solar flat collectors 2016;135:284–90. doi:10.1016/j.solener.2016.05.049.

[34] Mcmanus MC. Environmental consequences of the use of batteries in low carbon systems: The impact of battery production. Appl Energy 2012;93:288–95. doi:10.1016/j.apenergy.2011.12.062.

[35] Fukurozaki SH, Zilles R, Sauer IL. Energy Payback Time and CO2 Emissions of 1.2 kWp Photovoltaic Roof-Top System in Brazil. Int J Smart Grid Clean Energy 2013;2:164–169.

[36] Terna. Statistical data on electrical energy in Italy - in Italian. 2017.

[37] Vietnamese Ministry of Industry and Trade - General Directorate of Energy. Viet Nam's Power Development Plan. 2017.

[38] ISPRA. Atmospheric emission factors of greenhouse gases and other gases in the electricity sector - in Italian (Fattori di emissione atmosferica di gas a effetto serra e altri gas nel settore elettrico). 2018.

[39] Ministero dello Sviluppo Economico. Decreto Ministeriale 14 febbraio 2017. Disposizioni Per la Progressiva Copertura del Fabbisogno Delle Isole Minori Non Interconnesse Attraverso Energia da Fonti Rinnovabili. Italy: 2017.

[40] Garofalo E, Gargiulo A, Lembo E, Marazzi R, Rondena E, Moneta D, et al. Sviluppo delle Fonti Energetiche Rinnovabili nelle Isole minori non interconnesse. 2015.

[41] Worldbank, ESMAP, SOLARGIS. Global Solar Atlas n.d. https://globalsolaratlas.info.

[42] Legambiente. Isole sostenibili. Osservatorio sulle isole minori. Le sfide per le isole minori italiane e le buone pratiche nel mondo. 2019.

[43] Mattiazzo G. State of the Art and Perspectives of Wave Energy in the Mediterranean Sea: Backstage of ISWEC. Front Energy Res 2019;7.

[44] Crainz M, Curto D, Franzitta V, Longo S, Montana F, Musca R, et al. Flexibility Services to Minimize the Electricity Production from Fossil Fuels. A Case Study in a Mediterranean Small Island. Energies 2019;12. doi:10.3390/en12183492.

[45] Municipality of Pantelleria. Sustainable Energy Action Plan of Pantelleria. 2015.

[46] Bertini I, Cosentino V, Favuzza S, Graditi G, Ippolito MG, Massaro F, et al. Studio di fattibilità e progettazione preliminare di dimostratori di reti elettriche di distribuzione per la transizione verso reti attive. Report 1 – Caratterizzazione delle reti attuali e analisi di possibili scenari di sviluppo. 2010.

Chapter Seven – Conclusions

7.1. Main contents

The work described in this PhD thesis proposes a methodological framework to assess and minimise the life cycle impacts and the costs related to buildings with high-energy performance. The driving force behind the development of this project is the inclusion of the Life Cycle Thinking approach in the current decarbonisation of the building sector since this is one of the most energy-intensive sectors in industrialised countries. Policy makers should always take into account the application of the Life Cycle Thinking since it allows a deep and conscious analysis of processes and products, avoiding the phase-shifting phenomenon.

The methodology included the optimisation of buildings considering both the scales of single building and the clusters of building since both levels are currently of great interest for the international scientific and technical communities. Although the approach was illustrated regarding specific software tools, databases, objective functions and climate contexts, this method was conceived to be as generic as possible, in order to be applicable to different conditions. Both the design of new buildings or refurbishment of existing ones may be analysed, investigating the optimal techniques and interventions for the envelope and the equipment. The evaluation of the energy performance of the single building was included in a simulation-based optimisation through a quasi-steady state or a dynamic method. Furthermore, the adoption of optimisation techniques allowed identifying the best compromise solutions between many OFs, investigating very large search spaces that would be prohibitive for classical approaches as parametric analyses.

Another key point of the method was the preference for free-of-charge databases and software. Although these generic data may risk being not strictly representative of the specific conditions of each project, the adoption of average values has a duplex advantage: first, allowing to draw generic guidelines on the best interventions to adopt; secondly, it is to be preferred in a preliminary design phase, when the supplier is still unknown.

This thesis begins with an introduction on the main topic discussed in the document, illustrating the motivations behind the development of the PhD research project and the international policy context. Subsequently, a background on the main methods and techniques deepened for the research project was illustrated. This section was provided to enable the reader to be comfortable with the various topics and techniques included in the methodology. Moreover, two literature reviews, the first on the optimisation of the life cycle impacts of buildings and the second on the optimisation approaches employed for low-energy buildings, were included in the thesis to provide the reader with the status of the art on the various aspects of the project, creating a basic context to be further deepened in the subsequent sections. Furthermore, the review process allowed identifying the currently existing research gaps to be addressed in the project. The development of the method was thus illustrated and discussed, highlighting strengths and weaknesses and comparing its main features with the few previous works available in the literature. The main outcome is that this method should be employed for a comparison among many alternatives, as in the common practice of optimisation studies, since some detailed aspects are often neglected in order to attain the optimal solution. This aspect mainly regards the energy hub model employed for Step 2 of the single building optimisation and for the clusters optimisation. More detailed simulation-based optimisation studies might be conducted renouncing to take into account for the computational burden.

The application of the method was then shown concerning two different contexts for each scale, namely Southern and Northern Europe for the single building optimisation and a developed and a developing country in warm climate for the cluster of buildings optimisation. The contexts were differentiated according to the local climate, influencing the energy demand, economic conditions and technological development, impacting on the LCA and economic indicators. The validation and calibration of the simulation model was performed only for one study, namely the case developed in Danish context, since the Be18 results were compared with actual measurements and some parameters related to the occupancy habits were fine tuned to make the results adhere with the reality. Other aspects, as a sensitivity analysis on the input parameters, were also neglected in this thesis, since the main aim of the case studies was to show the feasibility of the method and only secondarily to identify the optimal interventions to be applied on each context, since the optimal solution is often very case-specific and providing generic guidelines is usually hard and risks to be misleading. For what above, the results of the case studies should be considered as an indication rather than a design guideline.

7.2. Advancements in the state of the art

The methodology illustrated in this thesis incorporates and harmonises several existing features and techniques usually employed in the analysis of the energy performance of buildings. The main benefits deriving from the application of this approach are summarised here below:

- *Applying building physics, LCA, economic analysis and multi-objective optimisation in a single study.* Although many applications of each of these techniques to the buildings were already performed, the original contribution of this work lies in the simultaneous employment of all of them, since no other similar approach was noticed in the existing literature;
- *Identifying and developing a bigger, generic framework where all the existing building optimisation studies may be included.* Previous studies can be considered as partial applications of the present methodological framework. For example, some existing studies applied a SOO study using only one LCA impact or only costs as objective functions, while other studies involved the MOO of many LCA impacts assessing the use phase performance with building physics and disregarding the economic aspects.

These works might be considered as adopting a partial application of the present methodology;

- *Collecting, comparing and suggesting free-of-charge databases and software tools.* The large availability of commercial and research tools may scare and confuse the beginners, preventing them from adopting some advanced approaches as the LCA, even because of their cost. The selection of free available tools and data should encourage novices and young designers in embracing these techniques. Moreover, the comparison of the main features summarised in this thesis should drive researchers in the selection of the correct tool for their application;
- *Supporting the decision making in energy saving policies*. Although politicians often keep themselves away from the academic discussions, the diffusion of the three dimensions of the sustainable development, *i.e.* economic, environmental and social dimensions, is gaining a large audience in the last decades. These dimensions can be incorporated properly through the application of the Life Cycle Thinking, as illustrated in Chapter 2. With specific detail on the building sector, the method here depicted may support this process, suggesting the correct direction to be promoted by policy makers. For example, although the NZEBs are currently seen as the future of the built environment, the preliminary results of the case studies illustrated in this document suggest that the *Net Zero target* might be too demanding to be reached, if the embodied energy term is taken into account;
- *Supplying the construction industry with a powerful design tool*. Since the final customers are becoming more and more sensitive to environmental issues, construction companies adopting this methodology might advertise their solutions to be really green and supported by scientific criteria. The widespread adoption of the method developed in this project, or similar methods, should be seen as the key for the decarbonisation of our cities and society.

7.3. Results of the case studies and guidelines

7.3.1. Single buildings optimisation

The three case studies on single building optimisation demonstrated the feasibility and effectiveness of the method developed in this PhD project. Although the first and the third cases show some similarities, some conclusions may be drawn from each study independently on the others. The first conclusion, common to all the studies, is that the two impact functions, namely GWP and CED, proved to be non-conflicting objectives. Since these are among the most employed impact assessment indicators in literature, and even the reports from IEA EBC Annex 56, focused on the LCA of buildings renovation, suggested the adoption of these two indicators, this aspect reveals that it is sufficient minimising one of these two functions. Furthermore, this aspect should stimulate the scientific community in identifying other relevant couples of indicators for the multi-objective optimisation of buildings.

Another main outcome is that the three OFs were highly minimised in all the case studies, with respect to the dimension of the search space, with energy, carbon and economic payback times being always lower than 6 years. Moreover, this target was reached with reasonable computational efforts, being always lower than three hours per each optimisation study. This result was obtained performing some preliminary assessment of the algorithm input parameters, selecting the best combination for each case.

An important result is that, although the local renewable energy production was always considered among the variables, the NZEB or plus-energy levels were never identified in the optimal solutions. This evidence should suggest that pushing only on the reduction of the use phase energy demand to the *Net Zero target* might be a blind policy and might be the cause of the phase shifting, if the embodied energy term is not taken into account. Nevertheless, this feature has still to be further investigated.

The selection of the best compromise solution was performed without including any weight to the OFs since this aspect would involve decision making rather than scientific considerations, and the utopia point criterion was always employed. The scalarization technique, employed for Step 2 as well as for the cluster optimisation, allowed having a reduced Pareto front, simplifying the identification of the best compromise even for decision-makers.

The development of the case study involving a fictitious building allowed confirming the feasibility of the methodology described in this thesis on the single buildings optimisation for the first time. Due to the input parameters, the concrete layer was preferred to hollow bricks to increase the thermal mass, while the glass wool outperformed both EPS and rock wool for the envelope insulation. These interventions were selected with very low values of thickness. The optimal equipment combination was given by the maximum installable PV size, *i.e.* about 3 kW_p, an average size for HP (4 kW_{cool}), 7 STC modules and about 5 m^3 of hot water sensible storage. With an annualised expense of about 1500 €, this system's payback time is lower than 6 years, while the primary energy and equivalent carbon emissions operating savings allow compensating the embodied impacts for envelope and equipment in less than one year.

The outcomes of the case study in oceanic climate suggest that a step-wise optimisation should be performed for the equipment, reducing the number of variables and the dimensions of the search space to avoid errors in the results. In Step 1 the search space was composed of 40 discrete variables and $5.84 \cdot 10^{17}$ alternatives, while the whole building optimisation included 46 discrete variables, 2 continuous variables and $8.98 \cdot 10^{20}$ alternatives. The envelope optimisation suggested walls insulation and low glazing values while including the equipment the district heating was awarded as best heating technology, neglecting the solar energy exploitation for both electricity and heating production.

The solution of the case study in Mediterranean climate allowed managing 54 discrete variables, 4 continuous variables and comparing $2.66 \cdot 10^{19}$ alternatives. The best envelope had limited or null additional insulation, limited additional thermal mass but high performing glazing for windows, shading from the high solar radiation during summer. The RES technologies installation selected the maximum size available in each case, disregarding the electrical storage mainly due to its high cost, while the optimal solution was also based on the installation of an HP with 6.4 kW_{cool} and a very large hot water storage, namely about 40 m^3. Another important result of this case was that the best performing envelope solution was disregarded when the operating impacts and costs were assessed through the building service equipment. This feature suggests that the second optimisation step should be performed on all the envelope solutions form Step 1, and is the main aspect supporting a whole-building optimisation in lieu of a multi-step approach.

All the optimal retrofit actions somehow mirror the common practice in these locations, mainly relying on envelope insulation and district heating in Denmark and on solar technologies, heat pumps and limited insulation in Southern Italy, confirming the reliability of the results.

7.3.2. Clusters of building optimisation

The cluster optimisation model was fruitfully employed to identify the best equipment synthesis, design and operation of three microgrids, namely a fictitious urban district in developed and a developing contexts, both of them located in warm climate, and on a Mediterranean island. This application was an original contribution of the PhD project to the international literature since LCA of microgrids were hardly developed in the past, and never in an optimisation process. Nevertheless, a correct LCA of microgrids should also take into account for many other aspects, as the equipment connection to the buildings or the impacts related to the control system. The latter would influence the absolute final values because of the high impacts due to the integrated circuits, although the optimal equipment combination should not be affected.

According to the results of the single building optimisation, one of the two LCA impact was only assessed rather than minimised in these studies, reducing the number of simulations to be performed. The urban district study was one of the first integrating electricity, heating and cooling demands in the multi-objective optimisation of an energy hub model, illustrating a methodology to optimise costs and environmental impacts related to the energy demand. The optimisation was performed adopting average seasonal standard days for electricity, space heating and space cooling demands. The difference between the cost-optimal and the carbon-optimal combinations of technologies in Italian context is that the sizes of PV, STO_{el} and STO_{th} systems were higher in the GWP optimisation, while NGB was preferred according to the economic criterion. The sizes of STC and HP systems did not depend on the optimisation criterion. The Vietnamese cluster optimisation led to preferring the installation of AC and STO_{el} in the GWP optimisation and STO_{th} and NGB in the cost-optimal solution, while PV and HP sizes were the same in the two solutions. The CHP was always disregarded. The comparison between the two contexts neglected the different architectural features of the countries, and also the higher pollution concentration in Hanoi that may reduce the direct radiation collected by solar technologies. This phenomenon, known as the urban haze, should be taken into account in detailed studies in highly polluted cities.

Since the cost and GWP optimisations of the energy system in Pantelleria were both oriented at minimising the gas oil consumption, the differences in the OFs between the cost-optimal and carbon-optimal scenarios were limited. In detail, 9.7 MW of PV, 3230 m^2 of STC and 10 MWh of STO_{el} were installed in the cost-optimal solution, against 13.2 MW of PV and 10 MWh of STO_{el} in the carbon-optimal scenario. The simultaneous installation of these components with the optimal management of DES and HWSS during the year allowed a 43% of cost-saving and 74% of equivalent emissions reduction in the economic optimisation and a 39% reduction of the annualised costs and 75% of avoided equivalent emissions when GWP was minimised. Although the STC was designed to cover the 99% of the island's DHW demand in the cost-optimal solution, it was totally disregarded when the GWP was minimised. Anyway, the results show that the energy system of the island of Pantelleria presents considerable room for improvements and different actions may prove similar effects.

7.3.3. Generic guidelines

It is important to stress the fact that the optimisation studies performed in this thesis were illustrated to provide the readers and the international scientific community with a useful and powerful method that should be applied in many technical and social aspects, namely the combination of Life Cycle Thinking and optimisation approach. The results related to the design and renovation of single or clusters of buildings should instead be evaluated case-by-case, without deriving general results from the case studies illustrated in this document, although the optimal interventions obtained in the case studies were often in line with common practice in building and technical sectors.

Thus, as generic guidelines, the results recommend the assessment of the energy, environmental and economic performance at least of the main aspects of a design or renovation project to make efficient and decarbonise the building sector. Only three indicators were chosen as objective functions for this project, being the key performance indicators most commonly adopted in the current policies and investment projects. Results show that the insulation materials with natural origin should be preferred to synthetic ones, even with larger thicknesses, also allowing the installation of low-performing glazed surfaces. Solar technologies were highly recommended in warm climatic contexts, as well as HPs, due to their high efficiency that overbalances the embodied impacts and investment costs, while these systems were disregarded by the Be18 calculation method in Northern Europe. The low attractiveness of solar RES may be even due to the large adoption of wind farms in Denmark that contributes to reducing the impact of the electricity from the grid. On the opposite, the outcomes of the study in the Vietnamese context recommended to massively adopt electrical RES and storages due to the impacting power mix of this country, while cogeneration and gas-fired boilers were disregarded. The thermal technologies are less useful in this context since the demand in this climate is low, while the combination of thermal storage and absorbing chiller was selected to minimise the equivalent carbon emissions.

The reliability of these results is provided by a comparison with the common practice. For example, the insulation of buildings in Southern Italy is being considered only in recent times, and mainly for the economic incentives rather than for a true need of reducing thermal transmittance of the envelope that should be instead designed mainly to shift the heat wave during summer. Instead, solar RES are having a great success due to a combination of economic profitability and higher useful life of modern systems. In Danish context, solar technologies are usually considered only in few projects as NZEBs, as in BOLIG+, the first Danish NZEB, while the common practice is to develop offshore wind farms and to exploit the thermal energy of biomasses and wastes to power the district-heating networks.

As future developments of the research illustrated in this thesis, further aspects might be included among the objective function, as additional LCA impacts or indoor comfort indicators. Regarding the latter, the assessment of indoor thermal conditions was quite unnecessary in these studies, since the buildings final energy requirement was evaluated simulating ideal HVAC systems with infinite power able to keep the temperature equal to the set-point, but other models may require also evaluating lighting or acoustic indoor conditions. The economic analysis may be further deepened, conducting to a proper LCC study, as well as the inclusion of the social aspects might enable to obtain a Social LCA, that was hardly assessed in building sector up to date. An interesting direction to develop the model used for the cluster of buildings would be the verification of the optimal results with a detailed simulation model and the inclusion of transport losses to identify the optimal location to install each component.

As a final remark, I really hope that the content of this thesis, where the outcomes of a three-year-long path were illustrated, helps the future researchers investigating building energy performance in the development of their studies, pursuing the target of driving the mankind to a next step, where societies are based on the respect for the planet as well as for the others.